MECHANISTIC STUDIES OF HIGH TEMPERATURE REACTIONS OF HYDROCARBONS

This thesis is submitted by

STEPHEN KOLAWOLE LAYOKUN; M.Sc., D.U.C. (Biochem-Eng)

for the award of

THE DEGREE OF DOCTOR OF PHILOSOPHY,

in the Faculty of Engineering of

THE UNIVERSITY OF LONDON

The work described herein was carried out

at the Department of Chemical Engineering and

Chemical Technology, Imperial College, London S.W.7.

during the years 1972 - 1975

ABSTRACT

A study of the reactions of propane is carried out between 600° and 800°C with a view to elucidating the mechanism and kinetics. This is effected by continuous sampling of the reaction products through an MS10-C2 mass spectrometer and the results are compared with computer predictions.

The mass spectrometer is used to identify the reaction products. Quantification of the products is done by resolving the superimposed mass spectra with the aid of a novel matrix-inversion computer programme. This programme should be very useful in pollution studies as well.

The numerical integration programme employed is based on the semi-implicit trapezoidal rule. It is tested on two well studied experimental systems - the gas phase oxidations of acetaldehyde and formaldehyde. The predicted results showed very good agreement.

The above two experimental techniques are then employed in analysing the following systems.

(a) The pyrolysis of propane in a flow system between 600° and 800°C. A 19-reaction-step model based on generation and interaction of free radicals in the propane system is proposed with the appropriate rate constants and integrated. The main products are CH_4, C_2H_4, C_3H_6, H_2 and C_2H_6. The predictions fit very well the experimental data.

(b) The "perturbation-pyrolysis" of propane between 600° and 750°C. This is a new technique. Small amounts of acetone (a potential source of methyl radicals) and acetaldehyde (a methyl radical source and a branching intermediate) are added separately into the propane system and their individual effects on the mechanism and kinetics of propane decomposition are discussed. In both cases, there is acceleration of propane decomposition and a reduction of the induction period with increase in the concentration of the additive. Methane and ethane increase in concentration, ethylene

remains the same while propylene and hydrogen decrease, relative to the unperturbed propane pyrolysis system. Acetone system, a 21-reaction-step model fits the experimental data while a 24-reaction-step model fits the acetaldehyde perturbed system data.

(c)Oxidative pyrolysis of propane between 600° and 700°C. Literature on this topic is very sparse for temperatures above 600°C. In this work, small amounts of oxygen are added into the propane stream such that the oxygen will only participate in the early stages of reaction, thus throwing some light on the nature of the initiation reactions in pyrolysis and oxidation systems. The results show that oxygen first of all abstracts a hydrogen atom to form hydroperoxy radical, HO_2. The hydroperoxy radical then engages in recombination reaction to form water, but as reaction proceeds and oxygen is consumed, pyrolysis takes over from oxidation and the hydroperoxy radical then engages in hydrogen atom abstraction to form hydrogen peroxide. The hydrogen peroxide then pyrolyses to yield hydroxy radicals which are the dominant radicals in high temperature oxidation. A 28-reaction-step model fits the experimental data.

ACKNOWLEDGEMENTS

I would like to express my thanks to:

The Department of Chemical Engineering and Chemical Technology, Imperial College, for the opportunity to do this work and for the provision of research equipment.

Dr. D.H. Slater and Dr. D.L. Trimm for suggesting this topic, and particularly to Dr. D.H. Slater for his supervision, constant guidance and encouragement throughout the research work.

The members of the Glassblowing, Engineering and Electronic workshops for their assistance.

The University of Ife, Nigeria for its financial assistance.

Miss Cathy Maxwell for her patience and typing of the thesis.

Finally, I thank Dr. T.A. Sutherley for help in proof reading.

CONTENTS

CHAPTER V

Perturbation pyrolysis kinetics of propane

Propane pyrolysis perturbed by acetone

Abingdon vaporizer

Propane pyrolysis perturbed by acetaldehyde, mechanism and kinetics

CHAPTER VI

Oxidative pyrolysis of propane

Composition profiles

Effect of oxygen concentraion

Mechanism of reaction

High temperature reactions of alkyl and radicals with oxygen

CHAPTER I

Chapter I

1.1 INTRODUCTION

Two important systems involving high temperature reactions of hydrocarbons are pyrolysis and oxidation. Mechanistic studies have shown that both involve the generation and interaction of free radicals. The primary object of any kinetic study is to establish a mechanism for the succesive breakdown and fate of the parent hydrocarbon molecule and of any intermediate. A complete mechanistic description not only requires an identification of all the elementary steps and their sequence in the network, but also a quantitative knowledge of the pre-exponential factors and activation energies for each step. Much of the present evidence concerning the elementary steps is of an indirect nature, inferred from the isolation of relatively stable intermediate products during the course of reaction.

(a) PYROLYSIS

The spectrum of products from hydrocarbon pyrolysis encompasses an enormous number of compounds extending from hydrogen and methane at the low end of the molecular-weight scale to very high molecular-weight polynuclear aromatics, tars and coke at the upper extreme. The same principal products are normally present in effluents from all feedstocks, but their relative proportions vary widely and are dependent upon the composition of the feedstock and the conditions under which they are carried out.

Up to the time of the first world war, there was little incentive for applying industrially the pyrolysis of gaseous hydrocarbons. The war created a demand for benzene, toluene and olefins which brought about a study of their production by the pyrolysis of oils as well as hydrocarbon gases. Interest in benzene and toluene declined with the termination of the war, but the manufacture of chemical derivatives from hydrocarbons received an impetus from chemical warfare activities. The last decade has witnessed the development of diversified industries. Alcohols, ethers,

acids,esters, resins, pharmaceuticals, carbon black and many other products are made from light unsaturated hydrocarbons.

(b) OXIDATION

The combustion of hydrocarbons is an exothermic process; chemical energy released can be transformed into mechanical energy and utilized. The wide applications of combustion processes have stimulated interest in, for example, low pollution combustion devices. More complete understanding of the mechanisms of the reactions involved is essential in order to explain abnormal engine behaviour and its connection with anti-knock additives and exhaust gas composition. Apart from the numerous products formed, the well established obervation of several distinct regions of combustion under different conditions of pressure and temperature are definitive features. These features are; (a) an autocalytic development of the reaction with time following an induction period during which no apparent reaction occurs; (b) a negative temperature coefficient when reactions slow down with rising temperature; (c) the catalytic effect of additives such as peroxides and aldehydes. All these indicate the complexity of a combustion system and the need for full kinetic details to be determined.

Although, in the past, both pyrolysis and oxidation have engaged the interest of the chemical and petroleum industries and developments within the industries have stimulated research of a fundamental type: i.e., improvements in experimental and analytical techniques, the intimate understanding of the chemistry/mechanism necessary demands further consideration. The approach so far confirms the fact that empirical technology has always been well in advance of theoretical understanding. Current research aims to bridge this gap. There is a considerable amount of evidence which indicates that hydrocarbon reaction processes are propagated by minute concentrations of free radical species. The direct identification of these species and measurement of the concentrations involved are problems which are only recently being solved in complex systems. Hence, knowledge concerning the rate parameters of the individual elementary steps is becoming available and current

research is directed mainly at establishing the elementary steps and their sequence in these chain processes.

In general, chain reactions consist of three main steps: initiation, propagation and termination.

$$A \longrightarrow R. \qquad \text{Initiation}$$

$$R. + A \begin{cases} \nearrow R'. + \text{products} \\ \rightarrow 2R'. \\ \searrow R. + R'. \end{cases} \qquad \text{propagation}$$

$$R. + R'. + M \longrightarrow \text{Inert}$$
$$R'. + \text{Wall} \longrightarrow \text{Inert} \qquad \text{Termination}$$

in which A is a molecule and R. is an active centre (free radical). The rate, W, of a single step reaction such as $nA \longrightarrow$ Products is usually defined as $W = K[A]^n$ where K is the rate constant and n is the order of reaction which will be an integer. In chain reactions the constant K is replaced by a function of all rate constants K_1, K_2, K_3 ..... K_n and the order n may or may not be an integer.

The kinetic description of the Vant-Hoff-Arrhenius Law as represented by the equation

$$W = Ae^{-E/RT}$$

is that every molecule has a certain stability and resists chemical reaction even when the net overall potential energy would decrease. The molecule requires an excess energy E to overcome this inertia and to undergo reaction, the excess energy being the activation energy of the system. In 1923 Christiansen and Kramers gave a general formula for chain reactions as $W = K_i n \exp(-E/RT)$ in which W is the number of activated molecules reacting in unit time (reaction velocity), K_1 is the rate constant and n is the concentration of active molecules.

Every elementary reaction is thus associated with two kinds of energy, namely, the activation energy, E, and the enthalpy H of the reaction. Any liberated energy will be collisionally distributed among all molecules. Hence, at high temperatures, radical concentrations will be high. Further-

more the lower kinetic order of dissociation with respect to recombination means that radical concentrations will tend to exceed the local equilibrium values and will only return to them relatively slowly.

Although, as a result of the high temperature, all reactions will be correspondingly faster, radical-radical reactions, despite their low activation energies, become progressively more significant and the nature of the dominant active intermediates is also likely to change.

1.2 PYROLYSIS OF HYDROCARBONS

The chemical reactions which occur when hydrocarbons are decomposed under the influence of heat are complex, the degree of complexity increasing with increasing molecular weight of the hydrocarbon being pyrolyzed and with increasing conversion. F.O. RICE [1,2,3] established in the 1930's that hydrocarbon decomposition by pyrolysis involves the production and subsequent reaction of free radicals, and was able to rationalize the distribution of the principal products resulting from the pyrolysis at low conversion of several of the C_2 to C_6 paraffin hydrocarbons. Despite this big step forward, the reaction even for the simplest compound of interest, ethane, are sufficiently complex that it has not yet been possible to rationalize the complete product distribution especially at high conversion. This has probably been due mainly to:

(i) Misinterpretation of experiments involving inhibitors leading to a belief in the participation of molecular reactions.

(ii) Inadequate allowance for the involvement of surface processes.

(iii) Neglect of the effect of trace impurities.

(iv) Complexities associated with polymerization [4] and self-inhibtion [5] reactions.

These problems are now better appreciated and over the last decade a body of work has appeared which is capable of satisfactory interpretation and the free radical mechanism is now a powerful tool in guiding predictions and correlations of pyrolysis data.

1.2.1. FREE-RADICAL MECHANISMS

As indicated, chains of elementary free radical links is made up of the three major steps:

(a) Initiation (b) Propagation and (c) Termination.

(a) Initiation

In a saturated hydrocarbon, initiation may occur by cleavage of either a C-C bond or a C-H bond. If this is a unimolecular dissociation, then a theoretical estimate can be made of its rate.

The factor in The Rice-Ramsperger-Kassel-Marcus(R.R.K.M.) expression for the high-pressure limiting rate characteristic of the particular process is:

$$\frac{q_r^+}{q_r^*} \quad \frac{\prod^{s} \nu_i^*}{\prod^{s-1} \nu_i^+} \quad \exp\,(-Eo/KT)^4 \qquad (1)$$

where q_r^+ and q_r^* are the rotational partition functions for the transition state and the energised state respectively; ν_i^+ and ν_i^* are the corresponding vibration frequencies; S is the number of oscillators and Eo the critical energy. Strengths of C-C bonds in C_2- C_8 hydrocarbons lie in the range 325-350 KJ $mole^{-1}$ while C-H bonds have typical dissociation energies of 410-427, 393 and 381 KJ/mole for primary, secondary and tertiary positions respectively. Even in the most unfavourable case the temperature-dependent terms will lead to rates of C-C scission at least ten times faster than the corresponding C-H rupture at temperatures up to $1500^{o}K$. It is therefore reasonable to assume that the primary initiation process involves unimolecular rupture of C-C bonds in the molecule, although the contribution of surface reactions cannot be excluded.

Thus, ethane splits into two methyl radicals

$$C_2H_6 \longrightarrow CH_3 + CH_3 . \qquad (2)$$

A methyl radical then reacts with another ethane molecule to give methane and an ethyl radical:

$$CH_3 + C_2H_6 \rightarrow CH_4 + C_2H_5 \cdot \quad (3)$$

The ethyl radical decomposes into an ethylene molecule and a hydrogen atom:

$$C_2H_5 \rightarrow C_2H_4 + H \cdot \quad (4)$$

The hydrogen atom then attacks an ethane molecule to produce a molecule of hydrogen and a new ethyl radical:

$$H + C_2H_6 \rightarrow H_2 + C_2H_5 \cdot \quad (5)$$

The ethyl radical formed by reaction 5 decomposes by reaction 4, thus generating another hydrogen atom. Hence reactions 4 and 5 constitute a chain reaction, the net effect of which can be represented by the simple stoichiometry:

$$C_2H_6 \rightarrow C_2H_4 + H_2 \cdot \quad (6)$$

Reactions(3)and(4)are propagation reactions in which the radicals formed by the initial splitting reaction undergo further reactions in which they are not regenerated and by which the radicals required to establish the chain mechanism are formed.

If the chain mechanism represented by reactions 4 and 5 were able to continue uninterrupted, it would be necessary for only one molecule of ethane to decompose by reaction 2, and all other ethane disappearance would be attributable to reaction 5. However the chain cycle will be terminated if either an ethyl radical or a hydrogen atom should react with another radical in any of the following ways:

$$H\cdot + H\cdot \rightarrow H_2 \quad (7)$$

$$H\cdot + CH_3\cdot \rightarrow CH_4 \quad (8)$$

$$H\cdot + C_2H_5\cdot \rightarrow C_2H_6 \quad (9)$$

$$CH_3\cdot + C_2H_5\cdot \rightarrow C_3H_8 \quad (10)$$

$$C_2H_5\cdot + C_2H_5\cdot \rightarrow C_4H_{10} \quad (11)$$

This is the classical mechanism described as the Rice-Herzfeld theory of thermal decomposition. At the higher levels encountered in commercial

pyrolysis, however, the chain termination reactions become important, and the olefins containing three or more carbon atoms, formed during the early stages of pyrolysis, themselves become degraded to a significant extent.

Thus, when considering the pyrolysis of propane and heavier hydrocarbons it is convenient to consider the reactions as occurring in two stages.

(a) The first stage is designated as the primary reactions wherein the reactants are decomposed by the free-radical chain mechanisms into principal primary products: H_2 CH_4, C_2H_4 and/or propylene, and olefins up to C_{n-1} where n is the number of carbon atoms in the feed hyrocarbon. In the cases of propane and iso-butane, substantial yields of C_n olefin are also realized, but from other paraffinic hydrocarbons, both straight chain and branched, the C_n olefins are produced in only minor quantity.

(b) The second stage encompasses secondary reactions which can be classfied into three types:

1. Reactions involving further pyrolysis of the olefins produced by the primary reactions.
2. Hydrogenation and dehydrogenation reactions wherein paraffins, diolefins, and acetylenes are produced from the olefins.
3. Condensation reactions wherein two or more smaller fragments combine to produce larger stable structures such as cyclodiolefins and aromatics.

The two stages are successive only to the extent that the primary reactions must have progressed far enough to have produced quantities of products sufficient to initiate the secondary reactions. Thus, both primary and secondary reactions are usually occurring simultaneously. At low conversion level of the primary reactant, the secondary reactions are relatively unimportant. The olefins formed are mostly more refractory than the feed and thus are being cracked at relatively low rates. Any degradation of these olefins by second order condensation reaction is also

proceeding very slowly because of the low partial pressures of these constituents. As the conversion of the primary reactant is raised toward higher levels, the secondary reactions become more significant. The proportion of the remaining reactant disappearing per unit time is rising as the temperature of the reacting mixture is elevated, but since the quantity of unreacted feed is decreasing, the absolute amount of reactant undergoing degradation per unit time passes through a maximum and starts to diminish. At the same time, the partial pressures of the primary products increase rapidly due both to their high rate of production and to simultaneous disappearance of the reactant. Consequently cracking of the primary olefins takes place at an accelerated rate, acetylenes and olefins appear in increasing concentrations, and the production of benzene and other aromatics becomes substantial.

A plot of the quantities of the various constituents in the reacting mixture against conversion of reactant shows that at low conversion levels, the yields of primary reaction products are described by straight lines through the origin. As conversion increases, the primary curves start to exhibit curvature, generally, upward for methane, but downward for propylene, butanes, and other higher olefins as their cracking rates become significant. The curve for ethylene may bend in either direction or remain approximately straight, depending upon whether the rate of formation of ethylene from the pyrolysis of the higher olefins is greater than, equal to, or less than the rate of conversion of ethylene to secondary products. Depending upon reactor conditions, a substantial proportion of the ethylene may be hydrogenated to ethane and a lesser amount dehydrogenated to acetylene. In addition it could undergo condensation reactions.

When the heavier feedstocks such as naphthas are being cracked, the severity level is often carried to a point such that the original reactants have been, for all practical purposes, completely consumed. Under these conditions, all the reactions occurring in the vicinity of the reactor out-

let can be classified as secondary.

1.2.2. THE KINETICS

Various investigators of the vapour-phase pyrolysis of individual hydrocarbons have found that the rate of disappearance of the reactant is generally independent of both the pressure and the surface to volume ratio in the reactor[6]. Thus, the disappearance can be considered to follow an overall first-order mechanism as predicted by the simple Rice-Herzfeld mechanism. A first order mechanism has been reported[7,8,9,10] for propane. Martin et al,[11] reported an order of 1.5 and in 1969 Crynes and Albright[13] claimed an order slightly greater than unity at temperatures above 750°C for propane.

A first-order mechanism can be described by the following integrated form of the rate equation;

$$K_t\Theta = 2.3 \log_{10}\left(\frac{1}{1-\alpha}\right) \qquad (12)$$

where:

K_t = Disappearance reaction velocity constant evaluated at temperature t (sec^{-1}).

Θ = Time, secs.

α = Fractional disappearance of reactant.

The reaction velocity constant, K, varies with temperature in accordance with the Arrhenius equation;

$$K = A \exp(-E/RT) \qquad (13)$$

where

A = Frequency factor sec^{-1}.

E = Activation energy KJ/mole.

R = Gas constant 8.31 J/g-mole. °C.

T = Absolute temperature °K.

Equation (13) may be written in the more convenient form:

$$\log K = B - (C/T) \qquad (14)$$

where: $B = \log A$ and $C = E/2.3R$ (^{o}K)

Thus, for any specific compound which reacts according to the first-order mechanism, the logarithm of the reaction velocity constant varies linearly with $1/T$. Values of constants of equations 13 and 14 are shown in Table 1 - 1 .

TABLE 1 - 1

MOLECULE	B = LogA	C = E(2.3R(^{o}K)	E(KJ/mole)
ETHANE	14.67	15,829	302.5
PROPYLENE	13.83	14,715	281.2
PROPANE	12.61	13,082	250.0
ISOBUTANE	12.32	12,559	240.0
n-BUTANE	12.25	12,329	235.6
n-PENTANE	12.25	12,140	232.0

The reaction velocity constants for the above compounds are plotted in Fig 1.1

Since propylene is seldom cracked by itself, but usually in admixture with propane or ethane, the propylene curve shown reflects the accelerated decomposition encountered under such circumstances. The initial and rate-determining reaction in each case involves splitting of a C-C bond in a manner analogous to that given in equation 2 for ethane. Consequently, activation energies for the decomposition of various compounds normally comprising pyrolysis feedstocks vary over a relatively narrow range. The constant C in equation 14, is, therefore of similar magnitude for all the important feedstock constitutents, and plotting log K versus $1/T$ results in a series of nearly parallel lines.

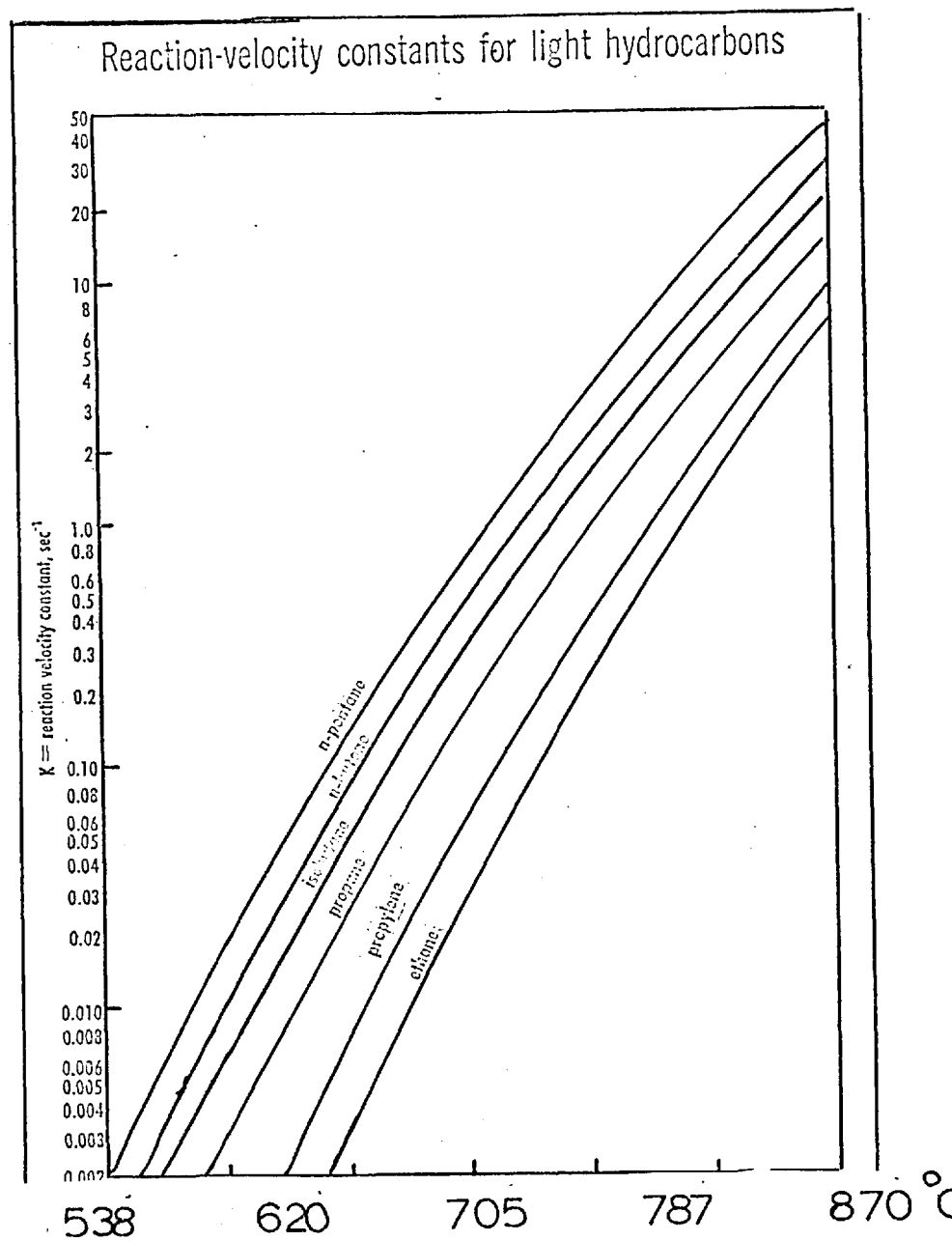
Reaction-velocity constants for light hydrocarbons
K = reaction velocity constant, sec⁻¹
50
40
30
20
10
8
6
5
4
3
2
1.0
0.8
0.6
0.5
0.4
0.3
0.2
0.10
0.08
0.06
0.05
0.04
0.03
0.02
0.010
0.008
0.006
0.005
0.004
0.003
n-pentane
n-butane
isobutane
propane
propylene
ethane
538
620
705
787
870 °C

Fig 1-1

In making cracking calculations, it is often required to solve equation 12 either for $K\Theta$ at a specific conversion or to find the conversion, α, corresponding to a speicfic $K\theta$ product. The linear semi-log graphical solution of equation 12 given in Fig. 1 - 2 is a convenience in making such computations. It is apparent from equations12 and 14 that a specified conversion of any individual hydrocarbon can be achieved by an infinite number of combinations of time and temperature. If the reactant is instantaneously heated to a constant temperature t, maintained at this temperature for time θ, the applicable reaction velocity constant can be found by equation 14 or Fig. 1 - 1, and the fraction of the reactant converted is then given by equation 12 or Fig. 1 - 2.

At any other temperature, the applicable value of K is different and a different residence time is required to effect the same conversion. Thus, if it is desired, for example, to achieve 85% conversion of normal pentane, equation 12 and Fig. 1 - 2 indicate that $K\theta$ must be 1.9. This condition will be met by any of the combinations shown in Table 1 - 2.

θ, sec	Kt, sec^{-1}	t. ^{o}C
100	0.019	594
50	0.038	630
10	0.190	660
2	0.950	715
0.5	3.800	765
0.1	19.000	832

Table 1.2

For a constant $K\theta$ product, equation 14 leads to the following relationship between time and temperature:

$$\log \quad = \quad (C/T) \quad + \quad D \qquad (15)$$

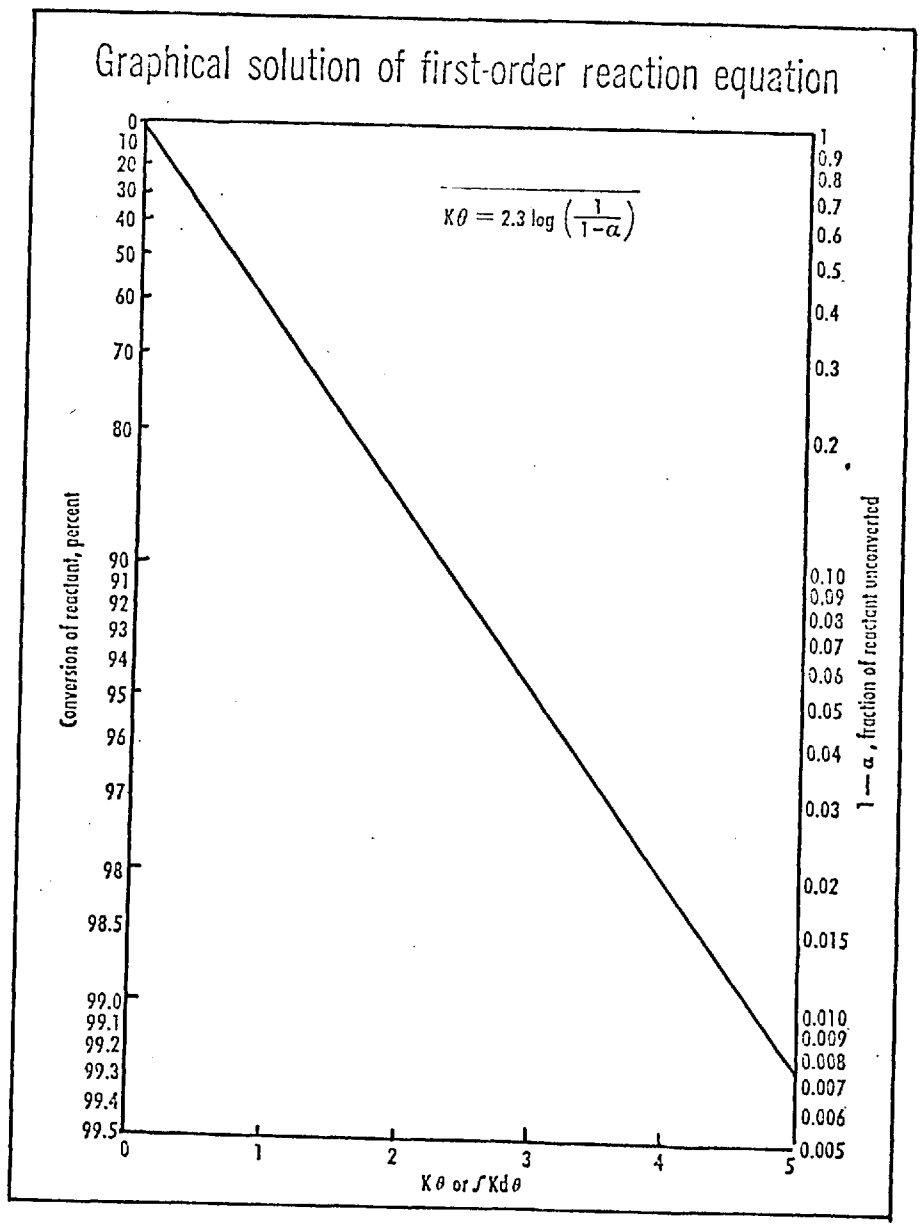
Graphical solution of first-order reaction equation
$K\theta = 2.3 \log \left(\frac{1}{1-\alpha}\right)$
Conversion of reactant, percent
0
10
20
30
40
50
60
70
80
90
91
92
93
94
95
96
97
98
98.5
99.0
99.1
99.2
99.3
99.4
99.5
1 — α, fraction of reactant unconverted
1
0.9
0.8
0.7
0.6
0.5
0.4
0.3
0.2
0.10
0.09
0.08
0.07
0.06
0.05
0.04
0.03
0.02
0.015
0.010
0.009
0.008
0.007
0.006
0.005
0
1
2
3
4
5
Kθ or ∫Kdθ

Fig 1-2

D is a constant specific to the compound being cracked and to the K product under consideration. It has the value $D = K\theta/A.$, A being the frequency factor. The reaction velocity constants plotted in Fig. 1-2 indicate, in the temperature range employed for pyrolysis in tubular reactors for olefins production, that the reactant disappearance rate doubles for each (4.5 - 13°C) increase in temperature.

In any sort of practical apparatus, it is not possible to achieve instantaneous heating of the reactant to some desired temperature and then to maintain the temperature constant for some specific length of time. Generally the temperature rises gradually up to a maximum, remains constant for a length of time and then falls. Where the isothermal region can not be identified, it becomes necessary to consider the time-temperature history of the reactant as it passes through succesive small increments of coil length in order to calculate $\int K d\theta$ for the entire coil and thereby to predict the conversion at the outlet. This brings in the concept of equivalent time - the time which, if the reactant could be raised instantaneouly to the reference temperature and held there, would effect the same conversion as achieved in the actual variable-temperature apparatus.

$$(\theta_{eq})_t = \frac{\int K d\theta}{K_t} \qquad (16)$$

where:

$(\theta_{eq})_t$ = equivalent time, sec, at reference temperature t,

K_t = reaction velocity constant at reference temperature t.

For example, if in some specific apparatus 80% conversion of n-pentane is effected, $\int K d\theta$ from fig. 1-2 is 1.6. The rate constant K, at 815°C (1500°F) is 13. Hence the equivalent time at 815°C is 1.6/13 = 0.12 sec. Usually the reactor outlet temperature is taken as the reference when comparing the performance of two reactors. If in reactor A, 80% conversion

of n-pentane is realized with outlet temperature of 760°C, the equivalent time θ_{eq} = 1.6/3.3 = 0.48 sec. In a second reactor B, if the same conversion is attained at an outlet temperature of 815°C with θ_{eq} of 0.12 sec, it can be concluded that the effective residence time in the first reactor, A, is about four times that in reactor B.

1.2.3. PREDICTING CONVERSIONS

The equivalent time, θ_{eq}, is a unique function of the reactor design. Consequently, if the coil-outlet temperature is known for one conversion level for a specific feed component, then the coil-outlet temperature can be predicted within close limits for higher or lower conversion levels. A cracking furnace designed to effect 60% conversion of ethane at a coil-outlet temperature of 827°C (1520°F) would have $\int Kd\theta$ = 0.92 (fig. 1-2) and K at 827°C is equal to 2.0 [fig. 1-1]. This means an equivalent time at the outlet temperature for this coil of 0.92/2.0 = 0.46 sec. If it is desired to operate this furnace at 50% conversion at which $\int Kd\theta$ = 0.70, then the outlet temperature must be reduced to a value corresponding to K = 0.70/0.46 = 1.52 or 817°C.

When two or more constituents are cracked simultaneously in admixture in a reactor, the time-temperature history for all constituents is identical, and the conversions of two such constituents a and b are related by:

$$\frac{\log[1/(1-\alpha_a)]}{\log[1/(1-\alpha_b)]} = \frac{\log(1-\alpha_a)}{\log(1-\alpha_b)} = \frac{K_a}{K_b} \qquad (17)$$

Considering constituent b as a reference, equation (17) may be written:

$$\log[1-\alpha_a) = -\frac{K_a}{K_b} \cdot \frac{K_b}{2.3} \qquad (18)$$

The ratio of the rate constants varies little with temperature, and for most practical purposes K_a/K_b can be considered as a constant. Equation (18), therefore, indicates that a plot of $\log(1 - \alpha_a)$ versus K_b is a straight line of slope $- K_a/2.3\ K_b$ having an intercept at $K_b = 0$ of $\log (1 - \alpha_a) = 0$ which is equivalent to $1 - \alpha_a = 1$ or $\alpha_a = 0$.

A plot of this type is represented in fig. 1.3 for a number of light feedstocks. Ethane is the reference hydrocarbon and the abscissa scale represents $\int K d\theta$ for this compound. The reaction velocity constant ratios are evaluated at (815°C) from fig. 1-1. If a mixture of ethane, propane and normal butane is to be cracked such that the conversion of propane is 80% then the corresponding conversions of ethane and butane will be approximately 43 and 96.9% respectively.

The above kinetic considerations hold well for feedstocks of up to five carbon atoms, that is, pentane. Reliable velocity-constant data for the heavier paraffins and naphthenes are meagre. Consequently it is more convenient to relate their velocity constants to that for normal pentane at the same temperature.

$$K_i = A_i e^{-Ei/RT} \qquad (19)$$

$$K_5 = A_5 e^{-E_5/RT} \qquad (20)$$

where K_i = velocity constant for any normal paraffin of carbon number greater than 5, and K_5 = velocity constant for n-pentane.

Hence $$\frac{K_i}{K_5} = \frac{A_i}{A_5} \cdot \exp\ (-E_i + E_5)/RT \qquad (21)$$

The activation energies for all normal paraffins having five or more carbon atoms can be assumed to be equal without serious error. Such assumption causes the exponential term of equation (21) to become unity, so that

$$\frac{K_i}{K_5} = \frac{A_i}{A_5} \qquad (22)$$

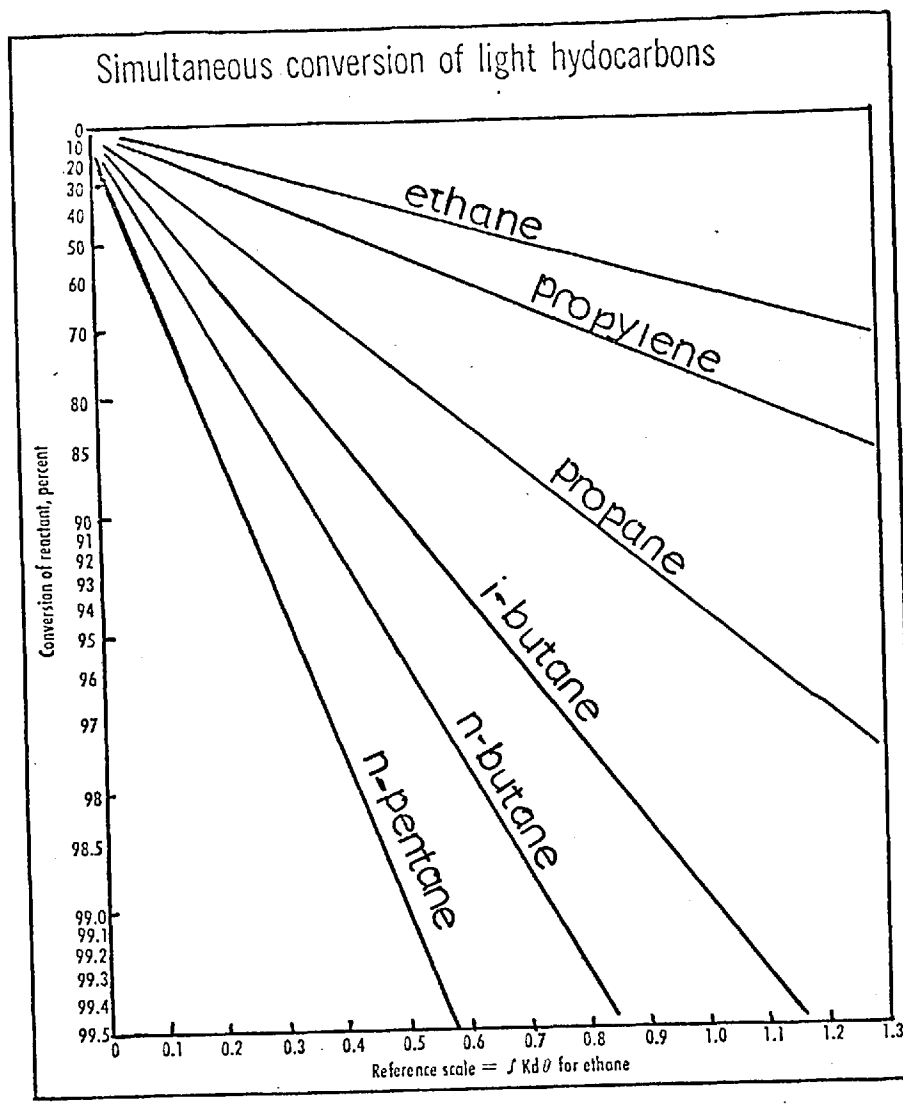
Simultaneous conversion of light hydocarbons
ethane
propylene
propane
i-butane
n-butane
n-pentane
Conversion of reactant, percent
0
10
20
30
40
50
60
70
80
85
90
91
92
93
94
95
96
97
98
98.5
99.0
99.1
99.2
99.3
99.4
99.5
0
0.1
0.2
0.3
0.4
0.5
0.6
0.7
0.8
0.9
1.0
1.1
1.2
1.3
Reference scale = ∫ Kdθ for ethane

Fig 1-3

If it now be further assumed that the frequency factor for this class of compounds is a power function of the carbon number n:

$$A = g(n)^h \tag{23}$$

where g and h are constants, then

$$\frac{A_i}{A_5} = \left(\frac{n_i}{5}\right)^h = \frac{K_i}{K_5} \tag{24}$$

This leads to:

$$\log \frac{K_i}{K_5} = h \log n_i - 0.70\,h \tag{25}$$

In 1967, Worrell et al.[14] reported first-order velocity constant for a wax consisting of 95% normal paraffins and having an average carbon number of 20.5. At 621°C, they reported a K value of 0.41 sec^{-1}. At this temperature the value for n-pentane (Fig. 1.1) is 0.050 substituting these values into equation (25) yield a value for h of 1.5, so that equation (25) can be rewritten:

$$\text{Log} \frac{K_i}{K_5} = 1.5 \log ni - 1.05 \tag{26}$$

This is the relationship used by Zdonik et al.[15] to construct curve 1 in Fig. 1-4. It seems to rationalize reasonably well the data obtained by Knaus et al[16] who reported 88% conversion of normal hexane when subjected to a temperature of 760°C for a residence time of 0.5 sec. From fig. 1.4, K_6/K_5 = 1.31. From fig 1.4, K_5 at 760°C = 3.3. Hence, K_6 = 1.31 x 3.3 = 4.37, and $K_6\theta$ = 4.37 x 0.5 = 2.19. The corresponding conversion of n-hexane from fig. 1.2. is 88.7% which is in good agreement with the reported 88%. Similar calculation for n-heptane at the same cracking condition would predict a 93.4% conversion; Knaus reported 90% conversion.

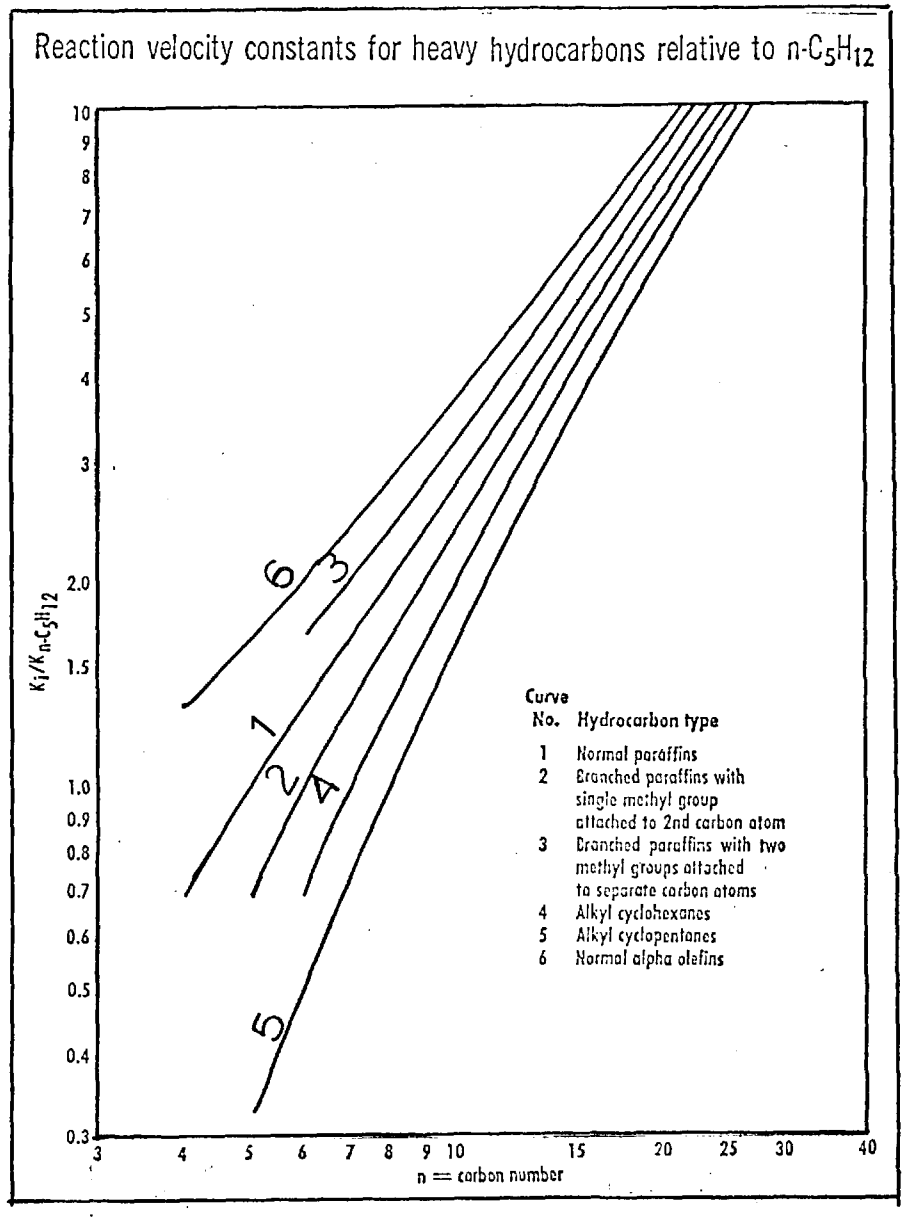
Reaction velocity constants for heavy hydrocarbons relative to n-C5H12
Kt/Kn-C5H12
10
9
8
7
6
5
4
3
2.0
1.5
1.0
0.9
0.8
0.7
0.6
0.5
0.4
0.3
3
4
5
6
7
8
9
10
15
20
25
30
40
n = carbon number
Curve No. Hydrocarbon type
1 Normal paraffins
2 Branched paraffins with single methyl group attached to 2nd carbon atom
3 Branched paraffins with two methyl groups attached to separate carbon atoms
4 Alkyl cyclohexanes
5 Alkyl cyclopentanes
6 Normal alpha olefins

Fig 1-4

Information on branched paraffins is even more sparce than for the straight chain compounds. Data for isopentane and 2-methyl hexane [17,18] indicate that the reaction velocity constant for paraffins containing a single methyl group on the second carbon is very close to that for the normal paraffin of one less carbon number; which means that the velocity constant for isopentane is almost equal to that for normal butane, and that for 2-methylpentane is similar to the value for normal pentane. This is represented by curve 2 in fig. 1-4. Such a curve tends to approach the curve for normal paraffins at high carbon numbers in accordance with the logical supposition that as the chains become longer and the differences between the two types of structure diminish, there should be a smaller percentage difference in velocity constant at any specific carbon number.

K_6/K_5 = 1.0 at 760°C for 2-methylpentane. $K_6=K_5$ = 3.3, and for a residence time of 0.5 sec, $K_6\theta$ = 1.65 ; fig. 1.2 indicates a predicted conversion of 81%. For these cracking conditions Knaus and Patton [19], reported 83% conversion which shows an excellent agreement.

Isoparaffins having two methyl side chains attached to the same carbon are more refractory than those of the same carbon number having a single methyl group for example 2,2 dimethylpropane (neopentane) [20] cracks less readily than isopentane. On the other hand, compounds having two or more side chains attached to separate carbon atoms have higher velocity constants than normal paraffins having the same number of carbon atoms. Thus 2,3 dimethylbutane [17] is pyrolyzed more readily than normal hexane. Curve 3 of fig. 1-4 has been drawn on the basis that the velocity constant for such a compound is approximately equal to that for the normal paraffin of one higher carbon number.

The naphthenic compounds, characterised by saturated ring structures containing 5 and 6 carbon atoms, are substantially more resistant to

pyrolytic decomposition than either normal or isoparaffins, especially when they are cracked in the pure state. Velocity constants calculated from cracking data for cyclopentane, methyl cyclopentane, cyclohexane, methylcyclohexane, and dimethylcyclohexanes exhibit serious inconsistencies [15]. There is little doubt however that the five-membered ring compounds are more refractory than those having six carbon atoms in the ring structure. Zdonik et al [15] did suggest that the velocity constants for alkyl cyclohexanes are approximately equal to those of normal paraffins of 2 fewer carbon numbers, and the constants for alkyl cyclopentanes are equal to those of normal paraffins of 3 fewer carbon numbers.

Aromatic compounds as a class are pyrolytically very stable. Their presence in olefin plant feed stocks makes an almost negligible contribution to the gaseous products, although some methane is produced by hydrodealkylation of xylenes to toluene and toluene to benzene, and a small amount of hydrogen is derived from dehydrogenation of ethylbenzene to styrene. The most important reactions of aromatics during pyrolysis are condensation reactions leading to the formation of polycyclic structures of high molecular weight. These are the principal constituents of the heavy-oil fraction boiling above the gasoline range and if allowed to grow to a sufficient extent, ultimately become tars and coke.

1.2.4 THE FORMATION AND CONSUMPTION OF THE OLEFINS FORMED

Olefins are products of primary reactions of paraffins and naphenes. They are degraded during secondary reaction stages. But, as yet, their reaction velocity constants are difficult to estimate. However, Rice, F.O. et al [21] and Hurd C.D. [22] established that the C-C bond located in the β position relative to the double bond of an olefin is significantly weaker than the C-C bond in paraffins, and that the C-C bond in the alpha position is substantially stronger. It could be predicted therefore that

propylene, isobutylene, and butene-2, in each of which the only C-C bonds are alpha to the double bond, would be more refractory than the corresponding paraffins, propane, isobutane, and normal butane respectively. Conversely, butene-1 and all normal alpha olefins of higher carbon number would be expected to decompose more readily than the corresponding normal paraffin.

These predictions are verified by the data of Hurd and Meinert [23], Hurd and Spence [24], Hurd and Goldsby [25] except in the case of butene-2, which appears to exhibit a higher velocity of disappearance than normal butane. This can be attributed, at least in part, to the fact that butene-2 undergoes isomerization to butene-1 during pyrolysis. As the carbon number increases, the structure of normal alpha olefins approaches more closely that of the corresponding normal paraffin, and it would appear logical to assume that the velocity constants for the two classes would approach each other. Curve 6 of fig. 1-4 has been drawn on the basis that the velocity constant for a normal alpha olefin is equal to that of a normal paraffin having two more carbon atoms than the olefin.

The initiating C-C cleavage is the principal determinant of the rate of decomposition. Consequently, if it were possible to introduce some radicals from another source into the reactant so that the chain mechanism could be initiated without the necessity for the C-C bond fracture, then the decomposition rate should be accelerated. Such acceleration of the decomposition of refractory compounds may be significant in the pyrolysis of naphthas. Kinney and Crowley [26] used dimethyl disulphide and 1,2 dichloroethane as sources of free radicals to accelerate the decompostion of propylene. An acceleration of the reaction rate by 20 to 50% was reported. Towell and Martin [27] and Davis and Williamson [28] both observed inhibition of ethane decomposition in the presence of propylene. They also noted a more significant increase in the propylene velocity constants by factors 9 to 12. These are attributable to a change in the mechanism

of propylene disappearance. In the absence of ethane, cleavage of the strong alpha C-C bond is required, the propylene molecule being split into a vinyl and a methyl radical:

$$C_3H_6 \longrightarrow C_2H_3 + CH_3 \qquad (27)$$

In the presence of pyrolyzing ethane, hydrogen atoms are present. These probably react with the propylene to form normal propyl radicals which are much more readily decomposed into ethylene and a methyl radical:

$$H + C_3H_6 \longrightarrow n\text{-}C_3H_7 \qquad (28)$$

$$n\text{-}C_3H_7 \longrightarrow C_2H_4 + CH_3 \qquad (29)$$

Thus, the disappearance rate of propylene is increased markedly, while the abstraction of hydrogen atoms from the system shortens the ethane reaction chains and results in a hindrance to ethane decompostion.

1.3 DETAILS OF PRODUCT FORMATION

Once the chain propagation radicals have been formed by the initiating C-C bond scission and by any subsequent transition reactions, the chain reactions proceed by extraction of a hydrogen atom from the reactant molecule, R_nH, to form a radical R_n having the same number of carbon atoms, n, as the reactant:

$$R + R_nH \longrightarrow RH + R_n \qquad (30)$$

The subsequent product distribution are determined by the relative probability of removal of primary, secondary and tertiary hydrogen atoms from the reactant molecule by the chain propagating radical R.. On the basis that the C-H bond for a tertiary hydrogen is weaker than a secondary hydrogen which in turn is weaker than a primary hydrogen, Rice[21] postulated that the logarithms of the relative rates vary linearly with the reciprocal of absolute temperature. These relative rates are plotted in fig. 1.5 against temperature.

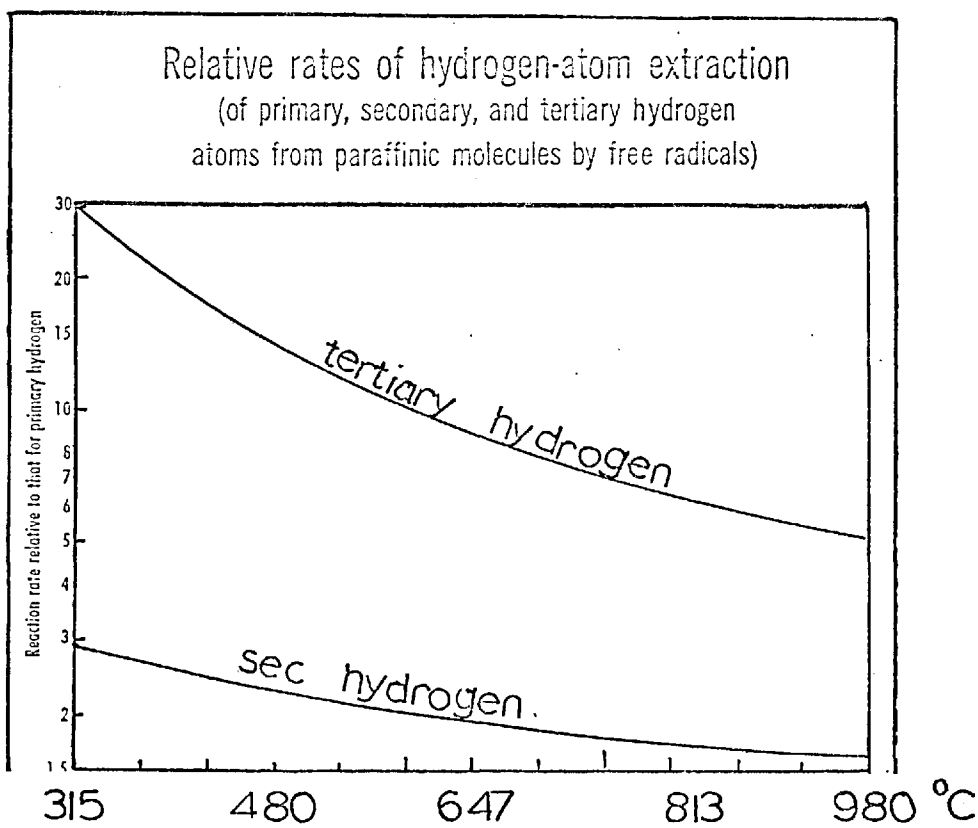
Relative rates of hydrogen-atom extraction
(of primary, secondary, and tertiary hydrogen
atoms from paraffinic molecules by free radicals)
Reaction rate relative to that for primary hydrogen
30
20
15
10
8
7
6
5
4
3
2
tertiary hydrogen
sec hydrogen
315
480
647
813
980 °C

Fig 1-5

The alkyl radical R_n then decomposes into an olefinic molecule and another radical R_1

$$R_n \longrightarrow C_m H_{2m} + R_1 \qquad (31)$$

If the radical R_1 contains two or more carbon atoms, it may either react with a feed molecule per equation 30 to produce the corresponding paraffin, or it may decompose further into another olefinic molecule and a smaller radical:

$$R_1 \longrightarrow C_m'H_{2m}' + R_2 \qquad (32)$$

The behaviour of R_1 depends on its structure as well as the conditions of temperature and pressure. Radicals of carbon number equal to and greater than 3 tend to decompose rapidly, especially at high temperature, so that very little reaction with feed molecules occurs, and the reactor effluent contains little heavy paraffin R_1H.

The radical R_2, if its $C \geq 2$, may behave in the same manner as R_1, i.e.,

$$R_2 \longrightarrow C_m''H_{2m}'' + R_3 \qquad (33)$$

In general, the alkyl radicals continue to decompose in the above manner into olefinic molecules until the remaining radical R is either a hydrogen atom or a methyl radical.

$$R_n \longrightarrow C_m H_{2m} + C_m'H_{2m}' + C_m''H_{2m}'' + \cdots + R \qquad (34)$$

The more complex products are formed as a result of secondary reactions, but the overall product distribution are dictated by:

(1) feedstock composition, (2) percentage conversion or severity level, (3) temperature level and residence time, and (4) hydrocarbon partial pressure.

1.3.1 HYDROGEN FORMATION

Molecular hydrogen is formed during pyrolysis by a two-stage process. The first stage involves the formation of a hydrogen atom. Radicals R., R_1., R_2. and R_3. in the above equations could be hydrogen atoms. Generally it is formed from processes or steps of the following type:

$$C_2H_5 \longrightarrow C_2H_4 + H \qquad (35)$$

the decomposition of isopropyl radical to form propylene, and the tertiary butyl radical to form isobutylene:

$$\begin{aligned} i\text{-}C_3H_7 &\longrightarrow C_3H_6 + H \\ i\text{-}C_4H_9 &\longrightarrow i\text{-}C_4H_8 + H \end{aligned} \qquad (36)$$

Similarly, it is formed during the primary conversion of naphthenes:

$$\text{Cyclohexyl} \longrightarrow \text{cyclohexene} + H \qquad (37)$$

Hydrogen atoms are also formed as primary decomposition products of olefins. Certain olefinic radicals decompose into a diloefin molecule and a hydrogen atom, and hydrogen atoms are generated by the reactions leading to aromatics production.

The second stage involves the abstraction of a second hydrogen from a neighbouring hydrocarbon molecule by collision. This is generally represented by the equation:

$$H + R_nH \longrightarrow H_2 + R_n \qquad (38)$$

Molecular hydrogen can also be formed by the combination of two hydrogen atoms:

$$H. + H. \longrightarrow H_2 \qquad (39)$$

But the energy liberated by this reaction is so great that unless a third body is present to absorb it, such as a hydrocarbon molecule or the wall of the reactor, the collision will not result in reaction. In addition, collisions between hydrogen atoms are relatively infrequent because of the small concentration of this species in the reaction mixture. Hence,

the percentage of the total hydrogen produced by this reaction is very small. It must be noted however that some may undergo addition reactions with olefinic molecules to generate paraffinic radicals such as:

$$H + C_3H_6 \longrightarrow n - C_3H_7 \qquad (40)$$

1.3.2. METHANE FORMATION

Formation of methyl radicals constitutes the first stage in the production of methane. They are formed by the C-C bond fracture which initiates the decompostion of paraffins and olefins:

$$C_2H_6 \longrightarrow CH_3 + CH_3 \qquad (41)$$

$$C_3H_6 \longrightarrow C_2H_3 + CH_3 \qquad (42)$$

They are also generated during the decomposition of numerous paraffinic and olefinic radicals:

$$n - C_3H_7 \longrightarrow C_2H_4 + CH_3 \qquad (43)$$

Significant quantities of methyl radicals are also produced by low-molecular-weight olefins, especially those containing no C-C bond beta to the double bond such as propylene and isobutylene.

As with hydrogen formation, the second phase of the methane-formation mechanism involves extraction of hydrogen atoms from the surrounding molcules to form methane and a radical:

$$CH_3 + C_2H_6 \longrightarrow CH_4 + C_2H_5 \qquad (44)$$

$$CH_3 + R_nH \longrightarrow CH_4 + R_n$$

A relatively small amount may be formed by the direct combination of methyl radicals and hydrogen atoms: $CH_3 + H \longrightarrow CH_4$.

Once formed, methane is apparently very stable at the temperatures normally employed in pyrolysis for olefins production and probably does not enter into further reactions. If it did, however, it would tend to be regenerated as illustrated by the following hypothetical series of reactions:

$$R_1 + CH_4 \longrightarrow R_1H + CH_3$$
$$CH_3 + R_2H \longrightarrow CH_4 + R_2 \qquad (45)$$

Consequently, with a given feedstock, the methane content of the effluent always continues to rise as cracking severity is increased.

1.3.3. ACETYLENE FORMATION

Acetylene occurs in pyrolysis effluents in relatively low concentrations at the temperatures and pressures normally employed for ethylene production. It's formation probably involves the elimination of hydrogen atoms from vinyl radicals:

$$C_2H_3 \longrightarrow C_2H_2 + H$$

It's formation is favoured by low pressures and high temperatures. In practice, the acetylene content to be expected in a pyrolysis effluent can be estimated by reference to the equilibrium constant for the molecular equation for dehydrogenation of ethylene:

$$C_2H_4 \longrightarrow C_2H_2 + H_2 \qquad (46)$$

The "partial pressure ratio", PPR (atm) for this reaction is defined by this relationship:

$$PPR = \frac{(PC_2H_2)(PH_2)}{PC_2H_4}$$
$$= \underline{P}\ \frac{(YC_2H_2)(YH_2)}{YC_2H_4} \qquad (47)$$

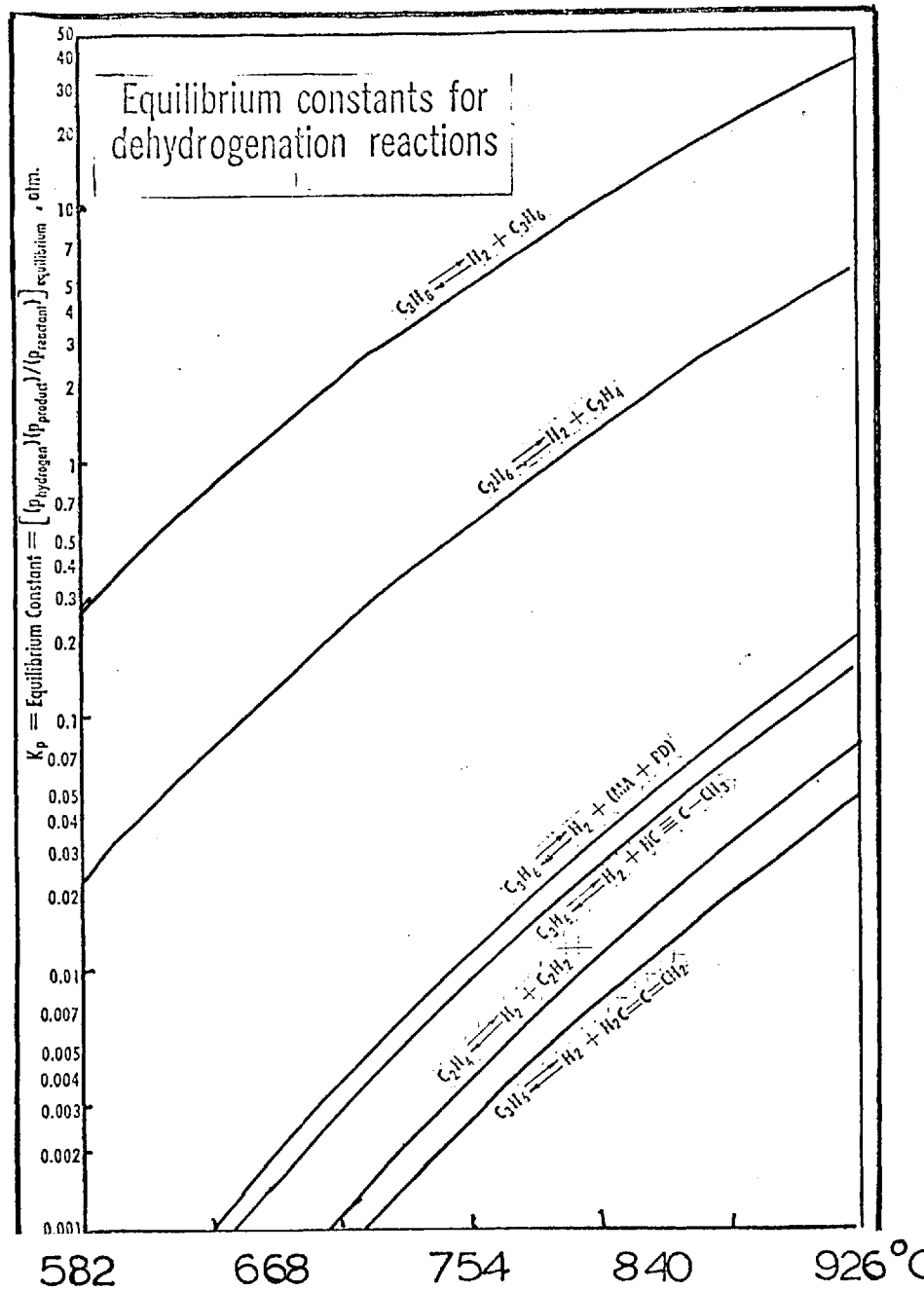
Equilibrium constants for dehydrogenation reactions
K_p = Equilibrium Constant = $\left[(p_{hydrogen})(p_{product})/(p_{reactant})\right]_{equilibrium}$, atm.
50
40
30
20
10
7
5
4
3
2
1
0.7
0.5
0.4
0.3
0.2
0.1
0.07
0.05
0.04
0.03
0.02
0.01
0.007
0.005
0.004
0.003
0.002
0.001
$C_3H_6 \rightleftharpoons H_2 + C_3H_4$
$C_2H_6 \rightleftharpoons H_2 + C_2H_4$
$C_3H_4 \rightleftharpoons H_2 + H_2C=C=CH_2$
$C_3H_4 \rightleftharpoons H_2 + HC\equiv C-CH_3$
$C_2H_4 \rightleftharpoons H_2 + C_2H_2$
$C_3H_4 \rightleftharpoons H_2 + H_2C=C=CH_2$
582
668
754
840
926°C

Fig 1-6

where: P = partial pressure of constituent, atm

$\underline{P}$ = total hydrocarbon pressure

Y = mole fraction of constituent in total hydrocarbon mixture.

Under equilibrium conditions, the PPR represents the equilibrium constant. The equilibrium constants for dehydrogenation reactions as calculated from thermodynamic data is plotted by Rosini et al[29] as a function of temperature as in fig. 1-6.

1.3.4 ETHYLENE FORMATION

Ethylene is formed during the primary pyrolysis of paraffinic and naphthenic hydrocarbons as one of the principal products from the decomposition of a large percentage of the radicals formed when hydrogen atoms are extracted from the reactant molecules, as per equation (34): For example, from normal pentane the following sequence takes place:

$$R + n - C_5H_{12} \longrightarrow RH + n - C_5H_{11}$$

$$n - C_5H_{11} \longrightarrow C_2H_4 + n - C_3H_7 \qquad (48)$$

$$n - C_3H_7 \longrightarrow C_2H_4 + CH_3$$

It can also be produced by the decomposition of ethyl radicals $C_2H_5 \longrightarrow C_2H_4 + H$, but the extent of this reaction depends upon operating conditions, being favoured by low pressure and high temperature. Similarly its formation can also occur by extraction of hydrogen atoms from hydrocarbon molecules by vinyl radicals:

$$C_2H_3 + R_nH \longrightarrow C_2H_4 + R_n \qquad (49)$$

This is an important source of ethylene during the thermal decomposition of light olefins particularly propylene. Although thermally rather stable, upon heating pure ethylene at atmospheric pressure and 815°C, Kinney and Crowley[26] reported that at 27.5% conversion, principal products were hydrogen, methane, ethane, propylene, butadiene and aromatic liquid, and

of the ethylene decomposed, about 83% by weight was converted to materials of molecular weight higher than 28.

1.3.5 ETHANE FORMATION

Ethane is produced principally by the reaction of ethyl radicals with surrounding hydrocarbon molecules:

$$C_2H_5 + R_nH \longrightarrow C_2H_6 + R_n \qquad (50)$$

The quantity of ethane produced depends primarily upon the relative amounts of ethyl radicals reacting in accordance with equation (50) to form ethane and equation (4) to form ethylene. A propensity for one reaction or the other, and hence the ethane formation tendency, is related to the temperature and pressure conditions under which the pyrolysis is being conducted. Ethyl radicals formed will react by one mechanism or the other, so that, when operating conditions encourage production of ethane, ethylene yield will tend to be reduced, and vice versa. Consequently, when the performances of alternative cracking processes are being correlated, it is often instructive to consider the yields of total C_2 constituents as well as the ethylene yields alone. The equilibrium constant for the reaction $C_2H_6 \rightarrow C_2H_4 + H_2$, was calculated by Rossini et al[29] and plotted as in fig. 1.6. The reaction $CH_3 + CH_3 \rightarrow C_2H_6$ also takes place but insignificantly, relative to abstraction reactions of methyl radicals.

1.3.6 FORMATION OF METHYLACETYLENE AND PROPADIENE

Methylacetylene and propadiene (allene) are probably produced by the loss of hydrogen atom from olefinic radicals having three carbon atoms, such as the allyl radical, in a manner similar to the formation of acetylene from vinyl radicals. Such radicals are produced during the secondary phase of pyrolysis when the primary olefinic products are undergoing decomposition.

Their concentration in pyrolysis effluents, like acetylene, is very small. Nevertheless, quantitative knowledge of their concentrations is important since facilities must be provided in the purification system for their recovery and removal.

The quantities of methylacetylene and propadiene can be predicted by consideration of 'approach to equilibrium' (PPR/equilibrium constant) of the molecular reactions for the dehydrogenation of propylene:

$$C_3H_6 \longrightarrow HC{\equiv}C-CH_3 + H_2 \qquad (51)$$

$$C_3H_6 \longrightarrow H_2C=C=CH_2 + H_2 \qquad (52)$$

The equilibrium constants for these two reactions are shown in fig. 1.6. Naphtha-pyrolysis data indicate that the total C_3H_4 content of the effluent represents an approach to equilibrium of about 0.05 - 0.10 which is the same range observed for acetylene.

1.3.7. PROPYLENE FORMATION

Propylene is one of the major products of both the primary disappearance of saturated hydrocarbons and the secondary decomposition of the resulting olefins of carbon number greater than 3. Propylene is formed during the decomposition of radicals formed from normal paraffins when a hydrogen atom is removed from the second-carbon atom. For example, 1-methylbutyl radical decomposes to a propylene molecule and an ethyl radical:

$$R + n - C_5H_{12} \longrightarrow RH + CH_3-(CH_2)_2-CH-CH_3 \qquad (53)$$

$$CH_3-(CH_2)_2-CH-CH_3 \longrightarrow C_3H_6 + C_2H_5 \qquad (54)$$

Similarly isopropyl radical from propane pyrolysis and numberous other branched paraffins, decomposes to propylene and hydrogen atom

$$i - C_3H_7 \longrightarrow C_3H_6 + H$$

Similarly, during the thermal decomposition of C_4 and higher olefins, allyl

radicals may be produced by fracture of the C-C bond beta to the double bond. These radicals are then converted to propylene by removal of a hydrogen atom from a neighbouring hydrocarbon molecule.

$$C_4H_8 - 1 \longrightarrow CH_3 + CH_2 = CH - CH_2$$

$$CH_2 = CH - CH_2 + R_nH \longrightarrow C_3H_6 + R_n \qquad (55)$$

It is thermally less stable than ethylene. It is more rapidly decomposed in the presence of ethane, and it is likely that other bimolecular reactions besides $C_3H_6 + H \rightarrow C_3H_7$, also play an important part in the disappearance of propylene in complex pyrolyzing mixtures. Addition reactions with vinyl radicals, for example, could lead to the formation of butadiene and isoprene, and reactions with diolefins are quite certainly involved in the production of aromatic compounds.

Kinney and Crowley[26] reported that the major products from propylene pyrolysis at 815°C and 9.3% conversion are hydrogen, methane, ethylene, propane, butadiene and pentadienes. Yield of aromatic liquid at this conversion level was only 4% by weight of the propylene converted, but rose rapidly to about 20% at 30% conversion and to 35% at 65% conversion. Because of the tendency of propylene to decompose at significant rates under pyrolytic conditions usually employed, as cracking severity is increased and the rate of propylene formation decreases due to depletion of the reactants from which it is formed, its yield eventually passes through a maximum, then declines as the rate of disappearance exceeds the rate of formation.

1.3.8 PROPANE FORMATION

Possible processes of formation of propane are through the reactions:

$$C_3H_7 + R_nH \longrightarrow C_3H_8 + R_n \qquad (56)$$

and $C_3H_7 + H \longrightarrow C_3H_8$ (57)

But at temperatures and pressures usually employed for ethylene production normal propyl radicals are readily decomposed to ethylene and methyl radicals and isopropyl radicals decomposed into propylene and hydrogen atoms. Consequently, propane formation by reaction (56) proceeds to a relatively small extent and the ratio of propylene to propane in the reactor effluent tends to be high for all feedstocks except those containing propane itself. Similarly reaction (57) is not quite significant. However, the propane content of pyrolysis effluents can be predicted by the equilibrium-approach concept. Calculated values for the equilibrium constant for the propane dehydrogenation equation.

$$C_3H_8 \longrightarrow C_3H_6 + H_2 \quad (58)$$

are plotted against temperature in fig. 1.6

1.3.9 C_4 FRACTION

Feedstocks containing constituents with carbon numbers of five and higher usually contain quantities of mixed C_4's, principally butenes and butadiene, in their pyrolysis effluents. Butanes are found in only very small concentration. Butenes are formed as decomposition products of aliphatic radicals formed during primary decomposition of straight chain and branched paraffins containing five or more carbon atoms. Normal paraffins yield only butene-1, while branched paraffins may produce one or more of the principal isomers, depending upon the structure of the reactant. Isobutylene is formed in substantial yield from isobutane. It is also a major decomposition product from compounds of higher carbon number having one or two methyl groups on the second carbon. Since the butenes, particularly butene-1 and butene-2, are less refractory than

propylene, they undergo decomposition even as they are being formed, and their peak concentration in the cracked products generally occurs at severities somewhat lower than those at which the propylene yield reaches its maximum.

Butene-1 and butene-2 decompose principally to H_2, CH_4, C_2H_4, C_3H_6 and aromatic liquid. Substantial isomerization of the reacting components takes place, but very little dehydrogenation to butadiene seems to occur [25] Butadiene is one of the major decomposition products from the pyrolysis of naphthenes having six carbon atoms in the ring, especially cyclohexane [31] High yields are also realized from C_5 and heavier olefins, pentene-2 is an especially prolific source of butadiene. It is relatively stable at normal cracking temperatures, being more highly refractory than the butanes. It does however enter into bimolecular reactions with the lower olefins leading to the eventual formation of aromatics. With increasing cracking severity of naphtha, concentration of butadiene in the C_4 fraction tends to increase.

1.3.10 PYROLYSIS GASOLINE

The mixture consisting of C_5's and heavier components having boiling points up to about 205°C is often designated by such terms as "pyrolysis gasoline", "cracked distillate", and "aromatic distillate". Their yield from distillate feedstocks such as naphthas and gas oils is substantial, ranging from about 15 to 35% weight of the hydrocarbon charged, the quantity depending principally upon the composition of the feed and the cracking severity. The C_5-and -heavier components appearing in the effluent from ethane, propane, and butane cracking must of necessity be essentially synthetic, being formed by condensation reactions among light molecules and free radicals existing in the pyrolyzing mixture. At high severity levels, only the most thermally stable compounds in the C_5 to C_{10} range

can exist, such as cyclopentadiene, benzene, toluene, xylenes, ethyl-benzene, styrene, and indene. The C_6 and heavier material is almost completely aromatic.[26]

1.3.11 C_6- C_8 FRACTION

This fraction is of particular interest because of its content of valuable aromatics. Aromatics are highly resistant to thermal decomposition. Hence, the aromatics contained in a feed naphtaha will issue from the reaction coil also as aromatics, although not necessarily in the same form as they existed in the feed. Some dealkylation occurs, as well as condensation to polynuclear structures of higher molecular weight. There still remains considerable uncertainty regarding the mechanism of aromatics synthesis but the weight of evidence seems to point towards condensation reactions between light olefins, such as ethylene and propylene, and diolefins such as 1,3-butadiene and isoprene. The total concentration of benzene, toluene, xylenes ethyl benzene, and styrene in the C_6- C_8 fraction from naphtha cracking is principally a function of cracking severity. Typically, the aromatics concentration is about 65-75 wt% at moderate severities and rises to over 90% wt. at the highest severities normally employed for light olefins production. At extreme severities, the concentration can be made virtually 100%.[32]

1.3.12 HEAVIER FRACTIONS - DOWN TO COKE

Coke formation is largely, the result of progressive cracking, polymerization and condensation reactions leading through naphthalene, higher polycyclic aromatics, tar to a more and more complex product of decreasing hydrogen content. The olefins resulting from the primary reactions, particularly those of higher molecular weight, polymerize readily

and in this way there are produced new compounds whose molecular weight tends to exceed that of the original stock. On prolonged exposure to high temperature or longer contact time, the polymerized material undergoes recracking with the formation of new unsaturated compounds which give rise to further polymerization.

Progressive reactions of this type, along with condensations of the ring compounds lead to the formation of more and more complex compounds of decreasing hydrogen-to-carbon ratio and with this decrease the material becomes more refractory. The final products are therefore:

(1) gaseous and low-boiling liquid compounds relatively high in hydrogen.

(2) liquid reaction products of higher molecular weight, tar and petroleum coke, possessing a very low ratio of hydrogen to carbon.

1.4 FREE-RADICAL CHAIN MECHANISM APPLIED TO SPECIFIC PARAFFINS

The Rice-Herzfeld free-radical chain mechanism has been applied by several workers to interpret the product distribution from pyrolysis of any individual paraffin at both primary and secondary levels. Some of the most significant revelations disclosed by such studies are briefly summarised:

1.4.1 PRIMARY PRODUCT DISTRIBUTION FROM NORMAL PARAFFINS

(1) Ethane produces only ethylene and hydrogen as primary products the theoretical ultimate yield of ethylene being 93% by weight. Hence ethane is an ideal feedstock in those cases where ethylene is the only olefinic product desired.

(2) The only primary products from propane and n-butane are hydrogen, and 65. to ethylene and methane. Commerical pyrolysis of propane at coil outlet temperatures of 815-845^{o}C confirm this primary distribution

when due account is taken of the secondary decomposition of primary propylene at the high conversion levels normally practised.

(4) Approximately 52% of n-butane decomposition is to propylene and methane, while the remaining 48% is converted to ethylene and hydrogen. Sandler and Chung[33] indicated 60 to 62% decomposition to propylene and methane.

(5) The calculated primary yields of both ethylene and propylene are higher from n-butane than from propane.

(6) The total primary yield of these olefins from n-butane is about 84% by weight, which is significantly higher than the 75% realised from propane. The higher olefin yields from n-butane are achieved at the expense of a correspondingly lower yield of residue gas.

(7) Propane and n-butane are outstanding feedstocks when C_3H_6 and C_2H_4 are desired as co-products with minimum production of by-products.

(8) The primary products from C_4 and heavier normal paraffins, are, in addition to hydrogen and methane, all the normal alpha olefins of carbon number up to n-1 where n is the carbon number of the feed paraffin. The C_4 and heavier olefins are produced in equimolar quantity.

(9) The calculated percent yield of primary ethylene remains remarkably constant at 46 - 49% for all n-paraffins with carbon numbers equal to or greater than 4. The yields of hydrogen, methane and propylene gradually become lower with increasing carbon number while the total yield of C_4 and heavier olefins gradually rises, reaching a value of 39% for n-decane.

1.4.2 BRANCHED PARAFFINS - PRIMARY PRODUCT DISTRIBUTION

Some of the more salient points are:

1. Branched paraffins do not follow a simple, orderly pattern with respect

to the primary products formed and their distribution.

2. They produce high yields of olefins having one less carbon atom than the reactant. Branched olefins of carbon number n-1 are always present and straight-chain isomers may also be formed.
3. The primary yield of C_3 and lighter constituents from a branched paraffin is substantially lower than from the corresponding normal paraffin. This difference becomes less with increasing carbon number, especially for the less-branched compounds.
4. The yields of H_2 plus methane and of C_4 and heavier olefins are higher. The weight ratio of primary propylene to ethylene tends to be much higher for branched paraffins than for the straight-chain counterparts. Thus, branched paraffins are desirable cracking stocks in those cases where a high propylene to ethylene ratio is desired.
5. Isobutane produces hydrogen, methane, propylene and isobutylene. Ethylene is not a primary product of isobutane, it is a secondary product derived from subsequent cracking of propylene and isobutylene.
6. Isopentane produces hydrogen, methane, ethylene, propylene, and the three major butene isomers. The yield of primary butenes is approximately 50% by weight.
7. Neopentane (2, 2-dimethylpropane) can undergo decomposition by only a single-chain mechanism into methane and isobutylene, which are the only predicted primary products. This is confirmed by the data of Frey and Hepp.[34]
8. Among the C_6 compounds, 2-methylpentane and 3-methylpentane both produce hydrogen, methane, ethylene, propylene, butenes and pentenes. Isobutylene is the only C_4 olefin produced by the former, while the latter yields both butene-1 and butene-2 but no isobutylene. Both reactants produce straight chain and branched C_5 olefins.

Because of the symmetry of the 2,3-dimethylbutane molecule, Only two reaction chains are operative. One, involving the extraction of tertiary hydrogen, leads to the formation of methane and 3-methylbutene-2. The other, wherein primary hydrogen is extracted, has two alternative routes for the R_n radical decomposition, the first producing hydrogen and propylene, and the second yielding methane and 2-methylbutene-1. No ethylene or any of the butenes is to be found among the primary products. The experimental data fo Frey and Hepp[34] confirm these predictions, except that very little 2-methylbutene-1 was found. This indicates that the R_n radical formed decomposes almost entirely to propylene and hydrogen and that the alternative route is virtually inoperative.

9. The three C_7 branched paraffins, 2-methyl hexane, 3-methylhexane and 2,3-dimethylpentane yield hydrogen, methane, ethylene, propylene butenes, pentenes and hexenes. Because of the nonsymmetrical molecular structures of these compounds, the number of reaction chains is high being 6 for 2-methylhexane and 2,3-methylpentane and 7 for 3-methylhexane.

10. Compounds with a single methyl group remote from the end of the molecule deviate more from normal paraffins than the compounds having the methyl group attached to the second carbon. Compounds with two methyl groups on different carbons show even greater deviation in behaviour from that of the normal paraffins. They tend to give high yields of branched C_{n-1} olefins.

1.4.3. PRIMARY PRODUCT DISTRIBUTION FOR NAPHTHENES

The naphthenes have not received nearly so much attention from the investigators of pyrolytic decomposition as have the paraffins. Consequently, the mechanisms of decomposition have not been well established and published

data are insufficient to permit estimation of the primary product distributions except for only three of the simpler compounds - cyclopentane, methylcyclopentane, and cyclohexane.

Rice and Murphy[35] proposed that cyclopentane decomposes by ring fracture, followed by decomposition of the resulting diradical into ethylene and a three-carbon diradical which reforms into propylene. It is possible, however, to postulate free-radical chain mechanism for the decomposition of cyclopentane which rationalize the observed product distribution. Two chains lead to the following resultant molecular equations:

$$\text{Cyclopentane} \longrightarrow H_2 + \text{cyclopentane} \qquad (59)$$

$$\text{Cyclopentane} \longrightarrow C_2H_4 + C_3H_6 \qquad (60)$$

Methylcyclopentane[35] has unsymmetrical configuration. It's decomposition is more complicated than that of cyclopentane. The chains lead to four basic overall molecular equations:

$$\text{Methylcyclopentane} \longrightarrow H_2 + \text{methylcyclopentenes} \qquad (61)$$

$$\text{Methylcyclopentane} \longrightarrow H_2 + C_2H_4 + C_4H_6 \qquad (62)$$

$$\text{Methylcyclopentane} \longrightarrow C_2H_4 + C_4H_8 \qquad (63)$$

$$\text{Methylcyclopentane} \longrightarrow 2C_3H_6 \qquad (64)$$

It is possible to describe the primary decomposition of cyclohexane[36] by three chain reactions which lead to the following molecualr equations:

$$\text{Cyclohexane} \longrightarrow H_2 + \text{cyclohexene} \qquad (65)$$

$$\text{Cyclohexane} \longrightarrow H_2 + C_2H_4 + C_4H_6 \qquad (66)$$

$$\text{Cyclohexane} \longrightarrow C_2H_4 + C_4H_8 - 1 \qquad (67)$$

One difficulty in establishing the primary products from naphthanes lies in the fact that these compounds are so highly refractory that some of the primary products are less stable than the reactant and consequently

undergo extensive decomposition in a very short time after formation. Hence, even at low conversion of the reactant, some of the constituents found may truly be secondary products.

1.4.4. PRODUCT DISTRIBUTION FROM OLEFINS AND FROM MIXTURES OF SATURATES

The decomposition of olefins has been the subject of considerable research reported in the literature; but as yet, the mechanisms involved have not been established to the extent necessary to permit confident prediction of the reaction products and their distribution.

The decomposition of ethylene is probably initiated by a bimolecular reaction such as:

$$C_2H_4 + C_2H_4 \longrightarrow C_2H_3 + C_2H_5 \qquad (68)$$

A propagation step would be:

$$C_2H_5 + C_2H_4 \longrightarrow C_2H_6 + C_2H_3 \qquad (69)$$

Rupture of the C-C bond in ethane would produce methyl radicals which would eventually become methane. Decomposition of ethyl radicals would lead to the formation of hydrogen atoms. Some of these may be converted to molecular hydrogen by extraction of another hydrogen atom from a molecule, but it seems more likely that most of the hydrogen atoms would undergo an addition reaction with ethylene to form ethyl radical: Collision of two vinyl radicals would result in the production of butadiene:

$$C_2H_3 + C_2H_3 \longrightarrow C_4H_6 \qquad (70)$$

Reaction of butadiene with ethylene or vinyl radicals would then lead to the formation of benzene with liberation of hydrogen, by a mechanism which is not yet well understood.

PROPYLENE DECOMPOSITION

Mechanisms of the thermal reaction of propylene have been proposed by many authors[37,38,39,40]. However, few mechanisms seem to account for the observed distribution at 700° to 850°C and atmospheric pressure, and Kunugi et al [41] who proposed a 48 steps-mechanism suggested that the initiation reaction must not be a reaction of propylene, but rather, a reaction of one of the products. Kunugi et al.[41] in fact claimed that at low conversion of propylene, around a few mole per cent, initiation is:

$$C_4H_8 - 1 \longrightarrow CH_3 + C_3H_5 \qquad (71)$$

$C_4H_8 - 1$ having been formed according to the following steps:

$$C_3H_6 \longrightarrow CH_3 + C_2H_3 \qquad (72)$$

$$CH_3 + C_3H_6 \longrightarrow sec - C_4H_9 \qquad (73)$$

$$sec - C_4H_9 \longrightarrow C_4H_8 - 1 + H \qquad (74)$$

There is no doubt then that the actual initiation is the rupture of a C-C bond according to equation (72). $C_4H_8 - 1$, being less refractory than propylene, would immediately decompose according to equation (71).

Ethylene and methane would be formed by extraction of hydrogen atoms from propylene by the vinyl and methyl radicals, respectively:

$$C_2H_3 + C_3H_6 \longrightarrow C_2H_4 + C_3H_5 \qquad (75)$$

$$CH_3 + C_3H_6 \longrightarrow CH_4 + C_3H_5 \qquad (76)$$

The allyl radicals thus formed are relatively stable and the principal method by which they are consumed is by polymerization reactions among themselves leading eventually to the formation of aromatic liquid and hydrogen.

The behaviour of isobutylene is similar to that of propylene, the reaction being initiated by C-C bond rupture followed by formation of methane and propylene by hydrogen extraction.

$$i - C_4H_8 \longrightarrow C_3H_5 + CH_3 \quad (71)$$

$$CH_3 + i - C_4H_8 \longrightarrow CH_4 + i - C_4H_7 \quad (72)$$

$$C_3H_5 + i - C_4H_8 \longrightarrow C_3H_6 + i - C_4H_7$$

The isobutenyl radicals formed behave similarly to the allyl radicals generated during propylene pyrolysis and upon combination lead to the formation of aromatic liquids. Since the decomposition rates of isobutylene and propylene are nearly equal, the propylene formed from isobutylene begins to decompose as soon as it is formed, and although ethylene is found in the decomposition products of isobutylene ethylene is undoubtedly a secondary product.[42]

Butene-1 and butene-2 undergo isomerization during pyrolysis[25] While it is possible to postulate a chain-reaction mechanism for butane-1 leading to formation of butadiene and hydrogen, the available data indicate that very little butadiene is formed. The mechanism of decomposition of the straight chain butenes appears, therefore, to proceed in a manner similar to those of propylene and isobutylene, with methane, propylene and aromatic liquid being prominent among the products.

PRODUCT DISTRIBUTION FROM MIXTURES OF SATURATES

The effluent composition from a specific feed constituent is affected by the presence of one or more other pyrolizable compounds, but this composition is not significantly different from that which one would calculate based on the individual yield structures at any conversion levels. This is the result one would expect based on consideration of the free-radical-chain reaction mechanisms of paraffin decomposition. The distribution of primary products from a particular compound is dependent only on:

1. The kinds of R_n radicals which are produced when radical R extracts a hydrogen atom from feed molecule R_nH, and

2. The molecules and radicals which result when the radical R_n decomposes. The kinds of R_n radicals which are formed depend only upon the structure of the reactant molecule and not upon the configuration of radical R which extracts the hydrogen atom. Consequently, it does not matter what the configuration of R is or from what source it originated. Considering the simultaneous cracking of ethane and propane, for ethane the reactions are:

$$R_1 + C_2H_6 \longrightarrow R_1H + C_2H_5 \quad (73)$$

$$C_2H_5 \longrightarrow C_2H_4 + H \quad (74)$$

For propane the following simultaneous reactions apply:

$$R_2 + C_3H_8 \longrightarrow R_2H + n\text{-}C_3H_7 \quad (75)$$

$$R_3 + C_3H_8 \longrightarrow R_3H + i\text{-}C_3H_7 \quad (76)$$

$$nC_3H_7 \longrightarrow C_2H_4 + CH_3 \quad (77)$$

$$iC_3H_7 \longrightarrow C_3H_6 + H \quad (78)$$

When ethane is cracked by itself, the radical R_1 of equation 73 is the hydrogen atom produced by equation 74, and R_1H is H_2. The primary products are thus ethylene and hydrogen.

When propane is cracked by itself, the radical R_2 of equation (75) may be either the methyl radical produced by (77) or the hydrogen atom produced by (78). It makes no difference, since the R_n radical produced by (75), $n\text{-}C_3H_7$, leads by (77) to one molecule of ethylene, and the methyl radical simultaneously formed eventually becomes a methane molecule. This comes about irrespective of whether the methyl radical became R_2 of (75) or R_3 of (76). Similarly, the radical R_3 of (76) may be either methyl or a hydrogen atom without having any effect on the product distribution.

When ethane and propane are cracked simultaneously, radical R_1 sometimes will be a hydrogen atom from (74) or from (78), and at other times may be a methyl from (77). Regardless of its kind or origin the

resulting C_2H_5. radical will produce an ethylene molecule and a hydrogen atom which later becomes a hydrogen molecule whether by (73), (75) or (76). Thus, as long as the basic mechanisms of these equations are in force, the product distribution from either of the two feed constituents is not influenced by the presence of the other.

However, at high conversion levels, where olefin concentrations become high and secondary reactions become significant, then the influence of a coreactant may be felt. In the ethane propane system, the relatively high quantity of hydrogen atoms produced by ethane decomposition will not only accelerate the decompostion of propylene derived from propane, but will also affect the products formed from it, resulting in a lower yield of aromatic liquid and a higher yield of ethylene and methane. Knaus et al [16] indicate successful prediction on the basis of the above considerations.

1.5 OTHER KINETIC CRITERIA EMPLOYED IN PYROLYSIS

1.5.1 KINETIC SEVERITY FUNCTION (KSF)

When high hydrocarbons are used as pyrolysis feed, it is convenient to use the percentage conversion of the principal reactant as an indication of cracking severity. Exceptions occur, however, when substantial yields of the constituent of interest result from the decompostion of one of the other components, and a decade ago, only the most imprecise terms were applied to such feedstocks as gas oils and distillates. These terms in some vague way were generally related to reactor-outlet temperature. Thus cracking naphtha at furnace-outlet temperature of 690° - $718^{\circ}C$ was referred to as "mild", 718° - $746^{\circ}C$ was "moderate" severity, and with any outlet temperature above $746^{\circ}C$. The term "severe" was used. The idea of using weight percent conversion to a particular product was an improvement, but neglected the important influences of feed composition

and time-temperature effects.

Zdonik et al[43] used a parameter termed "kinetic severity function" (KSF) which is defined by: $KSF = \int K_5 d\theta$ (79)

where: KSF = kinetic severity function

K_5 = reaction velocity constant for n-pentane

θ = time, sec.

This criterion has been very useful both for correlating yield data and for designing and evaluating the performance of cracking coils. Its most obovious advantage is that it recognizes and incorporates both time and temperature in a way that is consistent with the kinetics. Its most serious disadvantages are that it requires for its determination detailed knowledge of the temperature profile for the process stream flowing through the reaction coil and necessitates an integration which is best carried out on a digital computer.

When high precision analytical facilities exist to determine the normally small amount of pentane in the effluent, the KSF can be determined directly:

$$KSF = 2.3 \log (C_1/C_2) \quad (80)$$

where:

C_1 = concentration of n-pentane in feedstock, wt%

C_2 = concentration of n-pentane in effluent hydrocarbons. wt%

Cracking severity designated as "mild" is now equivalent to a KSF of about 0.6-0.8, "moderate" severity covers range of KSF = 0.8-1.5 and the "severe" cracking is approximately 1.5-2.0. Cracking furnaces being currently designed for high severity cracking of naphas and gas oils operate at values of KSF as high as 3.5.

From the definition of $KSF = \int K_5 d\theta$, and that of equivalent time $(\theta_{eq})_t = \int K d\theta / K_t$; an expression relating equivalent time referred to coil-outlet temperature and normal pentane disappearance becomes:

$$(\theta_{eq})_{cot} = \frac{\int K_5 d\theta}{(K_5)_{cot}} = \frac{KSF}{(K_5)_{cot}} \quad (81)$$

from which $KSF = (\theta_{eq})_{cot} \cdot (K_5)_{cot}$ (82)

Since the reaction velocity constant K is a function of temperature according to equation 14, the relationship between $(K_5)_{cot}$ and coil-outlet temperature may be written:

$$\log (K_5)_{cot} = B_5 - (C_5/T_{co}) \quad (83)$$

Now $\log KSF = \log (\theta_{eq})_{cot} + \log (K_5)_{cot}$

Hence $\log(KSF) = \log (\theta_{eq})_{cot} + B_5 - (C_5/T_{co})$

$$\log(KSF) = - (C_5/T_{co}) + [\log (\theta_{eq})_{cot} + B_5] \quad (84)$$

Where:

T_{co} = coil-outlet temperature

θ_{eq} = equivalent time, sec

B_5, C_5 = constants related to frequency factor and activation energy in Arrhenius equation for disappearance of n-pentane. Equation 84 indicates that, for a constant θ_{eq}, log (KSF) is proportional to the reciprocal of the absolute temperature at the coil outlet, and that for a constant T_{co}, KSF is directly porportional to equivalent time. The solution of equation (84) in terms of coil outlet temperature at several constant values of equivalent time is presented graphically in fig. 1.7.

For a specific type of feedstock being cracked at a specific pressure level, the equivalent time related to coil-outlet temperature is for practical purposes a constant whose value is a characteristic of the particular coil design. Hence determination of KSF at one coil-outlet temperature allows estimation of severity levels corresponding to other temperatures. For example, if a certain naphtha-cracking furnace has been found to effect a severity equivalent to KSF = 1.0 at 760°C , the equivalent

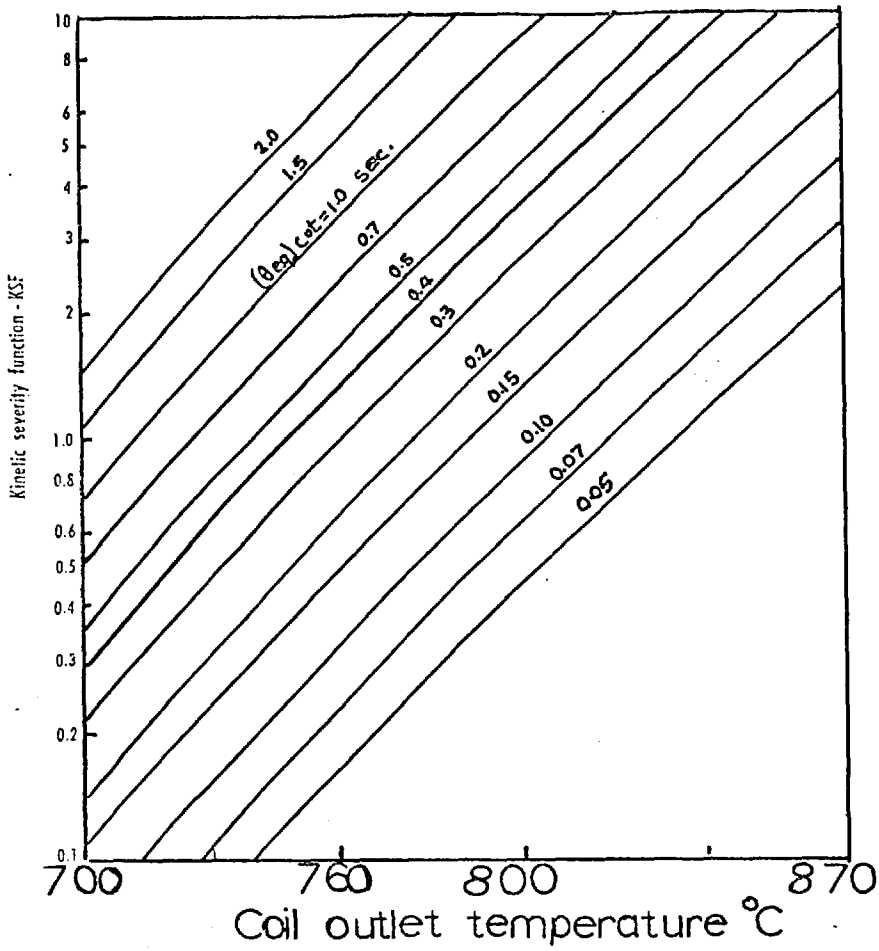

Fig 1-7 Distillate cracking—severity as function of coil-outlet temperature at constant equivalent time

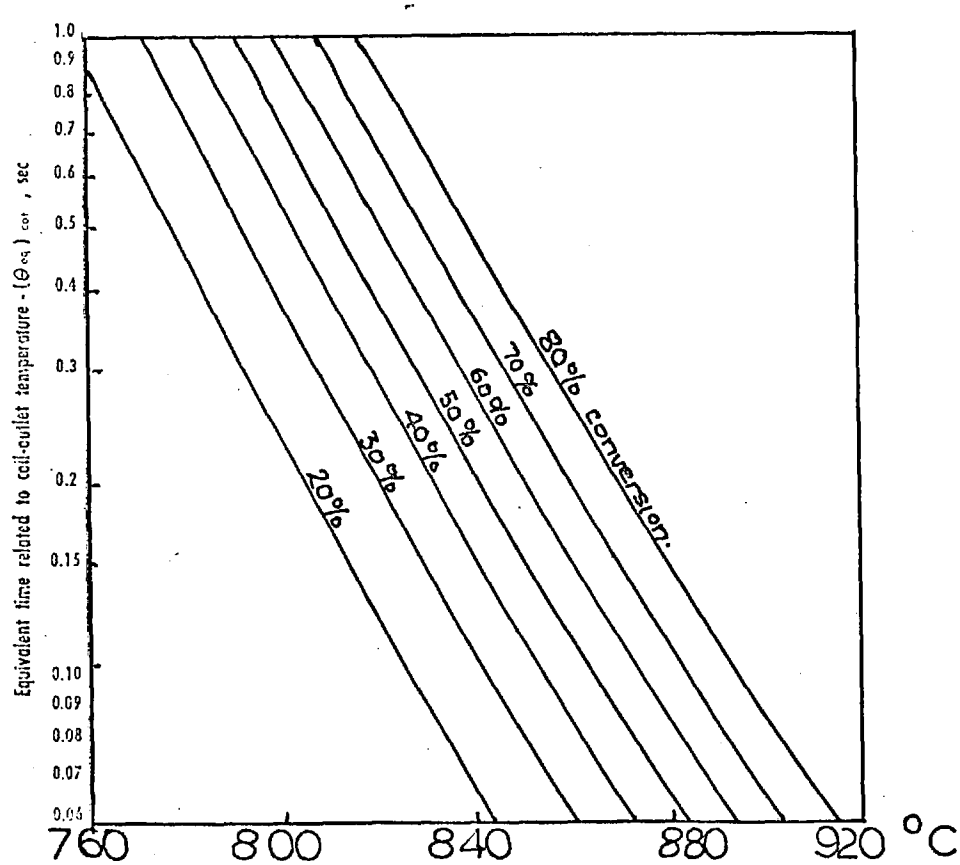

Fig 1-8 Ethane cracking—equivalent time as function of coil-outlet temperature at constant conversion

time is read from fig. 1.7 as 0.3 sec. To effect an increase in KSF to 2.0 would then require that the coil-outlet temperature be raised to about 790°C.

In gas cracking, conversion of a key feed constituent is the normal criterion of severity rather than $\int K_t d\theta$. A convenient form of graphical representation of the time-temperature-severity relationship is a plot of the logarithm of equivalent time against coil-outlet temperature with lines of constant conversion. Fig. 1.8 represents such a plot for ethane cracking.

It is apparent from this procedure that it is feasible to design a furnace whose radiant coil is suitable for cracking a wide variety of feedstocks at appropriate severities and coil outlet temperatures. It should be noted however, that when two different feedstocks are cocracked simultaneously in the same coil, the equivalent times are equal since the two materials are being cracked in accordance with a single time-temperature profile. Irrespective of the type of plot used to relate product distribution to severity, to be meaningful, the corresponding operating conditions must be specified, particularly those which have a bearing on the hydrocarbon partial pressure and the residence time.

1.4 DISTRIBUTION FOR DISTILLATES

Zdonik et al [44] showed qualitatively how the distribution of the major products from cracking a typical naphtha in a tubular reactor varies with severity expressed as KSF. Flow rates of hydrocarbon and dilution steam at constant coil-outlet pressure are assumed, such that the hydrocarbon partial pressure at the coil-outlet is approximately constant at the moderate and high severity levels where this variable is important. Similarly the equivalent time is constant. This qualitative profile is as shown in fig. 1.9.

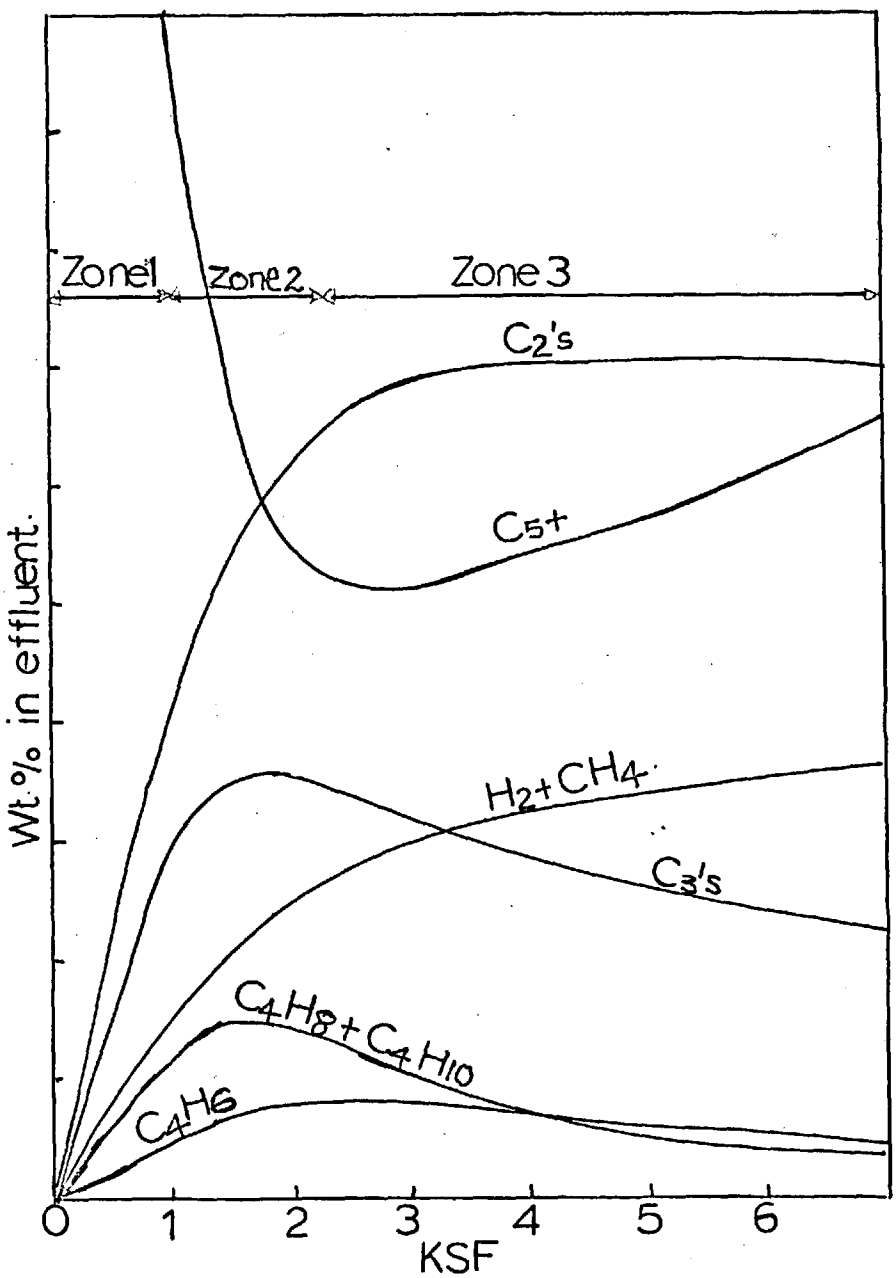

Fig1-9 Naphtha cracking—typical variation of product distribution with severity

The severity diagram can be divided into three zones. In zone 1, the zone of low severity up to a KSF of about 1, the principal reactions in progress are those involving the primary disappearance of the saturates in the feedstock. In zone 2, secondary reactions are becoming dominant. Primary reactions still continue as indicated by the still rapid decrease in C_{5+} constituents. This zone extends up to a KSF of about 2 - 2.5. Yields of hydrogen, methane, total C_2's, and butadiene continue to to increase rapidly, even though at a gradually diminishing rate. The concentrations of propylene and butylenes pass through maxima as their rates of formation is overtaken by their rates of disappearance.

In zone 3, the primary reactions have virtually ceased, and all further changes are due to secondary reactions. The C_5+ passes through a minimum as the original saturates become exhausted, and the formation of stable aromatics from the degradation of propylene and C_4's adds to the C_5+ yields as the severity is increased. Hydrogen and methane continue to rise, but the C_2's and butadiene curves eventually pass through maxima. Butadiene yield typically peaks at a KSF of about 2.5, while the C_2's pass through a broad maximum at about KSF = 5 as the rate of ethylene degradation finally reaches and then surpasses its rate of formation from the higher olefins.

1.5.2 EQUILIBRIUM CONSIDERATIONS

The reactions encountered in pyrolysis can be classified into three types:

Type I : $a \rightarrow b + c$ (85)

Type II : $d + f \rightarrow g + h$ (86)

Type III : $q + r \rightarrow s$ (87)

The equilibrium constants for these reactions in terms of the partial pressures in atmospheres of the reactants and products at equilibrium are given by the expressions:

$$(K_p)_I = [(P_b)(P_c)/(P_a)]_{equil} \quad (88)$$

$$(K_p)_{II} = \frac{(P_g)(P_h)}{(P_d)(P_f)}_{equil} \quad (89)$$

$$(K_p)_{III} = \frac{[p_s]}{[(P_q)(P_r)]}_{equil} \quad (90)$$

The kinetic significance of the equilibrium constant is that it equals the ratio of the forward reaction velocity to the velocity in the reverse direction.

$$K_p = K/K' \quad (91)$$

The equilibrium constant varies with temperature in accordance with the Vant Hoff equation:

$$\frac{d\ln K_p}{dT} = \frac{\Delta H}{RT^2} \quad (92)$$

where: H = heat of reaction, KJ/mole.

R = gas constant = 8.31 J/mole ^{o}K.

The integrated form of equation (92) assuming ΔH to be constant over the temperature interval of interest is:

$$\log K_p = -\frac{\Delta H}{2.3RT} + \text{const.} \quad (93)$$

It is apparent that for endothermic reactions, which absorb heat (ΔH + ve), K_p increases with rising temperature as the term $\Delta H/2.3RT$ becomes a smaller negative number. Conversely, for exothermic reactions K_p becomes smaller as the temperature is increased. Thus, increase in temperature favours the formation of products from endothermic reactions.

TYPE I REACTIONS

Such reactions are highly endothermic and most of the olefinic products formed during pyrolysis result from reactions of this type.

REACTIONS	ΔH (827°C)
$C_2H_6 \longrightarrow H_2 + C_2H_4$	+ 145.4 KJ
$C_3H_8 \longrightarrow H_2 + C_3H_6$	130 "
$C_3H_8 \longrightarrow CH_4 + C_2H_4$	77.8 "
$n\text{-}C_4H_{10} \longrightarrow C_2H_4 + C_2H_6$	88.3 "
$n\text{-}C_4H_{10} \longrightarrow H_2 + {}_2C_2H_4$	233.4 "
$n\text{-}C_4H_{10} \longrightarrow CH_4 + C_3H_6$	65.7 "

This is graphically illustrated in Fig. 1.6

These molecular equations merely represent the overall result of what is actually achieved through a series of free radical reactions. For example the decomposition of $n\text{-}C_4H_{10}$ to hydrogen and ethylene is a result of a chain mechanism involving two consecutive reactions:

$$H + n\text{-}C_4H_{10} \longrightarrow H_2 + {}_n\text{-}C_4H_9$$

$$n\text{-}C_4H_9 \longrightarrow C_2H_4 + C_2H_5 \qquad (94)$$

$$C_2H_5 \longrightarrow C_2H_4 + H$$

TYPE II REACTIONS

Bimolecular reactions of Type II are usually exothermic, thermaly neutral, or only slightly endothermic, and are typical of those by which hydrogen is extracted from saturated reactant during primary decomposition:

$$R_1 + R_nH \longrightarrow R_1H + R_n \qquad (95)$$

Any reaction of this type is characterised by a heat of reaction of virtually zero since one carbon-hydrogen bond is broken to satisfy formation of another except when R_1 is a hydrogen atom, in which case the reaction is slightly exothermic. The equilibrium constants for these reactions is therefore practically independent of temperature.

Reactions leading to the formation of aromatics are undoubtedly bimolecular. Although the mechanism is not firmly established, it is possible to write reactions which probably represent reasonably the overall result, for example,

$$C_2H_4 + C_4H_6 \rightarrow C_6H_6 + 2H_2 \qquad (95)$$

for which the heat of reaction in the vapour phase at 827°C is -547.6 KJ/mole. In view of the highly exothermic nature of this reaction, increasing temperature would be expected to shift the equilibrium away from aromatics formation. But the equilibrium constant for this reaction is high (875 KJ/g - mole). Hence the determining factor with respect to propensity toward aromatics formation would appear to be reaction rate rather than equilibrium considerations.

(a) EQUILIBRIUM APPROACH

If the term "partial pressure ratio" for a reaction of Type I be defined as:

$$(PPR)_I = (P_b)(P_c) / (P_a), \qquad (96)$$

where the partial pressures of reactant and products are those actually existing in the reacting system, then the equilibrium approach (EA) is defined as:

$$(EA)_I = (PPR)_I / (K_p)_I \qquad (97)$$

This represents a relationship between the partial pressures actually existing and those which would prevail under conditions of equilibrium.

At the onset of decomposition (PPR) is zero and EA is also zero. As the reaction proceeds, the partial pressure of the reactant falls and the partial pressures of products become greater, the value of (PPR) rises, as does the value of (EA). At some conversion level, (PPR) = K_p and EA becomes unity. Conversely by starting with a mixture of product constituents the equilibrium approach would start at infinity tending to unity as reactant was formed and products depleted.

COMPETING REACTIONS

While equilibrium treatment show how increasing temperature affects the rate of the forward reaction relative to the reverse rate for each of the three types of reaction, no conclusions can be drawn from these relationships as to how the increase in rate of forward reaction for one type compares with that for another type.

It is known that the heat of reaction is equal to the difference between the activation energies of the forward and reverse reactions:

$$\Delta H = E - E' \qquad (98)$$

The activation energy, E, is a measure of the rate of change of the velocity constant with temperature in the same way that ΔH is a measure of the rate of change of equilibrium constant with temperature.

$$\text{Log } K = \log A - \frac{E}{2.3\ RT} \qquad (99)$$

It has been demonstrated by experiment that activation energies for monomolecular reactions as exemplified by Type I, are substantially higher than those for bimolecular reactions of Types II and III. Type I reactions generally will exhibit much higher temperature coefficients of reaction velocity than reactions of the other two categories.

In support of this, Rice and Herzfeld[2] considered the two reactions of ethyl radical:

$$C_2H_5 \longrightarrow C_2H_4 + H, \quad \text{and}$$

$$C_2H_5 + R_nH \longrightarrow C_2H_6 + R_n$$

The first is a highly exothermic monomolecular reaction of Type I characterised by a high activation energy and a high temperature coefficient of velocity. The value of ΔH was 164 KJ/mole and that of E of approximately 206 KJ/mole.

In contrast, the authors estimated, for the second reaction, a ΔH equal to zero and an activation energy E of 84.2 KJ/mole. Thus the second reaction has a significantly lower temperature velocity coefficient which means that the rate of decomposition of ethyl radicals to ethylene and hydrogen atoms is enhanced at increasing temperatures with respect to that of the competing reaction leading to the formation of ethane.

(b) EFFECT OF HYDROCARBON PARTIAL PRESSURE

The partial pressure of the hydrocarbons in a pyrolyzing mixture affects chemical equilibria and reaction rates, and thereby influences the product distribution. For monomolecular reactions of Type I defined by equation 85.

$$a \longrightarrow b + c \qquad (85)$$

the equilibrium constant is given by:

$$(K_p)_I = [(P_b)(P_c) / (P_a)] \text{ equil} \qquad (88)$$

But the partial pressure of any constituent i in the pyrolyzing mixture is:

$$P_i = Y_i P \qquad (100)$$

the equilbrium constant in terms of concentrations is given by:

$$(K_p)_I = P[(Y_b)(Y_c) / (Y_a)] \text{ equil} \qquad (111)$$

where:

$\underline{P}$ = total pressure of hydrocarbons, atm.

Y = mole fraction of constituent in mixture

$$\text{Hence } (Y_c)_{\text{equil}} = \frac{(K_p)_I \quad Y_a}{\underline{P} \quad x \quad Y_b} , \tag{112}$$

and this leads to the important conclusion that the equilibrium concentration of olefin product corresponding to any specific concentraions of reactant and saturated product is inversely proportional to total hydrocarbon partial pressure:

If the term "mole fraction ratio" is defined as:

$$(MFR)_I = \frac{(Y_b)(Y_c)}{Y_a} \tag{113}$$

taking into account equations (96) and (97), the expression for partial pressure ratio becomes

$$(PPR)_I = \underline{P}(MFR)_I \tag{114}$$

and the equilibrium approach also becomes:

$$(EA)_I = \underline{P} \frac{(MFR)_I}{(K_p)_I} \tag{115}$$

Thus for specific concentrations of reactant and products at a specific temperature, the equilibrium approach is directly proportional to hydrocarbon partial pressure.

Similar consideration of bimolecular reactions of Type II as defined by equation (86).

$$d + f \rightleftharpoons g + h \tag{86}$$

indicates that the equilibrium is unaffected by the total hydrocarbon pressure, the partial mole fraction being identical, and the equilibrium approach is given by:

$$(EA)_{II} = \frac{(MFR)_{II}}{(K_p)_{II}} \qquad (116)$$

For bimolecular reactions of Type III:

$$q + r \longrightarrow s \qquad (87)$$

the approach to equilibrium is inversely proportional to hydrocarbon pressure:

$$(EA)_{III} = \frac{(MFR)_{III}}{\underline{P}(K_p)_{III}} \qquad (117)$$

For reactions of this type then, high hydrocarbon pressures result in low approach to equilibrium and an increased tendency to produce the condensation product. Low hydrocarbon pressures favour progress of equation 87 from right to left discouraging the formation of by-products by condensation reactions between radicals.

For reactions of Type I, the fractional disappearance of reactant concentration or partial pressure. This is apparent from the differential form of the first order equation:

$$-\frac{dC}{C} = Kd\theta \qquad (118)$$

which may be written :

$$\frac{-dC/C}{d\theta} = K \qquad (119)$$

where: C = concentration of reactant

K = first-order velocity constant, sec^{-1}.

Thus, reactions such as:

$$\begin{aligned} C_2H_6 &\longrightarrow CH_3 + CH_3 \\ C_3H_6 &\longrightarrow CH_3 + C_2H_3 \\ n\text{-}C_4H_{10} &\longrightarrow C_2H_5 + C_2H_5 \end{aligned} \qquad (120)$$

the rates of fractional disappearance of reactant species which are dependent upon first order initiating reactions, are independent of partial pressure.

On the other hand, the biomlecular reactions of Types II and III which lead to chain interruptions and production of by-products are of second-order. For such reactions, the fractional disappearance per unit time is directly proportional to the existing reactant concentration:

$$\frac{-dC}{C^2} = K_{II} d\theta \qquad (121)$$

which may be rewritten:

$$\frac{-dC/C}{d\theta} = C. K_{II} \qquad (122)$$

where K_{II} = second order velocity constant (conc) $^{-1}$sec^{-1}. Reducing hydrocarbon partial pressure, therefore, decreases the velocity of the bimolecular reactions, the effects on product distribution being similar to those resulting from increased temperature level and shorter residence time.

Reaction of radicals with reactant molecules to form saturates of the same carbon number as the radical is discouraged in favour of decomposition of the radical to olefin and a radical of lower carbon number. In addition, interruption of free radical chain mechanisms by Type III reactions between radicals, becomes less frequent, so that the reactant decomposes more selectively to the desired olefins with less formation of undesired by-products.

The net effect of the free radical chain mechanism of decomposition of ethane to ethylene and hydrogen can be expressed by the molecular dehydrogenation equation.

$$C_2H_6 \longrightarrow H_2 + C_2H_4 \qquad (123)$$

If the chain mechanism were not interrupted, and if none of the ethylene formed were itself pyrolyzed, then the reactor effluent would contain

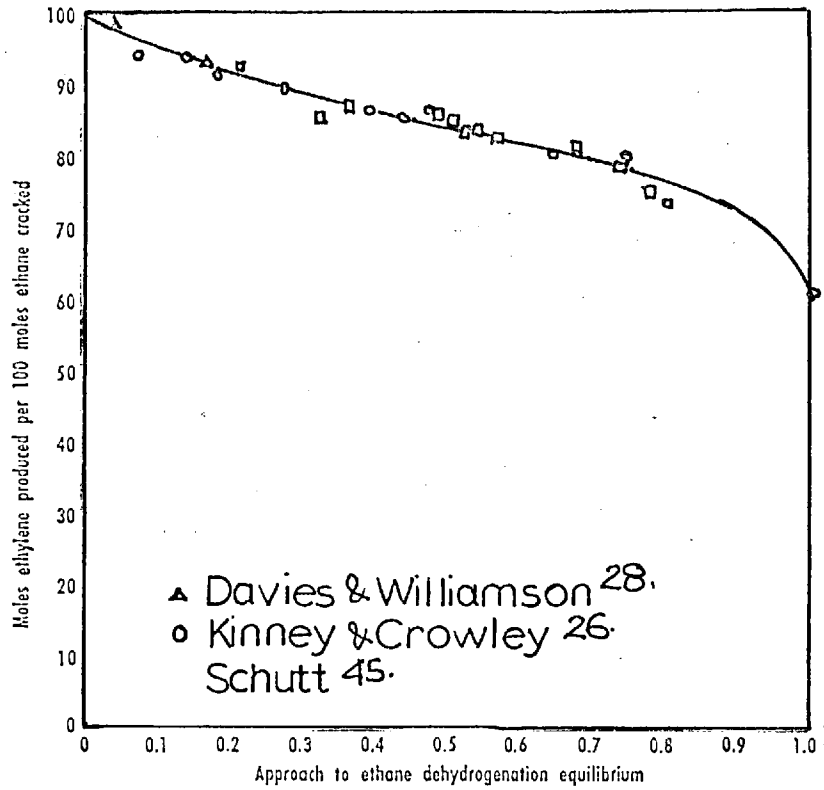

Fig 1-3 Equilibrium approach correlation

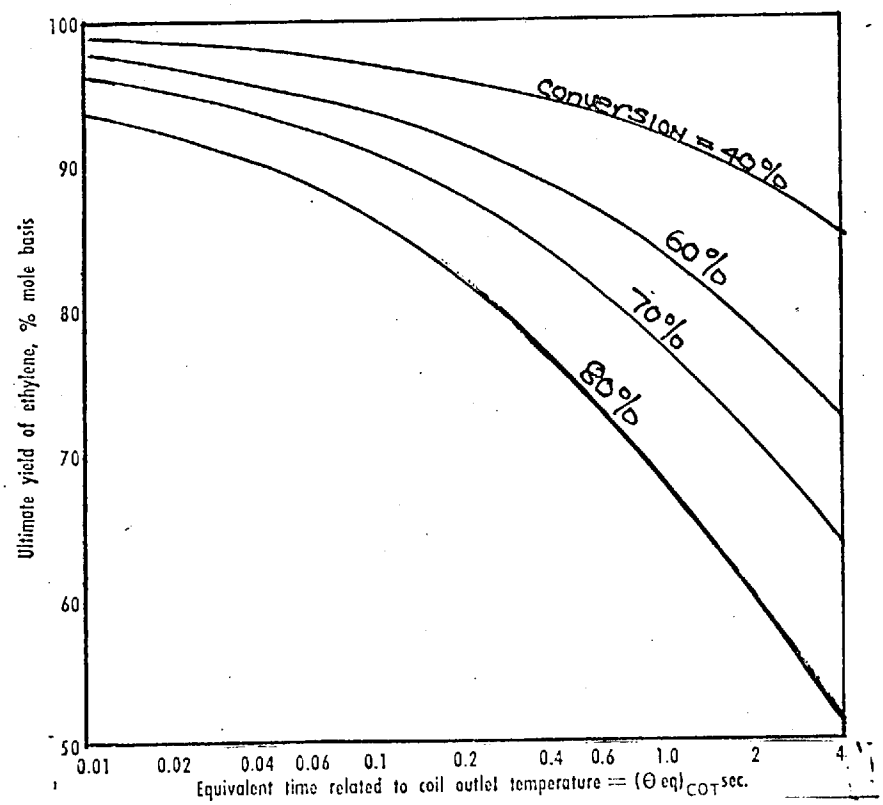

Fig 1-10 Effect of reaction time and conversion on ultimate yield of ethylene

one mole of ethylene and one mole of hydrogen for each mole of ethane decomposed. In practice however, ethylene yield is less than one mole because the chains are interrupted and ethylene itself is degraded. It was left to Schutt[45] to show that the ultimate molal yield of ethylene realized in commercial pyrolysis furnaces becomes farther removed from unity with increasing approach to equilibrium of reaction.(123)

$$EA = \frac{(P_{H_2})(P_{C_2H_4})}{K_p (P_{C_2H_6})} = P \cdot \frac{(Y_{H_2})(Y_{C_2H_4})}{K_p (Y_{C_2H_6})} \qquad (124)$$

The ultimate yield of ethylene appears to be a virtually unique function of approach to this equilibrium at reactor outlet conditions as indicated by the correlation based on the commercial data of Schutt[45] and the bench-scale data of Kinney and Crowley[26] and of Davis and Williamson[28] This is shown in fig. 1-13.

(c) ULTIMATE YIELD EQUATION

The mole fraction ratio MFR is a function of conversion and yield

$$EA = \frac{P(MFR)}{K_p}$$

$$= \frac{P[f(X, Y)]}{K_p} \qquad (125)$$

The three major variables which determine yield are incorporated into this approximate equation.

$$Y = 1 + \frac{1}{\frac{0.30\ P\ [\ \phi(X)]}{K_p}} \qquad (126)$$

where:

Y = ultimate yield of ethylene, moles of ethylene produced per mole ethane disappearance.

P = hydrocarbon partial pressure, atm

$$\phi(X) = \frac{X^2}{1- X^2}$$

X = fractional conversion of ethane

K_p = equilibrium constant ethane dehydrogenation reaction, atm.

The degree to which each of these three variables affects the yield as calculated by equation 126, based on the data of Schutt[45] is shown by plots presented in figs. 1-10, 1-11, 1-12.

It can thus be seen that high yield of ethylene or indeed any other component of reference is enhanced by:

1. Low hydrocarbon partial pressure
2. Low conversion corresponding to low value of $\phi(X)$.
3. High temperature-short time corresponding to high value of K_p.

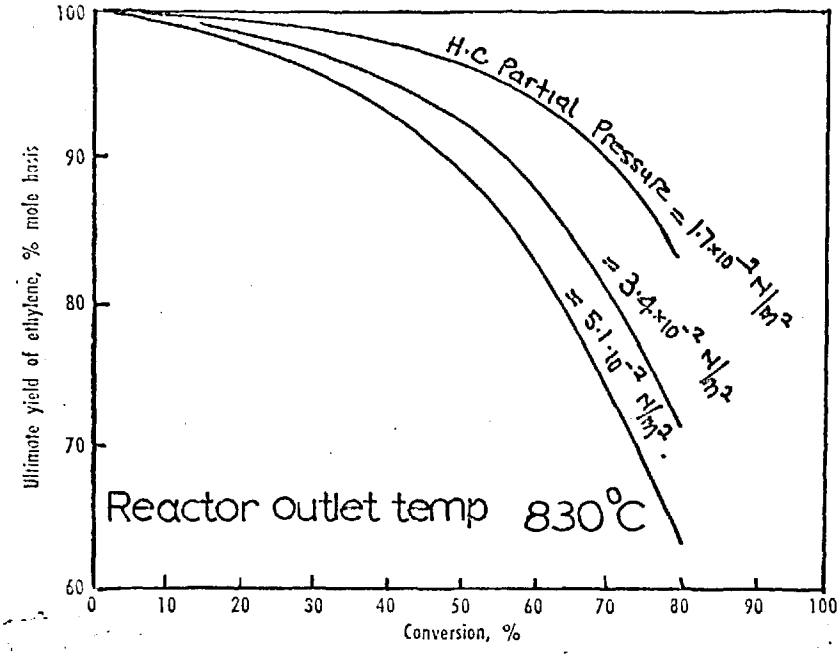

Fig1-11 Effect of conversion and hydrocarbon partial pressure on ultimate yield of ethylene

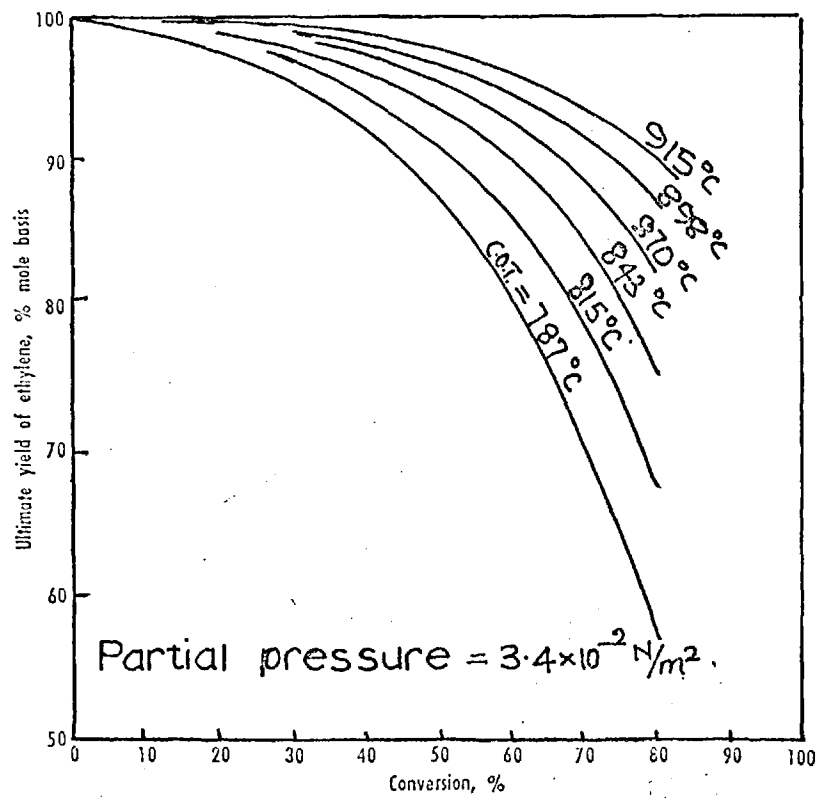

Fig1-12 Effect of conversion and reactor outlet temperature on ultimate yield of ethylene

COMBUSTION OF HYDROCARBONS

1.6.1 GENERAL INTRODUCTION ON OXIDATION

Organic oxidations can be divided roughly into low-temperature and high-temperature regimes, and most of the work reported so far have dealt with the low temperature regime. It is intended here to discuss the changes that occur in the behaviour of the involved radicals and this the changes in mechanism as the temperature increases.

The early theories concerning the mechanism of oxidation processes involving radicals were non-chain schemes such as the Hydroxylation[46] and Peroxidation[47] schemes. Although these theories successfully predicted the end products, they were unable to account for the autocatalytic nature of the reactions, the effect of inert gases, the nature of the vessel surface, and sensitisation or inhibition by small quantities of impurities. It soon became clear that these characteristics could only be explained on the basis of a chain process, a concept originally introduced by Bodenstein[48] and established by the work of Christiansen[49]. The theory of chain reactions was mathematically developed by Semenov who suggested the branched chain[50] and degenerately branced chain reactions[51]. The original hydroxylation and peroxidation theories were being gradually amalgamated to some extent in free radical chain mechanisms[52] until, in 1965, the position was summarised by Knox[53] as shown below.

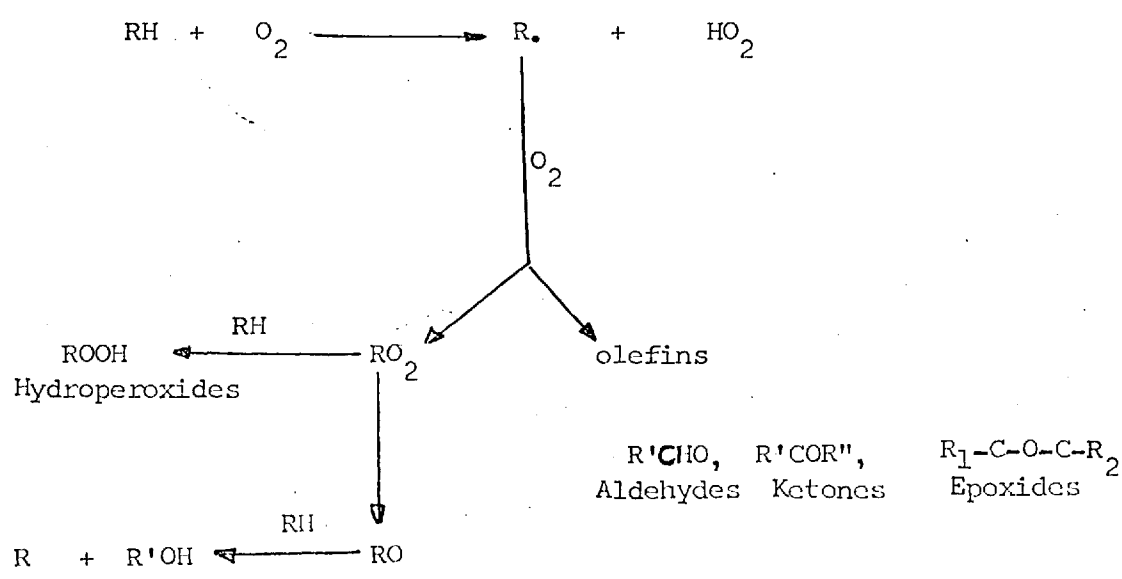

The reaction path and hence the product distribution is highly dependent on temperature. The detailed discussion of this reaction mechanism and the inferences that can be made from it, may best be initiated from consideration of the theory of chain reactions and of the chemistry of the individual free radicals involved in the combustion processes. Branching and degenerate branching chain reactions which are peculiar to oxidation as distinct from pyrolysis of pure hydrocarbons will be discussed first.

1.6.2 BRANCING CHAIN REACTIONS

If in a system, an active centre can produce more than one new centre, and these can initiate chain reactions in their own right, then the system is said to have branched. Generally, branching occurs either when a simple mono-radical reacts with a species containing a double bond or when a bi-radical reacts with a saturated molecule. Good examples are the branching reactions involved in the oxidation of hydrogen.

$$H\cdot + O_2 \longrightarrow \cdot OH + O\cdot$$

$$O\cdot + H_2 \longrightarrow \cdot OH + H\cdot$$

Since each hydrogen and oxygen atom produces two free radicals capable of initiating chain reactions like:

$$OH + H_2 \longrightarrow H_2O + H,$$

The system has a branched-chain mechanism.

If β is the probability of rupture of an unbranched chain at a particular link and δ is the probability of branching in a chain, then $\beta-\delta$ is the probability of a branched chain rupture. Representing the average chain length as ν (defined as the reaction rate divided by the rate of initiation of chain centres per unit volume), then the total length ν' of the branced chain can be represented as:

$$\nu' = \frac{1}{\beta-\delta} = \frac{\nu}{1-\nu\delta}$$

The rate of reaction W is then given as:

$$W = no\nu' = \frac{no\nu}{1-\nu\delta}$$

in which no is the number of primary reactions taking place in unit time due to thermal activation.

In the case of continuously branched chains,

$$\delta = 1-\beta$$
$$= \alpha$$

where α is the probability of production of a new active centre by a given centre at the beginning of the reaction.

Hence $$\nu' = \frac{1}{\beta-\delta} = \frac{1}{2\beta - 1}$$

The overall course of a branched chain can be represented by the differential equation:

$$\frac{dn}{dt} = n_o + (f - g)n$$

where: f is the coefficient for gas phase branching equal to $\delta/\Delta\tau$, and g is the coefficient of linear termination in the gas phase.

This equation can be integrated to give

$$n = \frac{no}{f - g} [\exp (f - g)t - 1]$$

which is also equivalent to:

$$W = \frac{n}{\Delta\tau} = \frac{no}{(f - g)} \frac{1}{\Delta\tau} [\exp(f - g)t - 1]$$

which is also equivalent to

$$W = \frac{n}{\Delta\tau} = \frac{no}{\delta - \beta} [\exp \frac{(\delta - \beta)t}{\Delta\tau} - 1]$$

$(f - g)$ is called the net branching factor and is usually represented as ϕ

Hence

$$W = \frac{n}{\Delta\tau} = \frac{no}{\phi\Delta\tau} (\exp \phi t - 1)$$

and $\emptyset$ is also equal to $\frac{\delta - \beta}{\Delta\tau}$

Representing the rate of reaction as $W = Ae^{\emptyset t}$, in which A would be equal to $\frac{no}{\emptyset\Delta\tau}$ or $\frac{no}{\delta - \beta}$; and considering the situation where

$\delta - \beta > 0$ ($\emptyset > 0$), the rate of reaction can be rewritten as

$$W = \frac{no}{\emptyset\Delta\tau} \cdot \exp(\emptyset t)$$

Under this situation, there will be continuous acceleration of the reaction which can lead to explosion for long reaction times.

On the other hand if $\emptyset < 0$, the rate of branching would be less than the rate of termination reactions, and hence no acceleration of reactions would be observed, and no explosion would take place.

The rates of branching and termination are proportional to the concentrations of atoms and free radicals formed since both branching and termination can involve radical-radical interactions or radical-intermediate product interactions[54].

Two types of chain interactions have been identified: (a) positive chain interaction in which the active and inactive radicals react with each other to produce two active centres leading to a very rapid reaction. Thus in the oxidation of hydrogen, the termination reaction,

$H\cdot + O_2 + M \longrightarrow HO_2\cdot + M$, where $HO_2\cdot$ is relatively inactive, competes with the reaction:

$H\cdot + HO_2\cdot \longrightarrow 2.OH + 376$ K Joules

The OH. radicals react with hydrogen to form hydrogen atoms which will propagate, thus leading to the rapid acceleration of the reaction.

$OH\cdot + H_2 \longrightarrow H_2O + H\cdot$

(b) Negative chain interaction, in which the radical loss occurs by combination, means that at low pressures the rate is not comparable with the termination rate either in the gas phase or at the wall, but at higher

pressures the branching would be so rapid that the gas is being heated and the chain explosion is reduced to a thermal chain.

1.6.3 DEGENERATE BRANCHING CHAIN REACTIONS

In general then, the rate of a branched reaction can be expressed by an equation of the form:

$$W = A \exp \phi t$$

where W is the rate of the reaction, ϕ is the net branching factor, A is a constant and t is time. Semenov[51] argued that the average life time of a chain centre is, at most, a fraction of a second. He estimated the smallest value of ϕ for a mixture of gases under atmospheric pressure to be one, i.e. the velocity of the reaction increases by e every second.

In the slow oxidation of hydrocarbons, the same exponential low holds, but the time of development of the maximum rate is frequently of the order of minutes or even hours. In order to explain this contradiction, he postulated the special case of 'degenerate branching'. In this theory, the primary chain is considered to be linear and not to undergo chain branching. But, as a result of the reaction of this primary chain, a relatively stable intermediate product is formed. This intermediate product can react independently to give the final product or to produce other centres capable of initiating other chains.

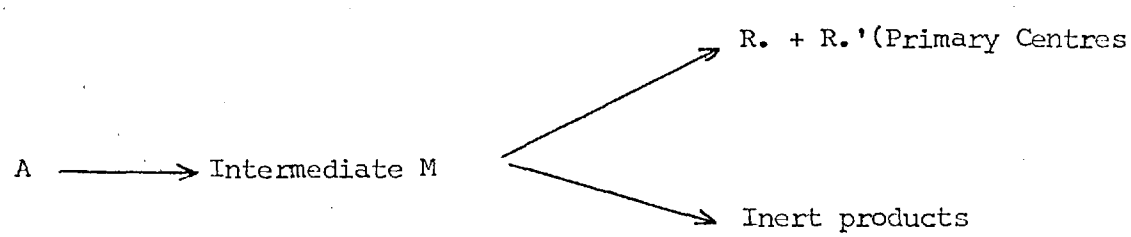

These secondary chains are considered to be branchings of the primary chains.

Two types of degenerately branched chain reactions are possible;

in the first, the maximimum rate of the reaction is governed solely by the rate of removal of the reactants. A typical process of this type can be represented by the scheme:

$$A + X \xrightarrow{Kp} M + X$$

$$M \xrightarrow{Kb} \text{products} + X$$

$$M \xrightarrow{Kd} \text{products}$$

$$X \xrightarrow{Kt} \text{Inactive}$$

Where A is a reactant; M the intermediate; X, the chain carrier and Kp, Kb, Kd, Kt are the rate constants for propagation, destruction of M leading to branching, destruction of M without production of new centres, and termination respectively.

If ν is the length of the main chain and No is the number of initially generated centres, then from the above scheme:

$$\frac{d[M]}{dt} = \nu No - Kb\,[M] + Kb[M] - Kd\,[M]$$

which can be abbreviated to:

$$\frac{d[M]}{dt} = a + \phi[M].$$

On integration at t = 0, [M] = 0, the concentration of M becomes, at time t,

$$[M] = \frac{a}{\phi}\,(e^{\phi t} - 1), \quad \text{and the rate of the reaction becomes}$$

$$W = \frac{[M]}{\tau} = \frac{a}{\phi\tau} \cdot \exp(\phi t - 1)$$

$$= A.\exp \phi t$$

where τ is the life time of the intermediate and $A = \frac{a}{\phi\tau}$. This scheme, therefore, predicts the exponential increase in rate with time. It should be noted however that both a and τ are functions of the chain length ν which, in turn, is a function of reactant pressure. Hence, both these terms will be constant to a first approximation only during the initial

stages of oxidation when reactant depletion is neglible.

The second type of degenerately branched chain reaction involves destruction of the intermediate M by the centres X which it itself generates. A representative scheme is:

$$A + X \xrightarrow{Kp} M + X$$

$$M \xrightarrow{Kb} \text{products} + X$$

$$M + X \xrightarrow{Kd} \text{products}$$

$$X \xrightarrow{Kt} \text{inactive}$$

This type of process exhibits a fairly short induction period, followed by acceleration to a maximum rate which remains steady even though the reactants are disappearing.

If the number of active centres generated by the branching step exceeds the number produced by initiation, then the number of active centres becomes proportional to the concentration of the intermediate, hence

$$\frac{d[M]}{dt} = \nu No - K_b[M] + \nu K_b[M] - K_d[M]^2 \qquad (1)'$$

which can be abbreviated to:

$$\frac{d[M]}{at} = a + f[M] - K[M]^2 \qquad (2)'$$

where $a = \nu No$, $f = K_b(\nu - 1)$: $K = K_d$

At the steady state:

$$\frac{d[M]}{dt} = 0 = a + f[M] - K[M]^2$$

whence $$[M] = \frac{f \pm \sqrt{f^2 + 4aK}}{2K}$$

$$= \frac{f \mp \sqrt{f^2 + 4aK}}{2K\tau}$$

If $f > K$, equation $(2)'$ can be integrated to give:

$$[M] = \frac{2a(e^{t\sqrt{a/K}} - 1)}{(f + \sqrt{q}) - (f - \sqrt{q})e^{t\sqrt{a/K}}}$$

where $q = f^2 + 4aK$.

If $f^2 \gg 4aK$, $\sqrt{q}$ can be replaced by f to give:

$$M = \frac{a}{f}\left[\exp(ft/K) - 1\right]$$

and the rate $w = \frac{a}{f\tilde{1}}\left[\exp(ft/K) - 1\right]$

$$\approx A.e^{\phi t}$$

Hence this scheme also predicts an exponential increase of rate with time. Further, the Semenov theory predicts that the pressure change of the system will increase exponentially, at least after the induction period.

$$P = \frac{B}{\phi^2} \cdot e^{\phi t} \quad ,$$

which also predicts that the acceleration rate will be exponential. Thus, from

$$W = \frac{B}{\phi} \cdot e^{\phi t} \quad ,$$

$$W = \phi \Delta P$$

Theoretically the rate increases continuously with time, but experimentally it reaches a maximum during the acceleration period due to consumption of reactants and then decreases and eventually falls to zero. According to the equation:

$\frac{dW}{dt} = K\frac{d[M]}{dt}$, the reaction rate is maximum when the concentration of M reaches its maximum [55], in other words.

$$\frac{d[W]}{dt} = 0 \text{ when } \frac{d[M]}{dt} = 0 .$$

1.6.4. THE REACTIONS OF FREE RADICALS IN COMBUSTION SYSTEMS

As discussed above, the understanding of combustion phenomena is equivalent to accurately interpret the behaviour of the free radicals that are involved in the branching chain reactions. When alkyl radicals are generated in the presence of oxygen, there are only a few primary reactions, but the radical products of these reactions evidently under numerous reactions. The following reaction is considered to be the initiation step of most combustion reactions:

$$RH + O_2 \longrightarrow R\cdot + HO_2$$

An oxygen molecule abstracts a hydrogen atom to form a hydroperoxy radical $HO_2\cdot$ and an altcyl radical R. for an oxygenated fuel, such as an aldehyde, a similar reaction occurs leading to the formation of an acyl radical RCO. and $HO_2\cdot$.

The propagation steps can follow different paths depending on the temperature. Generally the folllowing are usually encountered.

$$R\cdot + O_2 \longrightarrow RO_2 \qquad (1)$$

$$R\cdot + O_2 \longrightarrow \text{olefin} + HO_2 \qquad (3)$$

$$R\cdot + O_2 \longrightarrow R'CHO + R''O\cdot$$

$$RO_2 + RH \longrightarrow ROOH + R$$

$$RCO\cdot + O_2 \longrightarrow RCO_3$$

Thus while hydrogen abstraction leads to the production of alkcyl radicals R.,

$$\cdot OH + RH \longrightarrow H_2O + R\cdot$$

$$HO_2 + RH \longrightarrow H_2O_2 + R\cdot$$

oxygen can react with alkyl radicals to give other radicals as in reaction (2).

In the case of olefins or acetylene the oxygen is thought to be added to the double bond via HO_2 radicals:

$$RCH = CH_2 + HO_2 \longrightarrow RCHCH_2O + OH.$$

$$HC \equiv CH + HO_2 \longrightarrow HOOCH = CH$$

$$HOOCH = CH \longrightarrow CH_2O + HCO$$

Such reactions as these may lead to polymerisation especially when the oxygen concentration is low. Oxidation reactions will be autocatalytic when products such as ROOH and HOOH pyrolyze to give new free radicals,

$$ROOH = RO. + .OH$$

$$HOOH+M = \cdot OH + \cdot OH + M.$$

or when products such as aldehydes and olefins react with oxygen to give new free radicals by reactions such as:

$$R'CHO + O_2 \longrightarrow R'CO. + HO_2.$$

Disproportionation and recombination can effect chain termination:

$$R + R' \longrightarrow RR'$$

$$RO_2 + HO_2 \longrightarrow ROOH + O_2$$

$$RO_2 \longrightarrow QOOH$$

The last reaction is regarded as reaction type rather than as single reactions - i.e. it represents several distinct elementary steps. In the case of aldehydes the termination step is recombination of RCO and RCO_3. radicals;

$$RCO. + RCO. \longrightarrow (RCO)_2$$

$$RCO + RCO_3. \longrightarrow RCO\text{-}OO\text{-}OCR$$

$$RCO_3. + RCO_3 \longrightarrow RCO\text{-}OO\text{-}OCR + O_2.$$

It is the decomposition of certain radicals particularly at high

temperatures that over-shadow these termination steps.

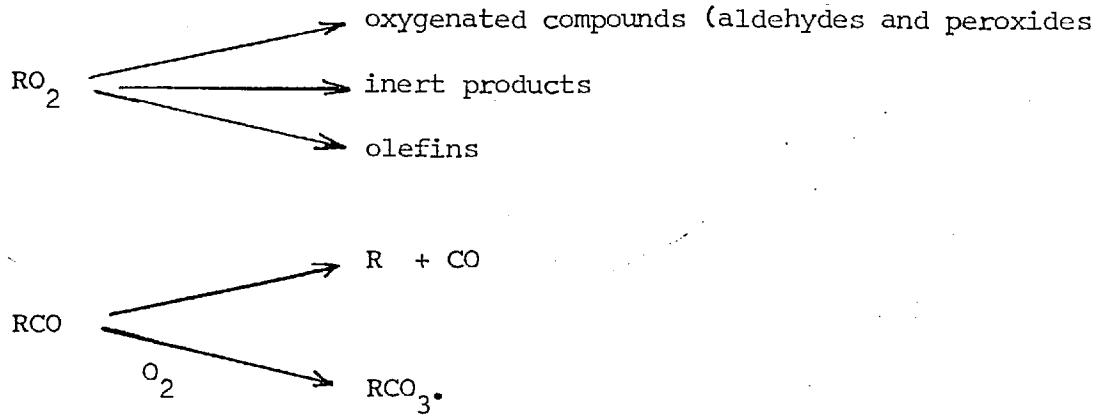

There is hardly any doubt that the decomposition of RO_2 radicals determines the different characteristics of low and high temperature combustion and explains the existence of the negative temperature coefficient.

1.6.4.1 TYPES OF RADICALS

There are two types of free radicals: σ and π free radicals. σ radicals are those containing an unpaired electron in a σ orbital and are conventionally shown as:

The ethynyl, vinyl, formyl, acetyl and phenyl radicals are of this type;

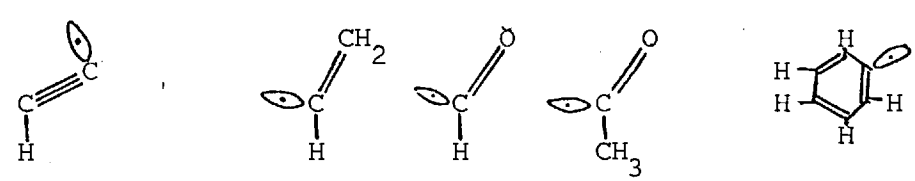

$\dot{C}\equiv CH$ $\quad$ $H\dot{C}=CH_2$ $\quad$ HCO $\quad$ CH_3CO $\quad$ C_6H_5

π radicals are those containing an unpaired electron in a P-orbital of their structure;

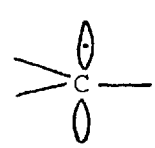

The alkyl, allyl, alkoxy, and phenoxy radicals are of the type;

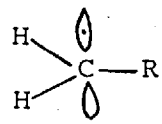
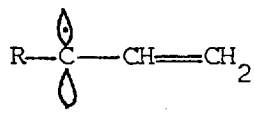
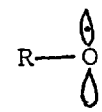
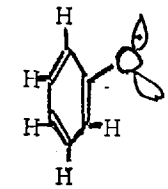

$R\text{-}\dot{C}H_2$ $\quad$ $R\text{-}\dot{C}H\text{-}CH = CH_2$ $\quad$ $R - O\cdot$ $\quad$ $C_6H_5O\cdot$

The two types of free radicals σ & π may exist in both planar and pyramidal form, with one configuration usually being more stable. For methyl radicals, the planar form is more stable.

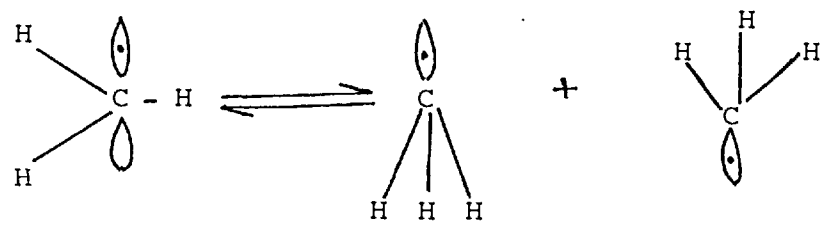

Planar form $\quad$ Pyramidal forms

Benson [58] and Knox [53] have examined π radical reactions with molecular oxygen and have shown that under normal conditions the equilibrium lies will to the right for saturated alkyl radicals. Where the π radical is resonance stabilized the equilibrium is reduced. Similarly σ radicals which are not resonance stabilised possess a low reactivity towards oxygen [59] The low reactivity exhibited by σ radicals towards molecular oxygen is a consequence of the symmetry of the σ orbital. Approach of a π radical along the molecular axis of oxygen gives the correct symmetry for successful bond formation in contrast to the same approach for a σ radical. Further, if there is the possibility of conjugation or hyperconjugation in the radical, then this will favour the stability of the π form over the σ form.

1.6.4.2. ALTERNATIVE REACTIONS OF FREE RADICALS

Mayo [60] classified the general reactions of free radicals as shown in table 1-5 below.

No.	Type of reaction	Examples
-1^1	Dissociation	$R_2 \underset{1^2}{\overset{-1^1}{\rightleftharpoons}} 2R. \xrightarrow{2^2} RH$
1^2	Combination	
2^2	Disproportion	
		1^1 D^1
D'	Diffusion from cage	[2R.]
3^2	Abstraction, transfer.	$R. + XY \xrightarrow{3^2} RX + Y.$
4^2	Addition.	$R. + A = B \underset{}{\overset{4^2}{\rightleftharpoons}} RAB.$
-4^1	Scission	-4^1
5^2	Displacement	$R. + X = YZ \xrightarrow{5^2} RXY + Z.$
6^1	Rearrangement (Isomerization)	$R. \xrightarrow{6^1} R^1.$

Which of these possible steps will predominate depends on the temperature and the structure of the radicals involved; and of course on the reaction medium. Diffusion from the cage is basically a liquid phase phenomenon. The decomposition of peroxides or of azo compounds produces a pair of radicals according to reaction -1^1 (dissociation) and these radicals may interact in pairs according to reaction 1^2 (combination). Abstraction is perhaps the most important of free radical reactions, as this leads to the production of a stable molecule and another radical capable of initiating chain transfer. Reaction 4^2 (addition) covers the addition

of an atom or radical to a double or triple bond (or to oxygen) and is usually accompanied by reaction 3^2 (abstraction). Scission is the reverse of addition, eliminating olefin units from alkyl radicals.

$$C_3H_7 \longrightarrow C_3H_6 + H.$$

Reaction 5^1 is the displacement of Z by radical R. and reaction 6^1 (rearrangement) corresponds to unimolecular abstraction or to other transference of atoms of groups within radicals.

In all these reactions, dissociation, diffusion from cage, scission and rearrangement steps are first order. Combination, disproporation, abstraction, addition and displacement are second order except addition which can occasionally be of third order.

In the gas phase, the conditions are usually such as to limit the bimolecular and termolecular processes. Chain termination reactions like combination and disproportionation, as well as propapation steps like abstraction and addition are the important steps as in halogenation, oxidation, and polymerization processes.

1.6.5. SPECIFIC REACTIONS OF SOME FREE RADICALS IN COMBUSTION SYSTEMS

Among the many free radicals encountered in combustion systems are alkyl, allyl, alkynyl, phenyl alkoxy, formyl, acyl, alkylperoxy, hydroxy, hydroperoxy, performyl, peracyl and diacyl radicals.

1.6.5.1 REACTIONS OF ALKYL RADICALS R.

The fate of a given alkyl radical R· depends not only on its structure but also on the conditions of the combustion system in which it is generated. It may decompose, add to oxygen or isomerize. Its interaction with oxygen must involve, as a first step, the formation of some species

which may be formally written as $C_nH_{2n+1}\cdots O_2$ This may be a fairly stable "thermalised" radical which can exist for relatively long periods of time, or a vibrationally excited radical having the energy released by formation of the C-O bond randomly distributed throughout the radical, or an activated complex in which the vibrational energy is organized in a specific way and which will decompose or rearrange within the period of a single vibration. It is generally believed that at low temperatures ($< 250^{\circ}C$) $C_nH_{2n+1}O$ radicals are stable, but at high temperatures ($> 400^{\circ}C$) an $HO_2\cdot$ radical and an alkene are the products of alkyradical-oxygen interactions.

$$C_nH_{2n+1}\cdot + O_2 \longrightarrow C_nH_{2n+1}O_2 \qquad (127)$$

$$C_nH_{2n+1}\cdot + O_2 \longrightarrow C_nH_{2n} + HO_2 \qquad (128)$$

$$C_3H_7\cdot + O_2 \longrightarrow C_3H_6 + HO_2$$

$$C_3H_7\cdot \longrightarrow CH_3\cdot + C_2H_4 \qquad (129)$$

In the intermediate temperature range (250° to $400^{\circ}C$), which is the region in which cool flames propagate during the oxidation of hydrocarbons, both alkenes and oxygenates are formed in significant amounts. Thus, in the oxidation of ethane[62] and 2-methylpropane[63,64] about 80% of the initial oxidation product is the conjugate alkene. Thus it can be seen that at intermediate temperatures there will be competition between reactions (127) and (128) but at high temperatures the competition is between reactions (128) and (129) where the predominant route of oxidation will then depend on the structure of the radical $C_nH_{2n+1}\cdot$.

1.6.5.2 REACTIONS OF ALKYL PEROXY RADICALS RO_2

The alkyl peroxy radicals are very stable at low temperatures, but decompose easily at high temperatures. When stable, by far the most common

routes of disappearance are by reaction with fuel molecules to produce hydroperoxides

$$RO_2 + RH \longrightarrow ROOH + R\cdot$$

or by an internal rearrangement of the type suggested by Fish[61]

e.g. $CH_3-CH(OO\cdot)-CH_2-CH_2-CH_3 \rightarrow CH_3-CH(OOH)-CH_2-CH-CH_3$

$$\longrightarrow CH_3-\underset{\diagdown O \diagup}{CH}-CH_2 + \cdot OH + CH_2=CH_2$$

The rates of abstraction of hydrogen atoms depends on whether the hydrogen atoms are tertiary, secondary or primary. Since the strengths of tertiary, secondary and primary C-H bonds are respectively 383, 395 and 409 KJoules per mole[58,65,66] and $D(RO_2 - H)$ = 376 KJoules per mole, the enthalpy changes and activation energies are:

				ΔH	E
RO_2 +	+ert	$>C-H$	$\rightarrow ROOH + >C\cdot$	7.10 KJ	32.2 KJ/mole
RO_2 +	sec	$>CH-H$	$\rightarrow ROOH + >\dot{C}-H$	18.8 KJ	41.8 KJ/mole
RO_2 +	prim	$-CH_3$	$\rightarrow ROOH + -\dot{C}H_2$	33.4 KJ	58.5 KJ/mole

If the peroxy radical does decompose, then several alternative reactions may occur such as,

$$CH_3O_2 \longrightarrow HCHO + OH$$

$$C_3H_7O_2 \longrightarrow CH_3CHO + CH_3O$$

$$H_3C-C(CH_3)(OO\cdot)-CH_2-CH_2-CH_3 \rightarrow CH_3-CO-CH_3 + C_3H_7O$$

$$\longrightarrow CH_3-CO-CH_3 + C_2H_4 + CH_3O\cdot$$

Peroxy radicals may also react with HO_2 radicals to give hydroperoxide

$$RO_2\cdot + HO_2 \longrightarrow ROOH + O_2$$

The probability of reaction also depends on the radical concentration.

Perfr and peracetyl radicals can either abstract hydrogen atoms to form the corresponding peracids or decompose.

$$RCO_3 + RH \longrightarrow RCO_3H + R\cdot$$

$$RCO_3 \longrightarrow RO_2\cdot + CO\cdot$$

1.6.5.2. REACTIONS OF ALKOXY RADICALS RO

Alkoxy radicals are formed mainly by decomposition of peroxides;

$$ROOH \longrightarrow RO + OH$$

$$ROOR' \longrightarrow RO + R'O\cdot$$

They are markedly involved in abstraction reactions and may decompose or react with oxygen. The reactions of ethoxy radical C_2H_5O are typical of the other alkoxy radicals. This is shown schematically below.

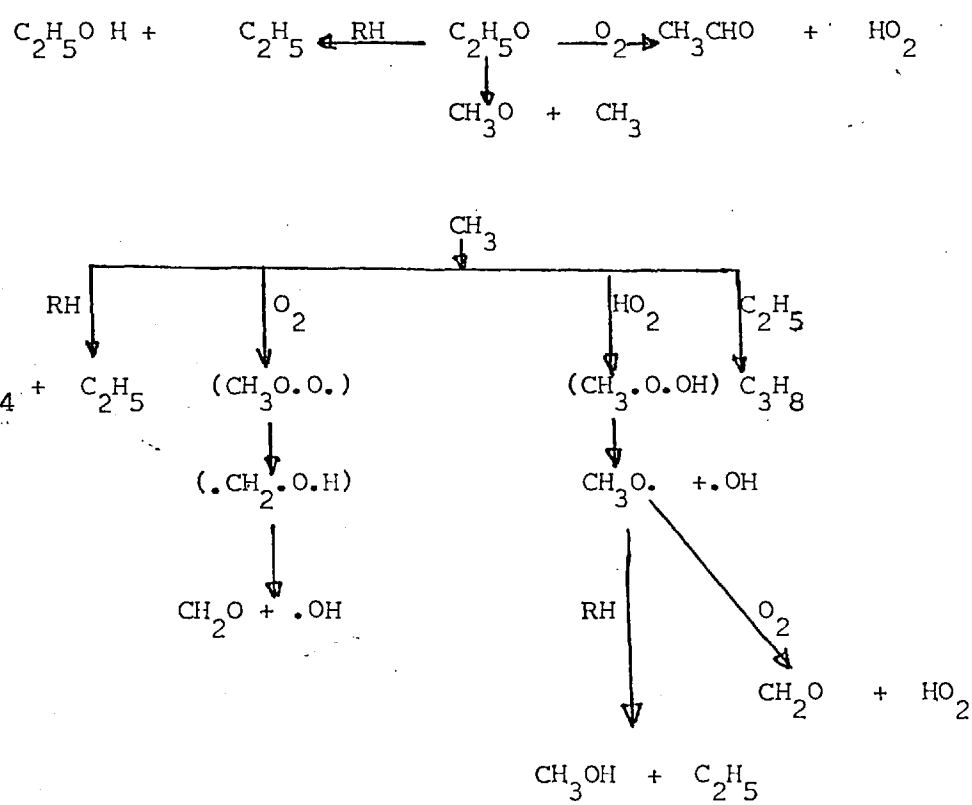

This scheme is likely to play an important role in explaining the spectrum of products obtained at intermediate and low temperatures when $RO_2\cdot$ radicals are fairly stable and able to abstract hydrogen atoms to form the hydroperoxides which eventually decompose into alkoxy radicals. At higher temperatures when $RO_2\cdot$ radicals, which abstract protons to give hydrogenperoxide, which in turn gives OH radicals, the hydroxyl radicals OH. should play a major role in propagation steps.

1.6.5.3. REACTIONS OF HYDROPEROXYL RADICALS

Hydroperoxy radicals can be formed by either the reaction of a hydrocarbon with oxygen or by the reaction of an alkyl radical with oxygen at higher temperatures.

$$RH + O_2 \longrightarrow R\cdot + HO_2\cdot$$

$$R + O2 \longrightarrow \text{olefin} + HO_2\cdot$$

Thsy may also interact to give hydrogen peroxide and oxygen:

$$2HO_2 \longrightarrow H_2O_2 + O_2$$

They can decompose homogeneously to give OH radicals[59] at high temperatures.

$$HO_2\cdot + HO_2\cdot \longrightarrow 2OH + O_2 \qquad H = 25 \text{ KJ/mole}$$

which is endothelmic.

Although the experimental evidence is not clear-cut, Sampson[67] suggested that a small proportion of the carbon monoxide and formaldehyde may arise through ethylene. The possible mode of formation of the CO, CH_2O, and methane through ethylene is shown in the following scheme.

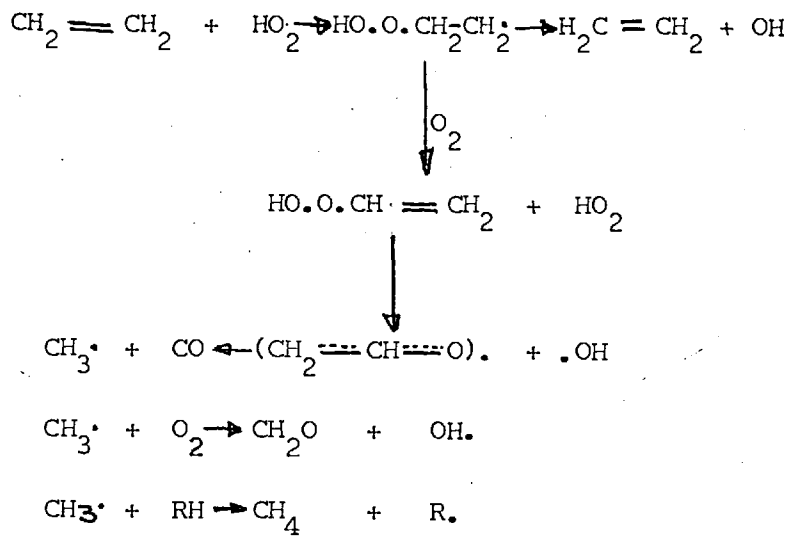

He also claimed that part of the carbon monoxide must arise through formaldehyde:

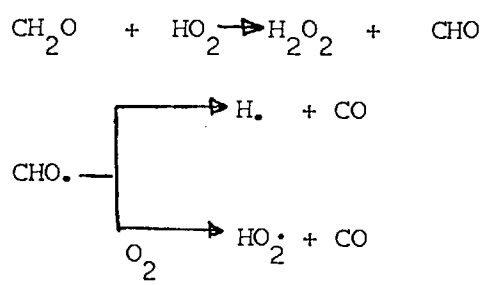

The other important reactions of hydroperoxy radicals are disproportionation with RO_2 radicals;

$HO_2 + RO_2 \longrightarrow ROOH + O_2$, and external hydrogen abstraction from the fuel molecule;

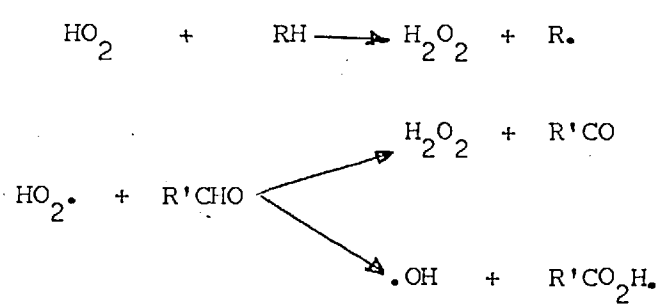

1.6.5.4. REACTIONS OF HYDROXYL RADICALS .OH

Hydroxyl radicals are usually produced by the decomposition of hydro-

peroxides (during the branching steps) or hydrogen peroxide at high temperatures. They are engaged mainly in abstraction reactions.

$$OH + RH \longrightarrow H_2O + R$$

They may also react with other fragments in the system. Fish [61] reported that hydroxyl radicals are the main propagating radicals involved in cool flame combustion.

1.6.6. COMBUSTION REGIONS ASSOCIATED WITH HYDROCARBON OXIDATION

The reaction of oxygen with hydrocarbons or their simple derivatives in the gas phase gives rise to many diverse phenomena. Some of these can be described by reference to the ignition diagram[68] fig. 1 - 14 which shows the pressure-temperature diagram for a 1:1 propane-oxygen mixture in a silica vessel. These observed phenomena can be more closely defined in terms of the lower slow combustion region (A), the upper slow combustion region (B), the lower cool-flame zone (C), the upper cool flame zone (D), the low temperature ignition region (E) and the high temperature ignition region (F).

At any temperature T, shown by a horizontal line in the ignition diagram, branching reactions are favoured by increasing the pressure of the system up to a critical point when cool flames or true ignition/ explosion phenomena occur. The locus of these critical points is drawn as the ignition boundary. Similarly at a given pressure P (represented by the vertical line x - x'), the process exhibits diverse rates of reaction and hence different kinetic and mechanistic characteristics.

Newitt and Thornes[68] observed that below 275°C, a slow reaction occurred, accompanied by a pressure change. Between 275° and 285°C a faint luminosity developed after several minutes and remained until the reaction was nearly complete. At 290°C, the luminosity was followed by a pale

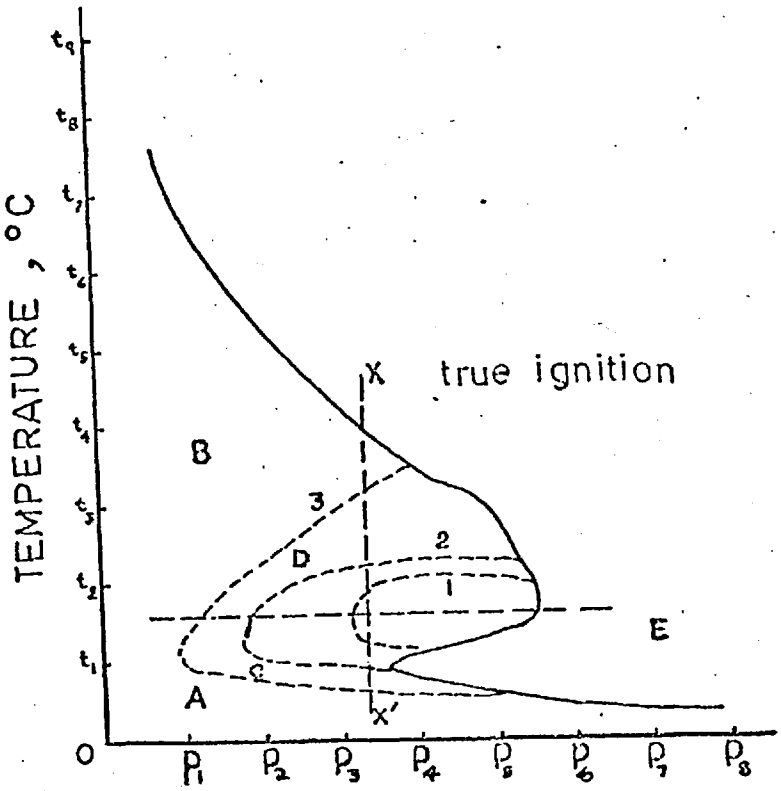

Fig1-14 PRESSURE , mm.Hg.

A TYPICAL IGNITION DIAGRAM FOR COMBUSTION OF HYDROCARBONS UNDER VARIOUS CONDITIONS

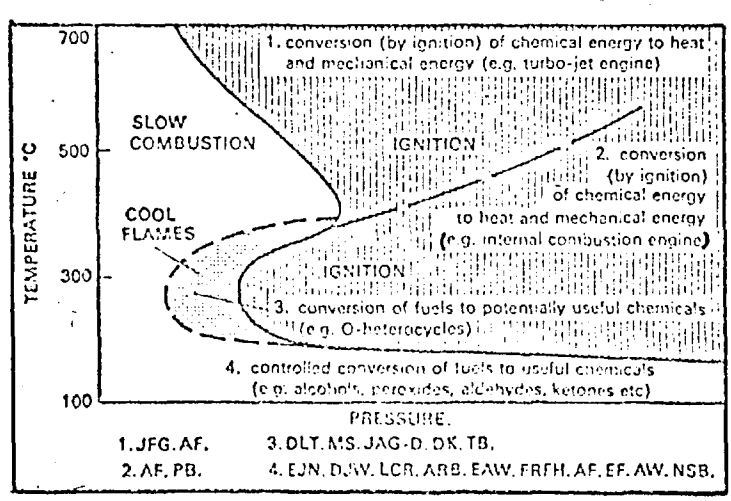

Fig1-15

blue "cool flame" of low intensity which started near the centre of the vessel and spread outwards, giving rise to a pressure pulse. After the passage of the flame, the luminosity persisted for several seconds. Between 300° and 340°C, the luminosity appeared immediately on filling the vessel and was succeeded by three to five cool flames at intervals of several seconds, each of which traversed the whole vessel before extinction and gave rise to a pressure pulse. Between 340° and 385°C only one, cool flame was observed. The intensity of these flames increased as their number diminished. Above 350°C, however, the single cool was raised, while the luminosity increased in intensity until, at 425°C, it was succeeded by a bright blue flame. At a slightly higher temperature, this changed to the characteristic yellow flame associated with true ignition. Another phenomenon sometimes observed is delay ignition. In the region where multiple cool flames are expected, a simple cool flame occurs followed after an appreciable period by a second cool flame and ignition. The appearance of delayed ignition suggests that cool flame transfers the system from the low temperature region to the high-temperature region, the increased rate of reaction there and the consequent increase in heat production then leading to thermal explosion.

Thus, the parameters used in describing combustion systems can be chosen in such a way as to favour the occurence of a particular phenomenon, the various reactions taking place favour the production of certain types of chemicals according to the regime of operation. A brief summary of the importance of each zone is as shown by Cullis[69] in Fig. 1-15.

VARIATION WITH TIME OF THE RATE OF COMBUSTION

The typical pressure-time curves for slow combustion of organic compounds in a static system is represented in Fig. 1-16[70]. The usual type, curve a, shows the induction period, τ, with negligible

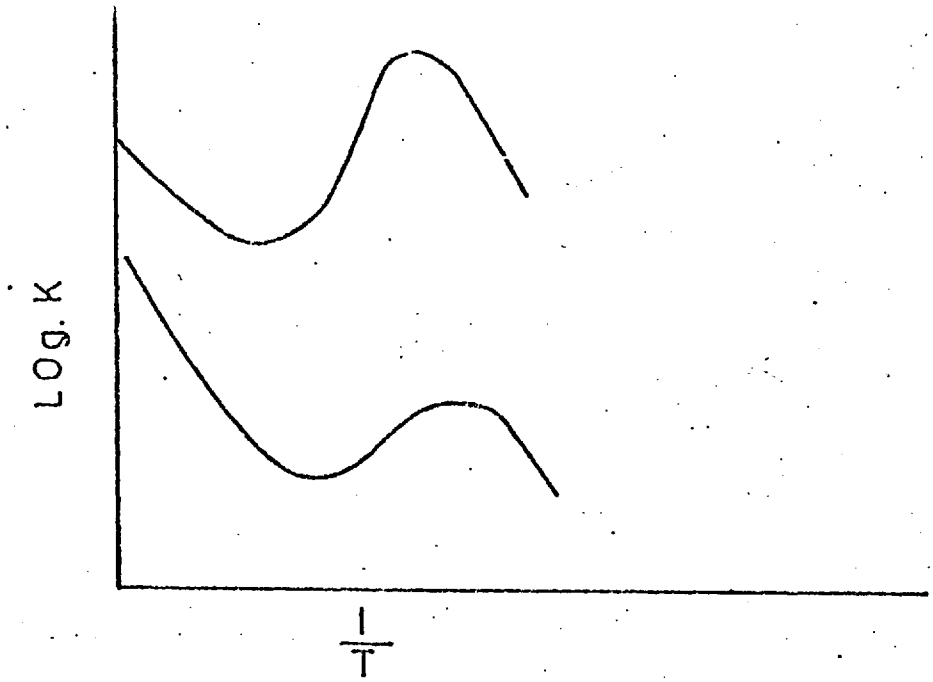

Fig 1-17

Arrhenius curve for hydrocarbons

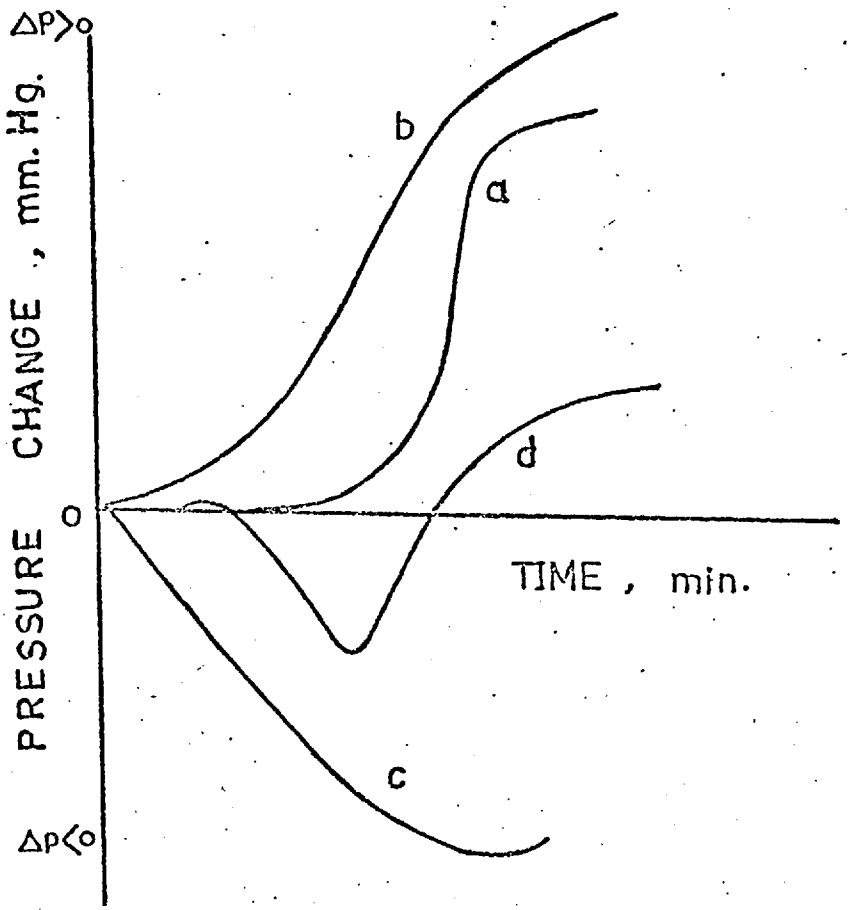

PRESSURE TIME CURVES FOR COMBUSTION REACTIONS

Fig1-16

pressure change, followed by an acceleration of the rate to its maximum after which it falls to zero. The acceleration to the maximum rate is exponential, i.e. $\Delta P = A \exp(\phi t)$ where ϕ is the net branching factor. The Arrhenius curve of logK versus the reciprocal of absolute temperature is shown in Fig 1-17. The net branching factor ϕ can be calculated from the slope of a plot of $\log_{10}\Delta P$ versus time, fig. 1- 18.

In some cases this typical pressure-time curve a is modified as in the case of the slow combustion of methanol (curve b), acetaldehyde at low temperatures (curve c) and for hexene-1 (curve d). When using flow systems, it is not easy to obtain oxidation rates. To follow the reaction throughout its course necessitates analysing the effluent mixture at a series of increasing residence times in the reactor. Even if only the concentrations of fuel and oxygen are determined it can be laborious to find, for example - $d[O_2]/dt$.

1.6.7 PRESENT WORK

As has been discussed, it is generally agreed that the reactions of hydrocarbons are propagated by free radicals generated in the reaction systems. Beyond this, there is very little detailed agreement. The present studies were initiated in order to try to establish the high temperature reaction mechanism of hydrocarbons with particular reference to propane in a flow system between 600 and 800°C, the temperature range usually encountered in commercial apparatus. To accomplish this, it has been necessary to adopt the following procedure.

(1) To employ the mass spectrometer as the analytical tool rather than chromatography. This necessiatated the writing of a matrix inversion programme to resolve the superimposed mass spectra of pyrolysis products. Such a programme should be useful in pollution studies as well.

(2) The results obtained from the mass spectra have been compared

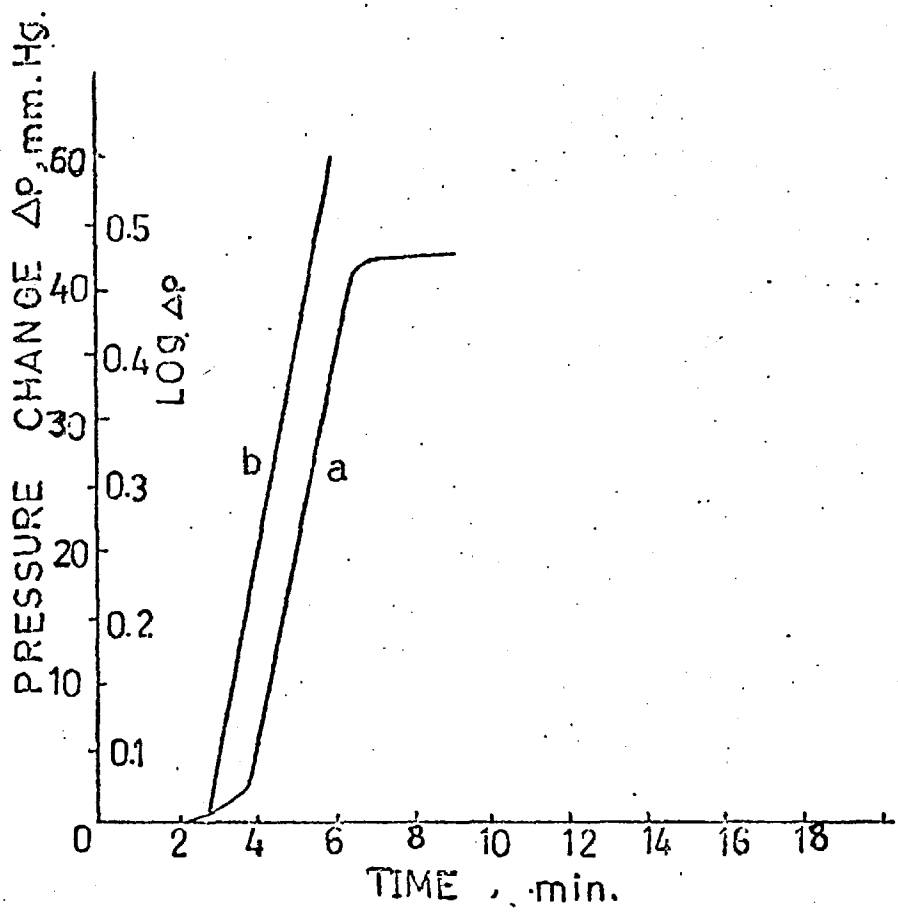

Fig 1-18
a) pressure - time curve
b) Logarithmic pressure - time curve

with computer predictions. The numerical integration program is based on the semi-implicit trapezoidal rule and devoid of the steady-state limitations. The programme was tested by modelling acetaldehyde and formaldehyde oxidation mechanisms and comparing the results with literature data.

(3) Pyrolysis of propane between 600-800°C, to establish the mechanism and the kinetics. The self-inhibition reactions of propane have been considered as these have been neglected in most literature.

(4) To establish the mechanism and kinetics of propane perturbed with small amounts of acetone and acetaldehyde. Both acetone and acetaldehyde are potential sources of methyl radicals, and, in addition, acetaldehyde is an intermediate in combustion systems. This type of experiment has not been reported in the literature.

(5) To establish the mechanism of the oxidative reactions of propane in the presence of small amounts of oxygen between 600° and 700°C, and the effect on the products distribution. Literature data on such reaction above 600°C is sparse.

The results in all cases have been compared with computer predictions as reported below and the literature pertinent to individual sections is summarized at the start of the section.

CHAPTER II

CHAPTER II

KINETIC MODELLING OF GAS PHASE OXIDATION OF FORMALDEHYDE AND ACETALDEHYDE

2.1 INTRODUCTION

Gas phase reactions are very complex, and it is difficult to decide, a priori, on a method for predicting the course of a complex reaction or even being sure that the mechanism assumed is the only one possible. There may be alternative reaction paths which can lead to the same kinetic observations. In developing a theoretical model, problems occur both in choosing the important reaction steps to include in the model and also in selecting accurate parameters (energies of activation and pre-exponential terms) for each reaction step.

Most of the many reactions involved occur in the gas phase, but some reactions also occur at the walls of the reactor. As suggested by Herriot et al[71], the energies of activation can vary to at least some extent with temperature. Values to be used between 750° and 900°C may be different from values determined experimentally at much lower temperatures, and a difference of 1.KJ. $mole^{-1}$ may have a large effect on the predicted rate values. In addition, the exact mechanism of some of these specific reaction steps that may involve hot or activated radicals or molecules, may change somewhat as temperature is increased.

For laboratory studies of processes of industrial interest where transport processes can be better understood and held under closer control, attempts have been made to fit the data to more detailed chemical models. A number of parameter fits to such extended models have been published. In many of these there is a mistaken belief that the ability to achieve such a fit is, of itself, an indication of the correctness of the model and that the parameters obtained are of fundamental significance. This can result in the proliferation of misleading rate constants in the literature. Discrepancies hitherto observed can be attributed mainly to the inability of simplified models to describe adequately the complexity of the systems under investigation.

Errors in some of the numerical techniques used to solve the kinetic equations may also contribute to the deviations. Snow's procedure [72], which is typical of those employed, uses a standard numberical integration of the kinetic equations combined with a quasi-steady state approximation when the derivative of one (or more) of the free radical intermediates becomes small. The errors inherent in this computational approach have become increasingly apparent over the years and have recently been reviewed by Edelson[73]. Workers in computational kinetics have increasingly turned to an integration method originated by Gear [74] which works extremely well for these stiff differential equations and which is free of the problems which plague the steady state approximation. Any chemical problem is subject to the constraint of the conservation of matter. According to Edelson[73], this is also implicit in the differenetial equations. Linear single or multistep integration procedures maintain this condition. But, once steady-state procedures are invoked, chemical balance restrictions are lost because, according to Galinas [94], the active centres or intermediates do not reach the steady-state simultaneously. He argues that, although the error in overall stoichiometry may be small, the error in a particular component may be significant and that this error can propagate through the system because of the way in which the several components are coupled. Thus, the errors have the effect of redefining the system being modelled. Both Edelson and Calinas are of the opinion that conservation of matter must be considered a necessary (but not sufficient) condition for validation of the results of computation. It is, perhaps better to apply the steady state approximation after the last transient has reached the steady-state.

2.2 INTEGRATION PROGRAMME EMPLOYED IN THIS WORK

The numberical integration programme employed in the present work

has been developed by Kershenbaum et al;[75]. It is based on the semi-implicit trapezoidal rule coupled with a variable step size selection. Since it takes into account fast components which appear during the reaction as well as those which may be present initially, systems typified by autocatalytic and branched free radical reactions are easily solved. Like the Gear method, it is also without the limitations of the steady state approximation.

The basic features of the programme are:

(a) The concentrations of the chemical species satisfy the conservation equations:

$$\frac{dc}{dt} = \underline{f}\ ; \qquad \underline{C}\,(0) = \underline{CO}. \tag{1}$$

where $\underline{C}$ is an n-vector of concentration variables, $\underline{f}\ (\underline{C}, \underline{K}, T)$ is a non-linear, continuous n-vector valued function of reaction rates of the mass action form, and $\underline{K}$ is an n-vector of kinetic parameters.

(b) The general single step method for $\dot{\underline{y}} = \underline{f}\ (y)$ can be expressed as:

$$\underline{Y}_{s+1} = \underline{Y} + h[\ (1 - \mu)\ \underline{f}_{s+1} + \mu \underline{f}_s] \tag{2}$$

where

$\underline{Y}$ = general vector of state variables

$\dot{\underline{Y}}$ = vector of the rate of change of $\underline{Y}$

$\underline{f}$ = vector of rates of reaction

s = time interval

h = step size in integration

μ = free parameter in numerical integration method

(c) For a single linear equation, $\dot{y} = \lambda y$, where is the eigenvalue of Jacobian matrix, the characteristic root r of the differential equation is

$$r(\mu, \lambda, h) = \frac{1 + \mu \lambda h}{1 - (1 - \mu)\lambda h}$$

(d) For the implicit trapezoidal rule $\mu = 1/2$

The characteristic root r. then becomes

$$r(1/2,\lambda, h) = \frac{1 + 1/2\ h\lambda}{1 - 1/2\ h\lambda} \qquad (4)$$

This equation shows that as $h\lambda \longrightarrow -\infty$, $r \longrightarrow -1$ instead of being asymptotic to zero. As a result, oscillations appear in the successively computed values. In order to control these oscillations, the authors recommend that a small step size be used initially to simulate the component accurately and then to increase the step size progressively according to the rate of change of concentrations of components in the system.

(e) The method of detecting oscillations examines second order differences associated with the integration. Considering a vector of these differences, oscillations result in sudden changes in the sign of $\Delta^2 y_i$ before having any significant effect on the computed values. They, therefore considered an algorithm which controlled the amplitude of oscillations by changing the step size so that

$$h^2 |\Delta^2 y_i| < \delta . y_i \qquad (5)$$

where δ is an updating parameter.

The step size h is locally reduced until (5) is satisfied and then changes normally.

A plotting subroutine was incorporated to plot the concentrations of each species with time. Thus, the kinetic behaviour of the system could be readily observed and rates could be computed by adjusting the mechanism or the Arrhenius parameters, A and E, within limits to interpret practical results.

2.3 FORMALDEHYDE OXIDATION

The first detailed studies of the oxidation of gaseous formaldehyde by Hinshelwood [76] and Spence [77] showed that it did not react with oxygen below 250°C, but that the reaction rate increased rapidly above 350°C. It was also reported that, while the concentration of fuel affected the rate of reaction markedly, oxygen had little effect, but that the effect of surface on the reaction kinetics was marked. Subsequent studies have confirmed that the oxidation is a chain reaction [78,79,80, 77, 81] and that the rate is decreased by packing the reactor [80]. Spence[77] reported that in packed vessels containing high surface areas of glass, the products of reaction were CO_2 and H_2O, but in empty vessels, products such as CO, CO_2, H_2O, H_2, CH_4, HCOOH, HCO_3H, H_2O_2 and $(CH_2OH)_2O_2$ were observed.[82,83,84] Some of the divergence of products can be ascribed to alternative reactions of formyl radicals at different temperatures, oxidation giving way to thermal decomposition as temperature is raised [85]. It was reported that HO_2., HCO., HCO_3., and HCO_3H reacted differently on different surfaces. Consequently, the difference in products spectrum can be attributed to the alternative reactions of these radicals. Vardanyan and Nalbandyan[86] found that the kinetics of oxidation were similar in vessels of glass with and without a boric acid coating but to be different when potassium tetraborate was on the surface.

Hessam [87] in 1971 used a static system to study the oxidation of formaldehyde between 370° and 420°C and obtained an overall order of 2 with respect to formaldehyde concentration and an overall activation energy of 74.4 KJ. $mole^{-1}$. His analysis showed H_2O, CO, CO_2, H_2, HCOOH were the major products with H_2O_2 falling to a low value having passed through a maximum as a function of time. To explain his result the following kinetic scheme is devised.

2.3.1 MECHANISM OF FORMALDEHYDE OXIDATION

Initiation of the oxidation almost certainly involves the reaction:[83, 55, 78]

$$HCHO + O_2 \longrightarrow HCO + HO_2 \qquad (1)$$

with a heat of reaction calculated[89, 88] as

$$\Delta H_1 = Q(H - O_2) - Q(HCO - H)$$

$$= 197 - 367 = -170 \text{ KJ. mole}^{-1}$$

This is about twice the overall activation energy of formaldehyde oxidation. Initiation, presumably, thus occurs mainly on the reactor wall, a conclusion borne out by Griffiths[83].

Propagation of the chain appears to involve the following reactions;

$$HO_2\cdot + CH_2O \longrightarrow H_2O_2 + HCO\cdot \qquad (2)$$

$$HCO + O_2 \longrightarrow HCO_3 \qquad (3)$$

$$HCO_3 + CH_2O \longrightarrow HCO_3H + HCO \qquad (4)$$

$$HCO + O_2 \longrightarrow CO + HO_2 \qquad (5)$$

At high temperatures however, the rupture of HCO must be taken into account

$$HCO \longrightarrow H + CO \qquad (6)$$

Reactions (2) and (3) are exothermic:

$$\Delta H_2 = H_f(H_2O_2) + H_f(HCO) - H_f(HO_2) - H_f(CH_2O)$$

$$= -32.9 + 8.0 - 5.0 + 27.7 = -2.2 \frac{\text{Kcal}}{\text{mole}}$$

$$= -9.2 \text{ KJ. mole}^{-1}$$

$\Delta H_3 = H_f(HCO_3)$ which may be computed from the thermochemical equation:

$$Q(HCO - O_2) = H_f(CHO) + H_f(O_2) - H_f(CH_2O)$$

$$40.7 = 8.0 + 0 - H_f(HCO_3)$$

$$40.7 - 8.0 = H_f(HCO_3)$$

i.e., $\Delta H_f(HCO_3) = -32.7$ Kcal/mole.

$= -136.7$ KJ/mole.

Reaction (4) represents the abstraction of one hydrogen atom by performyl radical to produce perfomic acid which is unstable at high temperatures[83,85]. This product was identified experimentally be Hessam[87] who then concluded that performic acid must be involved in branching through the reactions.

$$HCO_3H \longrightarrow .OH + .OH + CO \quad \Delta H = 125.4 \text{ KH/mole}$$

$$\longrightarrow OH. + H + CO_2$$

He also identified a product with m/e = 94, which displayed a concentration profile with a maximum at the early stages of the reaction. If the product is $C_2H_6O_4$, possible conventional non-branching routes of production and decomposition are:

$$HCHO + HO_2 \longrightarrow H_2C(OOH)(O\cdot) \xrightarrow{HCHO} HO_2CH_2OCH_2O\cdot \xrightarrow{RH.} HO_2CH_2OCH_2OH$$

$$HCHO + HO_2 \longrightarrow HOCH_2O_2 \xrightarrow{HCHO} HOCH_2O_2CH_2O$$

$$\xrightarrow{RH} HOCH_2O_2CH_2OH$$

This product decomposes at temperatures above 200°C to give formic acid + hydrogen, or formaldehyde + hydrogen peroxide.

$$(CH_2OH)_2O_2 \longrightarrow 2HCO_2H + H_2$$

$$\longrightarrow 2CH_2O + H_2O_2$$

Other propagation reactions may be suggested:

$$HCO_2 + CH_2O \longrightarrow HCO + HCO_2H$$

$$HCO_2 \longrightarrow CH + CO$$

$$\longrightarrow H + CO_2$$

$$OH + CH_2O \longrightarrow HCO + H_2O$$

The HCO_2· must have been derived from formic acid $CHOOH \longrightarrow H\cdot + CHOO\cdot$

Side reactions occuring are:

$$HCO_2H \longrightarrow H_2O + CO$$

$$\longrightarrow H_2 + CO_2$$

$$2CH_2O \longrightarrow CH_3OH + CO$$

$$H_2O_2 \longrightarrow H_2O + \tfrac{1}{2}O_2$$

Under oxidizing conditions certain reactions are also possible:

$$HCO + CH_2O \longrightarrow CH_2OH + CO \quad ; \quad H = -58.5 \text{ KJ}$$

$$CH_2OH + CH_2O \longrightarrow CH_3OH + HCO \quad ; \quad H = -21 \text{ KJ}$$

Although Steacie et al[91], and Newton and Dodge[92] suggested that the direct decomposition of CH_2O to H_2 and CO accounted for the increase in the H_2 observed, later studies by Nalbandyan et al[93] categorically indicated that this reaction does not occur.

Termination of the oxidation process probably involves the reaction steps:

$$HO_2 \xrightarrow{\text{Wall}} \text{inert products}$$

$$2HO_2 \longrightarrow \text{inert products}$$

which are known to be surface reactions. The kinetic modelling was then tested on Hessam's system[87] to see if a satisfactory fit could be achieved

The following scheme explains the kinetic observation of Hessam. The composition profiles of the products are shown in Fig. 2 - 1. and the comparison with predicted values shown in Table 2-2.

TABLE 2 - 1

		A/sec^{-1}	E KJ/mole	
	Initiation			
1.	$CH_2O + O_2 \rightarrow CHO + HO_2$	2×10^9	121.20 KJ/mole	140
	Propagation			
2.	$CH_2O + HO_2 \rightarrow H_2O_2 + CHO$	2×10^9	32.60	141
3.	$CH_2O + HO_2 \rightarrow OH + HCOOH$	2×10^9	28.42	142
4.	$CH_2O + HO_2 \rightarrow OH + CO + H_2O$	2×10^9	28.42	142
5.	$HCO + O_2 \rightarrow CO + HO_2$	7×10^8	0.00	140
6.	$HCO + O_2 \rightarrow HCO_3$	7×10^7	0.00	142
7.	$HCO_3 + CH_2O \rightarrow HCO + HCO_3H$	4×10^9	30.10	142
8.	$HCO_3H \longrightarrow OH + OH + CO$	1.10^{12}	62.70	142
9.	$HO_2 + CH_2O \rightarrow OH + H_2 + CO_2$	2×10^9	28.42	144
10.	$OH + CH_2O \rightarrow HCO + H_2O$	2×10^9	16.72	145
	Termination			
11.	$HO_2 + HO_2 \rightarrow H_2O_2 + O_2$	$1.8.10^{12}$	0.00	146
12.	$CH_2O + H_2O_2 \rightarrow H_2 + HCOOH + ROO$	4.10^9	30.10	146

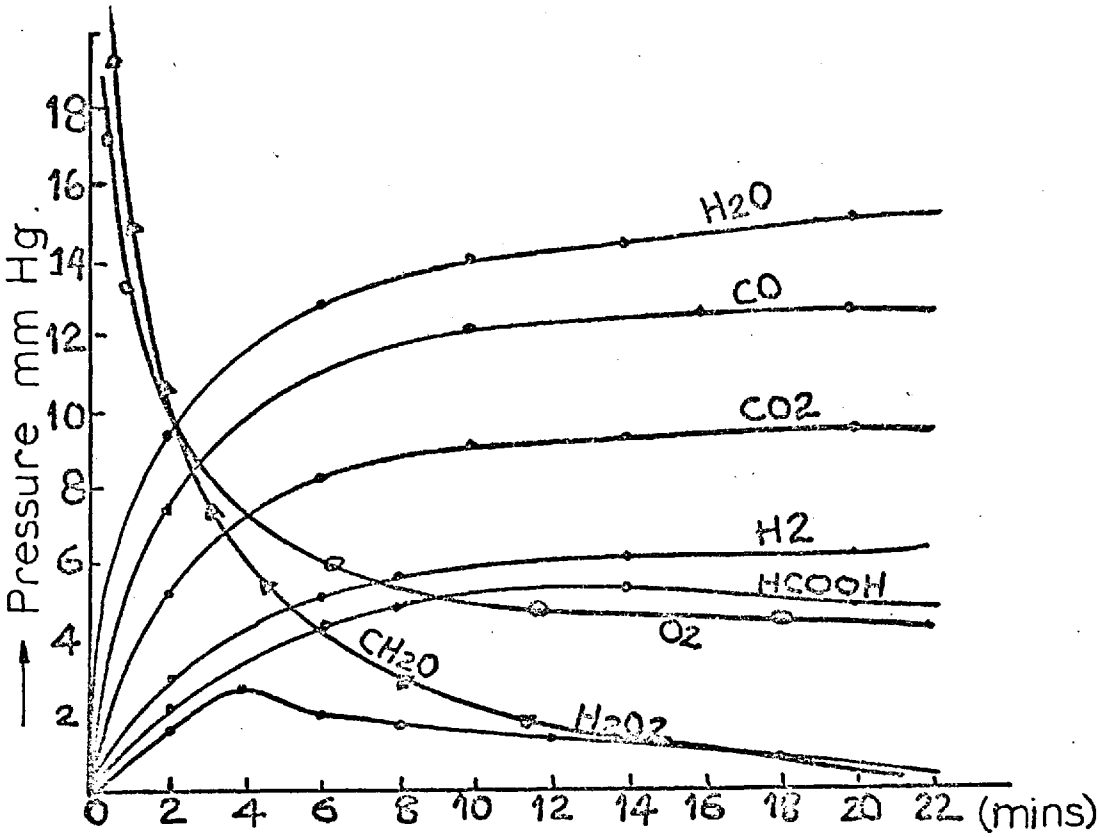

Fig 2-1 Product distribution from HCHO oxidation Hessams model at 400°C

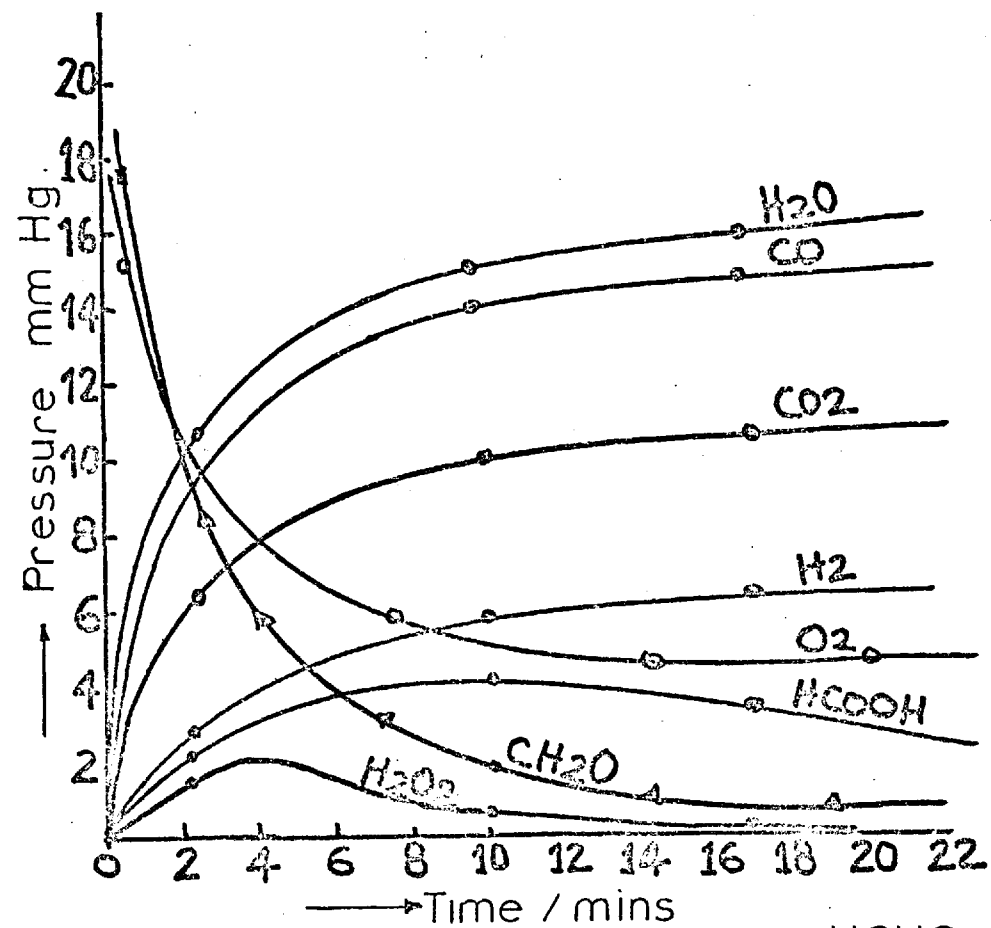

Fig 2-3 Product distribution from HCHO oxidation our extended model at 400°C

TEMPERATURE = 400°C

TIME (MINS)	4 MINS		14 MINS	
	HESSAM	PREDICTED	HESSAM	PREDICTED
CH_2O	5.76	6.00	1.26	1.22
O_2	6.82	7.00	4.70	4.60
H_2O	11.70	11.60	14.50	14.50
CO	10.00	9.80	12.00	12.60
CO_2	7.20	7.22	9.00	9.25
H_2	4.20	4.30	6.30	6.25
HCOOH	3.65	3.40	5.20	5.30
H_2O_2	2.70	2.80	1.20	1.20

TABLE 2-2 COMPARISON OF HESSAMS EXPERIMETNAL PARTIAL PRESSURES WITH COMPUTER PREDICTED VALUES

2.3.2 THE STEADY STATE APPROXIMATION

The steady state approximation permits the evaluation of the overall activation energy as well as the order of the reaction process under consideration. In general the concentration of any transient builds up to a maximum and then decreases to a constant value. This is also true of any branching intermediate like peracids, alkylperoxides and hydroperoxides. The rate of change in concentration of an intermediate A is the difference between the sum of its rates of formation and the sum of its rates of consumption, i.e.;

$$\frac{d[A]}{dt} = \sum r_{Af} - \sum r_{A,C} \qquad \text{where}$$

indices f and C represent formation and consumption respectively; At the steady state, the concentrations of being constant, its change with time is equated to zero:

$$\frac{d[A]}{dt} = \sum r_{A,f} - \sum r_{A,C} = 0$$

This procedure is carried out for each transient/intermediate and a set of n simultaneous equations with n unknowns (n = number of transients/intermediates) are obtained. These equations are solved to give the concentration of each steady state transient/intermediate. In addition certain reaction steps are found to proceed at almost equal rates after a long reaction time, i.e.; at the steady state. Considering the reactions.

$$A + B \xrightarrow{K1} C + D.$$

$$A + C \xrightarrow{K2} T$$, proceeding at rates r_1 and r_2 respectively. If $r_1 = r_2$, it follows that:

$$K\,[A][B] = K2\,[A][C]$$

i.e., $K1[B] = K2\,[C]$

Thus $[B] = \frac{K2}{K1}\,[C]$

Such a relationship can be substituted into the simultaneous equations (set up) Similarly, some rates may be small multiples of other reaction rates: e.g.; $r_1 = 2r_2$ etc. Rates which are too small in comparison to the others are neglected.

2.3.3 RESULTS AND CALCULATIONS

Transients: HO_2, HCO, OH, HCO_3.

Branching intermediate HCO_3H and H_2O_2.

It is found that at the steady state

$r_2 = r_3 = r_4 = r_5 = r_6 = r_7$.

$r_8 = r_9$.

$r_{10} = r_{11} = r_{12}$.

$$\frac{d[HO_2]}{dt} = 0 = -r_2 - r_3 - r_4 - r_{10} - r_{11} + r_5$$

But $r_3 = r_5$

$$\frac{d[HO_2]}{dt} = r_2 + r_4 + r_{10} + r_{11} = 0$$

i.e. $K2[HO_2][CH_2O] + K4[HO_2][CH_2O] + K10[HO_2][CH_2O] + K11[HO_2]^2 = 0$

$$K_2[CH_2O] + K4[CH_2O] + K_{10}[CH_2O] + K11[HO_2] = 0$$

$$K11[HO_2] = -[K2 + K4 + K10][CH_2O]$$

$$[HO_2] = -\frac{(K2 + K4 \quad K10)}{K11}[CH_2O]$$

From $r_2 = r_5$

$$K2[CH_2O][HO_2] = K5\,[HCO][O_2]$$

$$[HCO] = \frac{K2}{K5}\,\frac{[CH_2O]}{[O_2]}\,[HO_2]$$

$$= \frac{-K2}{K5}\left(\frac{K2 + K4 + K10}{K11}\right)\frac{[CH_2O]^2}{[O_2]}$$

$$\frac{d[HCO_3]}{dt} = r_6 - r_7 = 0$$

$$= K6[HCO][O_2] = K7[HCOH][HCO_3]$$

$$[HCO_3] = \frac{K6}{K7} \frac{[O_2]}{[CH_2O]} [HCO]$$

$$= -\frac{K6K2}{K5K7}\left(\frac{K2 + K4 + K10}{K11}\right)[CH_2O]$$

$$\frac{d[HCO_3H]}{dt} = r_7 - r_8 = 0$$

$$K7[CH_2O][HCO_3] = K8[HCO_3H]$$

$$[HCO_3H] = \frac{K7}{K8}[CHO_3][CH_2O]$$

$$= \frac{-K2\ K6}{K5\ K8}\left[\frac{K2 + K4 + K10}{K11}\right][CH_2O]^2$$

$$r_8 = r_9$$

$$K8[HCO_3H] = K9[CH_2O][OH]$$

$$[OH] = \frac{K8}{K9} \frac{1}{[CH_2O]} [HCO_3H]$$

$$= \frac{-K2\ K6\ K8}{K5\ K9\ K8}\left(\frac{K2 + K4 + K10}{K11}\right)\frac{1}{[CH_2O]}[CH_2O]^2$$

$$= \frac{-K2\ K6}{K5\ K9}\left[\left[\frac{K2 + K4 + K10}{K11}\right][CH_2O]\right.$$

The overall rate of reaction, w, is equal to the rate of consumption of CH_2O.

$$w = \frac{-d[CH_2O]}{dt}$$

$$= r_2 + r_3 + r_4 + r_7 + r_9 + r_{10} + r_{11}$$

r_1 is neglected being very small.

$$w = \frac{-d[CH_2O]}{dt} = K2\,[CH_2O][HO_2] + K3\,[CH_2O][HO_2] +$$

$$+ K4[CH_2O][HO_2] + K7\,[CH_2O][HCO_3] +$$

$$+ K9[CH_2O][OH] + K10;CH_2O][HO_2] + K11[HO_2]^2$$

$$= (K2 + K3 + K4 + K10)\,[CH_2O][HO_2] + K11[HO_2]^2$$

$$+ K7\,[CH_2O][HCO_3]$$

In addition from the steady state concentrations

$$K2 = K10\,,$$

$$K2 = K3 = K4$$

Hence substituting in the above equation

$$W = \frac{(4K2)(-3K2)}{K11}[CH_2O]^2 + \frac{K2K6}{K5}\left(-\frac{3K2}{K11}\right)[CH_2O]^2 +$$

$$+ \frac{K2K6}{K5}\left(-\frac{3K2}{K11}\right)[CH_2O]^2 + K11\left(-\frac{3K2}{K11}\right)^2[CH_2O]^2$$

$$= \left(-\frac{12K2^2}{K11} - \frac{6K2^2K6}{K5K11} + \frac{9K2^2}{K11}\right)[CH_2O]^2$$

$$= \left(-\frac{18K2^2}{K11} + \frac{9K2^2}{K11}\right)[CH_2O]^2\,, \qquad K5 \approx K6$$

$$= \frac{-9K2^2}{K11}[CH_2O]^2$$

$$= \frac{9A2^2}{A11}\, e^{-\frac{(2E2 - E11)}{RT}}\,[CH_2O]^2$$

Thus the overall activation energy

$$E = 2E2 - E11$$

$$= 2 \times 32.6 - 0.0 = 65.2 \text{ KJ/mole.}$$

which is of the same range as the experimental value of 74.4 KJ/mole obtained by Hessam.

It can also be seen that the overall order is 2 with respect

to formadehyde concentration and does not depend on the oxygen present.

At higher temperatures however, hydroformyl radical will decompose into hydrogen atom and carbon monoxide. Formic acid is expected to decompose and hydrogen peroxide will become a branching intermediate by producing most probably heterogeneously, hydroxyl radicals. Hence the following reaction steps were added to those in table 2.1 and integrated

			KJ/mole	
13.	$HCO \longrightarrow H + CO$	$2.5\ 10^{14}$	66.88	147
14.	$H + CH_2O \rightarrow H_2 + CHO$	1.10^{12}	0.00	148
			KJ/mol	
15.	$HCOOH \rightarrow CO + H_2O$	2.10^{8}	41.8	
16.	$HCOOH \rightarrow CO_2 + H_2$	2.10^{8}	50.16	
17.	$H_2O_2 + M \rightarrow OH + OH + M$	1.10^{12}	75.24	146
18.	$H_2O_2 \xrightarrow{WALL} H_2O + 1/2\ O2$	1.10^{8}	37.20	67

Between 500 - 600°C, the main products are in order of abundance, H_2O , CO, CO_2, H2. In fact the gap between H_2O and carbon monoxide narrowed as the temperature increased.

Representing the reaction rate constant K as

$$K = \frac{1}{t}\left[\frac{X}{aO(aO - X)}\right] \qquad \text{for a second order}$$

reaction, when aO is the initial concentration of formaldehyde and (aO - X) its concentration at time t, and X, its fractional disappearance, a graph of $\frac{X}{aO(aO - X)}$ versus t was a straight line, the slope of which is K This was done for different temperatures and the graph of $\log_{10}K$ against 1/T was plotted as shown in Fig. (2-2). The slope of this line represents E/2.3R

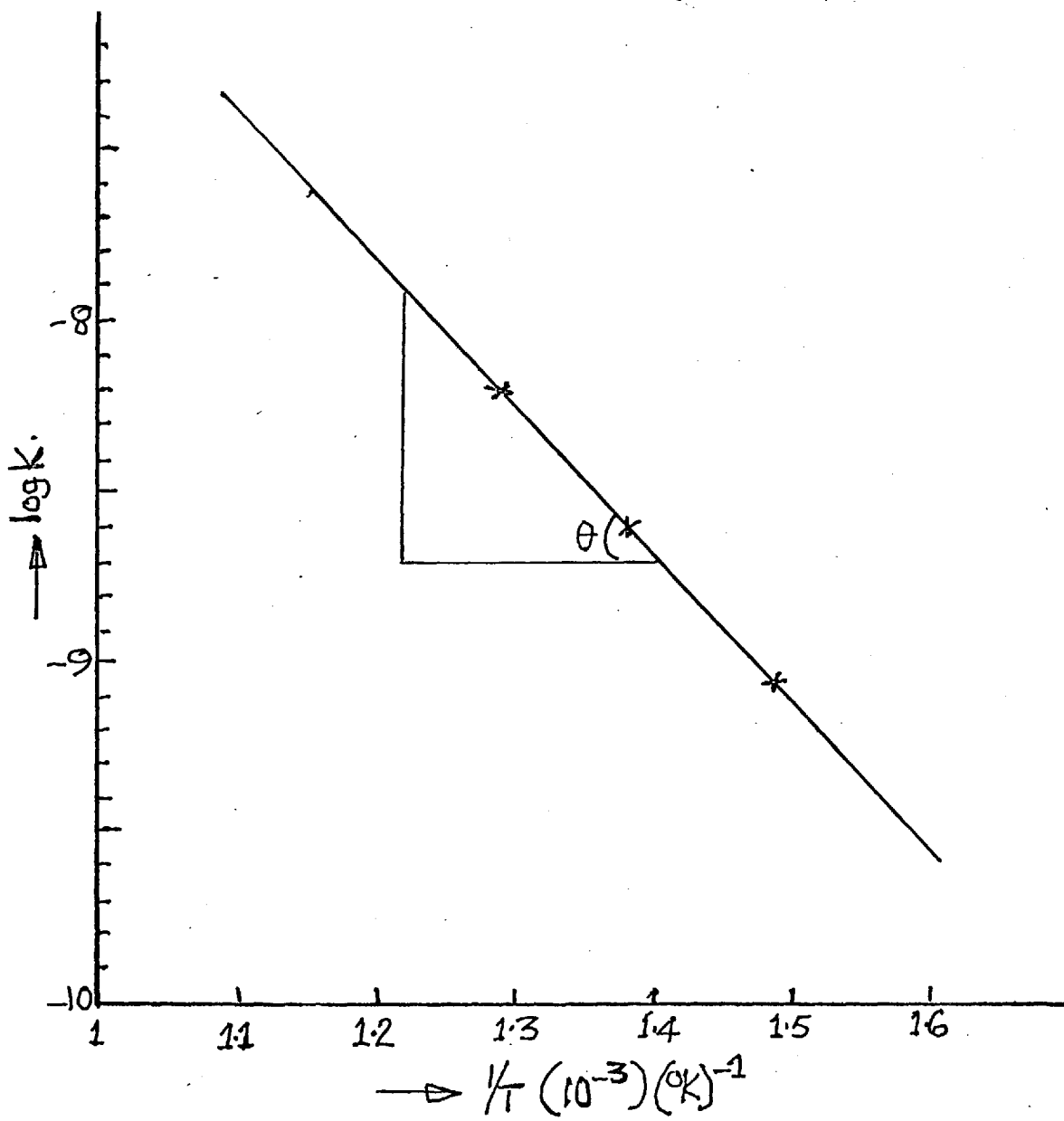

Fig 2-2. Calculation of the overall activation energy of HCHO oxidation

$$\text{Slope} = \frac{0.8}{0.185} = \frac{E}{2.3R}$$

$$E = \frac{0.8}{0.185} \times 2.3 \times 1.98 \quad \text{Kcal/mole}$$

$$= \frac{2.3 \times 1.98 \times 8}{1.85} \quad \text{Kcal/mole}$$

$$= 19.6 \text{ Kcal/mole} = 81.9 \text{ KJ/mole}$$

The mean value of $E = (15.6 + 19.6)\frac{1}{2}$

$$E = 17.6 \text{ Kcal/mole} = 73.6 \text{ KJ/mole}$$

It is thus concluded that the oxidation of formaldehyde involves a degenerate branched chain mechanism occurring at low temperatures by the decomposition of performic acid but at high temperatures hydrogen peroxide also acts as a degenerate branching intermediate.

The partial pressure profiles predicted by the extended model are shown in fig. 2-3, and the comparison with Hessams results and unextended model prediction is as shown in table 2-3. There is an increase both in water and carbon monoxide, clearly as a result of the termination reactions of HO_2. and the decomposition of formyl radical to generate more carbon monoxide. In addition there is a slightly faster consumption or decomposition of hydrogen peroxide and formic acid.

The extended model gave an activation energy of 81.9 KJ/mole which is still in the same range as that reported by Hessam but the average of the computed values 73.6 KJ. $mole^{-1}$ compares very well with the reported value of 74.4 KJ/mole.

TEMPERATURE = 400°C

TIME (MINS)	14 MINS		
	HESSAM	PREDICTED	EXTENDED MODEL
CH_2O	1.26	1.22	1.20
O_2	4.70	4.60	4.75
H_2O	14.50	14.50	15.50
CO	12.00	12.60	14.30
CO_2	9.00	9.25	10.20
H_2	6.30	6.25	6.20
HCOOH	5.20	5.30	3.80
H_2O_2	1.20	1.20	0.40

TABLE 2-3 COMPARISON OF HESSAMS EXPTAL RESULT WITH EXTENDED MODEL PREDICTION

2.4 ACETALDEHYDE OXIDATION

Gaseous acetaldehyde is relatively stable at moderate temperatures but a trace of oxygen accelerates its decomposition [55,85]. The combustion diagram of a mixture [18.8% CH_3CHO + 81.2% Air ($2N_2$ + $1O_2$)] is shown in fig. (2.4) Above 350°C its oxidation shows a pressure increase, but below 350°C, the reaction is accompanied by a rapid decrease in pressure at first, followed by a slow pressure increase. Below 295°C, a single cool flame occurs, but above 295°C. there are two cool flames.

The intermediate oxidation products in the lower slow combustion zone are mainly peroxides which decompose with temperature rise to produce more reactive free radicals. In the upper slow combustion region, the reaction starts with a rapid pressure increase due to rapid branching via decomposition of peroxy intermediates. The major products of acetaldehyde oxidation at about 400°C as reported by Hessam [87] are: H_2O CO, CO_2, H_2, CH_3COOH, HCHO and HCOOH, while the minor products are H_2O_2, CH_3OH, CH_4, $(CH_3)_2CO$, $(CH_3CO)_2$ and $(CH_3CO)_2O_2$. The intermediates reported are CH_3CO_3H and CH_3OOH.

At higher temperatures however, CH_3COOH, HCHO and HCOOH should decompose for example formaldehyde would pyrolyze to give hydrogen atom and formyl radical.

$$HCHO \longrightarrow H + CHO$$

The formyl radical would decompose to another hydrogen atom and carbon monoxide

$$CHO \longrightarrow H + CO$$

H. atoms would then engage in propagation reactions to boost H_2. Thus there would be an increase in CO as well as H_2 concentrations similarly formic acid may decompose into carbon monoxide and H_2O. Of course such compounds as $(CH_3)_2CO$, $(CH_3CO)_2$ and $(CH_3CO_2O_2$, would in all probability decompose. Their decomposition might be the source of methyl radicals

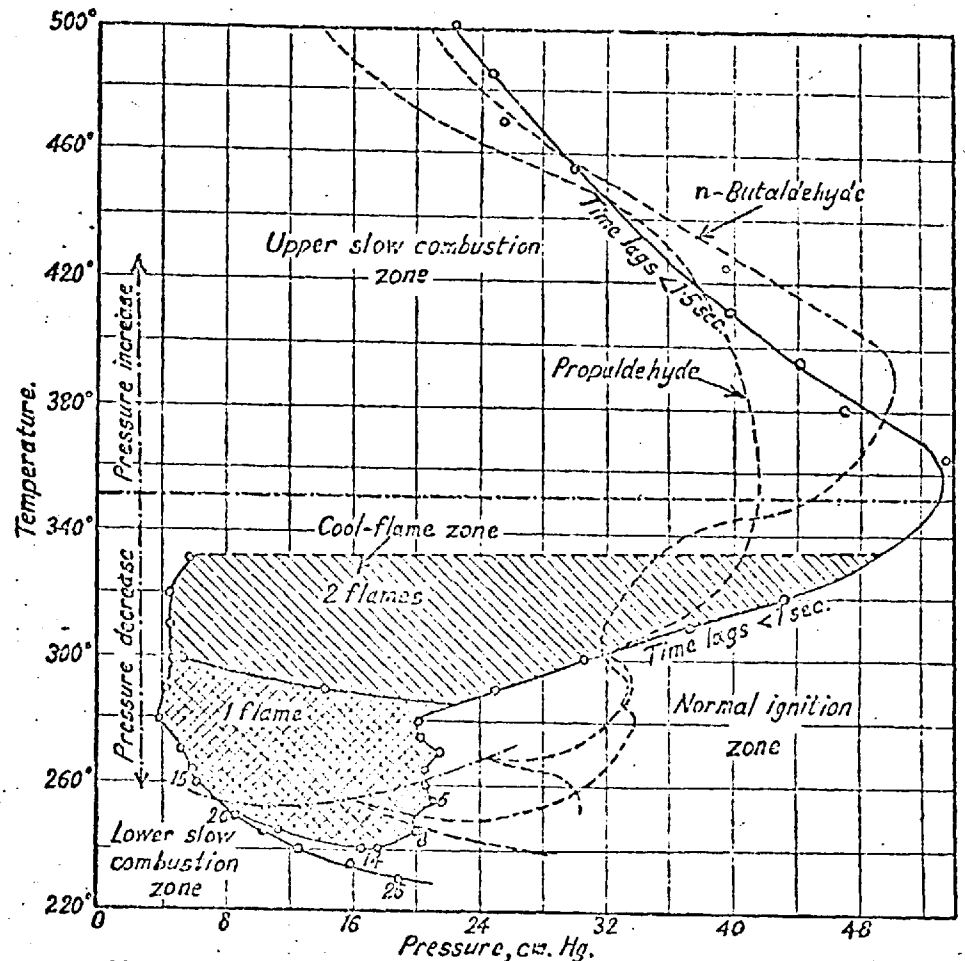

Fig 2-4 Combustion diagram of acetaldehyde.

which, by abstracting hydrogen atoms, yield the traces of methane observed. In addition hydrogen peroxide would be expected to play a more significant role as a branching intermediate as the temperature rises

$$H_2O_2 + M \longrightarrow .OH + .OH + M$$

Methyl hydroperoxide would likewise decompose homogeneously to give methoxy and hydroxyl-radicals.

$$CH_3OOH \longrightarrow CH_3O + .OH \qquad H = 133.7 \text{ KJ.mole}^{-1} \quad 18$$

Examining the reaction kinetics in the light of the reaction mechanisms postulated by other workers, it can be concluded that the reaction certainly involves a degenerately branched chain process.

The initiation step, as in all other alphatic aldehydes oxidation involves the reaction:

$$CH_3CHO + O_2 \longrightarrow CH_3CO + HO_2 \qquad (1)$$

which has an endothermicity of about 170 KJ.mole^{-1} 87 ·

ropagation involves all the reactions of CH_3CO and HO_2 and the subsequent decomposition of intermediates formed via these radicals.

The acyl radicals undergo reaction with molecular oxygen to produce peracyl and alkyl peroxy radicals;

$$CH_3CO. + O_2 \longrightarrow CH_3CO_3 \qquad (2)$$

$$CH_3CO + O_2 \longrightarrow CH_3O_2 + CO \qquad (3)$$

Peracyl radicals, CH_3CO_3. may either form peracids by abstracting hydrogen atoms or decompose to give other radicals:

$$CH_3CO_3 + CH_3CHO \longrightarrow CH_3CO_3H + CH_3CO \qquad (4)$$

$$CH_3CO_3 \longrightarrow CH_2O + HCO_2 \qquad (5a)$$

$$CH_3CO_3 \longrightarrow CH_3O + CO_2 \qquad (5b)$$

The radicals $CH_3O_2\cdot$, $CH_3O\cdot$ and $HCO_2\cdot$ can abstract hydrogen atoms from acetaldehyde to give CH_3OOH, CH_3OH and HCOOH respectively.

At high temperatures however CH_3CO will certainly decompose.

$$CH_3CO\cdot + M \longrightarrow CH_3\cdot + CO + M \qquad (6)$$

Methyl radicals will react with oxygen according to

$$CH_3\cdot + O_2 \longrightarrow CH_3O_2\cdot \text{ , or}$$

$$CH_3\cdot + O_2 \longrightarrow CH_2O + \dot{O}H \qquad (7)$$

Reaction (7) is certainly favoured at high temperatures.

The peracid, CH_3CO_3H, and methylhydrogperoxide CH_3OOH are responsible for branching at low temperature:

$$CH_3CO_3H \longrightarrow CH_3CO_2\cdot + \cdot OH$$

$$CH_3CO_3H \longrightarrow CH_3COOH + O \qquad (8)$$

$$CH_3OOH \longrightarrow CH_3O\cdot + \cdot OH \qquad (9)$$

The activation energies for (8) and (9) have been reported to be 18 ± 3[50] and 133.7[88] KJ/mole respectively. All three reactions might occur but reaction (9) is the most likely.

Reaction between acetaldehyde and peracidic acid may occur, possibly by two modes[83]. They are (a) aldolic and (b) ketonic condensations.

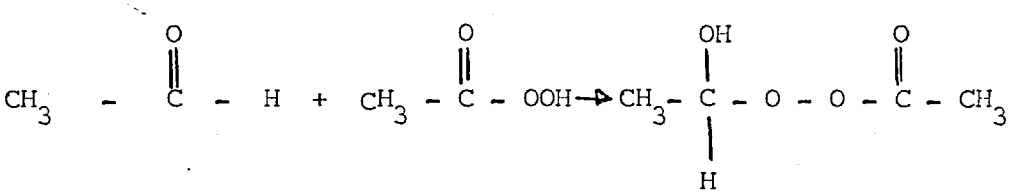

(A)

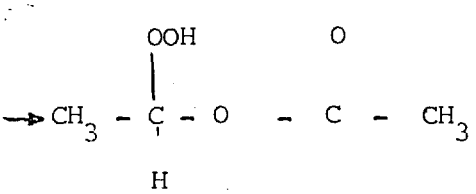

(B)

Compound (A) has a lower (O - O) dissociation energy than that of the parent peracid. Structure (B) is reported to have a bond dissociation energy about similar to that for normal hydrogperoxides [83]. Thus compound (A) is the more likely of the two. Even then both A and B can not stand high temperatures.

CH_3O_2H will decompose into CH_3O + OH. thus releasing .OH radicals for propagation.

$$CH_3CHO + OH \longrightarrow CH_3CO + H_2O \quad (10)$$

$$OH + CO \longrightarrow H + CO_2 \quad (11)$$

$$H + O_2 \longrightarrow HO_2 \quad (12)$$

$$CH_2O + OH \longrightarrow H_2O + CHO \quad (13)$$

$$CH\ O + O_2 \longrightarrow HCO_3. \quad (14)$$

$$HCO_3 \longrightarrow HO_2 + CO \quad (15)$$

$$HCO \longrightarrow H + CO \quad (16)$$

Hydrogen peroxide is formed as a result of the abstraction of hydrogen atoms by the radical HO_2;

$$HO_2 + CH_3CHO \longrightarrow H_2O_2 + CH_3CO \quad (17)$$

$$HO_2 + CH_2O \longrightarrow H_2O_2 + CHO \quad (18)$$

Hydrogen peroxide can then act as a branching intermediate

$$H_2O_2 \longrightarrow OH + OH \quad (19)$$

Hydrogen will be formed by abstraction reactions of hydrogen atoms.

$$H + CH_3CHO \longrightarrow H_2 + CH_3CO \quad (20)$$

Termination reactions would involve such reaction steps as:

$$CH_3CO + OH \longrightarrow CH_3COOH \quad (21)$$

$$OH + OH + M \longrightarrow H_2O_2 + M \quad (22)$$

$$H + H + \longrightarrow H_2 + M \quad (23)$$

$$CH_3CO_3 + OH \longrightarrow CH_3COOH + O_2 \quad (24)$$

$$CH_3O + CH_3O \longrightarrow (CH_3O)_2 \quad (25)$$

$$CH_3O + CH_3 \longrightarrow CH_3OCH_3 \quad (26)$$

$$CH_3COOH \xrightarrow{Wall} \text{Products} \quad (27)$$

$$H_2O_2 \xrightarrow{Wall} H_2O + \tfrac{1}{2}O_2 \quad (28)$$

2.4.1 ACETALDEHYDE OXIDATION MECHANISM

A mechanism comprising the following reaction steps was therefore proposed as accounting for the observed kinetics of the oxidation of acetaldehyde between 400 - 600°C.

TABLE 2.4

	REACTION	A/sec^{-1}	E(KJ/mole^{-1}
1.	$CH_3CHO + O_2 \longrightarrow CH_3CO + HO_2$	$1.11 0^9$	121.2 [140]
2.	$CH_3CO + O_2 \longrightarrow CH_3CO_3$	7.10^8	0.0 [142]
3.	$CH_3CO + M \longrightarrow CH_3 + CO + M$	1.66×10^{10}	56.43 [149]
4.	$CH_3 + O_2 \longrightarrow CH_2O + OH$	6.10^7	10.45 [150]
5.	$CH_3CO_3 + CH_3CHO \longrightarrow CH_3CO_3H + CH_3CO$	2.10^9	29.26 [151]
6.	$CH_3CO_3H \longrightarrow .OH + CH_3 + CO_2$	1.10^{12}	66.88 [152]
7.	$CH_3CHO + OH \longrightarrow H_2O + CH_3CO$	1.10^9	16.72 [153]
8.	$HO_2 + CH_3CHO \longrightarrow H_2O_2 + CH_3CO$	1.10^9	29.20
9.	$H_2O_2 + M \longrightarrow OH + OH + M$	$3.2.10^{14}$	150.50 [146]
10.	$OH + OH \longrightarrow H_2O_2$	7.6×10^{14}	0.0 [146]

11.	$CH_3CO + OH \longrightarrow CH_3COOH$	1.10^{11}	0.0
12.	$CH_2O + OH \longrightarrow H_2O + HCO$	2.10^{9}	20.00[154]
13.	$CH_2O + HO_2 \longrightarrow HCO + H_2O_2$	1.10^{8}	8.36[155]
14.	$CHO + O_2 \longrightarrow CO + HO_2$	2.10^{8}	0.00
15.	$OH + CO \longrightarrow H + CO_2$	$5.6.10^{8}$	4.18[156]
16.	$H + CH_3CHO \longrightarrow H_2 + CH_3CO$	1.10^{11}	20.90[157]
17.	$H. + O_2 + M \longrightarrow HO_2 + M$	$2.04.10^{11}$	68.97
18.	$H + H + M \longrightarrow H_2 + M$	$7.6.10^{11}$	0.00
19.	$CH_3CO_3 + OH \longrightarrow O_2 + CH_3COOH$	1.10^{10}	0.00[142]
20.	$CH_3COOH \longrightarrow$ Products	1.10^{14}	142.00
21.	$H_2O_2 \longrightarrow H_2O + 1/2\ O_2$	1.10^{8}	35.90[67]

Typical partial pressure profiles is as shown in Fig. 2.5. The homogeneous decomposition of hydrogen peroxide into hydroxyl radicals is branching step. But at the initial stages of the reaction, the termination reactions of peroxy radical HO_2 to give inert products is predominant. This must have led to the very small formation of hydrogen peroxide. Formaldehyde is formed in appreciable quantity but is easily attacked by the hydroxyl radicals.

CALCULATION

The steady state approximation is then applied to calculate the overall order as well as the overall energy of activation of the process.

(a) $r_7 = r_{11}$

$$K7\ [CH_3CHO][OH] = K11[CH_3CO][OH]$$

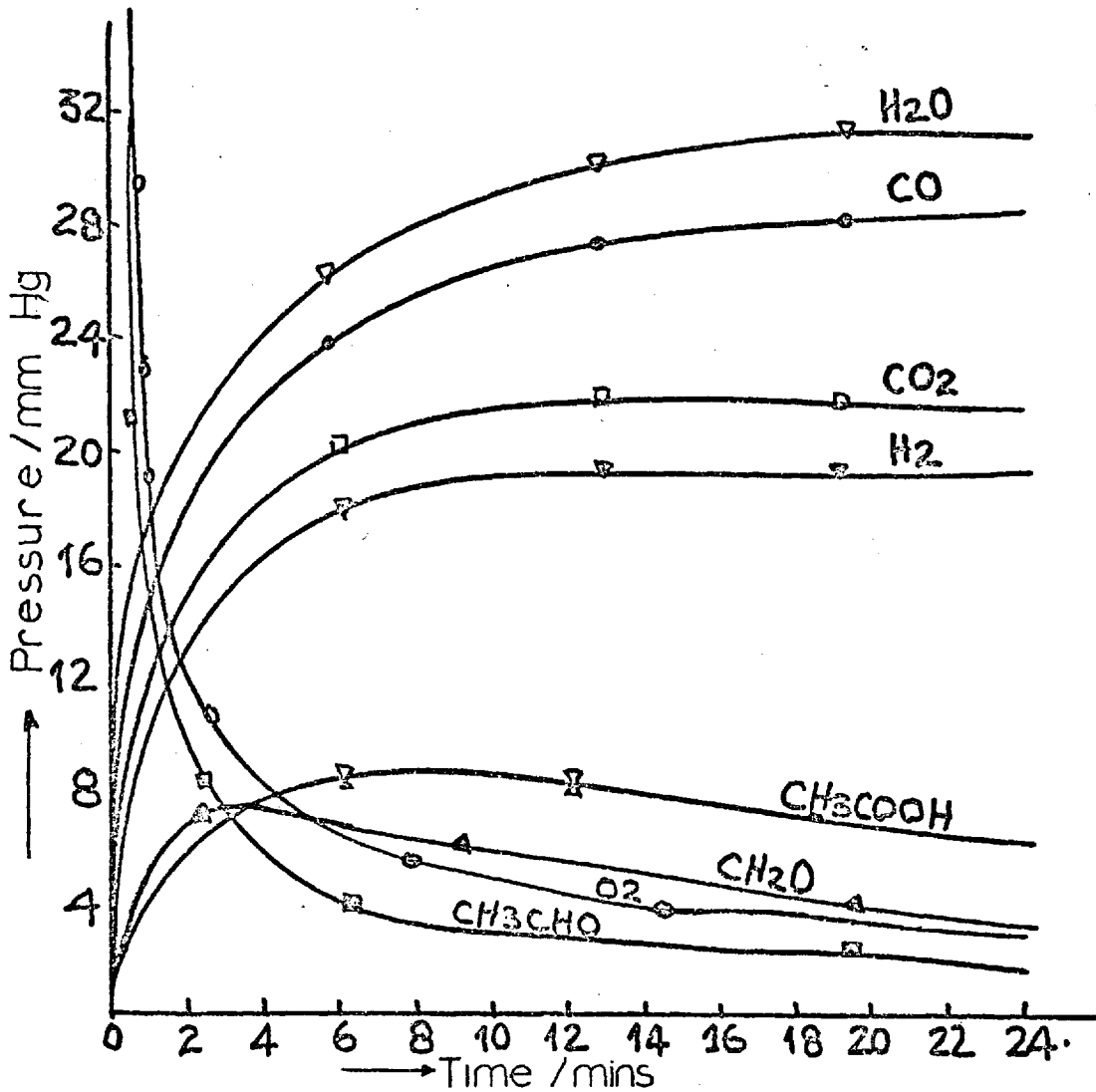

Fig 2-5 Product distribution from acetaldehyde oxidation at 500°C

$$[CH3CO] = \frac{K7}{K11}[CH_3CO][OH]$$

(b) $$\frac{d[CH_3CO_3]}{dt} = K2\,[CH_3CO][O_2] - K5\,[CH_3CO_3][CH_3CHO]$$

$$- K19[CH_3CO_3][OH] = 0$$

$$K19[CH_3CO][OH] = r_{19} \ll r_2 \quad or \quad r_5$$

$$\frac{d[CH_3CO_3]}{dt} = K2[CH_3CO][O_2] - K5\,[CH_3CO_3][CH_3CHO] = 0$$

Hence $$[CH_3CO_3] = \frac{K2}{K5}\frac{[CH_3CO][O_2]}{[CH_3CHO]}$$

$$[CH_3CO_3] = \frac{K2}{K5} \cdot \frac{K7}{K11}\,[O_2]$$

(c) $$r_4 = r_5$$

$$K4[CH_3][O_2] = K5[CH_3CHO][CH_3CO_3]$$

$$[CH_3] = \frac{K5}{K4}\,\frac{[CH_3CHO]}{[O_2]}\,\frac{K2}{K5}\cdot\frac{K7}{K11}[O_2]$$

$$[CH_3] = \frac{K2\ K7}{K4\ K11}\,[CH_3CHO] = \frac{K2\ K7}{K5\ K11}\,[CH_3CHO]$$

(d) $$r_3 = r_{10}$$

$$K3\,[CH_3CO] = K10[OH]^2$$

$$[OH]^2 = \frac{K3}{K10}\,[CH_3CO]$$

$$[OH]^2 = \frac{K3}{K10}\cdot\frac{K7}{K11}\,[CH_3CHO]$$

$$[OH] = \left(\frac{K3K7}{K10K11}\right)^{\frac{1}{2}}\,[CH_3CHO]^{\frac{1}{2}}$$

(e) $r_{10} = r_{16}$

$$K10[OH]^2 = K16[CH_3CHO][H]$$

$$[H] = \frac{K10}{K16} \frac{[OH]^2}{[CH_3CHO]}$$

$$= \frac{K3\ [CH_3CO]}{K16[CH_3CHO]}$$

$$= \frac{K3}{K16} \cdot \frac{K7}{K11} \frac{[CH_3CHO]}{[CH_3CHO]} = \frac{K3K7}{K11K16}$$

(f) $r_8 = r_5$

$$K8\ [CH_3CHO][HO_2] = K5\ [CH_3CHO][CH_3CO_3]$$

$$[HO_2] = \frac{K5}{K8}\ [CH_3CHO_3]$$

$$= \frac{}{K8} \frac{K2\ \ K7}{K11}\ [O_2]$$

$$= \frac{K2\ K7}{K8K11}\ [O_2]$$

The rate of reaction W is equal to the rate of acetaldehyde disappearance.

$$W = -\frac{d[CH_3CHO]}{dt}$$

$$= r_5 + r_7 + r_8 + r_{16}$$

$$= K5[CH_3CHO][CH_3CO_3] + K7[CH_3CHO][OH] +$$

$$= K8[CH_3CHO][HO_2] + K16[H][CH_3CHO]$$

$$= [CH_3CHO][K5[CH_3CO_3] + K7[OH] + K8[HO_2] + K16[H]$$

$$= [CH_3CHO]\frac{K2.K7}{K11}[O_2] + K7\left(\frac{K3K7}{K1OK11}\right)^{1/2}[CH_3CHO]^{1/2} +$$

$$+ \frac{K2K7}{K11}[O_2] + K16\frac{K3K7}{K11K16}$$

$$= [CH\ CHO]\frac{2K2K7}{K11}[O_2] + K7\left(\frac{K3K7}{K1OK11}\right)^{1/2}[CH_3CHO]^{1/2} + \frac{K8K7}{K11}$$

$$= K1[CH_3CHO]^{3/2} + K2[CH_3CHO][O_2] + K3$$

where $K1 = K7\left(\frac{K3K7}{K1OK11}\right)^{1/2}$

$K2 = \frac{2K2K7}{K11}$, and

$K3 = \frac{K3K7}{K11}$

It can be seen that the terms K2 and K3 are small in comparison with K1 Hence, the overall rate of reaction W can be represented as:

$$W = K1[CH_3CHO]^{3/2}$$

$$W = K7\left(\frac{K3\ K7}{K1OK11}\right)^{1/2}[CH_3CHO]^{3/2}$$

The overall order is thus 3/2

$$E = E_7 + 1/2(E_3 + E_7 - E_{10} - E_{11})$$

$$= 4+1/2(13.5 + 4 - 0)$$

$$= 4 + 17.5/2 = 4 + 8.75)$$

$$= 12.75 \text{ Kcal/mole} = (53.30 \text{ KJ.mole}^{-1})$$

The overall activation energy is thus 53.30 KJ/mole which compares favourably with the reported value of 57.60 KJ/mole. The rate of acetaldehyde oxidation can therefore be represented as:

$$W = A_7 \frac{3/2 \quad A_3^{1/2}}{(A_{10} A_{11})^{1/2}} \exp\left(\frac{-53.30}{RT}\right) [CH_3CHO]^{3/2}$$

$$= 1.47 \times 10^9 \exp(-53.30/RT)][CH_3CHO]^{3/2}$$

The following observations apply to both formaldehyde and acetaldehyde oxidation systems.

(1) The ratio CO/CO_2 decreases as the temperature increases, and also decreases as the reaction reactions proceed.

(2) The rate of formation and decomposition of hydrogen peroxide and other intermediates increases with an increase in temperature.

(3) The rate of formation of formic acid decreases as temperature is increased.

(4) At the early stages of reaction, water vapour is produced in greater amount at higher temperatures than at lower temperatures. This must be due to the fact that higher temperatures favour the formation of hydrogen peroxide which easily decomposes to give hydroxyl radicals, which, in turn, abstract hydrogen atoms to form water.

CHAPTER III

Chapter III

EXPERIMENTAL METHODS

3.1 MATERIALS:

Each chemical used showed no sigificant trace of impurity as indicated by its mass spectrum.

PROPANE

Propane was obtained from B.O.C. Special Gases. It was of C.P. Grade 99.5%, with specific volume 0.53. The cylinder valve outlet was CGA 510.

PROPYLENE

C_3H_6, 99.8% pure, with specific volume of 0.566 was also obtained from B.O.C. Special Gases.

ETHANE, METHANE, ETHYLENE

These gases were obtained from B.O.C. Special Gases, C.P. Grade. Ethane was 99.8% pure; with specific volume of 0.80; methane, had a specific volume of 1.48 and 99.5% purity: ethylene was 99.95% pure.

HYDROGEN

H_2 was obtained from Special Gases in special cylinders. It has a specific gravity of 0.0694 (referred to air), B.P. = 20.2^{o}K, M.P. = 13.8^{o}K, colourless gas and inflammable.

WATER

H_2O, with specific gravity of 1.00 (4^{o}C) in liquid form, and 0.915 (0^{o}C), colourless odourless, B.P. = 100^{o}C, and M.P. = 0^{o}C, was prepared by vaporization of de-gassed water maintained under low pressure in a trap, and then introduced into the mass spectrometer for calibration purposes. To de-gas the water a number of alternative freezing, evacuating and remelting processes were carried out.

ACETALDEHYDE

CH_3CHO, is a liquid with specific gravity of 0.783 at 18°C, is colourless, flammable and has a pungent odour. B.P. = 20.2°C, M.P. =123.5°C, vapour pressure = 740 mm. Hg. (20°C), flash point = -40°F (open cup) and miscible with water, alcohol and other solvents.

CARBON MONOXIDE

CO, with specific gravity of 0.806 (-195.1°C), [95] colourless, faint metallic odour, toxic, B.P. = -195°C, and M.P. = -207°C was obtained from B.O.C. with 99.7% purity. It was used mainly for the calibration of the mass spectrometer.

CARBON DIOXIDE

CO_2, with specific gravity of 1.101 (-37°C), liquid, 1.56(-79°C) solid, and 1.53 gas, colourless (gas or liquid), white snow-like solid, B.P. = -78°C and M.P. = -56.6°C (5.2 atm.) was 99.9% pure and obtained from B.O.C. It was used for calibration.

OXYGEN, AIR, N2

O_2, with specific gravity of 1.14 (-183°C), colourless, odourless, M.P. = -218.76°C, B.P. = -182.9% was obtained as C.P. grade (99.5% pure) from B.O.C. Air, also from B.O.C. was 99.9% pure. Nitrogen grade supplied by B.O.C. It has M.P. = -210°C and B.P. = -195°C.

3.2 APPARATUS

3.2.1 REACTION SYSTEM

Gas chromatography has been the main tool for analysing the products of pyrolysis. In this work, another versatile tool, the mass spectrometer, is employed to qualify and quantify such pyrolysis products and then proceed to establish the mechanism/model that best describes the kinetics of the observed products spectrum as a function of time and temperature.

The flow diagram is as shown in Fig. 3-1. It consists essentially of propane and nitrogen cylinders, flow meters (Rotameters purchased from

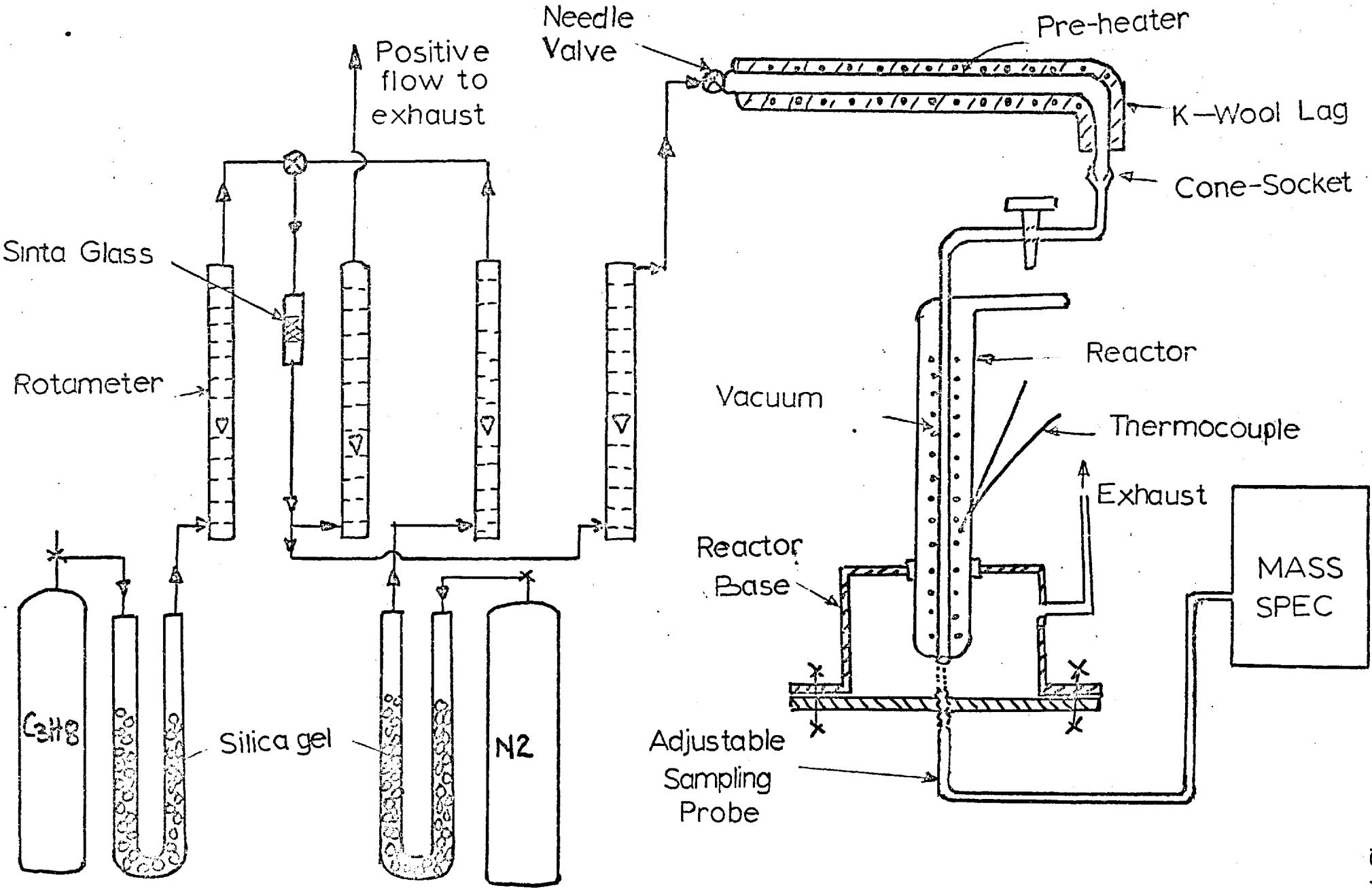

Fig 3-1 SCHEMATIC DIAGRAM OF THE FLOW SYSTEM

Rotameter Manufacturing Co. Ltd., Purley Way, Croydon), Sinta glass, reactor and reactor-base and a sampling probe of very narrow diameter that conveys the products into the mass spectrometer. Propane and nitrogen are separately passed through a U-tube containing silica-gel to remove any element of water. The Sinta glass effects perfect mixing of the gases and the idea of introducing positive flow is to eliminate fluctuation in flow-rate. The needle valve (purchased from Clockhouse Engineering and Instr. Co., Brookhill Road, New Barnet, Herts). and the tap T_3 apart from controlling flow-rates, could also act as a flame trap. The pre-heater is capable of attaining 100-150^{o}C and it is lagged with Triton Kaowool (from A.D. Wood (London) Ltd.) to prevent heat loss. The reactor which approximates to a plug flow (all flows being laminar) is made of quartz. It has a central bore of approximately one centimeter, surrounded by vacuum of 10^{-6} - 10^{-5} torr. The heating circuit is as shown in Fig.(3-2). The reactor is coupled to its base via a viton 'O'-ring and the sampling probe passing through the base of the flange is adjustable to permit sampling from any zone in the reactor, residual gases are let off into the fume chamber.

The schematic diagram of the reactor is as shown in Fig. 3-3. The thermocouple TC in the vacuum chamber indicates how much vacuum there is. If the temperature went up above 250^{o}C, it would mean that the vacuum was gone in which case the viton 'O'-ring would burn and there would be air-leakage into the system. The thermocouple is of chrom-alumel.

3.2.2 HEAT TRANSFER CONSIDERATIONS

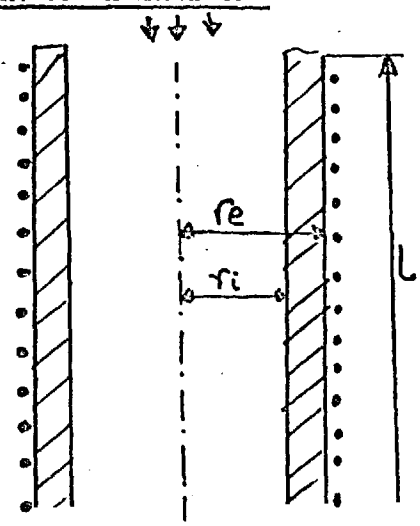

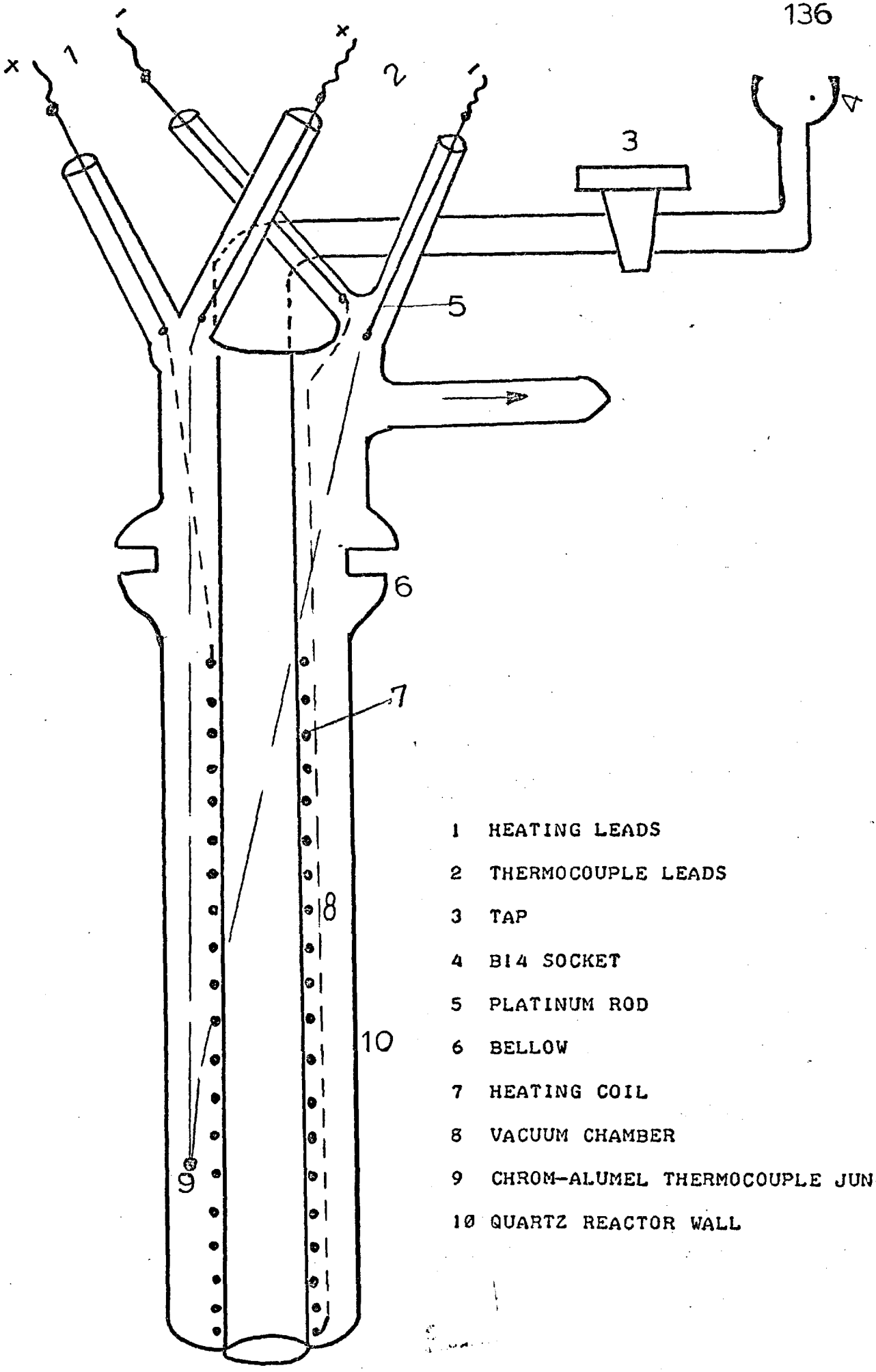

1 HEATING LEADS

2 THERMOCOUPLE LEADS

3 TAP

4 B14 SOCKET

5 PLATINUM ROD

6 BELLOW

7 HEATING COIL

8 VACUUM CHAMBER

9 CHROM-ALUMEL THERMOCOUPLE JUNCTION

10 QUARTZ REACTOR WALL

Fig 3-3 Schematic diagram of the reactor.

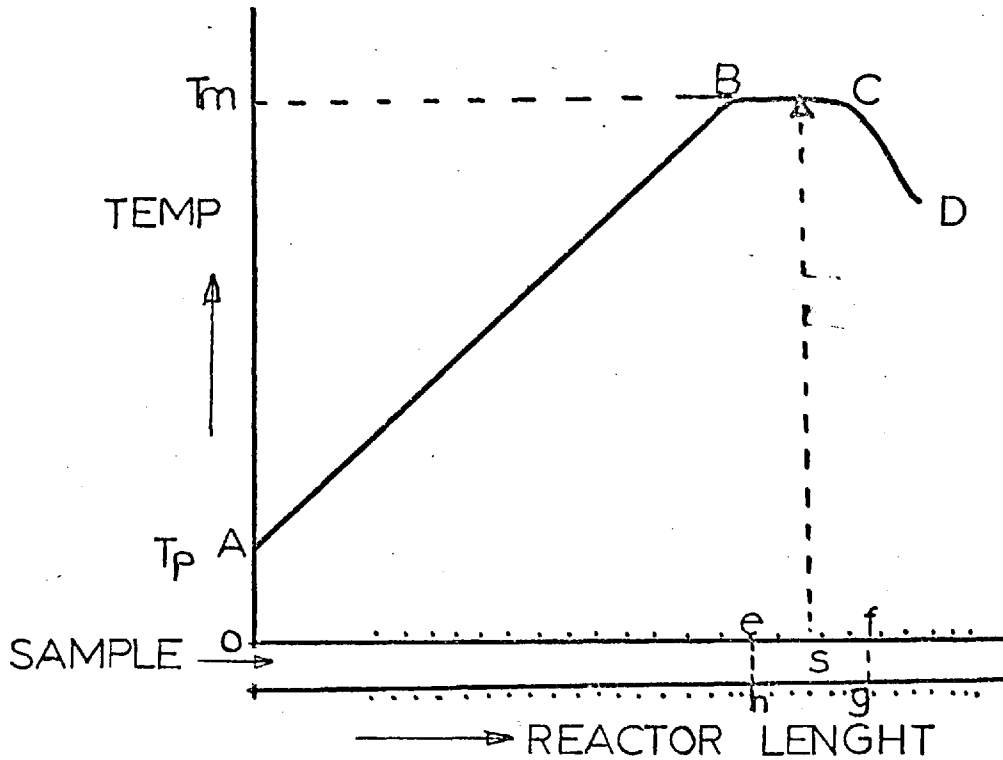

Fig 3-4. Temperature profile in the reactor.

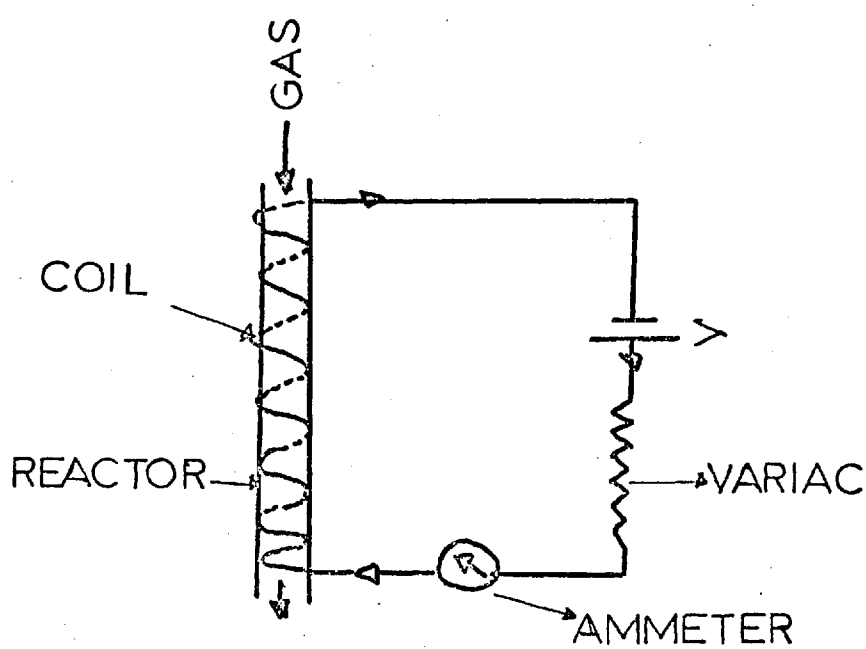

Fig 3-2 Heating Circuit.

Considering a length 1 of the reactor where r_i = inner radius, r_e = outer radius and $r_e - r_i = \delta$ = thickness of the inner tube, the heat characteristics can be expressed by isolating a thin coaxial segment.

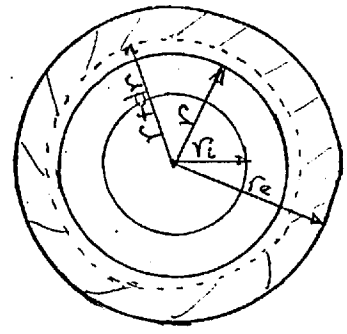

Total heat flux $Q = \frac{\lambda}{d\delta} A.\ dt$ (Kcal/unit time) (1)

$$Q = \frac{\lambda}{d\delta} 2\pi rl\ dt \qquad (2)$$

where; λ = thermal conductivity (Kcal/m.h. grd)

$\delta = r_e - r_i$

$d\delta = d_r$ = thickness of the thin section.

$A = 2\pi rl$ = laterial area of thin cylinder

l = heated length of cylindrical tube

dt = temperature change (^oC)

from equation (2)

$$Qdr = 2\pi rl.\ dt$$

$$\frac{dr}{r} = \lambda.\frac{2\pi l}{Q}\ dt$$

$$\int_{r_i}^{r_e} dr = \lambda.\frac{2\pi l}{Q} \int_{t_i}^{t_e} dt \qquad (3)$$

t_e, t_i represent temperatures on the outside and inside of the tube respectively.

$$\ln\left(\frac{r_e}{r_i}\right) = \lambda \frac{2\pi l}{Q} (t_e - t_i) \qquad (4)$$

From which heat flux, Q, can be expressed as: $Q = \lambda\ 2\pi l\ \frac{(t_e - t_i)}{\ln \frac{r_e}{r_i}}$

$$= \frac{\lambda}{r_e - r_i}\ 2\pi l\ \frac{r_e - r_i}{\ln r_{e/r_i}}\ (t_e - t_i) \qquad (5)$$

replacing $(r_e - r_i)$ with δ, and $(t_e - t_i)$ with t, and representing the mean radius r_m as

$$r_m = \frac{r_e - r_i}{\ln r_{e/r_i}} = \frac{r_e - r_i}{2.3 \log r_{e/r_i}}$$

the lateral area, A_m, can be expressed as: $A_m = 2\pi r_m l$.

r_m is the mean radius on log. basis. Thus Q, the heat flux, takes the form

$$Q = \frac{\lambda}{\delta}\ A_m .\ t \qquad (6)$$

Similarly the logarithmic mean diameter d_m can be expressed as:

$$d_m = \frac{d_e - d_i}{\ln \frac{d_e}{d_i}} = \frac{d_e - d_i}{2.3 \log \frac{d_e}{d_i}},$$

Hence $A_m = \pi d_m l$.

Q should be taken as the effective heat passing the reactor wall and thus available for pyrolysing the gas. Obviously some heat will be lost by conduction through the walls of the tube. The vacuum reduces convective and radiative heat transfer, thus protecting the 'O'-ring, so long as excessive heating is not applied.

The gas entering the heated reactor begins to take up heat and its temperature will thus rise as it passes through the reactor. Whether or not it pyrolyzes is dependent upon the amount of heat supplied and of course on the flow rate of the gas.

If V is the flow rate of the gas, S_g, its specific heat, and t', its change in temperature as it passes through the heated tube, then

$$Q = \frac{\lambda}{\delta}\ A_m \Delta t = V . S_g\ \rho_g . \Delta t' \qquad (7)$$

where ρ_g is the density of the gas.

Hence: $\Delta t' = \frac{\lambda}{\delta} \cdot \frac{A_m}{Sg . \rho g} \cdot \frac{1}{V} \cdot \Delta t'$

If T_o is the inlet temperature of the gas and T, its temperature at any point in the reactor $t' = T - T_o$

$$T - T_o = \frac{\lambda}{\delta} \frac{A_m}{\delta g \cdot \rho g} \frac{1}{V} \cdot \Delta t$$

$$T = \frac{\lambda}{\delta} \frac{A_m}{Sg \ \rho g} \frac{1}{V} \cdot \Delta t + T_o \qquad (8)$$

This temperature profile is as shown below:

3.2.3. REACTOR CALIBRATION

The typical temperature profile is as shown in Fig. 3-4. The pre-heated sample enters the reactor at a temperature T_p corresponding to OA. Segment AB shows a gradual rise in temperature as the gas flows from the inlet to the exit of the reactor. BC represents the isothermal zone which corresponds to the highest temperature T_m attainable under the existing conditions. This length BC is critical in the final analysis. Then follows section CD - a fall in temperature. The segment BC varies with changes in flow rates and temperatures. At a particular flow rate V_r and temperature T, an increase in T effects an increase in B - C, while an increase in V_r at constant T has the same effect. Thus a moving zone can be generated by varying V_r and T. The sampling point is at the mid-point of the segment B - C i.e. point S in the reactor. The kinetic reaction zone for the isothermal temperature T_m is the volume efgh, and the space time is defined as the volume of this, reaction zone divided by the gas flow rate [13]. The portion A - B becomes steeper with increase in temperature but reduces in slope with increase in flow rates. A chrom-Alumel thermocouple was employed for these temperature measurements.

3.3. ANALYTICAL SYSTEM (MASS SPECTROMETER)

3.3.1. INTRODUCTION

Mass spectrometry deals with the separation of gaseous ions of differing mass by the action of electric and magnetic fields, and with the

measurement of the abundance of the various ionic species revealed by this separation. The mass spectrometer thus identifies isotopes, measures their relative abundances, and makes possible tracer work with separated stable isotopes from more complex compounds. It usually forms ions by dissociation as well as by simple ionization, and gives a spectrum of masses which is characteristic of the compound for each set of ionizing conditions.

If a mixture is analysed, the resulting spectrum often yields a qualitative analysis by inspection, and a quantitative analysis may be made if calibrating spectra of the pure components are available. In many industrial applications, the spectrometer must compete with conventional methods of analysis, though economies can be effected only if a considerable number of samples are run each day. On the other hand, many complex analyses can be performed in no other manner, so that at least, access to a mass spectrometer for occasional use is almost a necessity for much research particularly in organic analysis. At present mass spectrometry is widely used to characterize or identify unknown compounds, to analyse mixtures, to trace compounds labelled with stable isotopes, to study the mechanisms and kinetics of reactions, and to determine ionization potentials and the strengths of chemical bonds. It is thus easy to visualise its playing an increasing role in the automation of chemical industry.

3.3.2. PRINCIPLES OF THE METHOD

When the molecules or atoms of a gaseous substance at very low pressure are bombarded by electrons from a heated filament or other source, both positively and negatively charged ions are produced. If the electrons are sufficiently energetic, they will not only produce molecular ions but will also break chemical bonds within the molecule. Some of the molecular fragments may be neutral, others will be positive ions having a deficiency of one, two, or more electronic charges, while still others may have excess electrons and be negative ions. If the pressure is low enough, the ions may travel over lengthy paths before losing their charges

by collisions with other molecules or with the walls of the container. While ionized, these gas molecules and fragments may be caused to move by applying an electric field. If such a field is produced between succesive parallel plates, positive ions moving towards the more negative plates can be collimated into a beam by suitable defining slits. In the absence of any other field, this beam will continue in a straight line, and its presence may be detected by its effect on a photographic plate or by the electrical effect of its net positive charge.

Such a beam of ions is deflected by any magnetic field which crosses its direction of flow. If the field is perpendicular to the motion, the deflection Y, of an individual ion is proportional to the strength of the magnetic field, H, and the ionic charge, e, and is inversely proportional both to the mass, m, and the velocity V, with which the ion moves. Thus:

$$y = k(eH/mV) \qquad (1)$$

If the moving ion is influenced by an electrical field of strength E in a direction also perpendicular to its motion, it will be deflected independently a distance x, given by:

$$x = k' (eE/m y^2) \qquad (2)$$

where k, k' are constants of the apparatus.

96

In the spectrograph devised by J.J. Thomson the electric and magnetic fields were arranged in the same direction such that the deflections x and y were at right angles to each other, and the locus of any ionic was defined, by combining equations (1) and (2), by

$$y^2/x = \frac{k^2}{k'} \frac{eH^2}{mE} = \text{constant} \qquad (3)$$

It can be seen from equation (3) that the locus defines a parabola, so that whenever ions of different masses are present, a number of separable parabolas are observed. The loci of various masses could be identified and m/e measured by their displacements, while the relative abundance of each ion could be estimated by the blackening produced on the photographic

plates. But the exact measurement of displacements was inconvenient if not impossible. This led Aston[97] and Dempster[98] to develop improved mass spectrometers with better resolutions and higher intensities using the same principles of electronic and magnetic deflection but different arrangement of fields with the x and y deflections separated by 180° instead of 90°, so that ion beams for various values of m/e were focussed at points along a straight line. This is the working principle of the MS10-C2 mass spectrometer employed in the present work.

3.3.3 MS10-C2 MASS SPECTROMETER

The schematic arrangement of the MS10-C2 mass spectrometer is as shown in Fig. (3 - 5). Samples are analysed by introducing them as gas into the analyser tube where the constituent molecules are ionised within the 'ion source cage' by subjecting them to bombardment by a controlled beam of electrons originating from a hot wire filament. The positive ions so formed are characteristic of the sample being analysed. Any charged particle (positive radical ions) acquires its velocity on falling through electrostatic potential difference V. Its potential energy eV must be the same as its kinetic energy after acceleration. Thus:

$$\frac{1}{2} mv^2 = eV . \qquad (4)$$

Hence mv^2 is a constant for monoenergetic particles. The accelerated particle enters the magnetic field where it is subjected to a field of Hev and a centrifugal force of mv^2/r. These two field forces must be equal.

$$Hev = \frac{mv^2}{} \qquad (5)$$

$$r = \frac{mv}{eH} \qquad (6)$$

If mv = constant, r is constant, i.e., particles of the same mass should define the same locus. The theoretical considerations governing the ion paths are indicated in Fig. (3.6).

Another particle of mass $m(1 + \delta)$ with velocity $v(1 + \varepsilon)$ would have

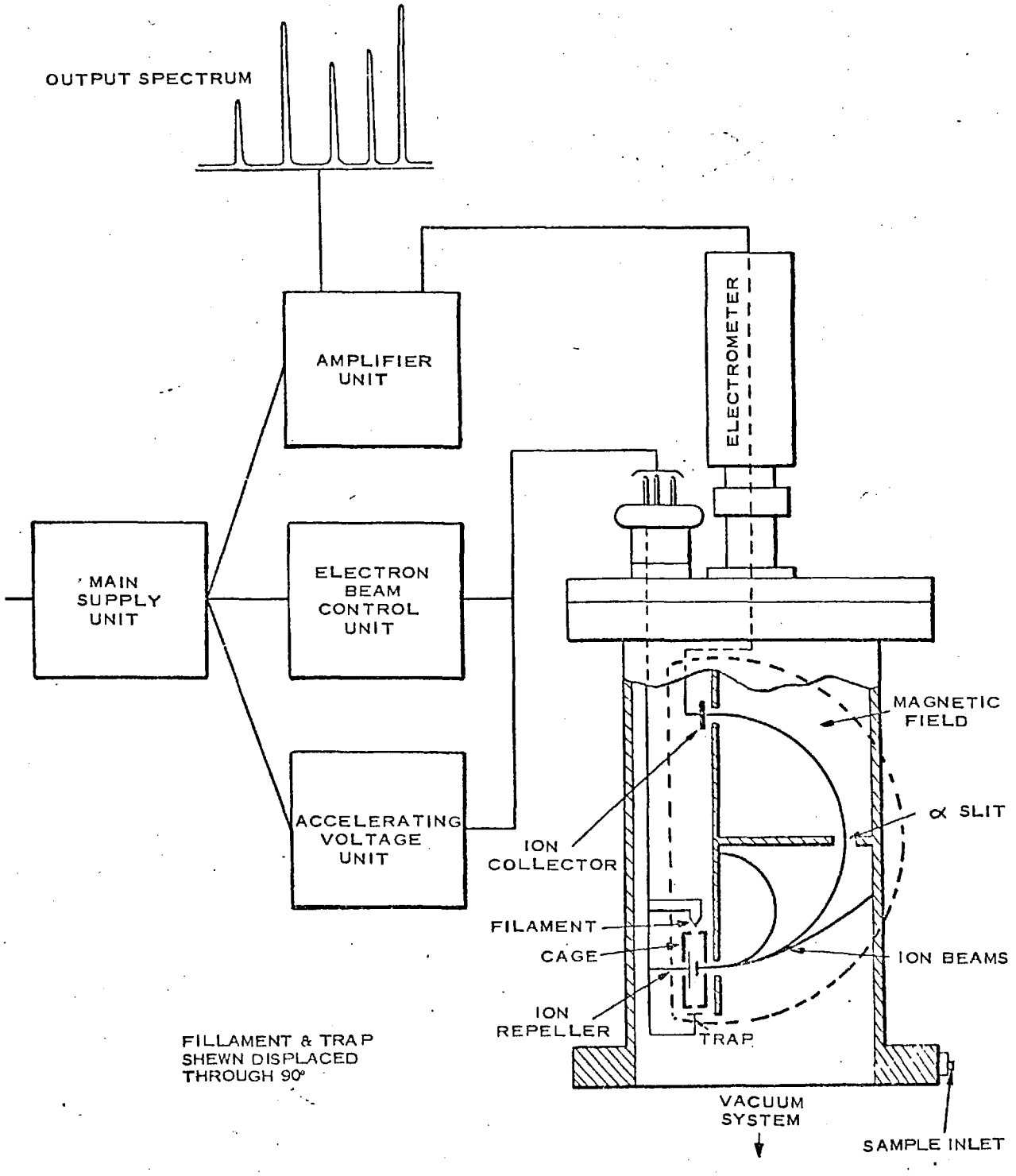

FIG.3-5 SCHEMATIC ARRANGEMENT OF THE MS10 MASS SPECTROMETER

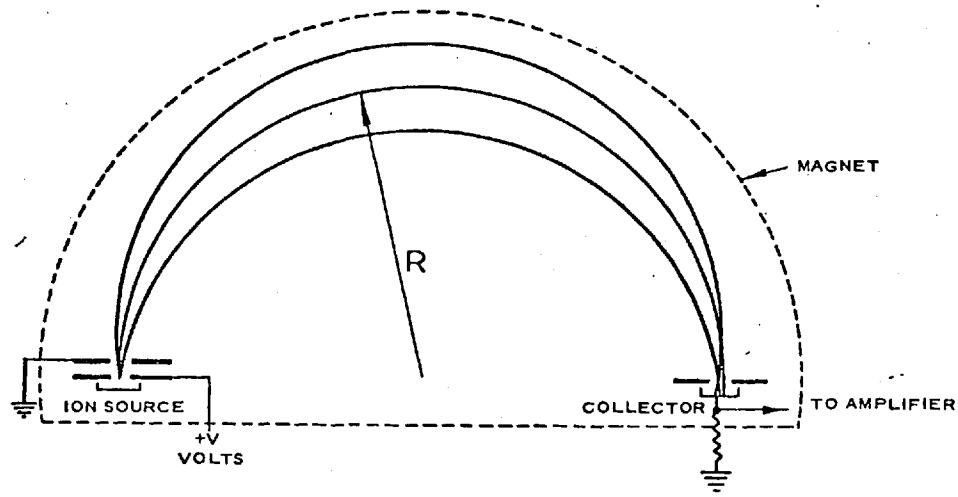

ACCELERATION IN THE SOURCE $eV = \frac{1}{2} mv^2$

RADIAL ACCELERATION IN THE MAGNET $\frac{mv^2}{R} = Hev$

HENCE $\frac{m}{e} = \frac{R^2H^2}{2V}$

V = ACCELERATING VOLTAGE

m = MASS OF ION

e = CHARGE ON ION

v = VELOCITY OF ION

R = RADIUS OF PATH IN MAGNET

H = STRENGTH OF MAGNETIC FIELD

FIG. 3-6 ION PATHS IN 180° DEFLECTION MASS SPECTROMETER

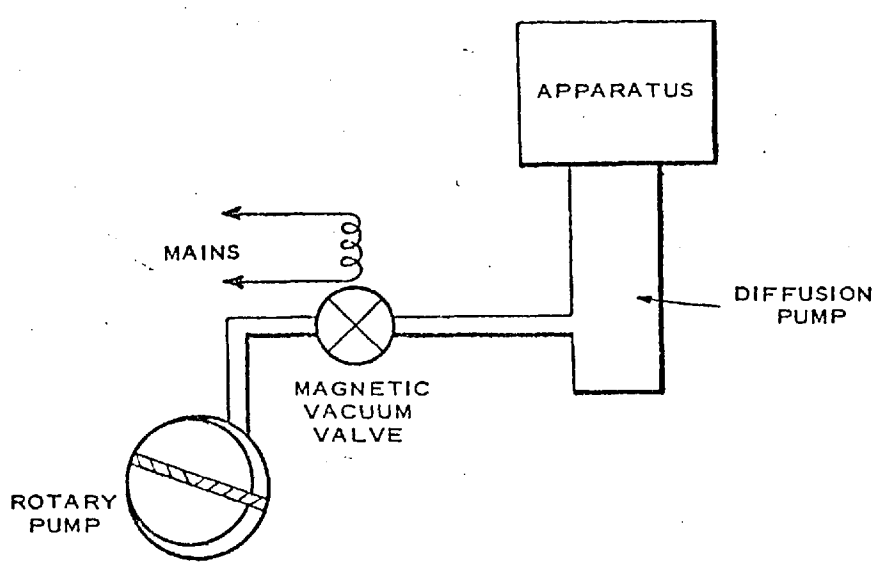

FIG. 3-8 SIMPLE ONE-VALVE 'FAIL SAFE' VACUUM SYSTEM

a momentum of $m(1+\delta)(1+\epsilon)r = m(1+\delta)v$, and its radius of curvature r, would be:

$$r = \frac{mv(1+\delta)}{eH} \qquad (7)$$

Hence, the magnetic field generates a momentum dispersion and δ is the measure of this dispersion. It can easily be seen that

$$v \propto (\sqrt{M})^{-1} \quad \text{and}$$

$$r \propto \sqrt{M} \quad ,$$

with the consequence that the momentum spectrum becomes a mass spectrum with a definite velocity associated with each mass. Combining equations (4) and (5),

$$\frac{m}{e} = \frac{r^2H^2}{2V} \qquad (8)$$

Equation (8) is the mass spectrometer equation.

By varying the value of accelerating voltage or the magnetic field force, individual beams can be brought in turn to focus on the collector where the ions give up their charge, the ion current so produced being detected by an electrometer amplifier whose output is displayed on a meter or recorder.

3.3.3.1 SPECIFICATIONS OF THE MS10-C2 MASS SPECTROMETER

The main components of the mass spectrometer are: (a) The pumping system, (b) The electromagnet (c) Ion source, (d) Filament, (e) Electrometer amplifier and (f) Ionisation gauge.

(a) Pumping System

The MS10 tube unit is mounted on a standard vacuum system comprising of a water cooled oil diffusion pump with stainless steel cold trap and GDR rotary backing pump. The diffusion pump is connected via a magnetic vacuum valve to the rotary pump. Liquid nitrogen was employed as the refrigerant in the 2.5 litres stainless steel cold trap. The wiring and

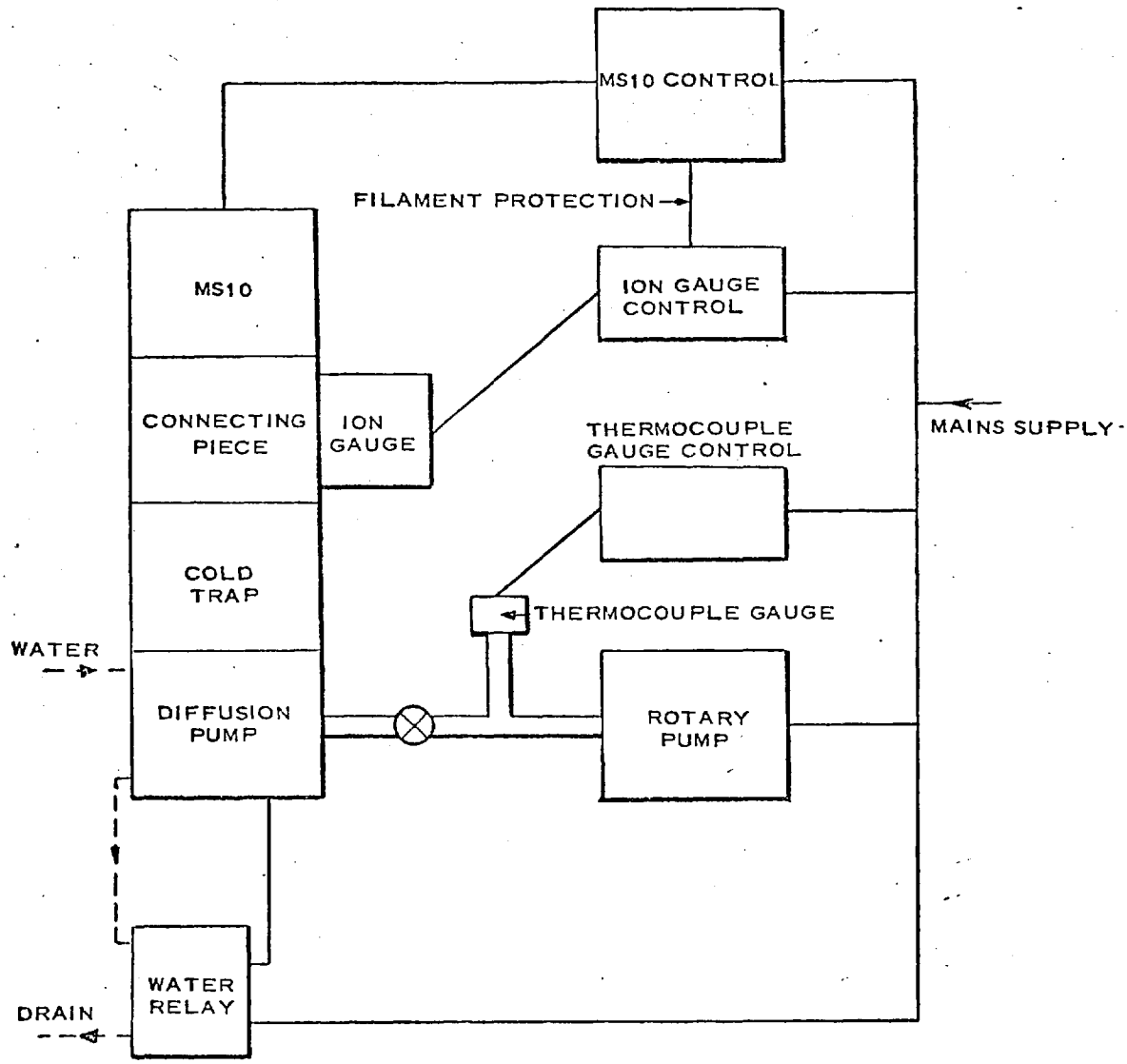

FIG. 3-7 WIRING AND PROTECTION OF MS10 PUMPING SYSTEM

protection of the pumping system is as shown in Fig. (3 - 7), and Fig. (3 - 8) shows the rotary pump-vacuum pump arrangement.

(b) Electromagnet

The assembly of magnet to tube unit is illustrated in Fig. (3 - 9). The electromagnet has a field intensity of 9 kilogauss. Its position must remain constant during all experiments as any slight displacement alters the sensitivity of any ion peak displayed on the recorder. The gap between the magnet yoke and tube unit is approximately $\frac{1}{2}$ inch.

(c) Ion source and collector

Both the ion source and collector are standard types. The source cable with moulded socket is connected to the 5-pin glass/metal seal as shown in Fig. (3 - 10). To avoid damaging the glass/metal seal the cable is supported by tying it to the cable of the electrometer box. The 6BA socket-head pinch screws should be tightened gently but firmly onto the leads of the source seal.

(d) Filament

The filament is a 0.178 mm diameter rhenium wire of 0.5 ohm resistance. It carries a current of 3.4 amp at 1.6/1.8 volts a.c at 50NA trap current setting. The performance of the filament varies from one type to the other. A new filament seems less efficient at the beginning by showing smaller peak height intensities for the same ions under identical conditions, but tends to function uniformly after bake and a small time usage.

(c) Electrometer-amplifier

The electrometer is type ME1403 with input resistance of 10^{11} ohms. The amplifier has a seven range sensitivity of 1000, 250, 100, 25, 10, 2.5 and 1. It permits input currents between 10^{-10} and 10^{-13} amp for full scale deflection on output meter. The amplifier can be conveniently calibrated against a potentiometer to check linearity in each range and

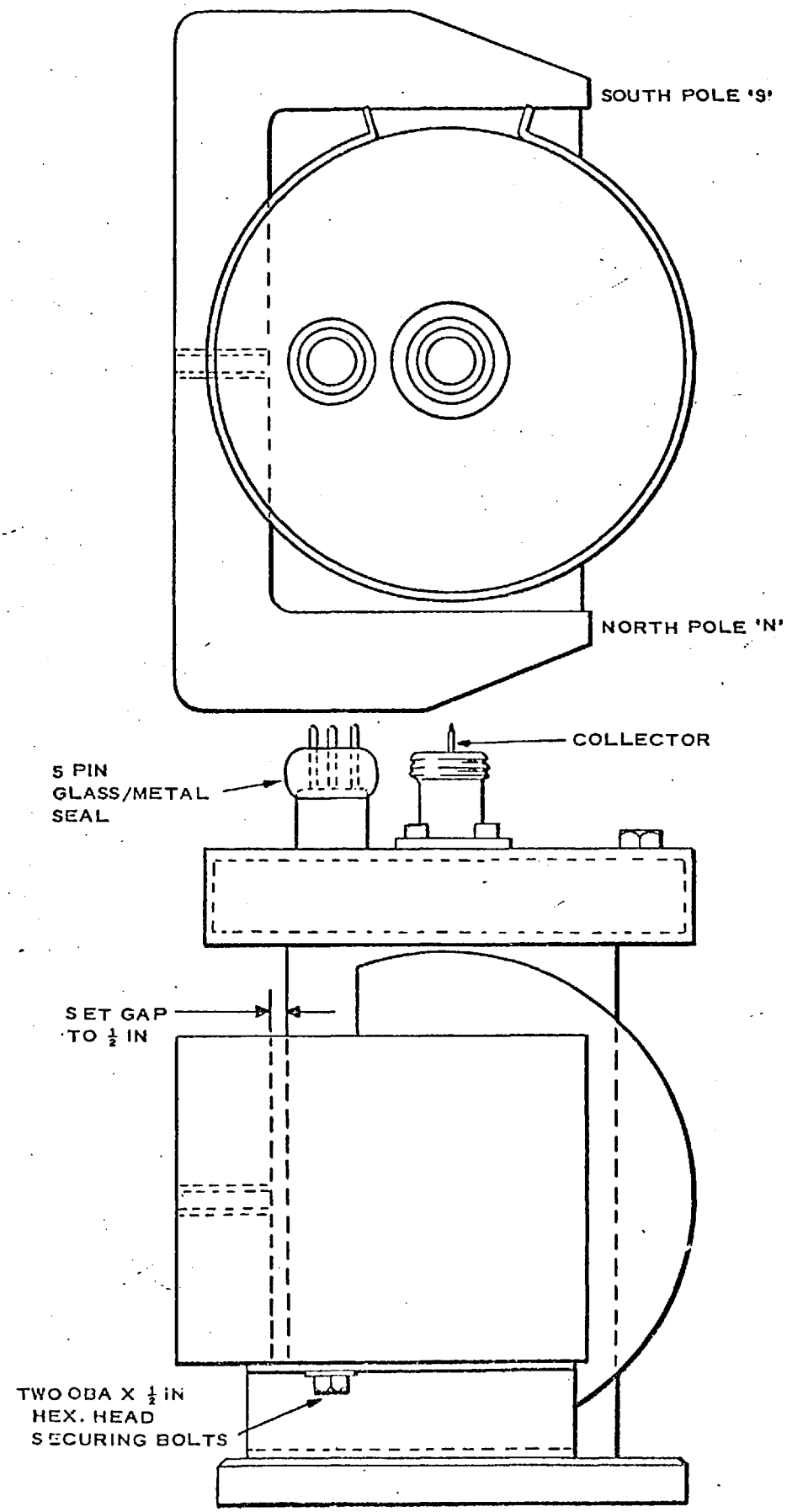

FIG. 3-9 ASSEMBLY OF MAGNET TO MS10 TUBE UNIT

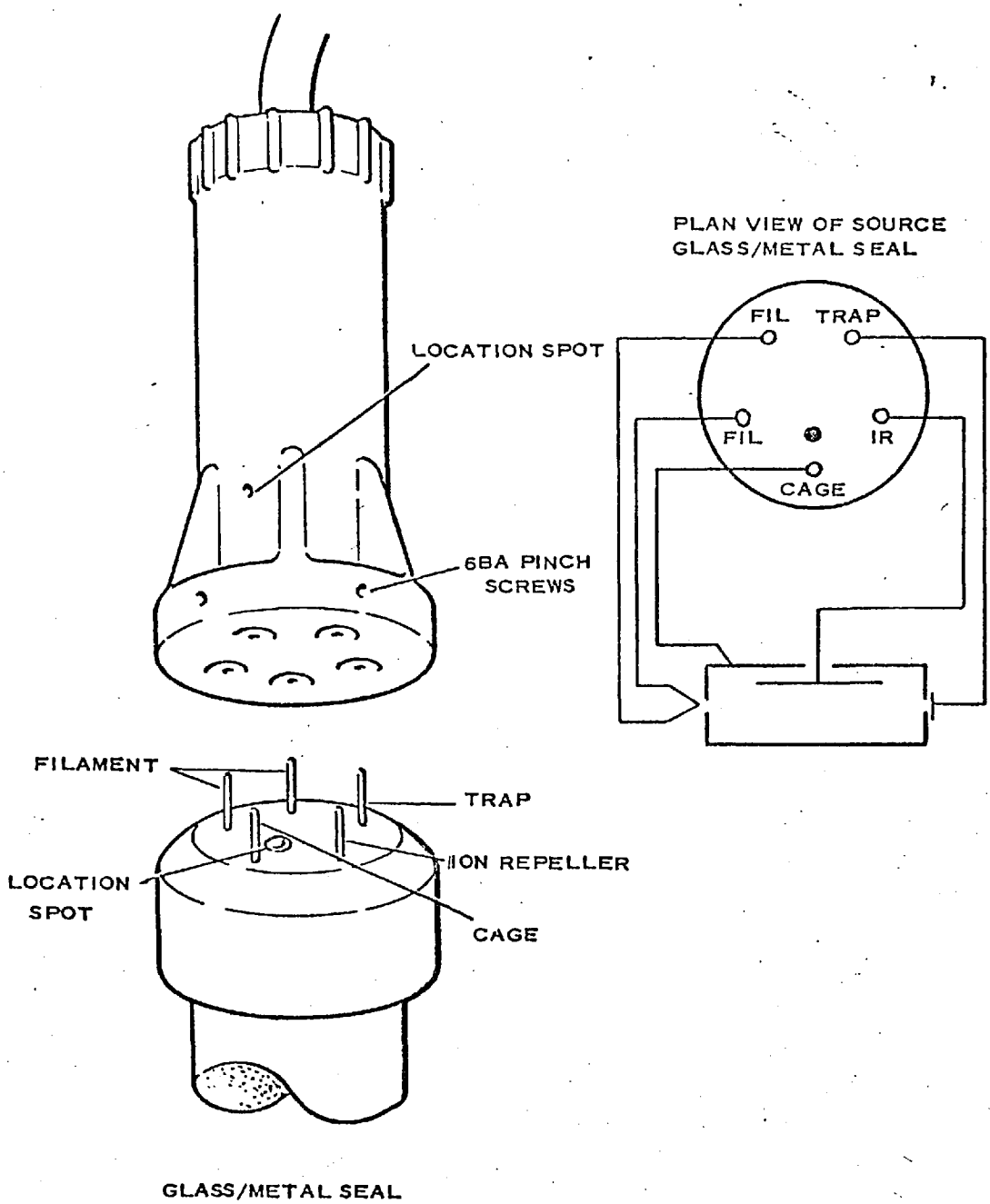

FIG. 3-10 SOURCE-SOCKET AND DEMOUNTABLE 5-PIN GLASS/METAL SEAL

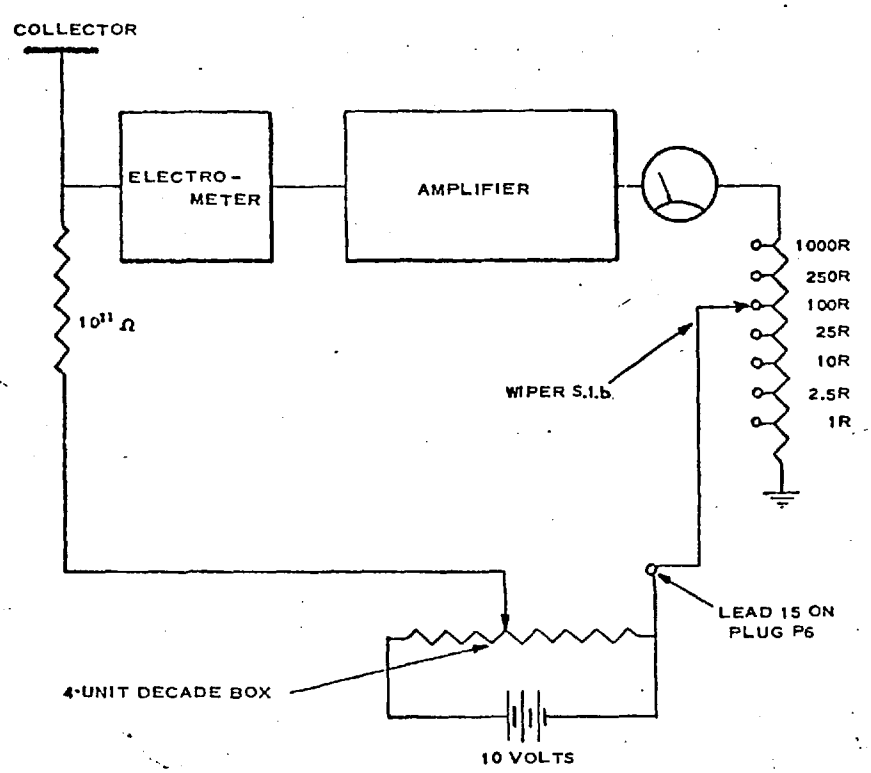

FIG.3-11 METHOD OF CALIBRATING AMPLIFIER

also that the correct ratio exists between ranges. A diagram of the method is illustrated in Fig. (3 - 11).

(f) Ionisation gauge

Type VC9 for pressure measurement in the range 10^{-4} and 10^{-7} torr in a single logarithmic scale was employed.

Fig. (11) shows the different parts of the mass spectrometer employed in this work. A Honeywell recorder was used. Other specifications are as follows:

The tube unit is made of stainless steel of 203 mm. height and stands on a 149 mm. diameter flange. Mass range: 1 - 400.

Resolving power: With a collector slit of 0.25 mm. fitted as standard, and 10% valleys between adjacent peaks the resolving power was 100.

Sensitivity: With standard conditions (electron beam energy of 70 eV, trap current of 50 μA and ion repeller voltage with respect to cage of + 1 volt), the sensitivity was about 4×10^{-5} amps/torr for N_2.

Working pressure: Maximum of 10^{-4} torr.

Accelerating voltage: Cage potential 20 to 2000 volts d.c. Source exit slit was 1.0 mm, defining (alpha slit) 0.25 mm. All flanges were sealed by gold-wire gaskets.

3.3.3.2 CALIBRATION OF PURE SAMPLES

In order to attain consistency in the mass spectrometer readings, certain conditions must be met.

1. The rate of gas flow should remain constant throughout the analysis.
2. The composition of the mixture feeding the ionization chamber should not change during the course of the analysis.
3. The feed must come to temperature equilibrium with the ionization source.
4. Erratic behaviour by the diffusion pump should have no significant effect on the gas pressure in the ionization chamber.
5. Anything that can minimise surface reactions should be undertaken.

6. All mixture peaks at any mass number should be linear superpositions of individual ion current intensities.
7. The pressure attained by the diffusion pump must be very low (we obtained about 2×10^{-7} torr) as this is essential in both the ionization and analyser chambers where the free mean path of the gas molecules must be always greater than the dimensions of any geometrical limitation in the system to gas flow.

These conditions are met. The gas flow was steady, the background pressure before commencement of experiment was around 10^{-7} torr, and never rose above 10^{-4} during experiments hot nitrogen gas was passed through the system to evacuate any adherent material. The products got quenched in the sampling probe so that the possibility of side reactions was eliminated. Further, the feed was allowed to run for about ten minutes so as to attain temperature equilibrium with the source. The fulfilment of the above conditions coupled with the fact that there was linearity between peak height and sampling pressure, assures linear superposition. Up to about 3 torr pressure the peaks are clean and sharp but above this they tend to flatten or diffuse at the tips indicating a saturation of the electrometer-amplifier. Consequently all readings were taken at pressures below 3 torr.

The saturation of the electrometer-amplifier was mainly by propylene, propane and traces of C4. This saturation was usually accompanied by a slight increase in the diffusion pump pressure, but the adherents were easily cleared away by low molecular-weight gases $H2 > CH4 > N2$. The sensitivity employed in this analysis is the ratio of the base peak height and the sampling pressure.

$$S = \frac{H}{P} \quad \text{(divisions/torr).}$$

3.4 COMPUTING THE PARTIAL PRESSURES OF INDIVIDUAL COMPONENTS

Ions produced in the mass spectrometer ionization chamber include,

parent ions, fragment ions, radical ions, rearrangement ions, isotopic ions and metastable ions (these may be dissociated during passage towards the collector), and are detected as peaks at individual mass-to-charge ratios. The intensity of the mass peaks is proportional to the partial pressure of the related parent compound in the ion source.[99,100] The ions produced and their relative intensities are characteristic of the parent molecule and defined as the "cracking pattern" or mass spectrum.

In a multicomponent system, each component shows its characteristic mass spectrum, but the peaks do superimpose and it is only by calibrating the instrument with the pure samples that a quantitative analysis is possible. Since Dalton's Law of partial pressures applies, the contributions of several gases to a specific mass peak are linearly additive, i.e., there is perfect linear superposition of all fragments of the same mass-to-charge ratio, such that:

$$\begin{aligned} h_{11}P_1 + h_{12}P_2 + \cdots\cdots + h_{1n}P_n &= H_1 \\ h_{21}P_1 + h_{22}P_2 + \cdots\cdots + h_{2n}P_n &= H_2 \\ &\qquad (A) \\ h_{m1}P_1 + h_{m2}P_2 + \cdots\cdots + h_{mn}P_n &= H_m \end{aligned}$$

where:

P_n = Partial pressure of component n in the inlet sample.

h_{mn} = Measured height of peak at mass in due to unit pressure of component n.

H_m = Measured height of peak at mass m in the mixture mass spectrum.

For simple systems where there is little superposition, the subtractive technique can be applied. This technique chooses n mass peaks in an n-component system such that the following set of linear simultaneous equations are satisfied.

$$P_1 h_{11} = H_1 \qquad (1)$$

$$P_1 h_{21} + P_2 h_{22} = H_2 \qquad (2)$$

$$P_1 h_{n1} + P_2 h_{22} + P_n h_{nn} = H_n \qquad (n)$$

From equation (a) the partial pressure P_1 can be obtained. The value of P_1 is substituted into equation (b) to obtain P_2. By repetition of this process, the partial pressures of all n components can be found. In complex systems choosing such a set of equations is not only difficult but is also bound to give errors in the partial pressures.

It is much better to solve the set of simultaneous equations (A). Unique answers can be obtained only when the number of unknowns is equal to the number of equations present whatever method of computation is used, it must reduce finally to the solution of n equations in n unknowns. It is reasonable to suppose that the most accurate solution would use all the given data, so a technique involving the least squares method is chosen. The basis of the least squares method is bound up with the mathematical theory of probability and the statistical idea of maximum likelihood.

If: $h_{r1}P_1 + h_{r2}P_2 + \ldots\ldots\ldots + h_{rn}P_n = H_r$, the sum of the squares of the residuals is given by;

$$\sum_{r=1}^{m} (h_{r1}P_1 + h_{r2}P_2 + \ldots\ldots\ldots + h_{rn}P_n - H_r)^2, \quad \text{and}$$

If this is a minimum with respect to the P_i, then

$$\frac{\partial}{\partial P_i}\left[\left(\sum_{r=1}^{m} h_{r1}P_1 + h_{r2}P_2 + \ldots\ldots\ldots + h_{rn}P_n - H_r\right)^2\right] = 0$$

for i = 1, 2, ... n.

The differentiation results in a set of equations typified by

$$\sum_{r=1}^{m} h_{ri}\,(h_{r1}P_1 + h_{r2}P_2 + \ldots\ldots\ldots + h_{rn}P_n - H_r) = 0.$$

There are now n linear equations for the n unknown P_i, i.e., the normal equations are now obtained and are amenable to inversion.

In practice some peaks are not very stable or suffer undue mass discrimination in the mass spectrometer. This is corrected for by multiplying each equation by the square root of a number called the "weight", and then minimising the weighted sum of squares of residuals.

The weight $w = (n' - 1)/\sum_{i=1}^{n'} (r_i' - m')^2$, where;

n' = m of readings

r_i' = values read

m' = mean of the n readings.

Thus the quantity to be minimized is.

$$\sum_{r=1}^{m} [\sqrt{W_r}(h_{r1}P_1 + h_{r2}P_2 + \ldots\ldots\ldots + h_{rn}P_n - H_r)]^2$$

and the normal equations are given by:

$$\sum_{r=1}^{m} [\, W_r h_{ri}(h_{r1}P_1 + h_{r2}P_2 + \ldots\ldots + h_{rn}P_n - H_r)] = 0$$

$$i = 1, 2, 3, \ldots\ldots\ldots n.$$

The peaks obtained are quite stable such that W(J) = 1, and the set of the simultaneous equations obtained after reduction of m to n can be inverted and solved as follows:

The sensitivities of the components are different and therefore, the set of simultaneous equations to be solved take the form:

$$\sum_{r=1}^{m} S_i h_{ri}(h_{r1}P_1 = h_{r2}P_2 + \ldots\ldots\ldots + h_{rn}P_n - H_r) = 0.$$

where S is the sensitivity of each component. For simplicity, it is desirable to regard as unknowns $S_i P_1 = x_i$, such that

$$\begin{aligned}
h_{11}x_1 &+ h_{12}x_2 + \ldots\ldots\ldots + h_{1n}x_n &&= H_1 \\
h_{21}x_1 &+ h_{22}x_2 + \ldots\ldots\ldots + h_{2n}x_n &&= H_2 \\
&\vdots \\
h_{n1}x_1 &+ h_{n2}x_2 + \ldots\ldots\ldots + h_{nn}x_n &&= H_n \\
h_{m1}x_1 &+ h_{m2}x_2 + \ldots\ldots\ldots + h_{mn}x_n &&= H_m
\end{aligned}$$

$m > n$, but after differentiation m becomes equal to n and it is this n x n matrix that is inverted and solved.

Thus, written in matrix form, the system becomes.

$$\begin{bmatrix} h_{11} & h_{12} \cdots\cdots\cdots & h_{1n} \\ h_{21} & h_{22} \cdots\cdots\cdots & h_{2n} \\ h_{31} & h_{32} \cdots\cdots\cdots & h_{3n} \\ & & \\ h_{n1} & h_{n2} \cdots\cdots\cdots & h_{nn} \end{bmatrix} \begin{bmatrix} x_1 \\ x_2 \\ x_3 \\ \\ x_n \end{bmatrix} = \begin{bmatrix} H_1 \\ H_2 \\ H_3 \\ \\ H_n \end{bmatrix}$$

or $$A\{x\} = \{H\}$$

The inverse of a matrix A is equal to A^- and

$$AA^- = I, \text{ the identity matrix.}$$

Therefore $$AA^-\{x\} = A^-\{H\}$$

from which $$\{x\} = A^-\{H\}$$

The solution of the equations may hence be written as

$$x_1 = \alpha_{11}H_1 + \alpha_{12}H_2 + \quad + \alpha_{1n}H_n$$

$$x_2 = \alpha_{21}H_1 + \alpha_{22}H_2 + \quad + \alpha_{2n}H_n$$

$$x_n = \alpha_{n1}H_1 + \alpha_{n2}H_2 + \quad + \alpha_{nn}H_n.$$

which is equivalent to

$$\begin{bmatrix} x_1 \\ x_2 \\ \vdots \\ x_n \end{bmatrix} = \begin{bmatrix} \alpha_{11} & \alpha_{21} \cdots\cdots & \alpha_{n1} \\ \alpha_{12} & \alpha_{22} \cdots\cdots & \alpha_{nn} \\ & & \vdots \\ \alpha_{1n} & \alpha_{2n} \cdots\cdots & \alpha_{nn} \end{bmatrix} \begin{bmatrix} H_1 \\ H_2 \\ \\ H_n \end{bmatrix}$$

$$x = A^-\{H\}$$

since $$x_i = S_i P_i$$

$$P_i = \frac{x_i}{S_i}$$

P_i generally differs from the total inlet pressure P. This is very small however but it is due to the formation of C_4 compounds formed in trace amounts.

3.4.1 THE MAIN SUBROUTINES OF THE PROGRAMME

(a) Linear Least-Squares Fit [LINSQ]

This subroutine fits data $y^{(i)}$ = 1, 2, ... N, by a function $F(x_1, x_2 \ldots x_M) = a_1 f_1(x_1, x_2 \ldots x_M) + \ldots\ldots {}_K f_K (x_1, x_2 \ldots x_M)$ linear in the parameters $_1\ _2 \ldots\ldots _K$. The minimum value of Q, where $Q(_1, _2, \ldots\ldots _K) = \sum_{i=1}^{N} W^{(i)} \left\{ F(x_1^{(i)}, x_2^{(i)} \ldots\ldots x_M^{(i)}) - Y^{(i)} \right\}^2$ and the corresponding parameters are computed. The conariance matrix and errors in parameters may also be requested.

In LINSQ(K,N, M, A, X, Y, W, DA, H, COV, QPRINT, QMN),

K is the number of functions.

N is the number of exerimental points.

M is the number of variables in each function $f_1(x_1, x_2, \ldots\ldots x_M)$.

AMIN is the computed minimum of the function Q.

A on return contains the parameters, $_1\ _2 \ldots\ldots _K$ at the minimum of the function Q. A must be of dimension K.

X contains the values $x_1, x_2 \ldots\ldots x_M$. It must be constructed in suh a way that the jth column contains the values $x_1^{(j)}, x_2^{(j)} \ldots x_M^{(j)}$ corresponding to the data $Y^{(j)}$ (j = 1, 2, ... N).

Y is a vector of dimension N in $Y^{(i)}$, i = 1, 2, ... N.

W is a vector of length K on return containing the statistical errors in the parameters $_1\ _2 \ldots\ldots _K$.

H on return contains the conariance matrix. It must be dimensioned (K,K+1)

COV { = 0. Only minimization is performed.
= 1. If errors and covariance matrix are also required.

QPrint { = 0. Results are not printed.
= 1. Results are printed out.

(b) Subroutine MATIN2 (E, NDIM, N, MDIM, M, INDEX, NERROR, DETERM).

MATIN2 will compute the inverse of matrix A, its determinant D as well as solve the system of linear equations AX = B. It uses Jordan's method with partial pivoting to reduce the matirix A to the identity matrix I through a succession of elementrary transformations:

$\lambda n \lambda n-1 \quad \cdots\cdots \quad {}_1A = I$. If these transformations are simultaneously applied to I and a matrix B of constant vectors, the result is A^{-1} and X where A = XB.

In the subroutine E is a two dimensional double precision array with NDIM as column size containing the matrix A of order N in its first N columns. The matrix of constant vectors, B, is stored in columns N + 1 through N + M of E.

NDIM is the column size of the two dimensional array E.

N is the order of the matrix A.

M is the number of column vectors in matrix B.

If M = 0 only the inverse of A and the computation of the determinant is carried out.

INDEX is a one dimensional array containing N locations and is used by MATIN2 for bookkeeping. The space for this array must be provided in the calling routine.

NERROR is an output parameter which is set on return to non zero, if at any elimination step the corresponding column of A contained only zeros.

DETERM is a double precision variable and contains on return the determinant A.

(c) Subroutine LINEQ2 (C, DIM1, N, DIM2, M, INDEX, NERROR, DETERM).

This is in double precision. The matrix equation AX = B is solved, where A is now a square matrix, and B is a matrix of constant vectors. The Gaussian elimination method with partial pivoting is used. If at any elimination step the pivot column contains only zeros, the elimination will be stopped, and error message NERROR will be set to -1.

C is a 2-dimensional array of size (DIM1, DIM2), containing the coefficient

matrix A and the matrix of constant vectors B.

DIM1 the dimensions of C in the calling program.

DIM2

N the order of the system.

M the number of columns in B (at least 1).

INDEX an internal vector with the dimension DIM1

NERROR error exit.

= 0. System is solved. No errors.

= -1. Pivot column contains only zeros. No solution.

DETERM will contain the value of the determinant A. On return the first m columns of C contain the solutions.

3.4

```
      PROGRAM MAS(TAPE2,INPUT,OUTPUT,TAPE5=INPUT,TAPE6=OUTPUT)
C
      DIMENSION DELTA(11),W(11),C(11)
      DIMENSION SH(11),MPE(11),R(11),RI(11,6),RIT(6,11),S(6)
      DIMENSION MP(11,6),NAME(6)
      DIMENSION MBASC(6),Y(11),A(6),P(6),NO(11),DA(6),H(6,7)
      REAL MP,MPE
      DOUBLE PRECISION H
C*****************************************************************************
C     SET
C     IC =1  TO CONNECT TO COLLIN'S PROGRAM
C     IX =1 TO CALCULATE MOLAR FRACTIONS
C     IR=1  TO CALCULATE RESIDUALS
C     OTHERWISE SET THEM TO ZERO
C*****************************************************************************
      COV = 1.
      QPRINT = 1.0
      IC = 0
      IX = 1
      IR = 1
    1 READ(5,10) M,N,PTOT,T
   10 FORMAT(2I5,2F10.5)
C          PRINT OUT TO CHECK DATA
      WRITE(6,100)M,N,PTOT,T,COV,QPRINT,IC,IX,IR
  100 FORMAT(////5X,2I5,4F10.2,3I5///)
    5 CONTINUE
C          CHECK ON IFL WHETHER TO STOP OR NOT
      IF(M.EQ.0) GO TO 500
    6 CONTINUE
C     SETTING W(M) AS IDENTITY
```

```
      DO 20 J=1,M
   20 W(J) =1.
C     READ IN CALIBRATION DATA OF PURE COMPONENTS
      WRITE(6,501)
  501 FORMAT(/////T25,'CALIBRATION DATA READ IS AS BELOW.',////)
      DO 22 I=1,N
      READ(5,11) NO(I),S(I),MBASC(I)
      READ(5,12) ((MP(J,I),RI(J,I)),J=1,M)
   11 FORMAT(I5,F10.5,I5)
   12 FORMAT(12F6.2)
C     WRITING OUT READ IN VALUES
      WRITE(6,11) NO(I),S(I),MBASC(I)
      WRITE(6,12) ((MP(J,I),RI(J,I)),J=1,M)
   22 CONTINUE
C     READ IN EXPERIMENTAL DATA FOR MIXTURES.
      READ(5,13) MBASE
      READ(5,14) ((MPE(J),R(J),SH(J)),J=1,M)
   13 FORMAT(I5)
   14 FORMAT(12F6.2)
C
C     WRITING OUT READ IN EXPERIMENTAL VALUES FOR MIXTURE.
      WRITE(6,502)
      WRITE(6,13) MBASE
      WRITE(6,144) ((MPE(J),R(J),SH(J)),J=1,M)
  144 FORMAT(1H0,12F8.2)
  502 FORMAT(/////T25,'EXPERIMENTAL DATA READ IS AS BELOW.',////)
C          CONVERTING PEAL HEIGHTS TO RELATIVE INTENSITIES
C          FOR CAL. DATA
      DO 25 I=1,N
      MBAS=MBASC(I)
```

```
      BPH=RI(MBAS,I)
      DO 26 J=1,M
   26 RI(J,I) = RI(J,I)/BPH
C          PRINT OUT
      WRITE(6,101) M,MBAS
  101 FORMAT(//5X,'PRINTING VALUES OF RELATIVE INTENSITIES FOR M,MBAS
     *AND COMPONENT DENOTED BY I.',2X,215///)
      WRITE(6,102) I,(RI(JJ,I),JJ=1,M)
  102 FORMAT(//X,'RI(JJ,I) FOR I= ',I2,(T20,5F10.3//)/)
   25 CONTINUE
C          GETTING Y(M)
      DO 28 J=1,M
      Y(J) = R(J)*SH(J)
   28 CONTINUE
C          PRINT OUT
      WRITE(6,104) (Y(J),J=1,M)
  104 FORMAT(////X,'Y(J) IS=',(T20,5F10.4//)/)
C          BEGIN LEAST SQUARES ESTIMATION
C          PREPARE INPUT TO LINSQ. COMPUTE TRANSPOSE OF RI
C          TRANSPOSE RI IS RIT
      DO 29 J=1,M
      DO 30 I=1,N
      RIT(I,J)=RI(J,I)
   30 CONTINUE
   29 CONTINUE
C          PRINT OUT
      WRITE(6,105) ((RIT(I,J),I=1,N),J=1,M)
  105 FORMAT(////X,'RIT IS.',(T20,5F10.4//)/)
C
      CALL LINSQ(N,N+1,M,N,A,RIT,Y,W,DA,H,COV,0PRINT,QMIN)
```

```
C          PRINT OUT
      WRITE(6,106)
  106 FORMAT(////T20,'HAVE COME OUT OF LINSQ',//)
C          CHECK IF RESIDUALS WANTED
      IF (IR.EQ.0) GO TO 2
C     CALCULATE RESIDUALS
      C(J) = 0.
      DO 31 J=1,M
      DO 33 I=1,N
   33 C(J) = C(J)+RI(J,I)*A(I)
      DELTA(J) = C(J) -Y(J)
   31 CONTINUE
      CALL MATPLY(RI,A,C,M,N,L)
      L=1
      WRITE(6,107) (DELTA(J),J=1,M)
  107 FORMAT(////X,'RESIDUAL MATRIX DELTA(M)',/,(T30,5E12.3//)/)
C          PRINT OUT
      WRITE(6,108)
  108 FORMAT(///T20,'HAVE COME OUT OF RESIDUALS',//)
    2 CONTINUE
C          CALCULATE PARTIAL PRESSURES FROM Y(M)
C          GET SI(N,N) FIRST A DIAG. MATRIX FORM S(N),AMENABLE TO
C                                   INVERSION
      DO 32 I=1,N
      P(I)=A(I)/S(I)
   32 CONTINUE
C          PRINT OUT
      WRITE(6,119)
  119 FORMAT(////T50,'PARTIAL PRESSURES ARE GIVEN BY P BELOW.',//)
      WRITE(6,110) ((P(J),NO(J)),J=1,N)
```

```
  110 FORMAT(////X,*P IS*,(T20,F10.4,I10//))
      IF(IX.EQ.0) GO TO 3
C     MOLAR FRACTIONS
      DO 34 J=1,N
      P(J)=P(J)/PTOT
   34 CONTINUE
C          PRINT OUT
      WRITE(6,112)
  112 FORMAT(////T50,'CONCENTRATIONS ARE GIVEN BY P BELOW.'//)
      WRITE(6,110)((P(J),NAME(J)),J=1,N)
    3 CONTINUE
C          OPTION FOR COLLINS PROGRAM TO BE INCLUDED  HERE
      IF (IC.EQ.0) GO TO 4
    4 CONTINUE
      GO TO 1
  500 STOP
      END
      SUBROUTINE MATPLY(RI,A,C,M,N,L)
C
C          MULTPLIES MATRICES.
C                                   C(M,L)=RI(M,N)*A(N,L)
      DIMENSION RI(M,N),A(N,L),C(N,L)
      DO 7 J=1,L
      DO 7 I=1,M
      C(I,J)=0.0
      DO 7 K=1,N
      C(I,J)=C(I,J)+RI(I,K)*A(K,J)
    7 CONTINUE
      RETURN
      END
```

```
C
      SUBROUTINE LINSQ(K,KPLUS,N,M,F,X,Y,W,DA,H,COV,APRINT,QPRINT)
      DIMENSION X(M,N),F(K),Y(N),W(N),H(K,KPLUS),DA(K)
      DIMENSION INDEX(100)
      DOUBLE PRECISION H,DETERM
C***  QPRINT IS SAME AS QMIN IE SUM OF SQUARES AT THE MINIMUM
      DO 11 I=1,K
      DO 11 J=1,KPLUS
   11 H(I,J)=0.
      IFLAG=1
      DO 2 I=1,N
      CALL FCN(K,M,F,X(1,I),IFLAG)
      IFLAG=4
      DO 2 K1=1,K
      AW=H(K1,KPLUS)
      H(K1,KPLUS) = H(K1,KPLUS)+W(I)*F(K1)*Y(I)
      AW = H(K1,KPLUS)
      DO 2 L=1,K1
      AW=H(K1,L)
      H(K1,L)=H(K1,L)+W(I)*F(K1)*F(L)
      AW=H(K1,L)
    2 CONTINUE
      DO 3 J=1,K
      DO 3 I=1,J
    3 H(I,J)=H(J,I)
      IF(COV)5,4,5
    4 CALL LINEQ2(H,K,K,K+1,1,INDEX,NERROR,DETERM)
      MM=1
      QPRINT=Q(K,KPLUS,N,M,F,X,Y,W,DA,H,MM)
      DO 7 I=1,K
```

```
    7 F(I)=H(I,1)
      IF(APRINT.NE.0.) GO TO 10
      RETURN
    5 CALL MATINP(H,K,K,K+1,1,INDEX,NERROR,DETERM)
      MM=K+1
      QPRINT=Q(K,KPLUS,N,M,F,X,Y,W,DA,H,MM)
      DO 6 I=1,K
    6 F(I)=H(I,K+1)
      DO 8 I=1,K
      HDA=H(I,I)
    8 DA(I)=SQRT(HDA)
      IF(APRINT.EQ.0.) RETURN
C     PRINTS ERRORS IN THE COEFFICIENTS
      PRINT 100
  100 FORMAT(45X,26HERRORS IN THE COEFFICIENTS)
      PRINT 101,(DA(I),I=1,K)
  101 FORMAT(5X,5G16.7)
C
C     PRINTS LOWER DIAGONAL COVARIANCE MATRIX
      PRINT 102
  102 FORMAT(///40X,26HVARIANCE-COVARIANCE MATRIX///)
      DO 9 I=1,K
      DO 12 J=1,K
   12 F(J)=H(I,J)
    9 PRINT 103,(F(JJ),JJ=1,I)
  103 FORMAT(10X,5G20.6//)
      DO 13 I=1,K
   13 F(I)=H(I,K+1)
   10 CONTINUE
C     PRINTS COEFFICIENTS AND SUM OF SQUARES
```

```
      PRINT 104,OPRINT
  104 FORMAT(///30X,15HSUM OF SQUARES=G20.6///)
      PRINT 105
  105 FORMAT(45X,12HCOEFFICIENTS///)
      PRINT 103,(F(I),I=1,K)
      RETURN
      END
      SUBROUTINE FCN(K,M,F,X,IFLAG)
C          CALCULATES FUNCTIONS FOR LEAST SQUARES ESTIMATION
      DIMENSION F(K),X(M)
      DO 16 J=1,K
      F(J)=X(J)
   16 CONTINUE
      WRITE(6,100) (F(J),J=1,K)
  100 FORMAT(2X,3HFCN,2X,4F10.3)
      RETURN
      END
      SUBROUTINE MATPLY(R,SH,M)
C          MULTIPLIES VECTORS TO RULE.  R(I)=R(I)SH(I)
      DIMENSION R(M),SH(M)
      DO 420 J=1,M
      R(J)=R(J)*SH(J)
  420 CONTINUE
      RETURN
      END
```

```
C
      FUNCTION Q(K,KPLUS,N,M,F,X,Y,W,DA,H,MM)
C     COMPUTES THE SUM OF SQUARES
      DIMENSION F(K),X(M,N),DA(K),H(K,KPLUS),Y(N),W(N)
      DOUBLE PRECISION H
      Q=0.
      WRITE(6,100) K,N,M
  100 FORMAT(2X,*FUNCTION Q   KNM*,3I5)
      DO 3 I=1,N
      CALL FCN(K,M,F,X(1,I),IFLAG)
      HSUM=0.
      DO 2 I1=1,K
    2 HSUM=H(I1,MM)*F(I1)+HSUM
      A=HSUM-Y(I)
      WRITE(6,101) I,A
  101 FORMAT (2X,*RESIDUAL A(*,I2,*)=*,1PE9.2)
      WRITE(6,103) (F(J),J=1,K)
  103 FORMAT(2X,3HFCN,2X,4E10.3)
    3 Q=(HSUM-Y(I))*(HSUM-Y(I))*W(I)+Q
      RETURN
      END
```

```
C
      SUBROUTINE  MATIN2 (A,DIM1,N1,DIM2,N2,INDEX,NERROR,DETERM)
C     MATRIX INVERSION WITH ACCOMPANYING SOLUTION OF LINEAR EQUATIONS
      DOUBLE PRECISION A,DETERM,DETER,PIVOT,SWAP
      INTEGER DIM1,DIM2,DIM,EMAT,PIVCOL,PIVCOL1,PIVCOL2
      DIMENSION A(DIM1),INDEX(DIM1)
      DETER=1.0D0
      N=N1
      EMAT=N+N2
      DIM=DIM1
      NMIN1=N-1
C     THE ROUTINE DOES ITS OWN EVALUATION FOR DOUBLE SUBSCRIPTING OF
C     ARRAY A.
      PIVCOL=1-DIM
C     MAIN LOOP TO INVERT THE MATRIX
      DO 11 MAIN=1,N
      PIVOT=0.0D0
      PIVCOL=PIVCOL+DIM
C     SEARCH FOR NEXT PIVOT IN COLUMN MAIN.
      PIVCOL1=PIVCOL+MAIN-1
      PIVCOL2=PIVCOL +NMIN1
      DO 2 I1=PIVCOL1,PIVCOL2
      IF(DABS(A(I1))-DABS(PIVOT)) 2,2,1
    1 PIVOT=A(I1)
      LPIV=I1
    2 CONTINUE
C     IS PIVOT DIFFERENT FROM ZERO
      IF(PIVOT) 3,15,3
C     GET THE PIVOT-LINE INDICATOR AND SWAP LINES IF NECESSARY
    3 ICOL=LPIV-PIVCOL+1
```

```
      INDEX(MAIN)=ICOL
      IF(ICOL-MAIN) 6,6,4
C     COMPLEMENT THE DETERMINANT
    4 DETER=-DETER
C     POINTER TO LINE PIVOT FOUND
      ICOL=ICOL-DIM
C     POINTER TO EXACT PIVOT LINE
      I3=MAIN-DIM
      DO 5 I=1,EMAT
      ICOL=ICOL+DIM
      I3=I3+DIM
      SWAP=A(I3)
      A(I3)=A(ICOL)
    5 A(ICOL)=SWAP
C     COMPUTE DETERMINANT
    6 DETER=DETER*PIVOT
      PIVOT=1./PIVOT
C     TRANSFORM PIVOT COLUMN
      I3=PIVCOL+NMINI
      DO 7 I=PIVCOL,I3
    7 A(I)=-A(I)*PIVOT
      A(PIVCOL1)=PIVOT
C     PIVOT ELEMENT TRANSFORMED
C     NOW CONVERT REST OF THE MATRIX
      I1=MAIN-DIM
C     POINTER TO PIVOT LINE ELEMENTS
      ICOL=1-DIM
C     GENERAL COLUMN POINTER
      DO 10 I=1,EMAT
      ICOL=ICOL+DIM
```

```
      I1=I1+DIM
C     POINTERS MOVED
      IF(I-MAIN) 8,10,8
C     PIVOT COLUMN EXCLUDED
    8 JCOL=ICOL+NMIN1
      SWAP=A(I1)
      I3=PIVCOL-1
      DO 9 I2=ICOL,JCOL
      I3=I3+1
    9 A(I2)=A(I2)+SWAP*A(I3)
      A(I1)=SWAP*PIVOT
   10 CONTINUE
   11 CONTINUE
C     NOW REARRANGE THE MATRIX TO GET RIGHT INVERS
      DO 14 I1=1,N
      MAIN=N+1-I1
      LPIV=INDEX(MAIN)
      IF(LPIV-MAIN) 12,14,12
   12 ICOL=(LPIV-1)*DIM+1
      JCOL=ICOL+NMIN1
      PIVCOL=(MAIN-1)*DIM+1-ICOL
      DO 13 I2=ICOL,JCOL
      I3=I2+PIVCOL
      SWAP=A(I2)
      A(I2)=A(I3)
   13 A(I3)=SWAP
   14 CONTINUE
      DETERM=DETER
      NERROR=0
      RETURN
```

```
15 NERROR=-1
   DETERM=DETER
   PRINT 100,MAIN,MAIN
   RETURN
100 FORMAT(18H MATINI ..... THE ,I10,50H. COLUMN OF THE MATRIX CONTAIN
   1S ONLY ZEROS AT THE ,I10,19H. ELEMINATIONSSTEP. )
   END
```

```
C
      SUBROUTINE LINEQ2 (A,DIM1,N1,DIM2,N2,INDEX,NERROR,DETERM)
      INTEGER DIM1,DIM,PIVCOL,PIVCOL1,TOPX,ENDX,TOPCOL,ENDCOL,EMAT
      DIMENSION A(DIM1),INDEX(DIM1)
      DOUBLE PRECISION A,DETERM,DETER,PIVOT,SWAP
      DIM=DIM1
      DETER=1.0D0
      N=N1
      EMAT=N+N2
      NMIN1=N-1
      PIVCOL=-DIM
C     MAIN LOOP TO CREATE TRIANGULAR
      DO 10 MAIN=1,NMIN1
      PIVOT=0.0D0
      PIVCOL=PIVCOL+DIM+1
      PIVCOL1=PIVCOL+N-MAIN
C     SEARCH PIVOT
      DO 2 II=PIVCOL,PIVCOL1
      IF(DABS(A(II))-DABS(PIVOT)) 2,2,1
    1 PIVOT=A(II)
      LPIV=II
    2 CONTINUE
C     IS PIVOT DIFFERENT FROM ZERO
      IF(PIVOT) 3,15,3
C     IS IT NECESSARY TO BRING PIVOT TO DIAGONAL
    3 IF(LPIV-PIVCOL) 4,6,4
    4 DETER=-DETER
      LPIV=LPIV-DIM
      I1=PIVCOL-DIM
      DO 5 I2=MAIN,EMAT
```

```
      LPIV=LPIV+DIM
      I1=I1+DIM
      SWAP=A(I1)
      A(I1)=A(LPIV)
    5 A(LPIV)=SWAP
    6 DETER=DETER*PIVOT
      PIVOT=1./PIVOT
C     MODIFY PIVOT COLUMN
      I1=PIVCOL+1
      DO 7 I2=I1,PIVCOL1
    7 A(I2)=A(I2)*PIVOT
C     CONVERT THE SUBMATRIX AND RIGHT SIDES
      I3=PIVCOL
      IROW=MAIN+1
      DO 9 I1=IROW,N
      I3=I3+1
      I4=PIVCOL
      I5=I3
      DO 8 I2=IROW,EMAT
      I4=I4+DIM
      I5=I5+DIM
    8 A(I5)=A(I5)-A(I4)*A(I3)
    9 CONTINUE
   10 CONTINUE
      DETERM=DETER
      NERROR=0
C     COMPUTE THE SOLUTIONS
      NO=N+1
      TOPX=NMIN1*DIM+1
      DO 13 I=NO,EMAT
```

```
      TOPX=TOPX+DIM
      ENDX=TOPX+N
      TOPCOL=N*DIM+1
      ENDCOL=TOPCOL+NMIN1
      DO 12 I1=1,NMIN1
      ENDX=ENDX-1
      TOPCOL=TOPCOL-DIM
      ENDCOL=ENDCOL-DIM-1
      A(ENDX)=A(ENDX)/A(ENDCOL+1)
      SWAP=A(ENDX)
      I3=TOPX-1
      DO 11 I2=TOPCOL,ENDCOL
      I3=I3+1
   11 A(I3)=A(I3)-A(I2)*SWAP
   12 CONTINUE
      A(TOPX)=A(TOPX)/A(1)
   13 CONTINUE
C     LEFTADJUST THE SOLUTIONS
      I=-DIM
      TOPX=NMIN1*DIM+1
      ENDX=TOPX+NMIN1
      DO 14 I1=NO,EMAT
      TOPX=TOPX+DIM
      ENDX=ENDX+DIM
      I=I+DIM
      I3=I
      DO 14 I2=TOPX,ENDX
      I3=I3+1
   14 A(I3)=A(I2)
      RETURN
```

```
C     ERROR EXIT
   15 NERROR=-1
      DETERM=DETER
      PRINT 100,MAIN,MAIN
      RETURN
  100 FORMAT(18H LINEQ1 ***** THE ,I10,50H. COLUMN OF THE MATRIX CONTAIN
     1S ONLY ZEROS AT THE  ,I10,19H. ELIMINATIONSTEP.  )
      END
```

CHAPTER IV

CHAPTER IV

PROPANE PYROLYSIS

4.1 INTRODUCTION

Although Propane is used commercially in large quantities as a reactant for the production of ethylene and propylene, the mechanism of the pyrolysis reaction is not fully understood. Molecular or at least partially molecular reaction schemes have been proposed by Blackmore and Hinshelwood[20] and Parsons et al[101] Hinshelwood[139] studied the inhibition of the reaction by nitric oxide, and found that under certain conditions some 14% was uninhibitable several investigations have shown that this residual reaction is not a molecular reaction Stevenson et al[111] studied the pyrolysis of propane containing radioactive carbon and concluded that isotopic mixing took place at the same rate, when the reaction was completely inhibited as when it was uninhibited. Hinshelwood[110] obtained the same result. Poltorak and Volevodsky[112] showed that when propane is pyrolyzed in the presence of D2, D atoms appear in the hydrocarbon fraction at a rate, relative to the rate of decomposition, that is independent of the amount of nitric oxide present.

All of these results show that free radicals are still important in the reaction occurring in the presence of No and provide no support for the view that a molecular mechanism plays a significant role in the propane pyrolysis. Evidence leading to the same conclusion is provided by the experiments of Neclause et al[113] which showed that in reaction vessels, the propane pyrolysis was completely inhibited by O_2; this would not be possible if a molecular mechanism occurred. The most recent studies of propane pyrolysis have led to general agreement that the reaction is entirely free radical in nature. Beyond this, however, there is little detailed agreement.

A number of earlier investigations on the propane pyrolysis[102,103,34,105,104].

indicated that the reaction is largely homogeneous and that the main decomposition products are H_2, CH_4, C_2H_4 and C_3H_6 according to the stoichiometry:

$$C_3H_8 \longrightarrow C_3H_6 + H_2$$

and $$C_3H_8 \longrightarrow C_2H_4 + CH_4$$

Essentially equal molar quantities of these products are obtained for low conversions at 550°C 650°C, as indicated by Laidler et al[9] and Steacie and Puddington[105]. Ethane, butadiene and heavier components are also sometimes obtained, especially at higher conversions and higher temperatures, as reported by Groll[106] Schneider and Frolich[107].

Although the thermal decomposition of propane is at least implicitly assumed in many cases to be a completely homogeneous gas-phase reaction, the influence of reactor surfaces has been demonstrated frequently, and this, in part, perhaps explains the discrepancies in the results obtained using different reactors. Laidler et al[9] and Poltovak et al[108], who used batch reactors at subatmospheric pressures reported that the surface acted both to initiate and terminate the reaction. Fusy et al[109] claimed that the wall was effective in terminating the chains. Additional information was obtained concerning the effects of treating the inside walls of a reactor with hydrogen surface and other gases. Corynes and Albright[13] had earlier reported results indicating the importance of such treatments in affecting the course of pyrolysis. Contacting H_2S with the reactor for several minutes at temperatures from at least as low as 100° to 800°C resulted in metal sulfide films on the reactor walls. This sulfide surface is relatively effective in preventing the formation of metal oxide surfaces when oxygen or steam is contacted with the reactors. Steam, when contacted for periods of 6 to 24 hours with such reactors, slowly converted some of the metal sulfides to metal oxides. These metal oxides promote coking reactions and the formation of larger amounts

of hydrogen. This investigation confirmed qualitatively that reactor history is a fairly important factor in the overall pyrolysis process since it affects the types of heterogeneous wall reactions which are especially important relative to coke (or carbon) and hydrogen formation.

The earlier works suggested that the kinetics are first order, but Martin, Dzierzynski, and Niclause[114] and Laidler, Sagert and Wojciechowski[9] found an order higher than 1. At higher temperatures and lower pressures the order approaches 3/2, while it is close to unity at lower temperatures and higher pressures. There is little effect of inert gases on the overall rates. Table 4.1 shows considerable spread in activation energy and frequency factor. Fig. (4.14) shows the Arrhenius diagram of the data obtained by De Boodt[115], Paul and Marek[7], Laidler et al[9], Kershenbaum[10] and Steacie[105]. In this work the temperature-time history of the pyrolysis of propane is followed using the mass spectrometer to analyse these products and compare the concentration profiles with computer predictions between 600° and 800°C.

4.2 CALIBRATION OF PURE SAMPLES

In order to quantify the products of pyrolysis as obtained from the mass spectrometer, it is essential to know the cracking pattern of each pure compound contributing to the mixture spectrum. The cracking patterns of the primary products are as shown in Table 4.2.

4.3 ANALYSIS OF RESULTS

Space time was obtained by dividing the volume of the reaction zone by the volumetric feed rate of the propane measured at the reaction temperature and pressure. This is basically the same method employed

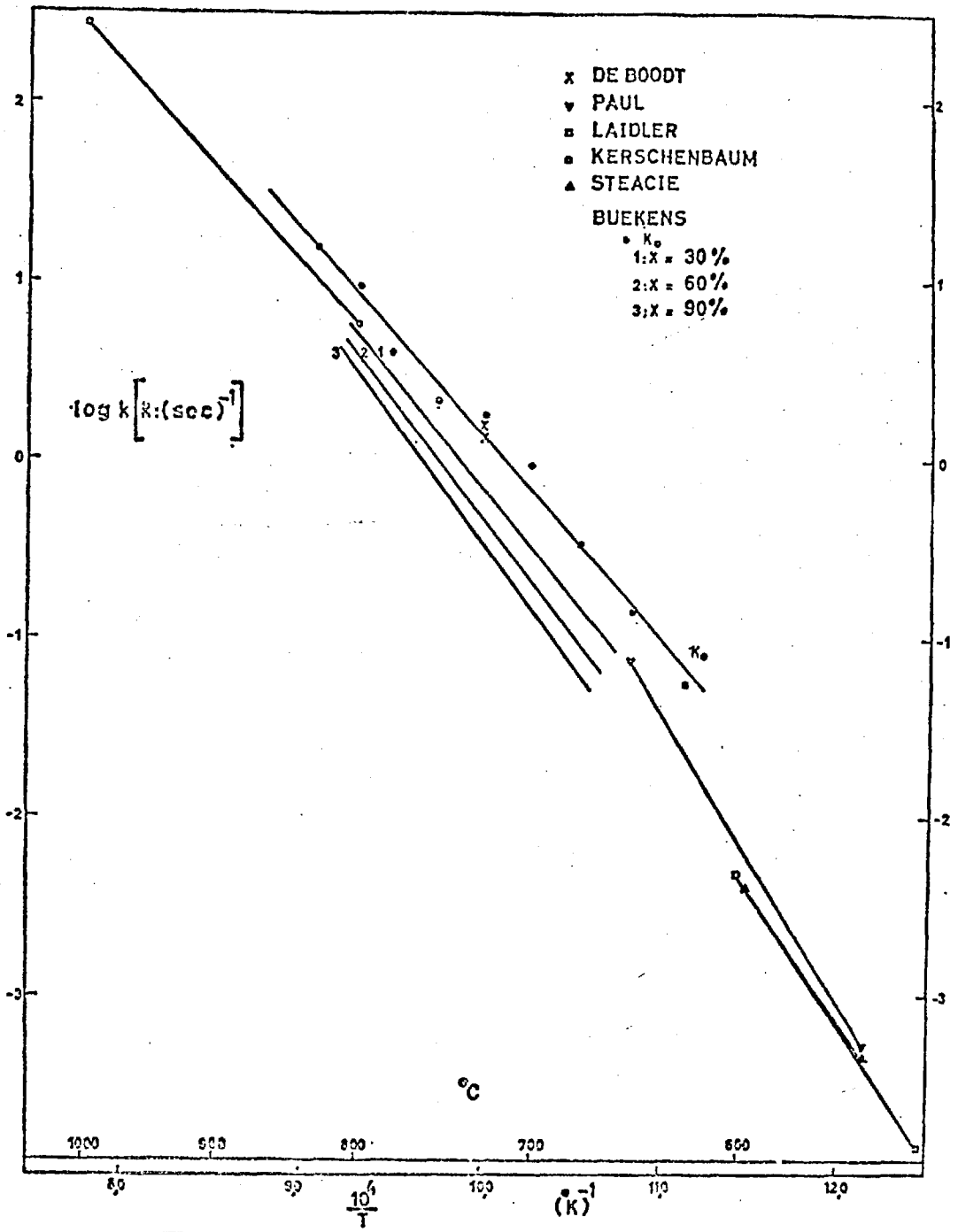

Fig 4-14 Figure Arrhenius diagram

Point values of rate coefficient, k

Table 4-1 Literature Data

Authors	*Order*	*Frequency Factor*	*Activation Energy, Cal./Mole*	*Temp. Range, °C.*
Paul and Marek (1934)	1	3.98×10^{16}	74,850	550–650
Engel *et al.* (1957)	...	...	71,000	500–590
Martin *et al.* (1964)	1.2–1.3	...	67,000	545–600
Laidler *et al.* (1962)	1	2.58×10^{15}	67,100	530–670
	1.5	8.50×10^{15}	54,500	
Steacie and Puddington (1938)	1	2.88×10^{13}	63,300	551–602
De Boodt (1962)	...	...	53,000	700–750
Kershenbaum (1967)	1	2.40×10^{11}	52,100	800–1000

TABLE 4-2

RELATIVE ION INTENSITIES FOR VARIOUS COMPOUNDS eV = 70V, Trap current = 50 μA. Ion repeller voltage = 1V, Mass spectrometer model MS10-C2.

COMPOUND	MASS NUMBER $\frac{M}{e}$	RELATIVE ION INTENSITIES	COMPOUND	MASS NUMBER M/e	RELATIVE ION INTENSITIES
C_3H_8	2.00	1.69	C_3H_6	2.00	3.17
	14.00	0.76		14.00	1.44
	15.00	4.06		15.00	3.05
	16.00	2.18		16.00	0.98
	25.00	0.94		19.00	1.47
	26.00	9.91		19.50	0.52
	27.00	39.55		20.00	1.10
	28.00	62.88		20.50	0.34
	29.00	100.00		25.00	1.44
	30.00	2.03		26.00	9.05
	37.00	3.77		27.10	27.30
	38.00	6.73		28.00	2.81
	39.00	25.46		36.00	1.47
	40.00	5.17		37.00	10.76
	41.00	26.37		38.00	16.49
	42.00	14.15		39.00	67.11
	43.00	33.96		40.00	26.78
	44.00	35.84		41.00	100.00
	45.00	1.03		42.00	72.15
C_2H_4	2.00	2.16	C_2H_6	2.00	1.03
	12.00	0.39		14.00	1.45
	13.00	1.05		15.00	3.10
	14.00	2.61		25.00	3.10

TABLE 4-2

COMPOUND	MASS NUMBER $\frac{M}{e}$	RELATIVE ION	COMPOUND	MASS NUMBER M/e	RELATIVE ION INTENSITIES
C_2H_4	24.00	2.09	C_2H_6	26.00	20.68
	25.00	9.41		27.00	30.36
	26.00	60.13		28.00	100.00
	27.00	62.75		29.00	22.23
	28.00	100.00		30.00	27.92
	29.00	2.35			
CH_4	2.00	0.62	H_2	2.00	100.00
	12.00	1.43			
	13.00	4.97			
	14.00	11.80			
	15.00	85.71			
	16.00	100.00			

by Crynes and Albright [18] except that they used stainless steel reactor while quartz was employed in this work. Each reaction zone is defined by a constant temperature. Hence by first plotting the concentrations against temperature and relating each temperature to the space time, the concentrations as function of space times can be plotted. The typical composition-temperature profile is as shown in Fig. (4.1) At low temperatures and low conversions the profile can be represented by curve OBCD. There is an induction period during which no appreciable amount of products is formed, followed by rapid formation (BC) and then CD where the rate of formation is becoming constant. As the temperature increases, the induction segment disappears with section BC becoming steeper and shorter while CD increases only slightly, flattens out or may even reverse its slope according to whether the product is being consumed or degraded or not.

At a flow rate V', different temperatures define different space-times and different concentrations. Thus at T_1, point 'a' defines a co-ordinate $a(C_1,t_1)$, T_2 gives $C(C_2,t_2)$ and T_3, $e(C_3,t_3)$. By changing the flow rate to V", at temperatures T_1, T_2 and T_3, co-ordiantes $b(C_1',t_1')$, $d(C_2',t_2')$ and $f(C_3',t_3')$ are defined respectively. Another flow rate would similarly define other loci. It was observed however that as the temperature increases ($> 650^{\circ}$) the space times became closer. Thus at the isothermal temperature T_1, the compositions against the space-times are well defined. This is as represented in Fig. (4.2).

The composition-time profiles obtained are as shown in Figs. 4.3, 4.4 and 4.5. The order of magnitude of the quantities of components obtained is CH_4 , C_2H_4 , C_3H_6 , H_2 , C_2H_6 , C_4. But at the beginning or onset of reaction, CH_4, C_2H_4, C_3H_6 and H_2 were formed at approximately equal amounts.

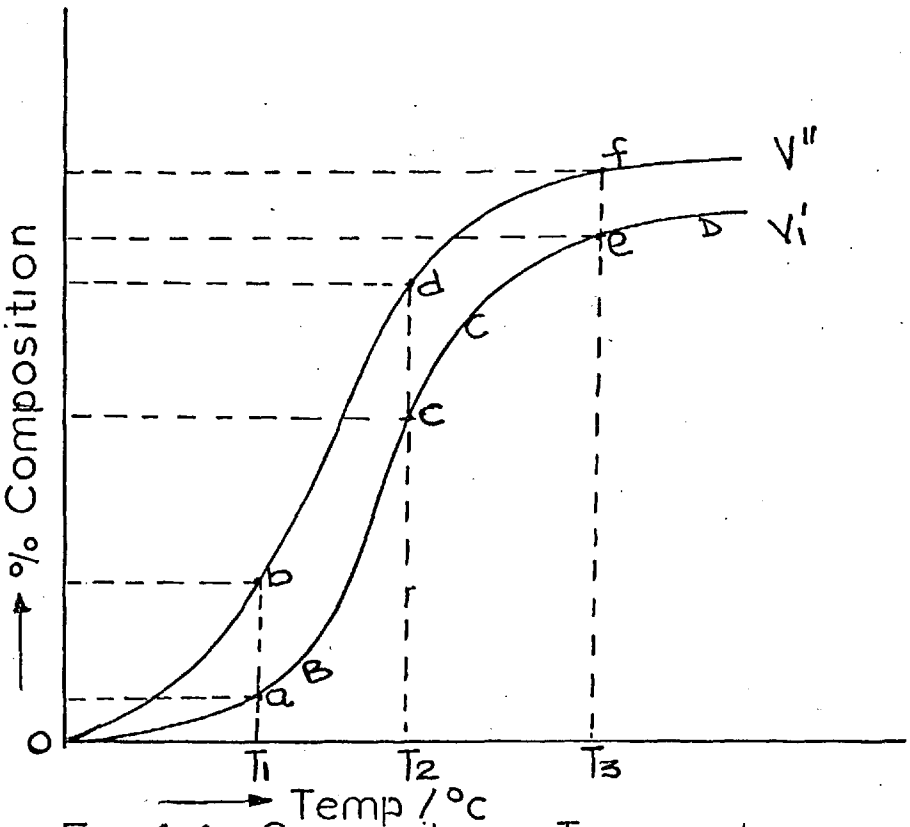

Fig 4-1 Composition Temperature profile.

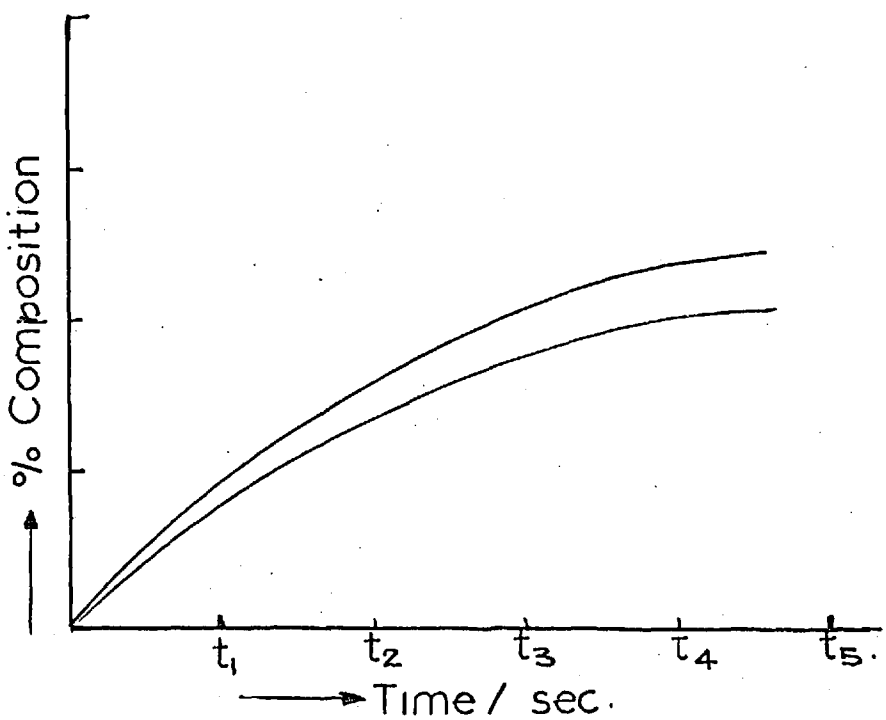

Fig 4-2 Composition–Time profile

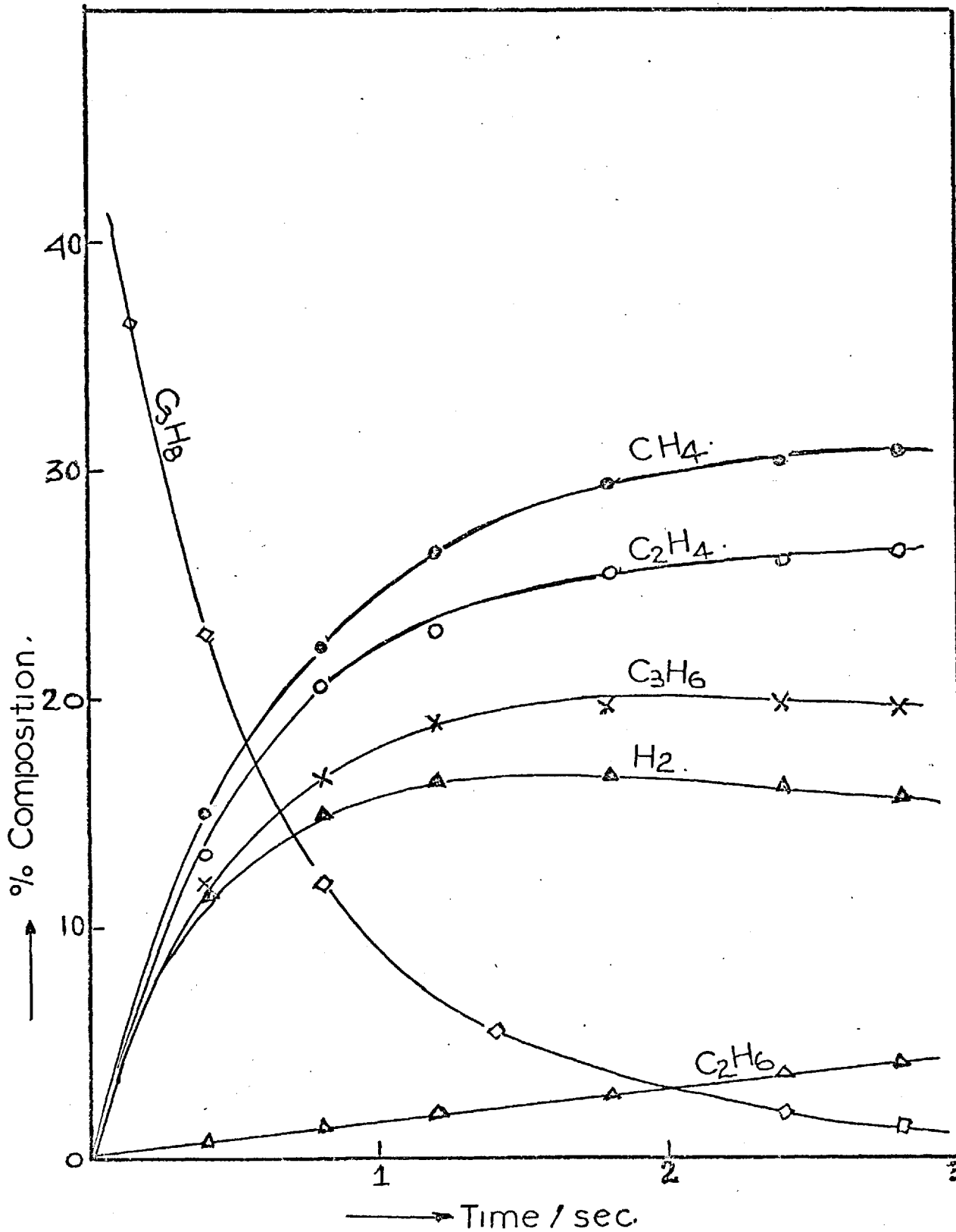

Fig 4-3 Product distribution from propane pyrolysis at 700 °C

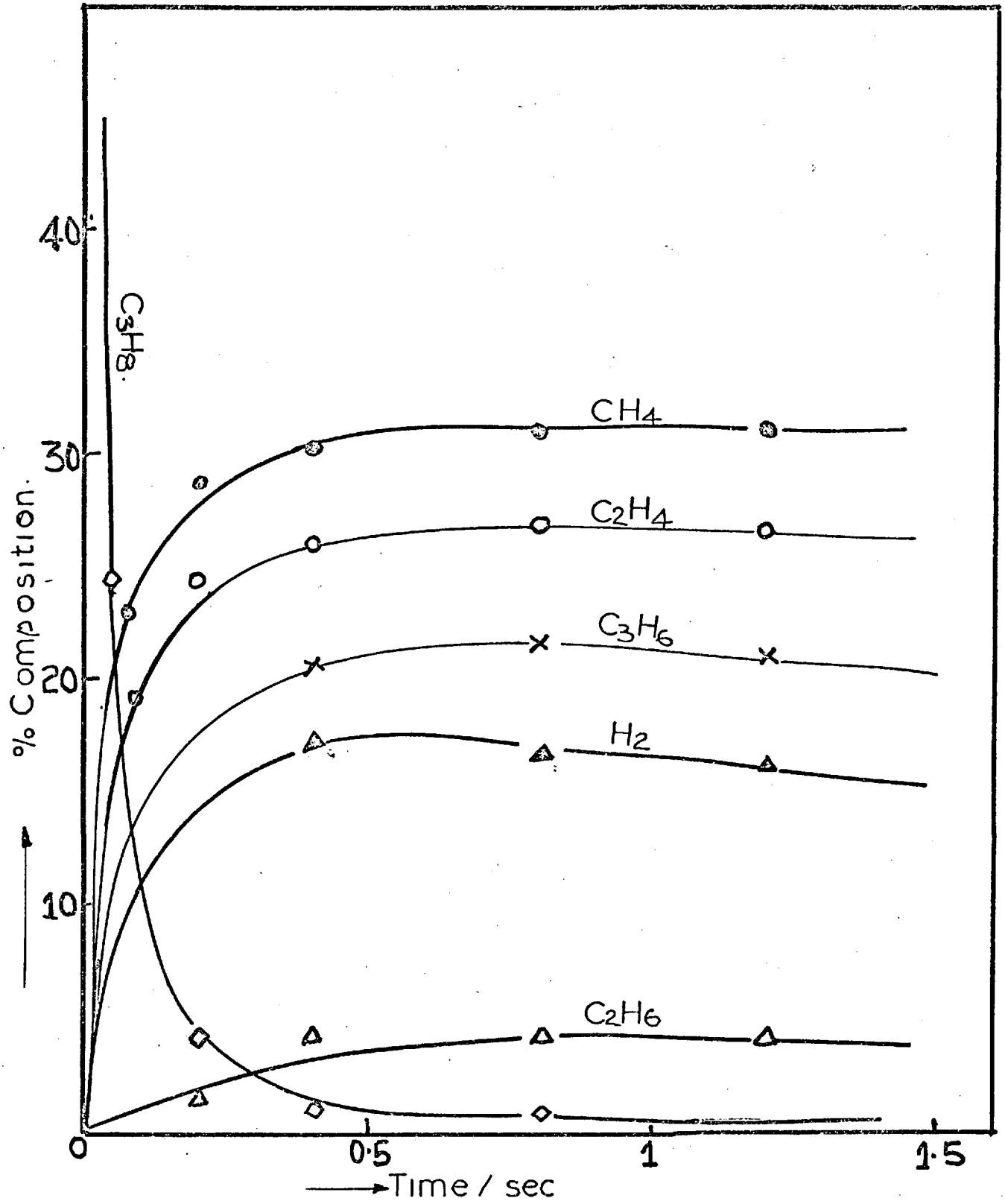

Fig 4-4 Product distribution from propane pyrolysis at 800°C.

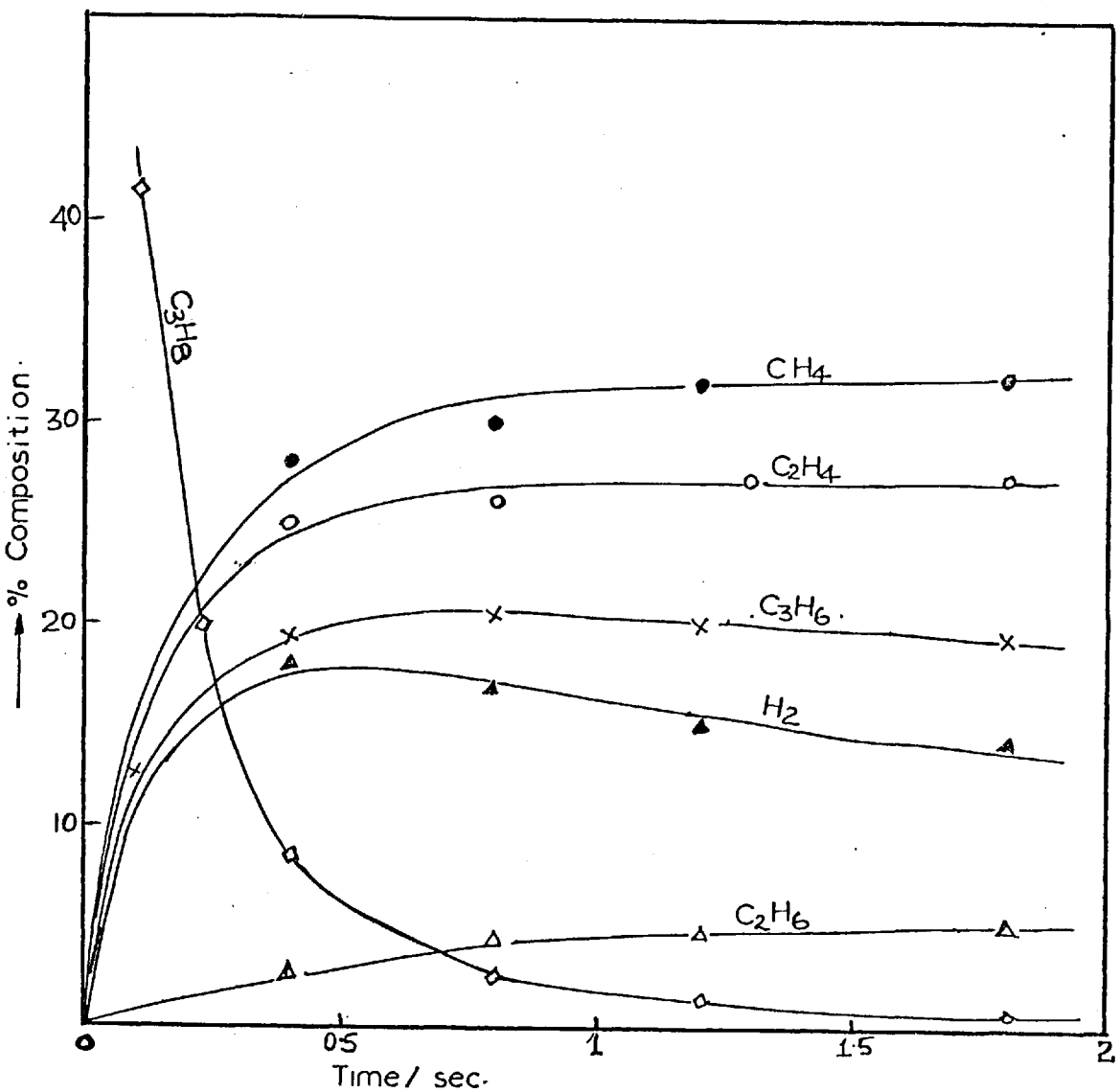

Fig 4-5 Product distribution from propane pyrolysis at 750°C

4.4 MECHANISM OF PROPANE PYROLYSIS

Breaking a C-H bond in propane is of limited importance as an initiation step because the C-H bond is stronger than a C-C bond in the propane. The key initiation step must certainly be as follows:

$$CH_3CH_2CH_3 \longrightarrow CH_3CH_2 + CH_3 \qquad (1)$$

propagation includes such steps as:

$$CH_3 + C_3H_8 \longrightarrow CH_4 + n\text{-}C_3H_7 \qquad (2a)$$

$$CH_3 + C_3H_8 \longrightarrow CH_4 + i\text{-}C_3H_7 \qquad (2b)$$

$$C_2H_5 + C_3H_8 \longrightarrow C_2H_6 + n\text{-}C_3H_7 \qquad (3a)$$

$$C_2H_5 + C_3H_8 \longrightarrow C_2H_6 + i\text{-}C_3H_7 \qquad (3b)$$

In addition the ethyl radicals will undergo some decomposition.

$$C_2H_5 \longrightarrow C_2H_4 + H \qquad (4)$$

and hydrogen atoms will engage in abstraction reactions:

$$H + C_3H_8 \longrightarrow H_2 + n\text{-}C_3H_7 \qquad (5)$$

$$H + C_3H_8 \longrightarrow H_2 + i\text{-}C_3H_7 \qquad (6)$$

Lin and Laidler[117] and many others have shown that normal propyl radicals decompose mainly into ethylene and methyl radicals:

$$CH_3\text{—}CH_2\text{—}CH_2 \longrightarrow C_2H_4 + CH_3 \qquad (6)$$

and isopropyl radicals mainly into propylene and hydrogen atoms:

$$CH_3\text{—}CH\text{—}CH_3 \longrightarrow H + C_3H_6 \qquad (7)$$

Actually in the isopropyl case the conversion into CH_3 and C_2H_4 proceeds with a lower activation energy than (7), but the frequency factor is low and (7) is therefore favoured under usual conditions.

The methyl and propyl radicals are now known to predominate in any propane pyrolysis reaction scheme, so that the most likely termination steps are:

$$CH_3 + CH_3 \longrightarrow C_2H_6 \qquad (8)$$

$$CH_3 + n\text{-}C_3H_7 \longrightarrow CH_4 + C_3H_6 \qquad (8a)$$

$$\longrightarrow i\text{-}C_4H_{10} \qquad (8b)$$

$$n\text{-}C_3H_7 + n\text{-}C_3H_7 \longrightarrow C_3H_6 + C_3H_8 \qquad (9a)$$

$$\longrightarrow n\text{-}C_6H_{14} \qquad (9b)$$

$$CH_3CH\text{-}CH_3 + CH_3CH\text{-}CH_3 \longrightarrow C_3H_6 + C_3H_8 \qquad (10a)$$

$$\longrightarrow (CH_3)_2 = CH\text{-}CH(CH_3)_2 \qquad (10b)$$

$$n\text{-}C_3H_7 + i\text{-}C_3H_7 \longrightarrow C_3H_6 + C_3H_8 \qquad (11a)$$

$$\longrightarrow CH_3(CH_2)_2\text{-}CH(CH_3)_2 \qquad (11b)$$

At high temperatures however the likelihood of reactions (9b), (10b) and (11b) occurring looks remote.

Hinshelwood et al.[110] reported that at pyrolysis temperatures the normal and isopropyl radicals are rapidly interconverted and that the reaction scheme could therefore be simplified by writing either radical as C_3H_7.

The relationship between the reaction mechanism and the overall kinetics behaviour must be considered with reference to the nature of the initiation, propagation and termination steps in which they are involved.

(i) β radicals are those that are involved in second order propagation steps; a hydrogen atom is a β radical in the propane decompostion since it undergoes the reaction:

$$H + C_3H_8 \longrightarrow H_2 + C_2H_6$$

(ii) μ radicals are those that are involved in first-order propagation steps. For example, if in a pyrolysis the C_3H_7 radical undergoes the propagation reaction $C_3H_7 \longrightarrow C_2H_4 + CH_3$, it is a μ radical.

But unimolecular reactions can have kinetics that are between first and second order, so that the radicals involved may be neither pure β or pure μ. but somewhere in between. The methyl radicals are β-radicals and if their recombination were the predominant chain-terminating step the kinetics would be 3/2 order. On the other hand if C_3H_7 were the predominant radical, and being a μ radical, the overall kinetics should be first order. In addition if reaction (8a) were predominant, the recombination would be a $\beta\mu$ type and the overall kinetics would still be first order. Any experimental result that shows an order of between 1 and 3/2 would be explained if both of these chain-terminating steps play some part with perhaps some smaller contribution from the reaction.

$$C_3H_7 + C_3H_7 \longrightarrow \text{stable products}$$

4.5 COMPUTER PREDICTION AND KINETICS

For a tubular plug flow reactor at constant total pressure, differential equations of the following type describe the system.

$$\frac{dCi}{d} = \frac{C_T}{Cro\,(1 + x)} \cdot \sum_{j=1}^{m} a_{ij} r_j - C_i \frac{dx}{dt}$$

$i = 1, 2, 3 \ldots\ldots\ldots n$

where

$$r_j = K_j \prod_{i=1}^{n} C_i^{-a_{ij}} - K'_j \prod_{i=1}^{n} C_i^{a_{ij}}$$

$a_{ij} < 0 \qquad a_{ij} > 0$

A = frequency factor in the Arrhenius expression (sec^{-1})

A_{ij} = stoichiometric coefficient of the i^{th} component in the j^{th} reaction; $aij < 0$ is a reactant; $aij > 0$ is a product

C = concentration, moles/cc .

C_T = total reactant gas concentration excluding diluent j-moles/C.C.

E = activation energy, Kcal/g-mole. or KJ/mole

K = forward rate constant, sec^{-1} or cc/g.mole(sec)

K' = reverse rate constant, " "

r_j = rate of j^{th} reaction moles/(cc)(sec)

X = fractional conversion of propane

= space time, secs.

i = refers to the component, moecular or free radical

j = refers to the reaction

m = total number of reactions

n = total number of components

After a detailed trial-and-error procedures using the integration programme described in Chapter (II), the model shown in Table 4.3 was solved using a CDC 6400 digital computer and was found to describe the pyrolysis results of propane for temperatures from 600 - 800°C at a pressure of approximately 1 atm.

TABLE 4.3

	REACTION	A	E	
1.	$C_3H_8 \longrightarrow C_2H_5 + CH_3$	6×10^{14}	326 JK/mole	158
2.	$CH_3 + C_3H_8 \longrightarrow CH_4 + C_3H_7$	1.5×10^{12}	20.5 KJ/mole	4
3.	$C_2H_5 + C_3H_8 \longrightarrow C_2H_6 + C_3H_7$	2×10^{10}	25 KJ/mole	158

4.	$C_2H_5 \longrightarrow C_2H_4 + H$	3×10^{11}	146.3 KJ/mole [159]
5.	$H + C_2H_5 \longrightarrow C_2H_5$ (4)	$7.5\ 10^{11}$	22.60 KJ/mole [158]
6.	$H + C_3H_8 \longrightarrow H_2 + C_3H_7$	1.8×10^{12}	19.20 KJ/mole [160]
7.	$C_3H_7 \longrightarrow CH_3 + C_2H_4$	4×10^{10}	133 KJ/mole [158]
8.	$C_3H_7 \longrightarrow H. + C_{3.6}$	3.6×10^{10}	133 KJ/mole [4]
9.	$H + C_3H_6 \longrightarrow C_3H_7$	1.8×10^{11}	4.18 KJ/mole [158]
10.	$CH_3 + C_2H_5 \longrightarrow C_3H_8$	$4.2\ 10^{12}$	10 KJ/mole [158]
11.	$C_2H_5 + C_2H_5 \longrightarrow C_2H_6 + C_2H_4$	1×10^{10}	0.0 KJ/mole [161]
12.	$CH_3 + C_3H_7 \longrightarrow C_3H_6 + CH_4$	1×10^{12}	0.0 KJ/mole [158]
13.	$CH_3 + C_3H_7 \longrightarrow C_4H_{10}$	1×10^{11}	0.0 KJ/mole [158]
14.	$C_3H_7 + H_2 \longrightarrow C_3H_8 + H$	5.6×10^{7}	92 KJ/mole [158]
15.	$C_2H_6 \longrightarrow CH_3 + CH_3$	1.2×10^{12}	248 KJ/mole [4]
16.	$CH_3 + C_2H_6 \longrightarrow CH_4 + C_2H_5$	8×10^{8}	50 KJ/mole [4]
17.	$H + C_2H_6 \longrightarrow H_2 + C_2H_5$	1.3×10^{11}	37.6 KJ/mole [161]

18.	$C_4H_{10} \longrightarrow C_2H_5 + C_2H_5$	8.7×10^9	167.2 KJ/mole	[162]
19.	$C_2H_5 + C_2H_5 \longrightarrow C_4H_{10}$	1×10^{11}	6.0 KJ/mole	[163]

The comparison of experimental results and with values calculated from the kinetic model shown in Table 4.4.

4.6 THE OVERALL ORDER AND ACTIVATION ENERGY OF REACTION

Suppose for example that a reaction is of the n^{th} order and involves substances that initially have a concentraion ao; such a reaction may be represented schematically as:

$nA \longrightarrow \underline{P}$

If X is the amount of A per unit volume that has disappeared in time t, the amount of A remaining is ao - X. The rate of reaction is thus:

$$\frac{-d(ao - X)}{dt} = \frac{dx}{dt} = K(ao - x)^n.$$

	873° K					
	OBTAINED	COMPUTED	OBTAINED	COMPUTED	OBTAINED	COMPUTED
SPACE TIME	0.8 SECS		1.5 SECS		2.2 SECS	
C_3H_8	97.90	98.10	95.00	94.6	90.32	89.90
C_3H_6	0.41	0.420	1.31	1.25	2.32	2.36
C_2H_4	0.022	.025	0.036	0.04	0.041	0.05
CH_4	0.47	.476	1.465	1.48	2.70	2.65
H_2	0.416	0.420	1.30	1.25	2.31	2.36
	973° K					
SPACE TIME	0.4 SECS		1.2 SECS		2.0 SECS	
C_3H_8	46.00	45.40	26.40	25.40	12.00	10.80
C_3H_6	11.50	11.52	19.00	19.00	20.00	20.00
C_2H_6	0.75	0.77	2.00	2.20	3.00	3.50
C_2H_4	13.50	13.75	23.00	23.60	25.70	26.00
CH_4	15.00	14.50	26.50	26.25	30.00	29.50
H_2	11.00	10.60	16.30	16.75	16.50	16.80

TABLE 4.4 COMPARISON OF EXPERIMENTAL DATA WITH COMPUTER PREDICTIONS

	1023° K					
	OBTAINED	COMPUTED	OBTAINED	COMPUTED	OBTAINED	COMPUTED
SPACE TIME	0.40 SECS		0.80 SECS		1.8 SECS	
C_3H_8	7.80	8.50	2.70	2.50	0.62	0.40
C_3H_6	19.00	19.80	20.40	21.50	19.50	20.50
C_2H_6	2.50	2.50	4.20	4.25	5.00	5.40
C_2H_4	24.70	25.00	26.70	27.00	27.50	27.40
CH_4	27.20	27.80	31.20	31.00	32.50	32.50
H_2	17.40	16.50	17.10	16.00	14.30	15.00
	1073° K					
SPACE TIME	0.2 SECS		0.4 SECS		0.8 SECS	
C_3H_8	4.25	4.10	1.50	1.00	0.67	0.40
C_3H_6	20.10	18.00	20.50	22.50	22.00	22.00
C_2H_6	2.20	2.00	4.20	5.00	4.52	5.00
C_2H_4	24.00	24.62	26.00	27.50	27.00	27.60
CH_4	28.00	29.60	30.40	31.50	31.20	32.00
H_2	16.80	16.50	17.50	18.00	17.80	18.30

TABLE 4.4 COMPARISON OF EXPERIMENTAL DATA WITH COMPUTER PREDICTION

This must be integrated subject to the boundary condition that x = 0, when t = 0.

If n is different from unity, the solution is:

$$K = \frac{1}{t\,(n-1)} \cdot \left[\frac{1}{(ao - x)^{n-1}} - \frac{1}{ao^{n-1}} \right]$$

but if n is unity;

$$K = \frac{1}{t} \ln \frac{ao}{ao - x}$$

Hence for a reaction of order 1, a graph of $\ln\left(\frac{ao}{ao - x}\right)$ against time t should be a straight line whose slope gives the rate constant K. for a 3/2-order kinetics, the applicable equation is

$$K = \frac{2}{t}\left[\frac{1}{(ao - x)^{\frac{1}{2}}} - \frac{1}{ao^{1/2}}\right]$$

and for a second-order reaction, the rate constant K. would be:

$$K = \frac{1}{t}\left[\frac{1}{ao}\left(\frac{x}{ao - x}\right)\right]$$

All of these are tested, but perfect agreement is obtained only in the 1st-order condition. The graphs of $\ln \frac{ao}{ao - x}$ us. t for different temperatures are as shown in Figs 4.7, 4.8, and 4.9 giving the corresponding K. values of 0.0384, 1.276 and 2.00 respectively.

$$K = Ae^{-E/RT}$$

$$\log K = \log A - \frac{E}{2.3\,RT}$$

A graph of log K us. 1/T should be a straight line whose slope is E/2.3R. This is presented in fig 4.10

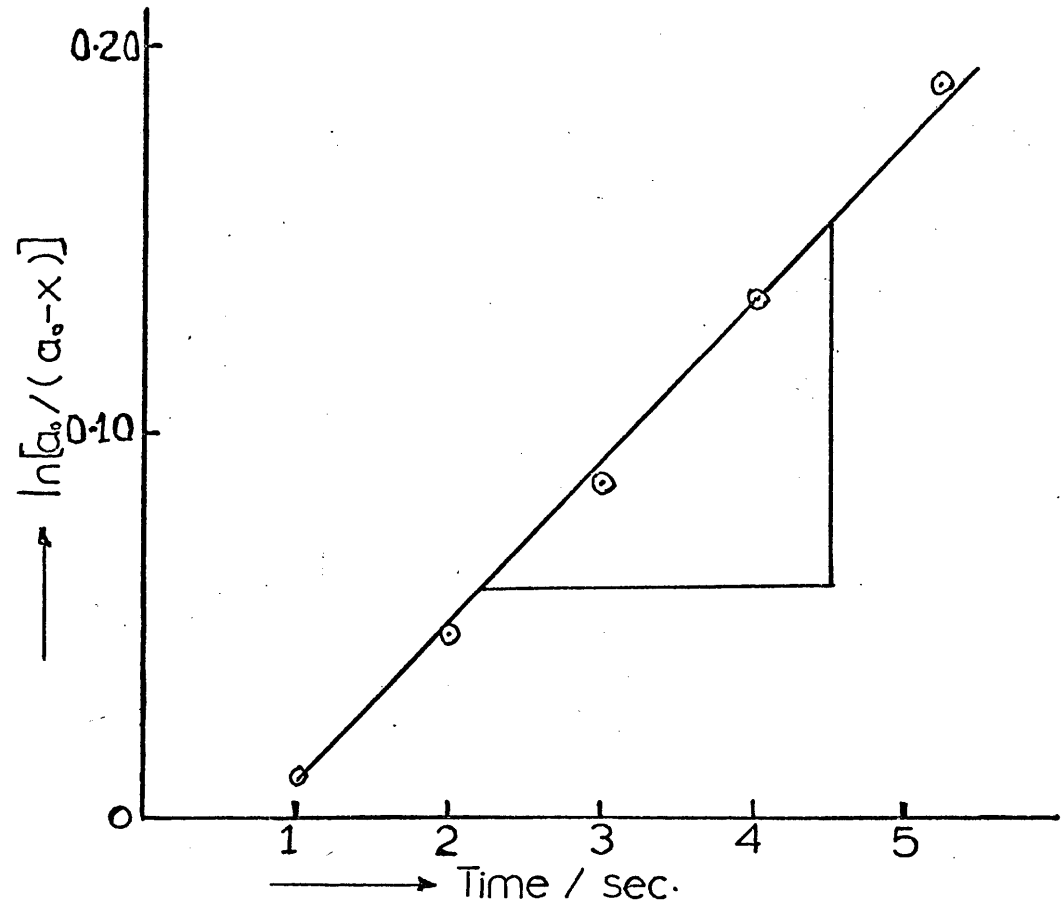

Fig 4-7· Determination of the rate constant, k, at 600°C

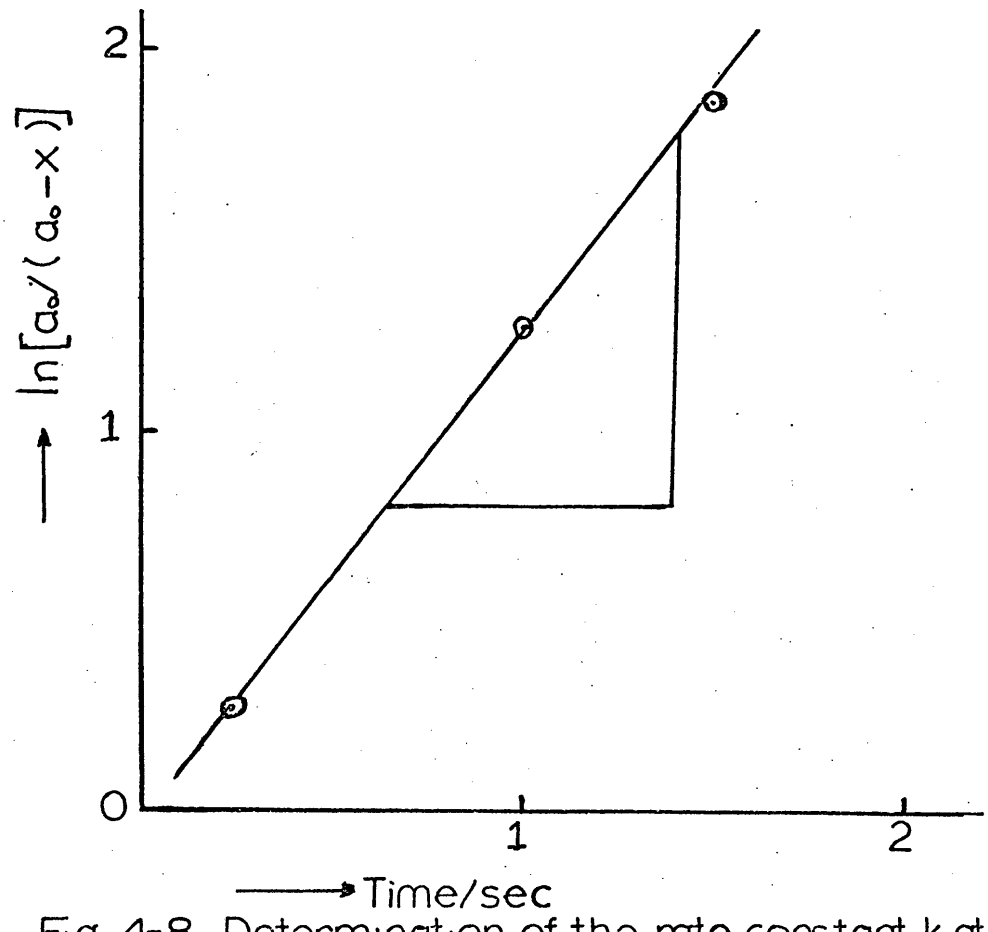

Fig 4-8· Determination of the rate constant k at 700°C

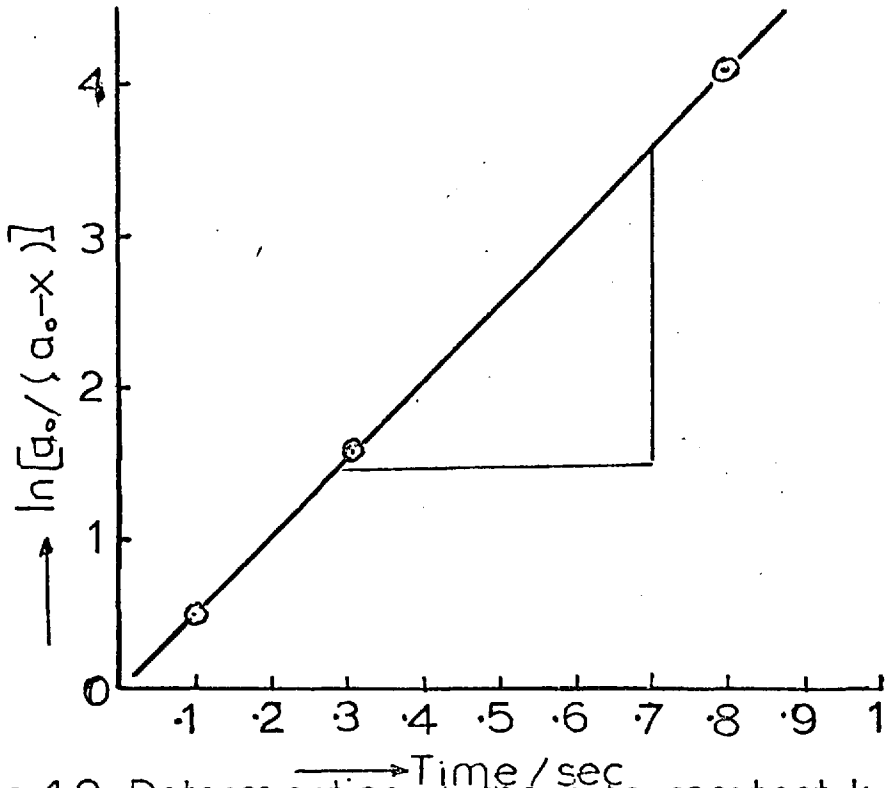

Fig 4-9 Determination of the rate constant, k, at 750°C

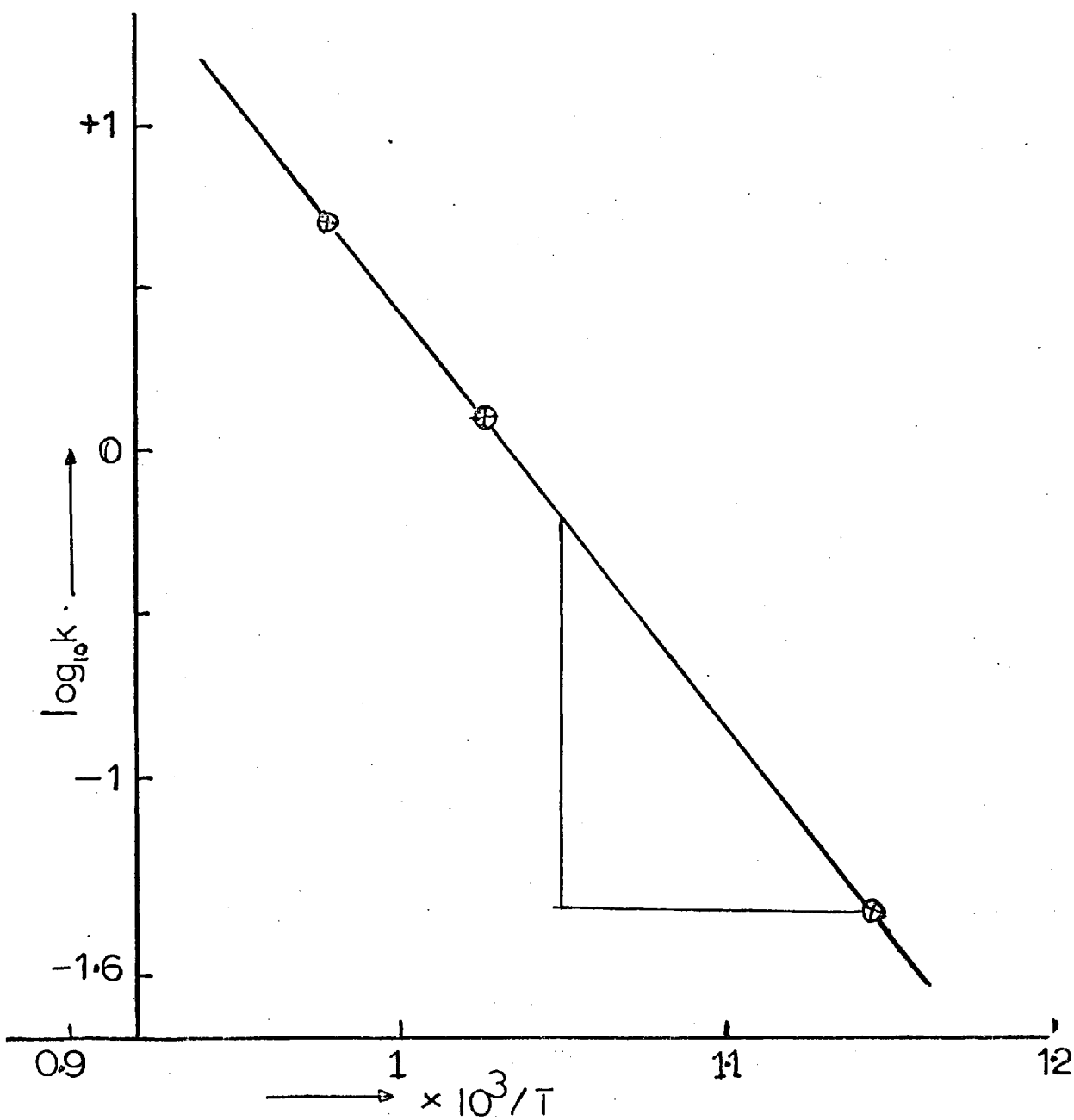

$$\text{The slope} = \frac{1.2}{0.093} \times 10^3$$

$$= 1.30 \times 10^4$$

$$E/2.3R = 1.30 \times 10^4$$

$$E = 1.30 \times 10^4 \times 2.3 \times 1.96 \text{ cals/mole}$$

$$= 5.86 \times 10^4 \text{ cals/mole}$$

$$= 58.6 \text{ Kcal/mole} = 245 \text{ KJ mole}^{-1}$$

Hence the overall activation energy is equal to 58.60 Kcal/mole.

Substituting this value in the rate equation

$$\log K = \log A - \frac{E}{2.3\,RT} \quad \text{, gives at } \frac{1}{T} = 1,$$

$$0.42 = \log A - \frac{58.60}{2.30 \times 1.96}$$

$$\text{i.e;} \quad \log A = \frac{58.60}{2.30 \times 1.96} + 0.42$$

$$\log A = 12.9991 + 0.4200$$

$$\log A = 13.4191 \text{ ,}$$

from which

$$A = 2.63 \times 10^{14} \text{ sec}^{-1}.$$

The overall reaction rate equation for the kinetics of propane pyrolysis between 600 - 800°C can thus be represented as:

$$W = 2.63 \times 10^{14} \, e^{-\frac{58.60}{RT}} \, [C_3H_8]^1$$

$$W = 2.63 \times 10^{14} \exp(-245/RT)[C3H8]^1 \quad E(KJ/mole)$$

4.7 DISCUSSION

It is concluded here that the kinetics of the primary decomposition of propane between 600° - 800°C and 1 atmosphere pressure is first-order with respect to propane concentration, and that the overall activation energy is 58.6 Kcals/mole. The data neither fits a 3/2 nor a second-order kinetics. As the mechanism indicates, propyl radical, $C_3H_7\cdot$, is the main radical. The methyl radicals present are mainly involved in abstraction to form methane so that their recombination does in no way predominate. Thus a 3/2 or higher order is not favoured. Termination reactions of the type $CH_3\cdot + C_3H_7\cdot$ products $\beta\mu$ combination, and $C_3H_7 + C_3H_7$ products which is a $\beta\beta$ combination supports the first-order kinetics. Hence Goldfinger's[116] theory seems validate.

Of all the primary products of propane, propylene is the most vulnerable to high thermal contact. Even then under the reaction conditions, it could only pyrolyze to a small extent to give mainly methane and ethylene. Methane is apparently not affected and together with ethylene, increase all of the time. Several reaction steps which are undoubtedly occurring, though not significantly, during propane pyrolysis include reactions such as:

$$C_3H_6 + CH_3 \longrightarrow C_4H_9$$

$$C_4H_9 \longrightarrow C_4H_8 + H$$

$$H_2 + C_4H_9 \longrightarrow C_4H_{10} + H$$

$$C_3H_7 + C_4H_8 \longrightarrow C_4H_7 + C_3H_8$$

$$C_4H_7 \longrightarrow C_4H_6 + H$$

$$C_2H_4 \longrightarrow 2C + 2H_2$$

There was soot deposited on the tips of the sampling probe at high temperatures which indicates the occurrence of coking reaction, most likely

$C_2H_4 \longrightarrow 2C + 2H_2$ and which may involve acetylene as an intermediate. Acetylene, apart from forming soot and hydrogen may be polymerized to benzene and other aromatics.

The overall activation energy of 245 KJ/mole compares favoourably with those of Laidler, De Boodt and Kershenbaum:

		E(kcal)	TEMP°C	E.
Laidler et al	(1962)	54,500	530 - 670	227.8 KJ/m
De Boodt	(1962)	53,000	700 - 750	221.5 "
Kershenbaum	(1967)	52,100	800 - 1000	218 "
This work		58,600	600 - 800	245 "

The comparative value of K is shown in fig. 4-11

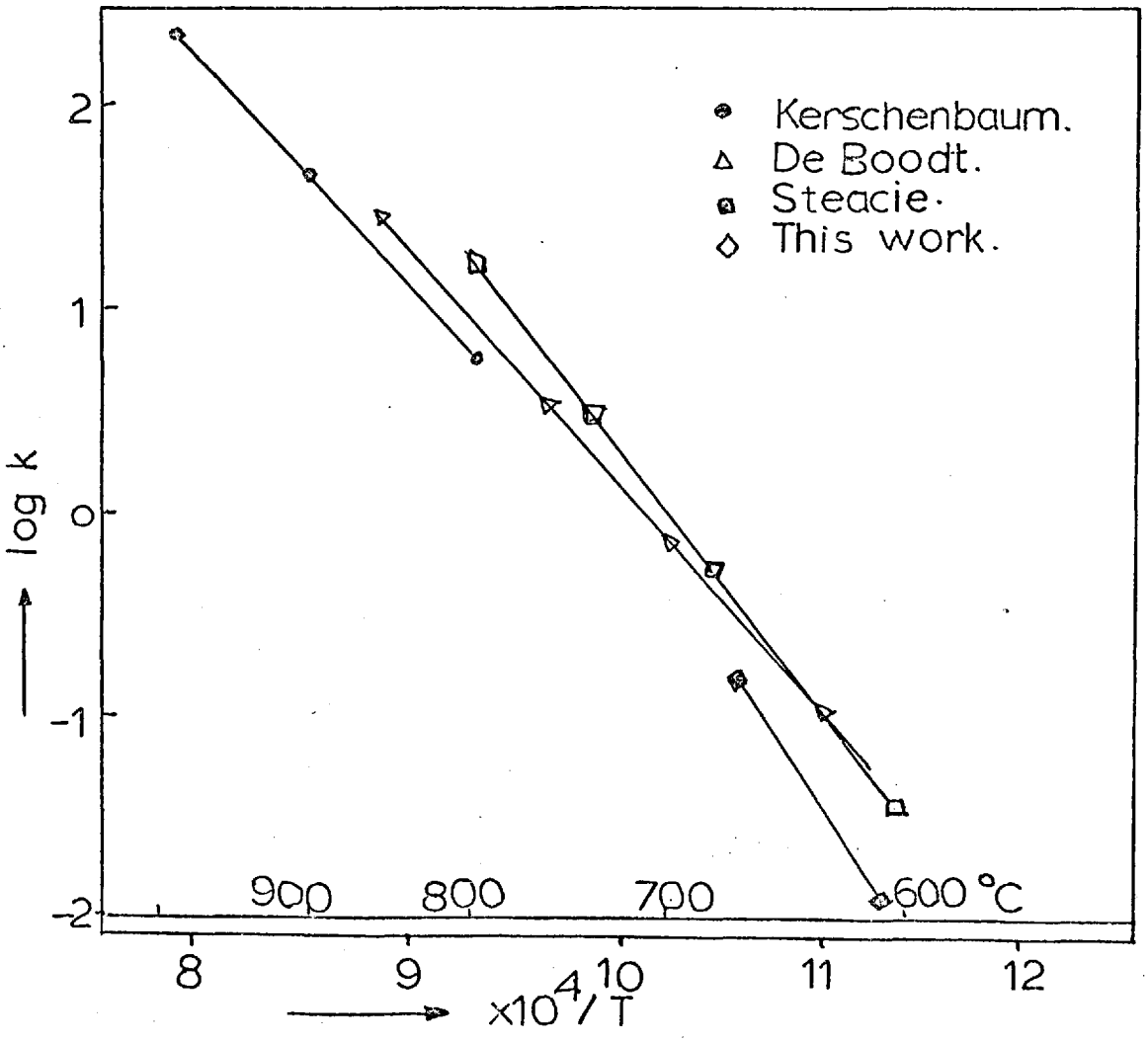

Fig 4-11 Comparison of kinetics with literature.

CHAPTER V

CHAPTER V

PERTURBATION PYROLYSIS KINETICS OF PROPANE

5.1 INTRODUCTION

As the results discussed in Chapter IV revealed, the kinetics of propane pyrolysis is first order with respect to propane concentration. It is generally true that impurities do affect the course of a chain reaction, either to hinder or accelerate its rate. They could therefore alter its mechanism. The free-radical chain reaction mechanism for the thermal decomposition of a paraffin requires first a scission of a C-C bond of the paraffin to generate free radicals which are necessary for initiation. This initiating C-C cleavage is the principal determinant of the rate of decomposition. Consequently, if it were possible to introduce some radicals from another source into the reactant so that the chain mechanism could be initiated by another reaction, then the decomposition rate should be altered.[121] To test both the mechanism and the mathematical modelling, the propane pyrolysis system is perturbed by artificially creating a higher rate of radical formation by introducing small amounts of acetone (regarded as a source of methyl radicals) and acetaldehyde(which, apart from being capable of generating methyl radicals, also plays an important role in the oxidation of hydrocarbons). The effect is measured experimentally between 600° and 750°C and compared with computer prediction to give an indication of its validity.

5.2 PROPANE PYROLYSIS PERTURBED BY ACETONE

The C-C bond in acetone is 343KJ per mole, i.e. is slightly weaker than that in propane of 352 KJ per mole[122]. Acetone can be thermally decomposed in two ways; namely either concertedly to give carbon monoxide and methyl radicals according to the equation:

$$CH_3COCH_3 \longrightarrow CO + CH_3\cdot + CH_3 \qquad \text{(i)}$$

or in two consecutive steps according to the equations:

$$CH_3COCH_3 \longrightarrow CH_3CO + CH_3 \qquad \text{(ii)}$$

$$CH_3CO \longrightarrow CH_3 + CO \qquad \text{(iii)}$$

The conclusion of Rice and Herzfeld[2] on acetone pyrolysis showed that acetone does not decompose concertedly. Hence the two-step decomposition is the most probable initiation reactions.

5.2.1 REACTION SYSTEM

The flow system is basically the same as in fig. [3 - 1] except that a vaporizer is placed between the flow meter and the preheater. This vaporizer was purchased from Longworth Scientific Instruments Co. Ltd., Abingdon, Berkshire, and its essential features are shown in fig. 5-1.

5.2.2 THE ABINGDON VAPORIZER

The vaporizer has a graduated knob on the front face which can be calibrated in volume percent of the volatile additive. When this knob is in the zero position, an internal mechanism closes the vapour chamber completely but permits free flow of propane or any other feed from the inlet to the outlet. The inlet tubes are fitted with PTFE (teflon) which is resistant to acetone. A minimum rotation of 20°, which is approximately 6mm of the scale length, is necessary to open the closing mechanism, and during this first 20° of rotation of the knob, there is virtually no output of any kind. Further rotation of the control knob will produce a gradually increasing output in accordance with the calibration marked on the dial. The calibration was carried out by opening the knob to a certain position while propane of known flow rate was passing and analysing

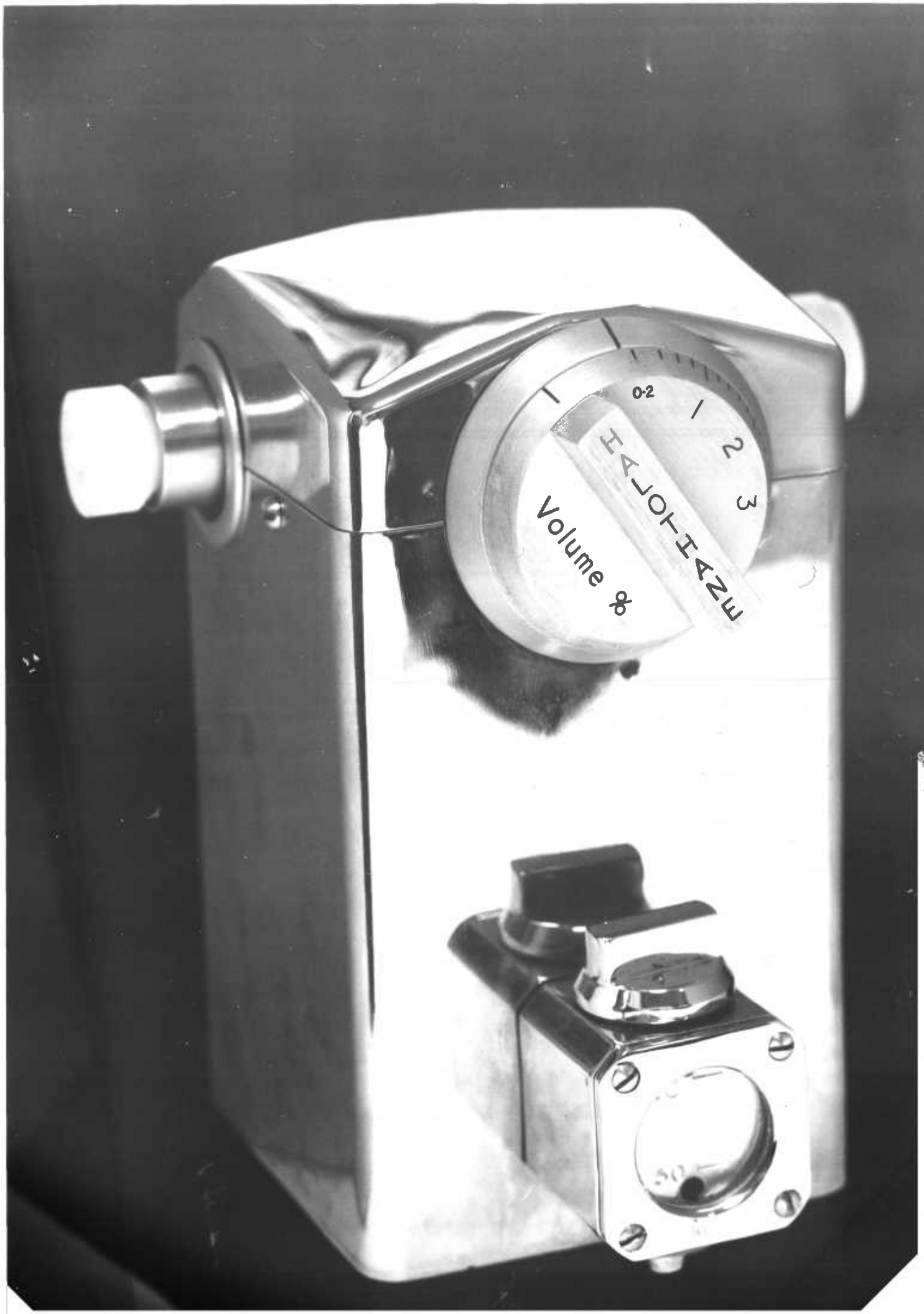
0-2
1
2
3
Volume

the putput mixture of propane and acetone with the mass spectrometer.

To fill the vaporizer, the control knob is turned to the zero position (it is then not necessary to turn off the gas supplies), the filler cap is unscrewed and the vaporizer filled with the appropriate volatile additive. The level indicator was calibrated at 50 and 150 ml volume and the vaporizer was filled until the level was between these marks. The top of the filler orifice is lower than the working parts of the vaporizer so that it is not possible to over-fill the vaporizer to a dangerous level. The filler cap is then replaced and tightened firmly with fingers only. To drain the vaporizer, the control knob should be turned to the zero position. The filler cap which exposes the head of the drain screw can then be removed. In one end of the bar on the filler cap is a hexagon socket to fit this drain screw. This must be used to loosen the drain screw which can then be opened with the fingers to release liquid into a bottle held below the filler block. The stainless steel wicks in the Abingdon Vaporizer retain very little liquid and it is possible to recover almost all of the additive.

The scale engraved on the knob was substantially accurate at flow rates between 0.30 and 8 litres per minute and at room temperatures between 18° and 32°C. In common with many other vaporizers, changes of ambient conditions may occasionally result in condensation of the volatile additive on the internal proportioning mechanism, which may temporarily reduce the output concentrations to a considerable extent. To avoid this difficulty, at the commencement of operation, the vaporizer control should be turned to 2% or more and a flow of 4 l/m passed for about 10 seconds. This would evaporate any condensation and ensure accuracy. Furthermore, when selecting a low concentration of less than 1., the control knob should be turned from zero to 1 and then back to the desired setting.

RELATIVE ION INTENSITIES FOR CERTAIN COMPONENTS. eV = 70V, Trap Current Trap Current = 50μA, Ion Repeller Voltage = 1V, Mass spectrometer model MS10-C2

TABLE 5.1

COMPOUND	MASS NUMBER M/e	RELATIVE ION INTENSITIES
CH_2O	12.0	3.30
	13.0	4.30
	14.0	4.40
	16.0	1.70
	28.0	30.90
	29.0	100.00
	30.0	88.50
	31.0	1.80
CH_3COCH_3	26.0	3.14
	27.0	4.83
	28.0	4.75
	29.0	3.07
	37.0	1.71
	38.0	1.96
	39.0	4.26
	42.0	6.72
	43.0	100.00
	44.0	4.65
	57.0	1.12
	58.0	37.35

COMPOUND	MASS NUMBER M/e	RELATIVE ION INTENSITIES
CH_3CHO	18.00	0.30
	21.0	0.10
	24.0	1.56
	25.0	4.76
	26.0	9.10
	27.0	4.54
	28.0	2.66
	29.0	100.00
	30.0	1.14
	41.0	3.86
	42.0	9.16
	43.0	j26.70
	44.0	45.70
	45.0	1.24

It is also essential that there should be no leakage. This can be ensured by turning on a supply of gas, thus partially blocking the outlet of the vaporizer to cause a positive pressure inside it, and with a syringe, run a small quantity of ether round the joint between the vaporizing chamber and body, and checking that no gas bubbles appear.

5.2.3. ANALYSIS OF RESULTS

The amount of acetone in the propane stream varied from 0.8 to 4% at 600° - 700°C but to a maximum of 3. at 750°C as the decay of propane was expected to be much faster at this temperature. In all cases however, there was an acceleration of propane decomposition, and the major products in order of magnitude are CH_4, C_2H_4, C_3H_6, H_2, C_2H_6, C_4 Methane and ethane increased in comparison to their values in the absence of acetone. Propylene and hydrogen were slightly reduced while ethylene remained virtually constant. Some of the concentration profiles are shown in Figs. 5.2 and 5.3.

5.3.1 MECHANISM AND KINETICS

Winkler and Hinshelwood[118] concluded that the thermal decomposition of acetone is almost completely homogeneous. This is supported by Allen[119]. Pyrolyzed on its own the Hertzfeld free-radical mechanism postulated the following reaction steps:

$$CH_3COCH_3 \longrightarrow CH_3 + CH_3CO.$$

$$CH_3CO + M \longrightarrow CH_3 + CO + M$$

$$CH_3 + CH_3COCH_3 \longrightarrow CH_4 + CH_3COCH_2$$

$$CH_3COCH_2 \longrightarrow CH_3 + CH_2CO$$

$$CH_3 + CH_3 + M \longrightarrow C_2H_6 + M$$

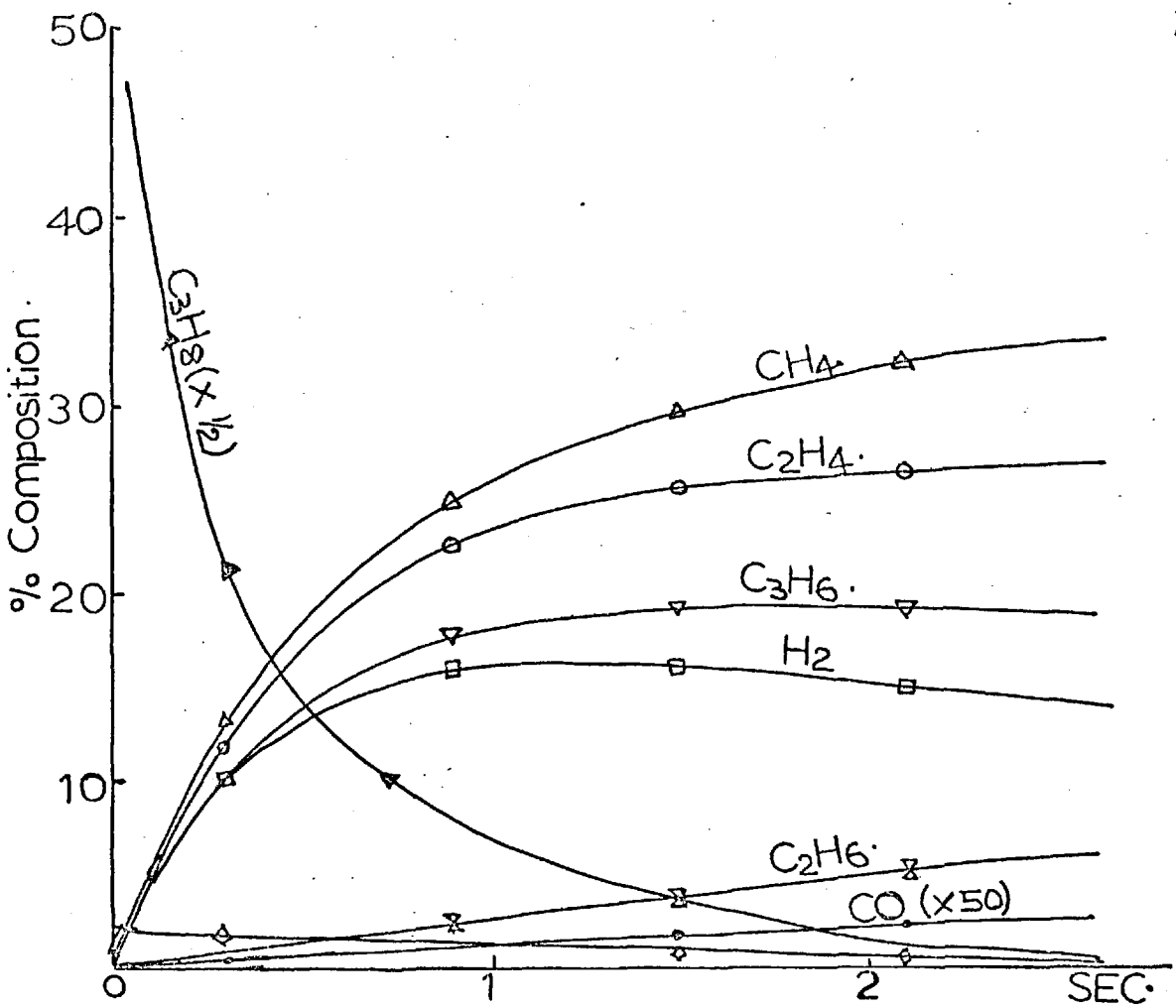

Fig5-2. Product formation from propane plus 2% acetone at 700 °C ◇= acetone

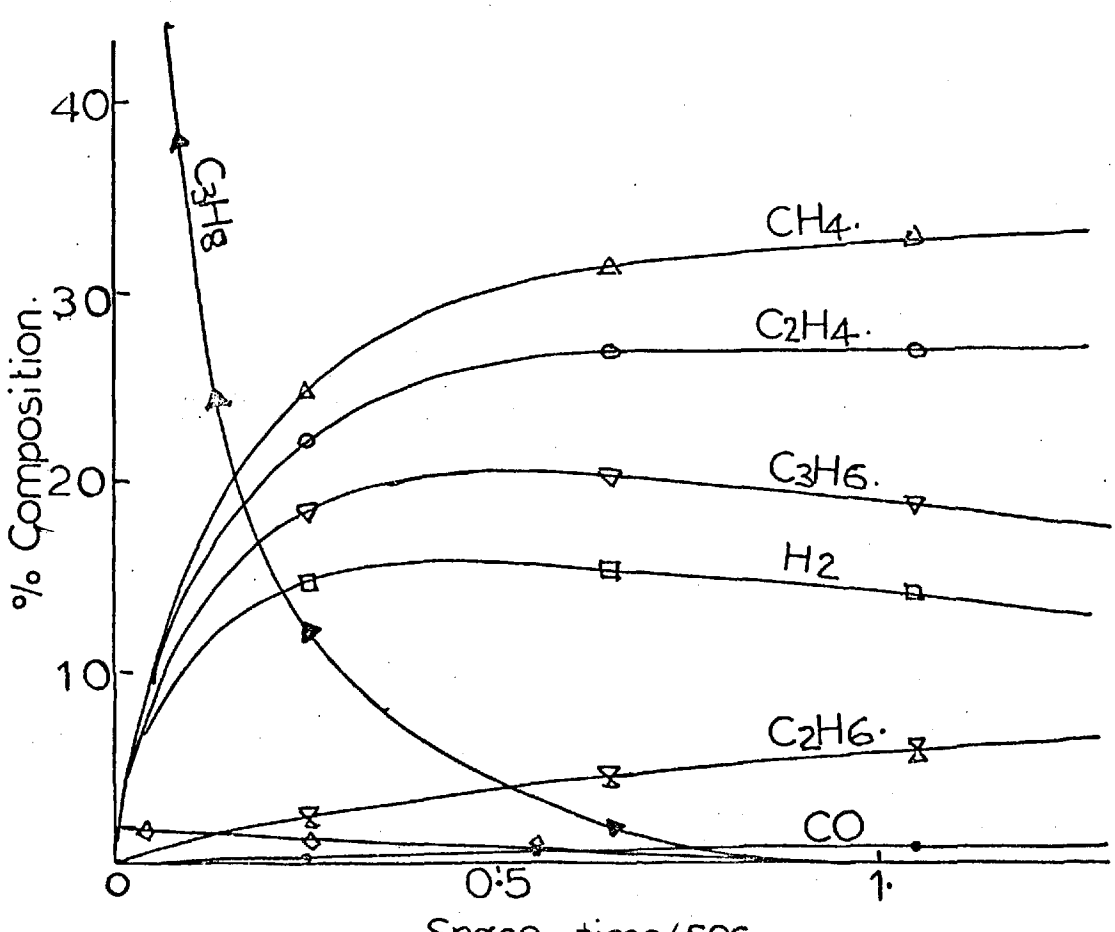

Fig 5 3 Product from propane plus 2% acetone at 750 °C ◇=acetone.

$$CH_3 + CH_3COCH_2 \longrightarrow CH_3COC_2H_5$$

$$2CH_3COCH_2 \longrightarrow (CH_3COCH_2)_2$$

At high temperatures both ketene, CH_2CO and CH_3COCH_2 as well as CH_3CO will be unstable and the main products at low conversion will be methane and ethane. At longer reaction times, the variation in the product spectrum relative to unperturbed propane will depend only on the total methyl concentration. Having established a mechanism for propane pyrolysis in Chapter IV, the rate equations appropriate to the following reaction scheme were integrated and found to describe very well the pyrolysis of propane perturbed by the addition of small amounts of acetone.

TABLE 5-2

	REACTION	A/SEC^{-1}	E/KJ/mole
1.	$C_3H_8 \longrightarrow CH_3 + C_2H_5$	6×10^{14}	326[158]
2.	$CH_3COCH_3 \longrightarrow CH_3 + CH_3CO$	3×10^{14}	300[164]
3.	$CH_3CO \longrightarrow CH_3 + CO$	1×10^{13}	67[149]
4.	$CH_3 + C_3H_8 \longrightarrow CH_4 + C_3H_7$	1.5×10^{12}	20.5[4]
5.	$C_2H_5 \longrightarrow C_2H_4 + H.$	$3\ 3 \times 10^{11}$	146.3[159]
6.	$H. + C_2H_4 \longrightarrow C_2H_5$	7.5×10^{11}	22.6[158]
7.	$C_2H_5 + C_3H_8 \longrightarrow C_2H_6 + C_3H_7$	2×10^{11}	25[158]
8.	$C_3H_7 \longrightarrow CH_3 + C_2H_4$	4×10^{10}	133.8[158]
9.	$H. + C_3H_8 \longrightarrow H_2 + C_3H_7$	1.8×10^{12}	19.2[160]
10.	$C_3H_7 \longrightarrow C_3H_6 + H.$	3.6×10^{10}	133.[4]
11.	$H. + C_3H_6 \longrightarrow C_3H_7$	1.8×10^{11}	4.18[158]

12.	$CH_3 + C_2H_5 \longrightarrow C_3H_8$	4.2×10^{12}	0.0	158
13.	$C_2H_5 + C_2H_5 \longrightarrow C_2H_4 + C_2H_6$	1×10^{10}	0.0	161
14.	$CH_3 + C_3H_7 \longrightarrow C_3H_6 + CH_4$	1×10^{12}	0.0	158
15.	$CH_3 + C_3H_7 \longrightarrow C_4H_{10}$	1×10^{11}	0.0	158
16.	$H_2 + C_3H_7 \longrightarrow H. + C_3H_8$	5.6×10^{7}	92.0	158
17.	$C_2H_6 \longrightarrow CH_3 + CH_3$	1.2×10^{12}	284	4
18.	$C_2H_5 + C_2H_5 \longrightarrow C_4H_{10}$	1.0×10^{11}	0.0	163
19.	$H. + C_2H_6 \longrightarrow C_2H_5 + H_2$	1.3×10^{11}	0.0	161
20.	$CH_3 + C_2H_6 \longrightarrow CH_4 + C_2H_5$	8×10^{8}	50.	4
21.	$C_4H_{10} \longrightarrow C_2H_5 + C_2H_5$	8.7×10^{9}	167	162

Table 5.3 shows the comparison between the calculated and computer predicted values which show very good agreement.

5.3.2 DISCUSSION

Fig. 5.4 shows clearly the accelerating effect of acetone on the rate of propane decomposition. This is due to the extra methyl radicals generated by acetone decomposition and it can be seen that as acetone concentration increases, the concentration of methyl radicals also increases and the overall effect is to diminish the induction period Fig. 5.5 reveals that the addition, at such low concentrations, is a direct boost rather than a deviation from the established first-order kinetics. The reaction rate constant, K, is almost constant as the plots of $\log_e[ao/(ao - x)]$ versus time, for the various concentrations of actone added, are almost parallel. The higher the acetone concentration the nearer to zero are the kinetic lines displaced indicating a shortening

TEMPERATURE = 600°C 4% ACETONE				
SPACE TIME	0.81 SECS		2.00 SECS	
	CALCULATED	COMPUTED	CALCULATED	COMPUTED
C_3H_8	93.45	93.60	84.00	84.28
C_3H_6	0.60	0.61	2.90	2.85
C_2H_6	0.002	0.002	0.02	0.018
C_2H_4	0.68	0.68	3.16	3.19
CH_4	0.69	0.68	3.20	3.22
H_2	0.63	0.61	2.80	2.83
CH_3COCH_3	3.80	3.79	3.62	3.60
CO	nil	traces	traces	traces
TEMPERATURE = 700°C, 4% ACETONE				
SPACE TIME	0.1 SEC.		0.96	
	CALCULATED	COMPUTED	CALCULATED	COMPUTED
C_3H_8	79.70	79.63	12.10	11.04
C_3H_6	3.92	3.96	17.90	18.20
C_2H_6	0.05	0.05	3.00	3.16
C_2H_4	4.40	4.43	23.50	23.56
CH_4	4.43	4.49	27.00	26.80
H_2	3.96	3.92	14.70	15.00
CH_3COCH_3	3.50	3.51	2.15	2.18
CO	0.008	0.008	0.04	0.043

TABLE 5.2 COMPARISON OF CALCULATED TO COMPUTED VALUES

of the induction period.

The effect remains the same at 700 and 750°C. The effect is illustrated in Fig. 5.6 at 700°C, but the profiles become very much closer due to the fact that, at this temperature, propane itself is being rapidly decomposed and the effect of the extra methyl radicals from acetone becomes relatively minor. The first order kinetic lines in fig. 5.7 are very close indeed. At 750°C, the same situation prevails as indicated in fig. 5.8 and fig. 5.9.

Propane decays faster in the presence of acetone because of the extra methyl radicals generated. This effect must be reflected in the concentration profiles of the pyrolysis products. The highest gain goes to ethane followed by methane boosted mainly by the increase in the concentration of methyl radicals. Ethane must have gained in addition as a result of methyl radical recombination.

$$CH_3 + CH_3 + M \longrightarrow C_2H_6 + M$$

The increase in the concentration of methyl radicals inevitably increases the rate of the propagating step.

$$CH_3 + C_3H_8 \longrightarrow CH_4 + C_3H_7$$

Thus at the onset of reaction, the following steps are accelerated.

$$C_3H_7 \longrightarrow C_2H_4 + CH_3$$

$$\longrightarrow C_3H_6 + H$$

$$H\cdot + C_3H_8 \longrightarrow H_2 + C_3H_7$$

This represents the boost for methane, propylene, ethylene and hydrogen particularly at 600°C when the dissociation of propane lags markedly behind that of acetone. As the reaction proceeds however, both propylene and hydrogen reduce in concentration and the ethane boost becomes more apparent. The boost for ethane is probably due to the combination of reaction of methyl radicals;

$$CH_3 + CH_3 + M \longrightarrow C_2H_6 + M$$

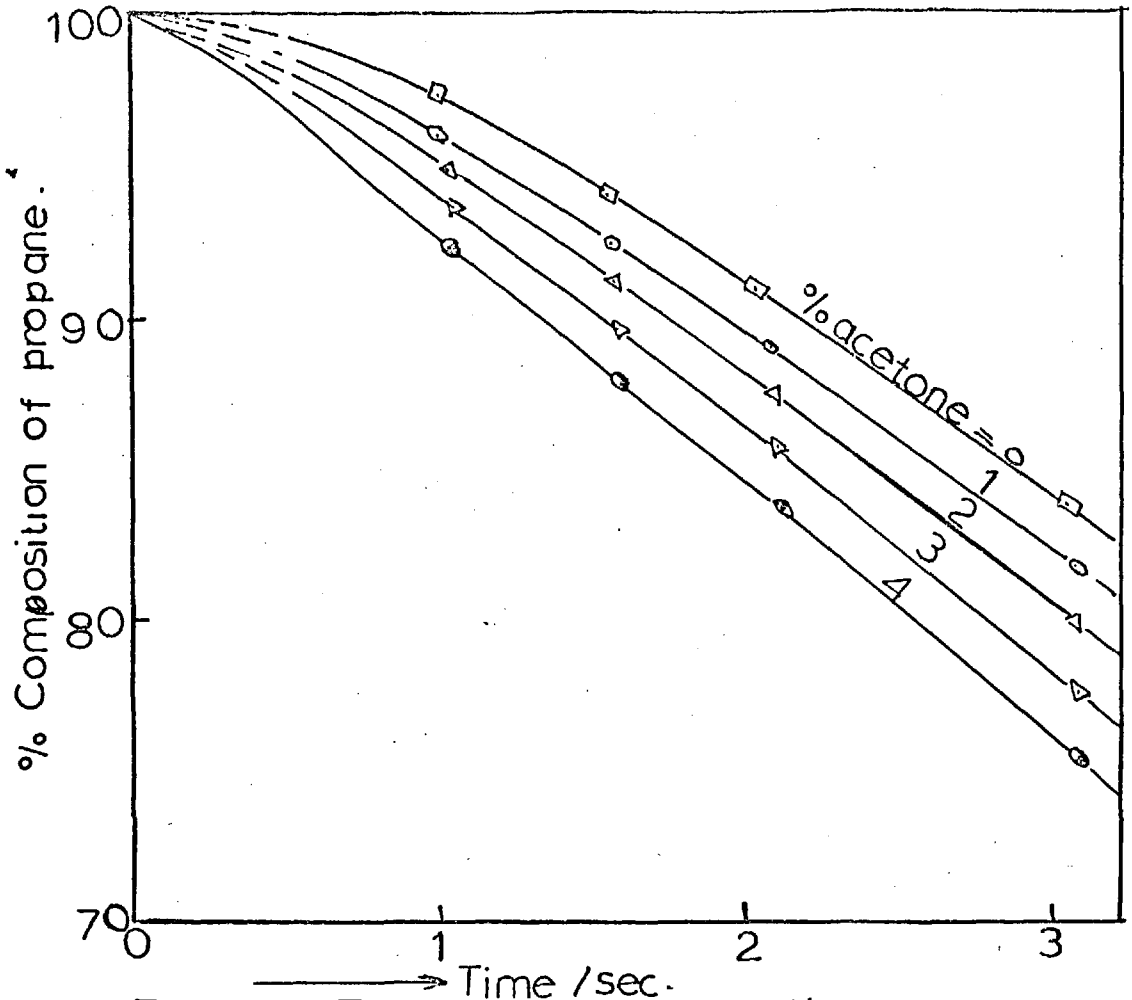

Fig.5-4. Effect of acetone partial pressure on propane decomposition at 600°C.

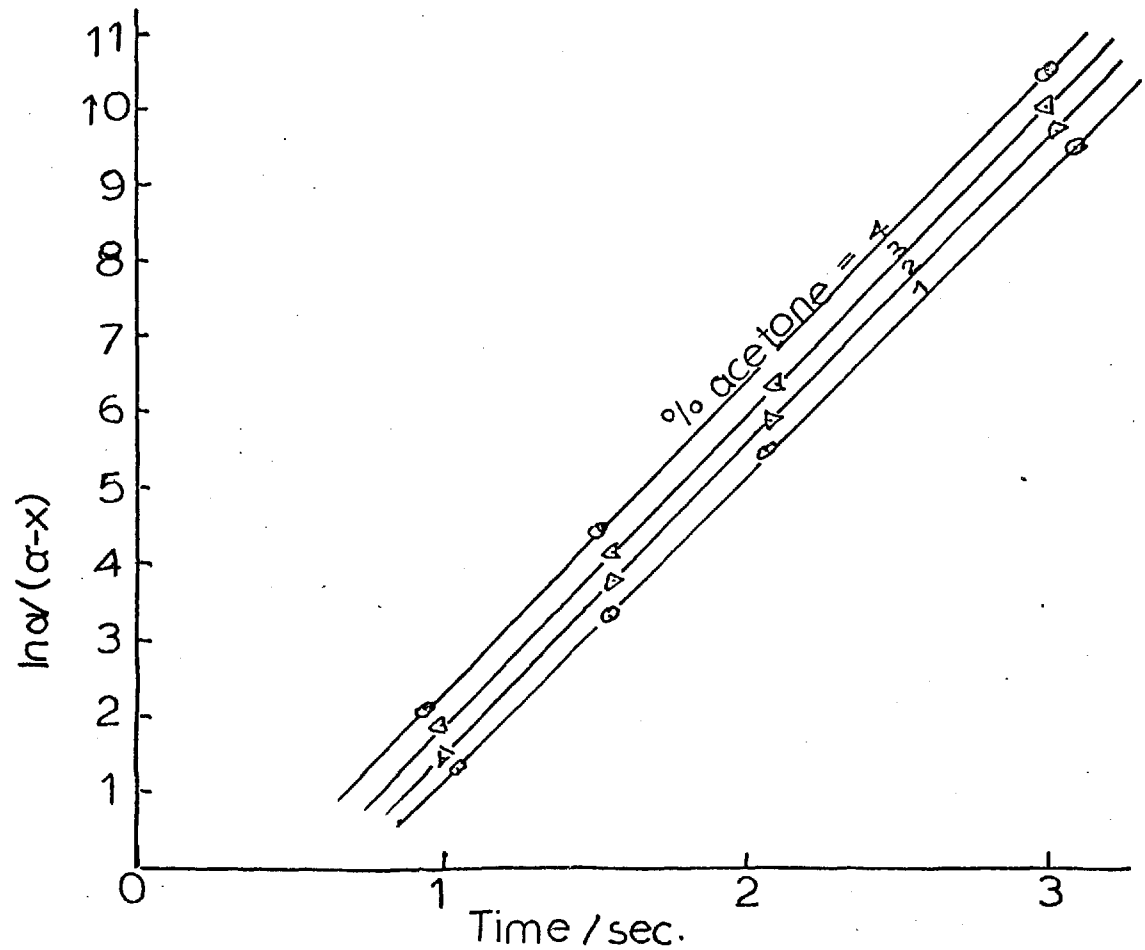

Fig.5-5. First order kinetics in presence of acetone.

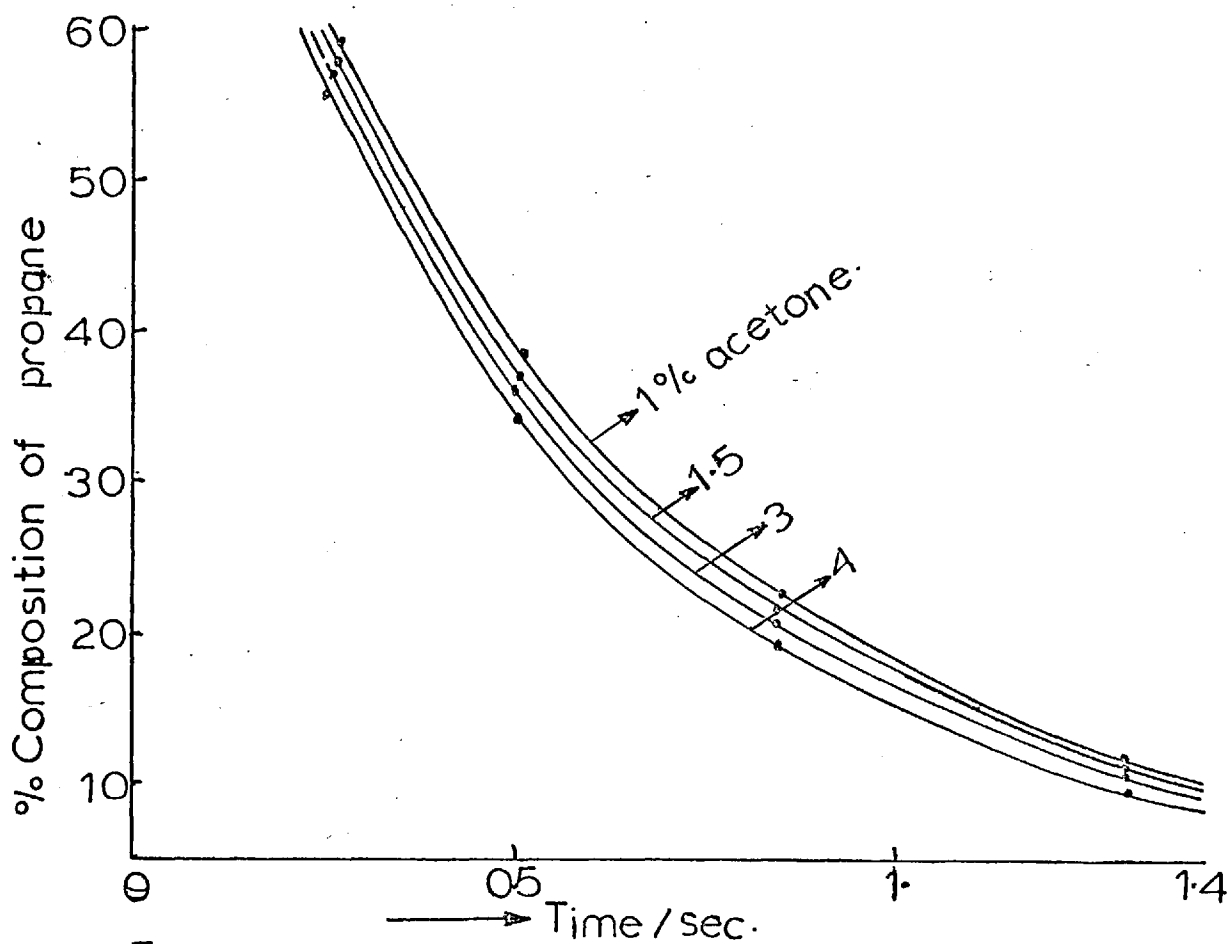

Fig 5-6. Effect of acetone partial pressure on propane decomposition at 700°C

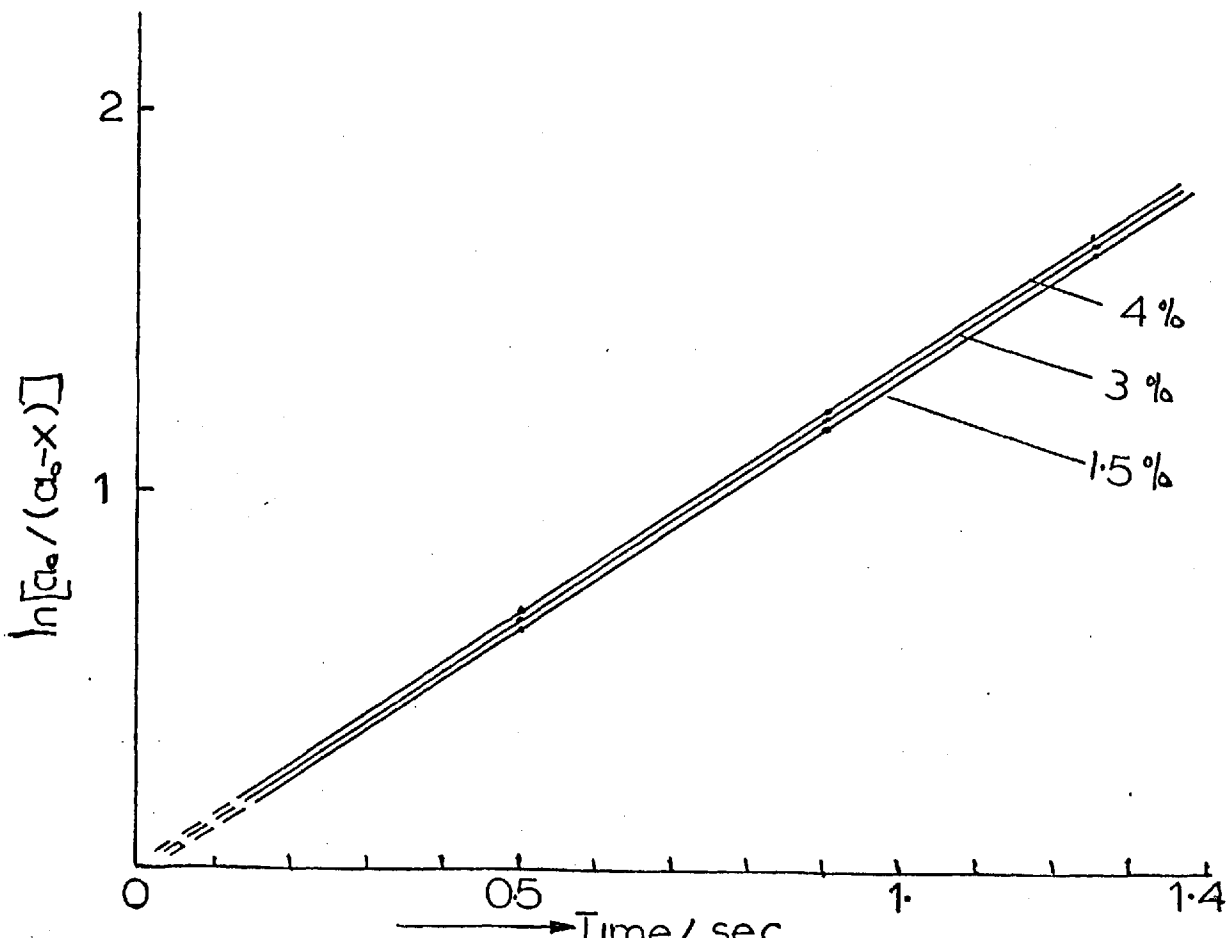

Fig5-7 First order kinetics in precence of acetone.

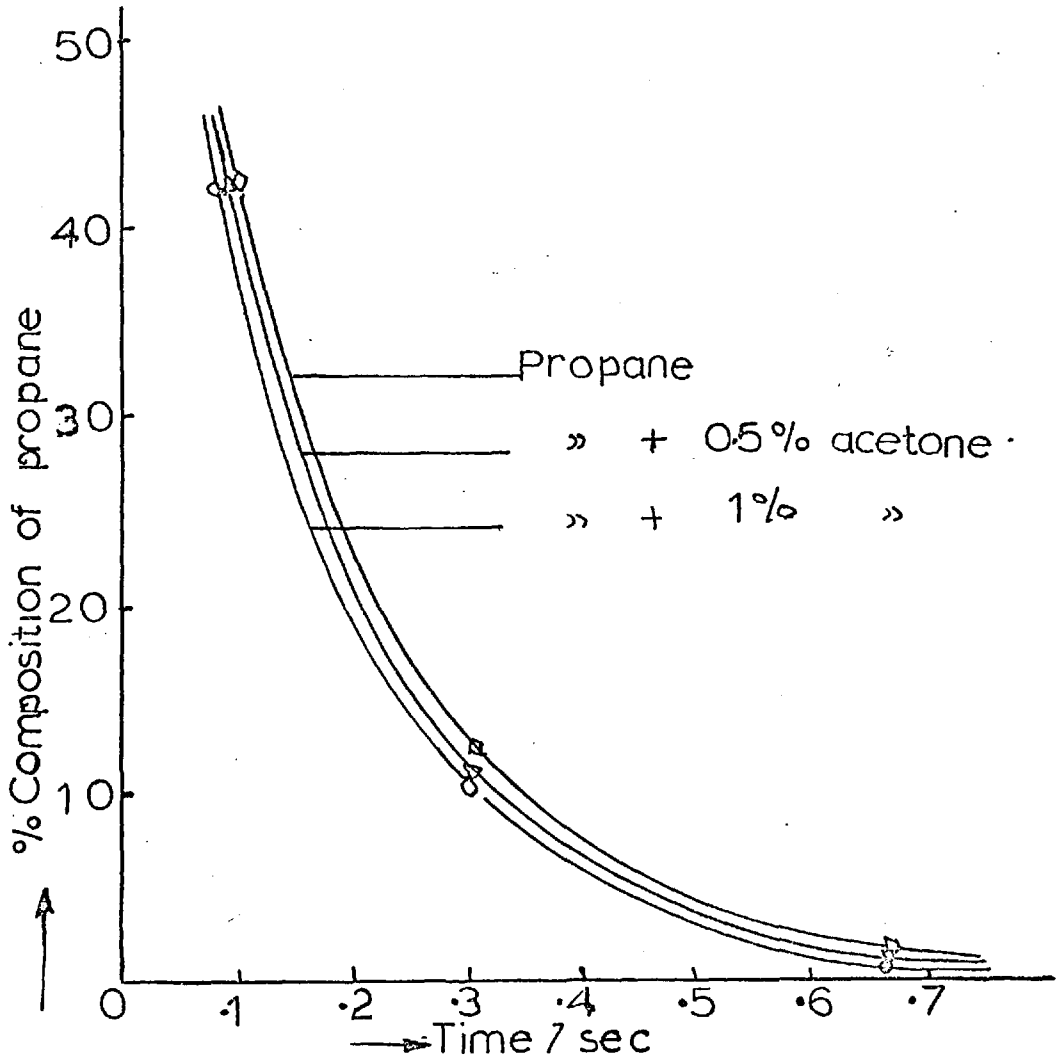

Fig 5-8 Effect of acetone partial pressure on propane decomposition at 750°c

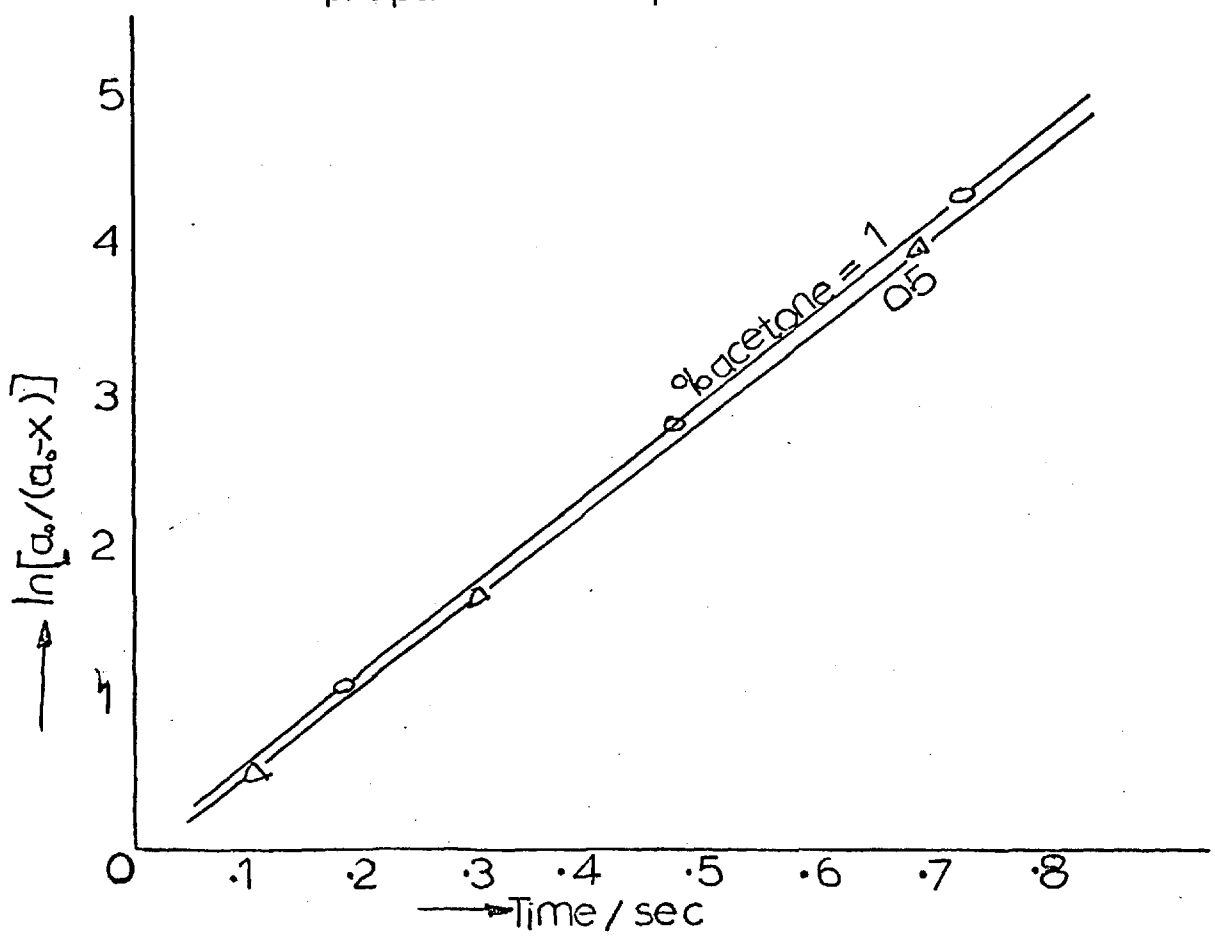

Fig 5-9 First order kinetics in presence of acetone

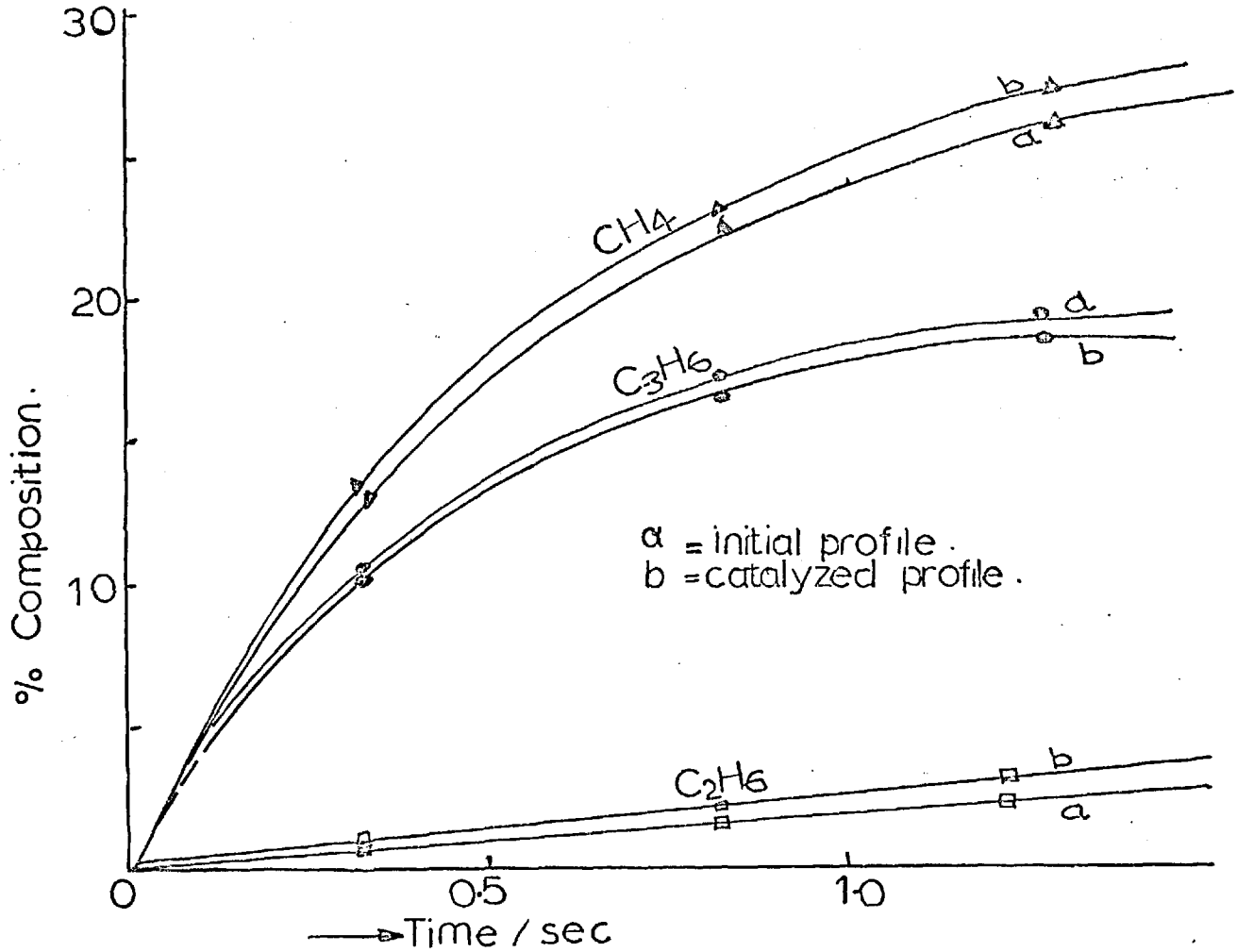

Fig 5-10 Effect of acetone on the yield of methane, propylene and ethane at 700°C

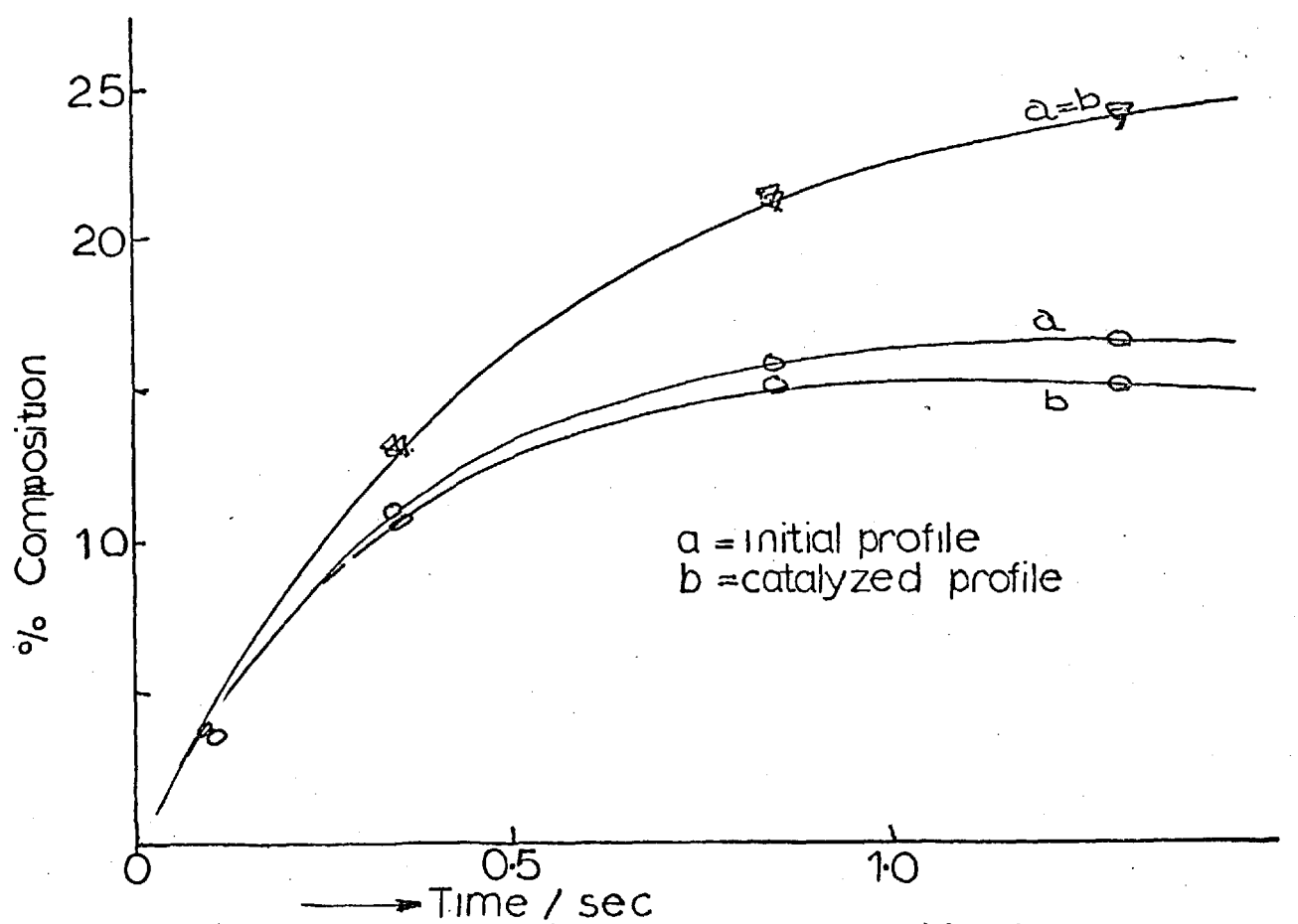

Fig 5-11 Effect of 4% acetone on the yield of ethylene and hydrogen at 700°C

But hydrogen atoms react with ethylene to give the ethyl radicals C_2H_5., which then abstract other hydrogen atoms to form ethane also.

$$H. + C_2H_4 \rightarrow C_2H_5$$

$$C_2H_5 + C_3H_8 \rightarrow C_2H_6 + C_3H_7$$

This could support the report of Bradley [4] that the combination of the lighter radicals are less important than their reaction with bulkier species due to the third body complication at elevated temperatures.

From the proposed mechanism, the additional methyl radicals from acetone attack propane and competition from hydrogen atoms in the system to form molecular hydrogen corresponding to equation (9) will lead to diminution of propyl radicals generated by this reaction step. Consequently the concentration of propylene obtained according to reaction steps (10) and (14), will be less than when acetone is absent. In addition certain reactions which may occur include steps such as:

$$CH_3 + C_3H_6 \longrightarrow C_4H_9$$

$$CH_3CO + RH \longrightarrow CH_3CHO + R$$

which will only diminish the concentration of propylene and that of propane in the system.

5.4 PROPANE PYROLYSIS KINETICS PERTURBED BY ACETALDEHYDE

Acetaldehyde is an important intermediate in the slow combustion of hydrocarbons where it probably participates in the role of a branching intermediate. Its oxidation has been well studied and it is known to accelerate the rate of hydrocarbon oxidation by reducing the induction period. The C-C bond strength in acetaldehyde is 334 KJ.per mole [122] compared to 343 KJ.per mole [122] in acetone. Hence, it is just slightly weaker than in acetone. As in the case of acetone, acetaldehyde is likely to accelerate the propane pyrolysis rate by furnishing methyl

radicals according to the equation:

$$CH_3CHO \longrightarrow CH_3 + CHO$$

The formyl radical, HCO, is unstable at high temperatures and should therefore decompose into carbon monoxide and hydrogen atom rather than engage in abstracting hydrogen atoms to form formaldehyde. The free-radical mechanism has been shown to explain perfectly the kinetics of acetaldehyde decomposition such that no molecular reaction step is involved when it is decomposed in the presence of other compounds.

The reaction system is the same as for the acetone additive experiments. The effect of acetaldehyde on the rate of decay of propane, and hence the changes in the concentration profiles of the pyrolysis products, is followed between 600° and 750°C at one atmosphere pressure using the mass spectrometer as the analytical tool.

5.4.1 RESULTS

The percentage by volume of acetaldehyde in the propane stream was varied from 1-4% at 600° to 750°C. There was an acceleration in the rate of decomposition of propane but this is smaller than in the case of acetone. The major products are CH_4, C_2H_4, C_3H_6, H_2 and C_2H_6. Relative to the unperturbed propane pyrolysis, the concentrations of CH_4 and C_2H_6 increased while those of propylene and hydrogen decreased with both increase and decrease not as much as in acetone perturbation Some of the concentration profiles are shown in fig. 5.12 and fig. 5.13.

5.4.2 MECHANISM AND KINETICS

The first chain mechanism for the decomposition of acetaldehyde was proposed by Rice and Hertzfeld in their fundamental work published in 1934. However some of the minor products obtained could not be

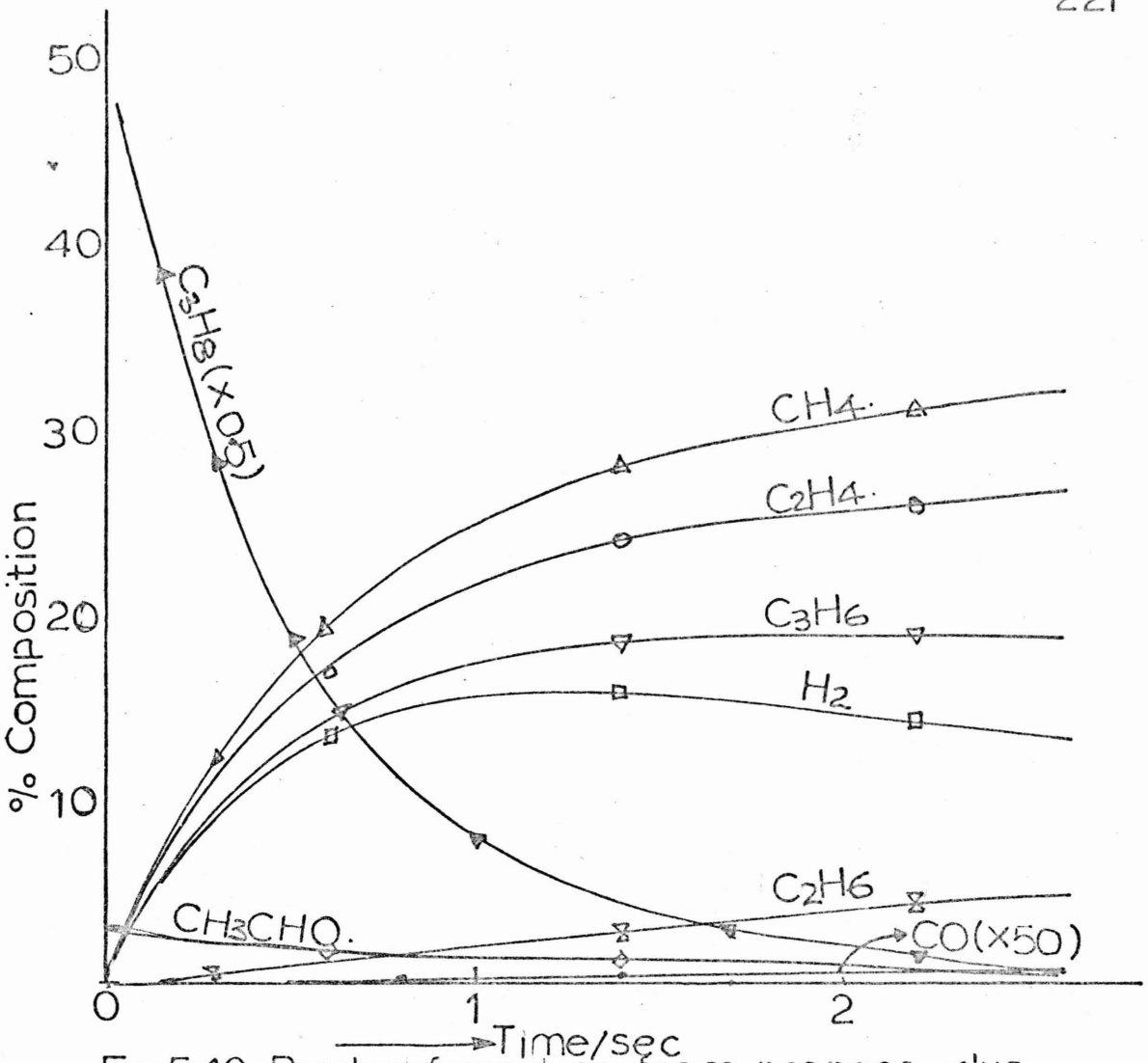

Fig 5-12 Product formation from propane plus 3% acetaldehyde at 700°C

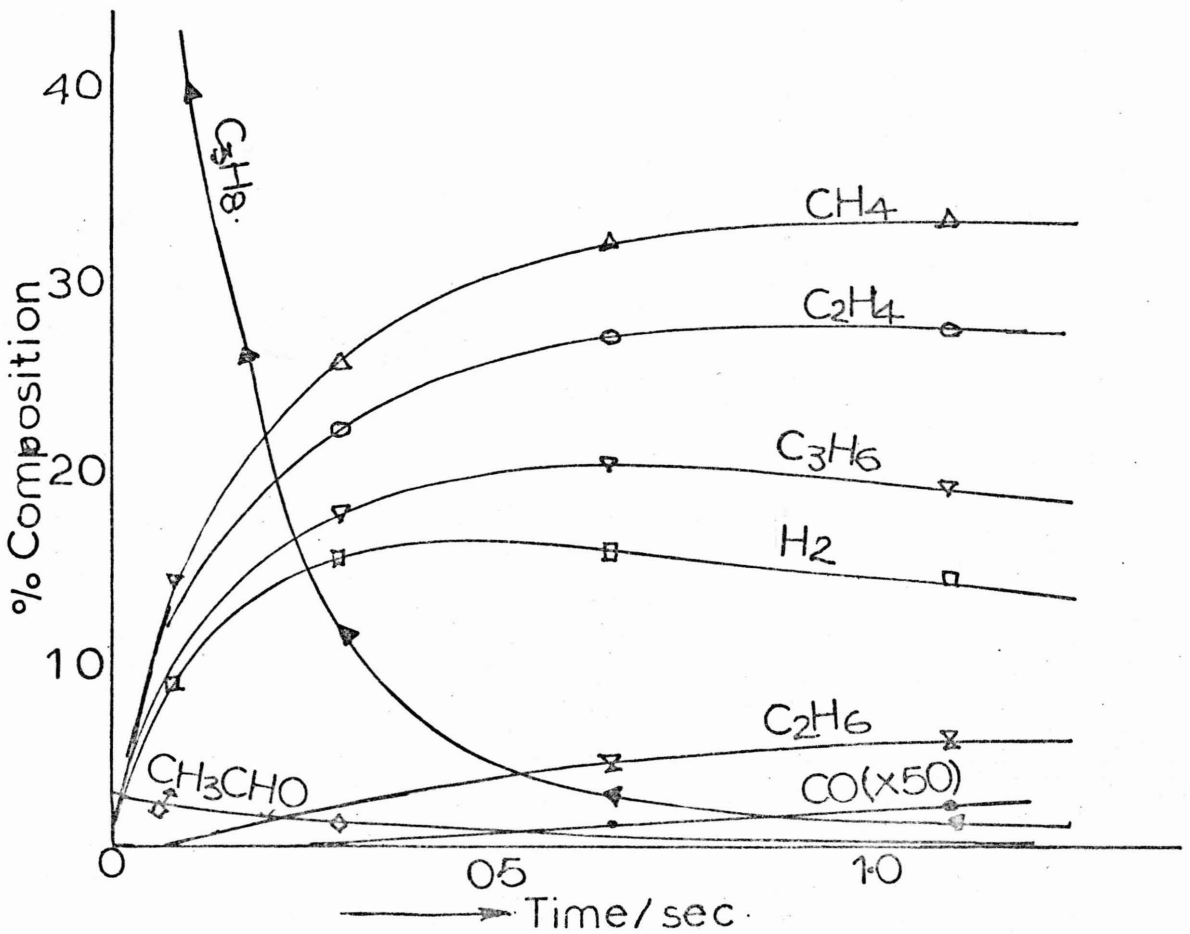

Fig 5-13 Product formation from propane plus 3% acetaldehyde at 750°C.

explained by their mechanism. A much more accurate kinetic scheme of the thermal decomposition was put forward by Laidler and Liu[120] obtained on the basis of the following mechanism.

$$CH_3CHO + M \longrightarrow CH_3 + CHO + M$$

$$CHO + M \longrightarrow H + CO + M$$

$$H\cdot + CH_3CHO \longrightarrow H_2 + CH_3CO \qquad (3)$$

$$CH_3 + CH_3CHO \longrightarrow CH_4 + CH_3CO$$

$$CH_3CO + M \longrightarrow CH_3 + CO + M$$

$$CH_3 + CH_3CHO \longrightarrow CH_4 + CH_2COH \qquad (6)$$

$$CH_2CHO \longrightarrow H + CH_2CO$$

$$CH_3 + CH_3 + M \longrightarrow C_2H_6 + M$$

It is to be expected then that at the initial stages of the reaction, when propane dissociation is very small, that methane, ethane and hydrogen should be produced. This was actually found to be the case. Reaction (3) is very much favoured over reaction (6) particularly when the perca percentage composition of acetaldehyde is very small compared to that of propane.

The following mechanism explains very well the product distribution in time at temperatures between 600° and 750°C when small concentrations of acetaldehyde are added into the propane fuel.

	REACTION	A/SEC^{-1}	$E/KJ.mole^{-1}$	
1.	$CH_3CHO \longrightarrow CH_3 + CHO$	2.5×10^{14}	312	164
2.	$HCO \longrightarrow H + CO$	1×10^{13}	67	147
3.	$C_3H_8 \longrightarrow CH_3 + C_2H_5$	6×10^{14}	326	158
4.	$CH_3 + CH_3CHO \rightarrow CH_4 + CH_3CO.$	1.7×10^{9}	35.5	149
5.	$H\cdot + CH_3CHO \longrightarrow H_2 + CH_3CO$	1×10^{9}	23.4	157
6.	$CH_3 + C_3H_8 \longrightarrow CH_4 + C_3H_7$	1.5×10^{12}	20.4	158

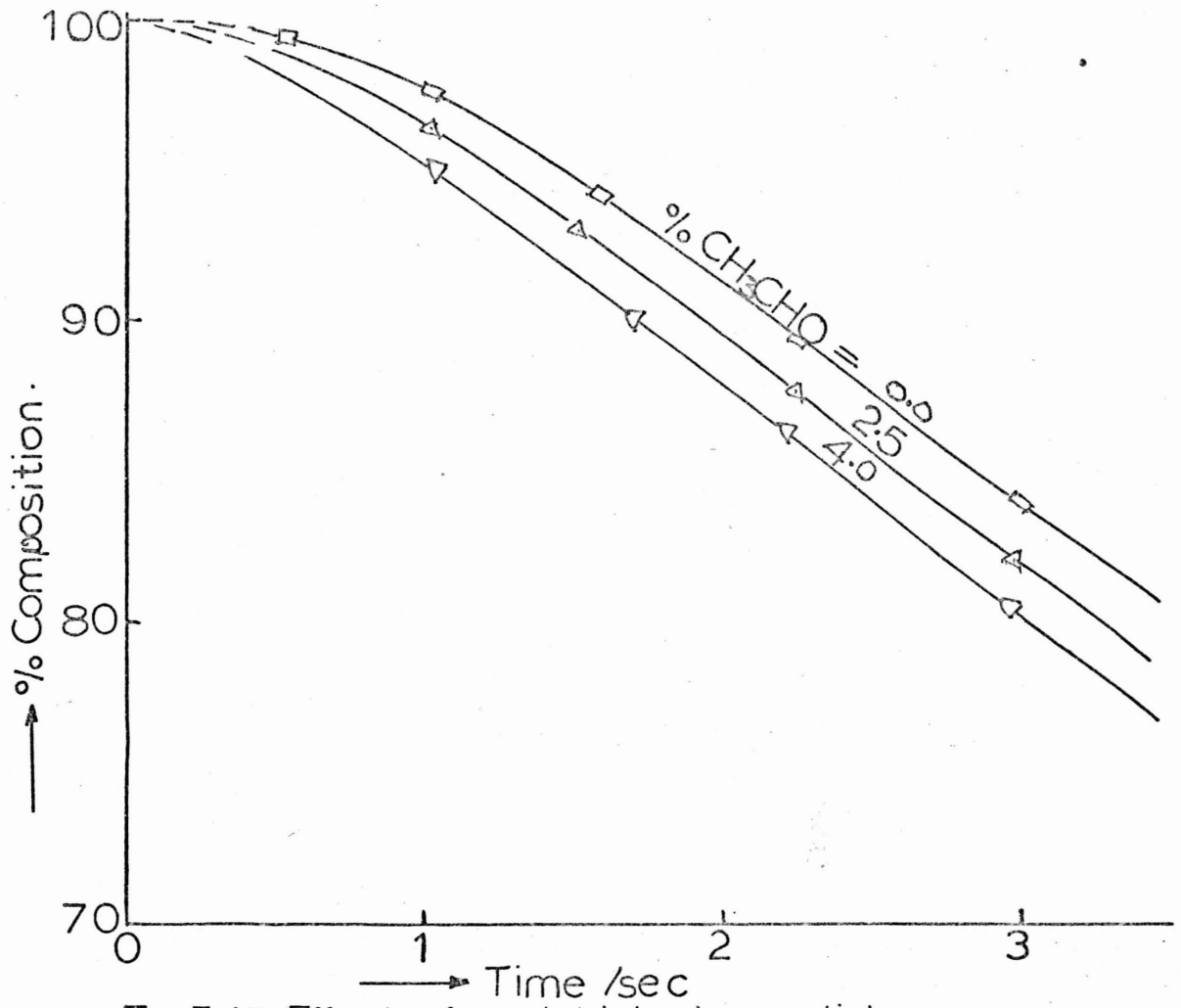

Fig 5-14 Effect of acetaldehyde partial pressure on propane decomposition at 600°C

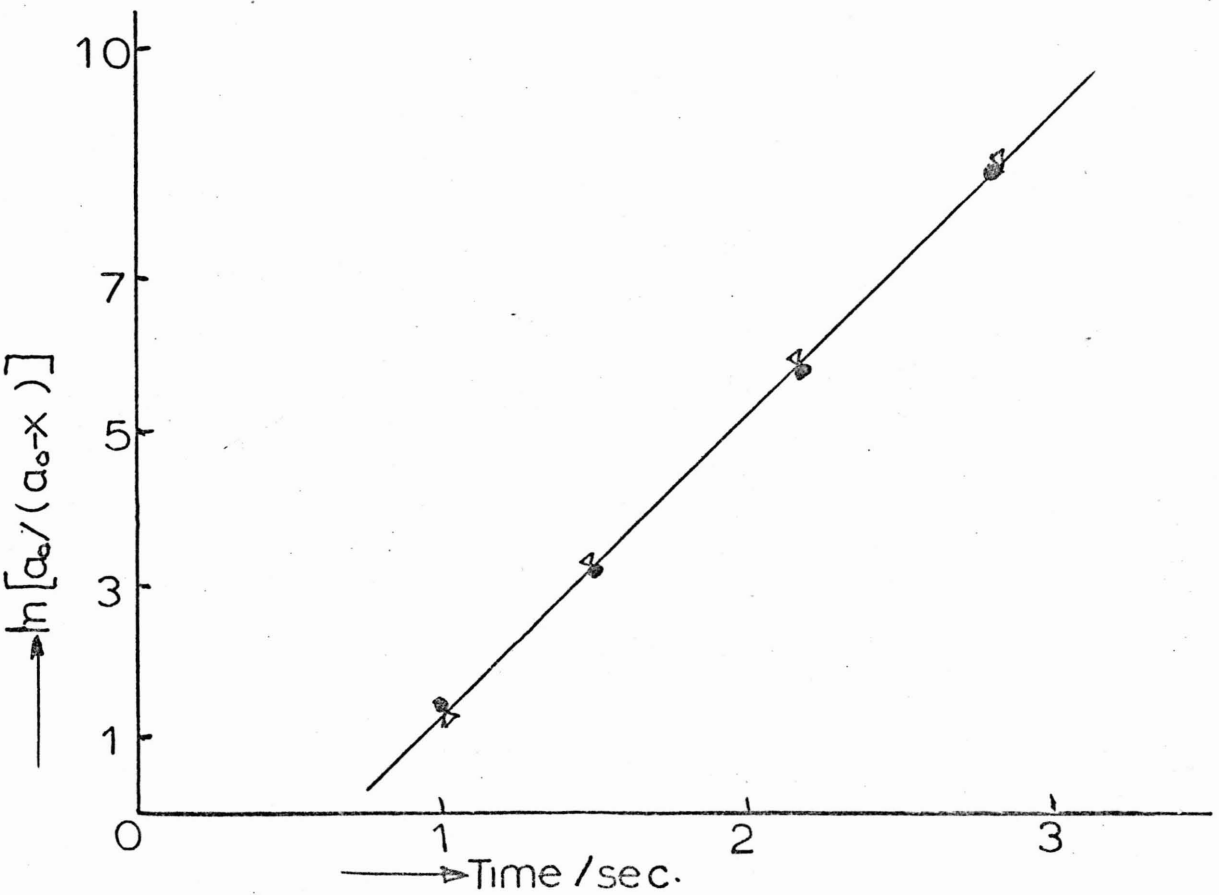

Fig 5-15 First order kinetic in presence of acetaldehyde.

7.	$CH_3CO \longrightarrow CH_3 + CO$	5×10^{12}	62.7	149
8.	$C_2H_5 + C_3H_8 \longrightarrow C_2H_6 + C_3H_7$	2×10^{10}	25.0	158
9.	$C_2H_5 \longrightarrow H + C_2H_4$	3×10^{11}	146.3	159
10.	$H. + C_2H_4 \longrightarrow C_2H_5$	7.5×10^{11}	22.5	158
11.	$H. + C_3H_8 \longrightarrow H_2 + C_3H_7$	1.8×10^{12}	19.2	160
12.	$C_3H_7 \longrightarrow CH_3 + C_2H_4$	4×10^{10}	132.	158
13.	$H. + C_3H_6 \longrightarrow C_3H_7$	1.8×10^{11}	4.18	158
14.	$C_3H_7 \longrightarrow H. + C_3H_6$	3.6×10^{10}	134.	4
15.	$CH_3 + C_2H_5 \longrightarrow C_3H_8$	4.2×10^{12}	0.0	158
16.	$C_2H_5 + C_2H_5 \longrightarrow C_2H_4 + C_2H_6$	1×10^{10}	0.0	161
17.	$C_2H_5 + C_2H_5 \longrightarrow C_4H_{10}$	1×10^{11}	0.0	163
18.	$CH_3 + C_3H_7 \longrightarrow CH_4 + C_3H_6$	1×10^{12}	0.0	158
19.	$CH_3 + C_3H_7 \longrightarrow C_4H_{10}$	1×10^{11}	0.0	158
20.	$H_2 + C_3H_7 \longrightarrow H. + C_3H_6$	5.6×10^{7}	83.6	158
21.	$C_4H_{10} \longrightarrow C_2H_5 + C_2H_5$	8.7×10^{9}	167	162
22.	$CH_3 + C_2H_6 \longrightarrow CH_4 + C_2H_5$	8×10^{8}	50	4
23.	$H. + C_2H_6 \longrightarrow H_2 + C_2H_5$	1.3×10^{11}	37.6	161
24.	$C_2H_6 \longrightarrow CH_3 + CH_3$	1.2×10^{12}	284	4

5.4.3 DISCUSSION

The accelerating effect of the addition of acetaldehyde is very well isllustrated in fig. 5.14. As in the case of aceone additive, the induction period is reduced, becoming smaller and smaller as the concentration of the additive increases. At two seconds reaction time, unperturbed propane suffers a conversion of about 10% at 600°C, but the

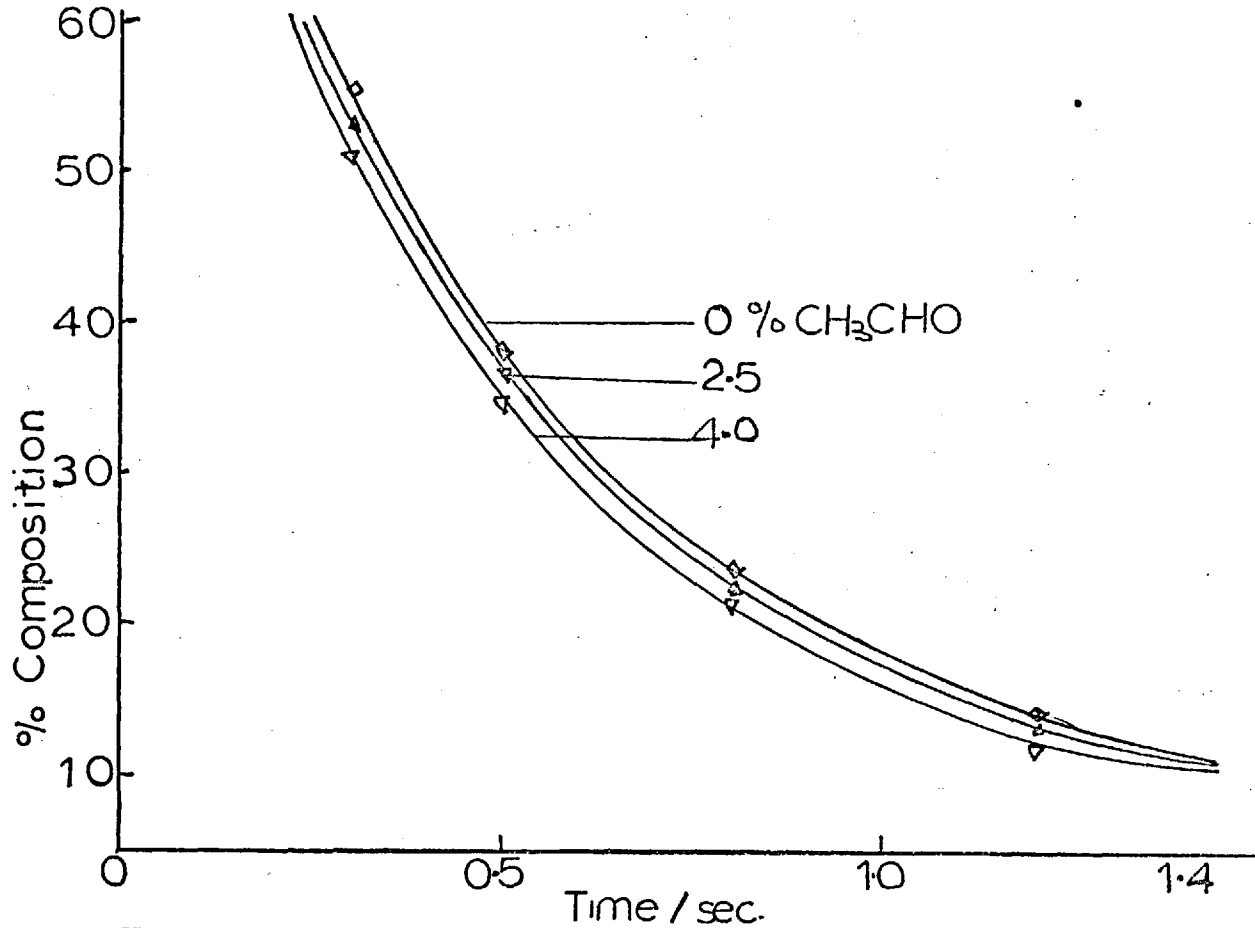

Fig 5-16 Effect of acetaldehyde on propane decomposition at 700°C

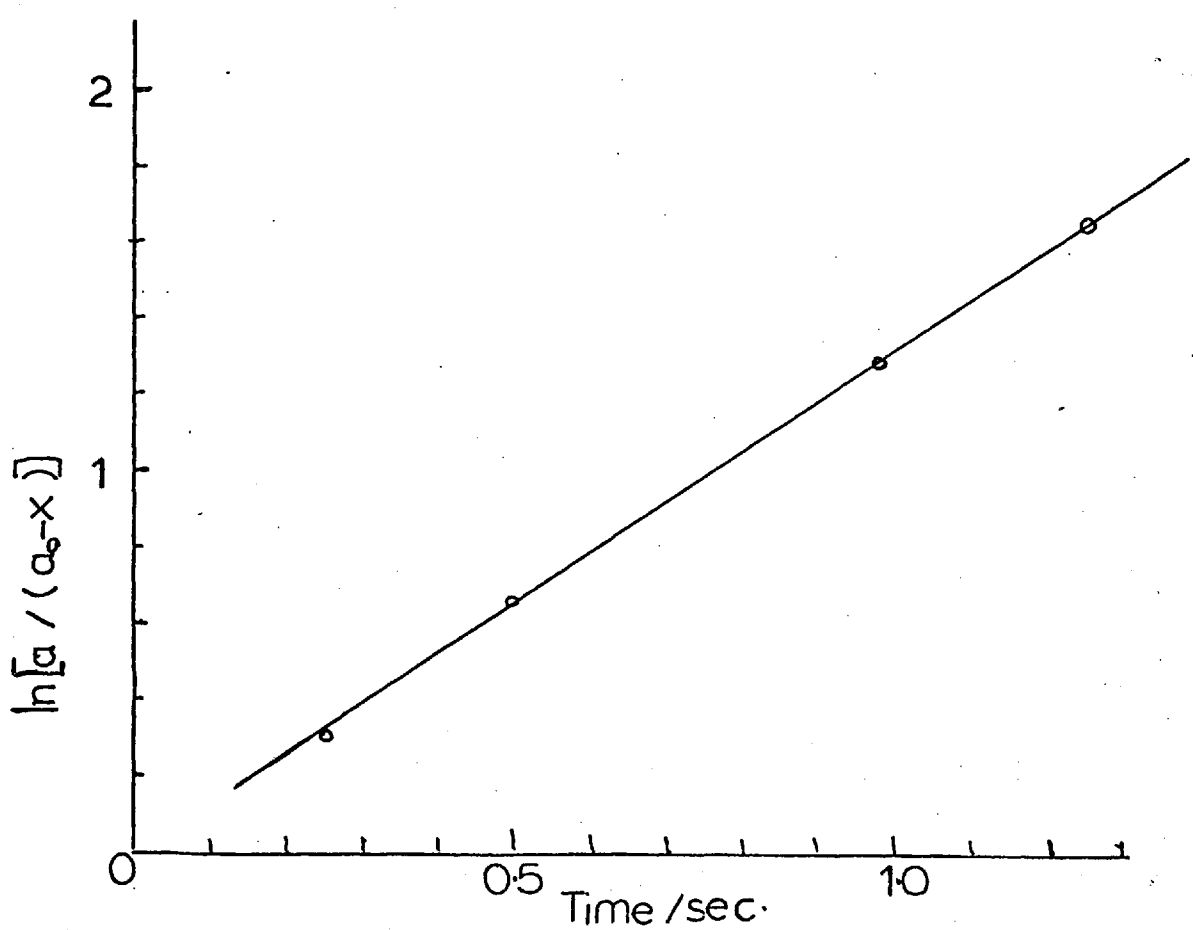

Fig 5-17· First order kinetics in precence of CH_3CHO 700°

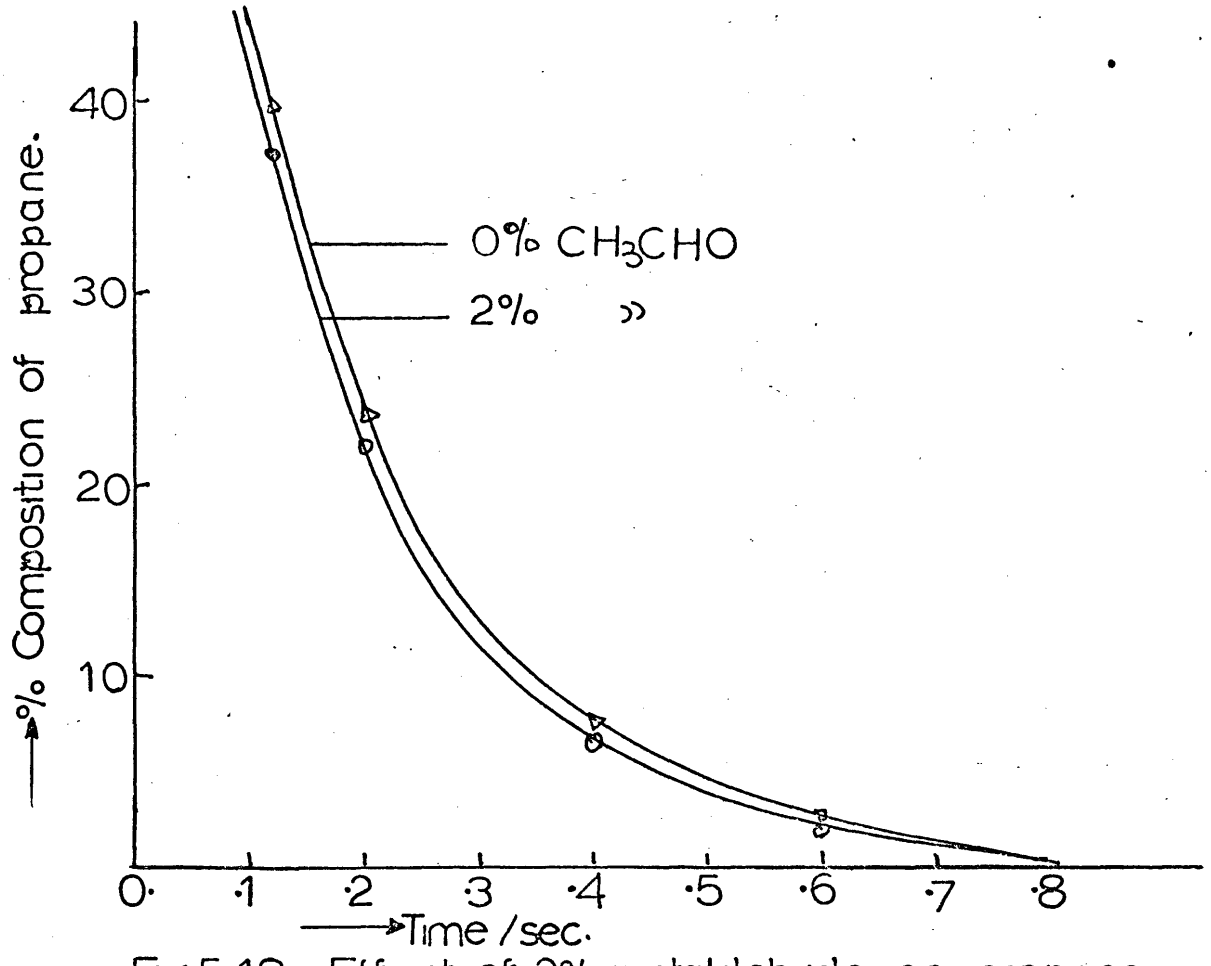

Fig 5-18 Effect of 2% acetaldehyde on propane decomposition at 750°C

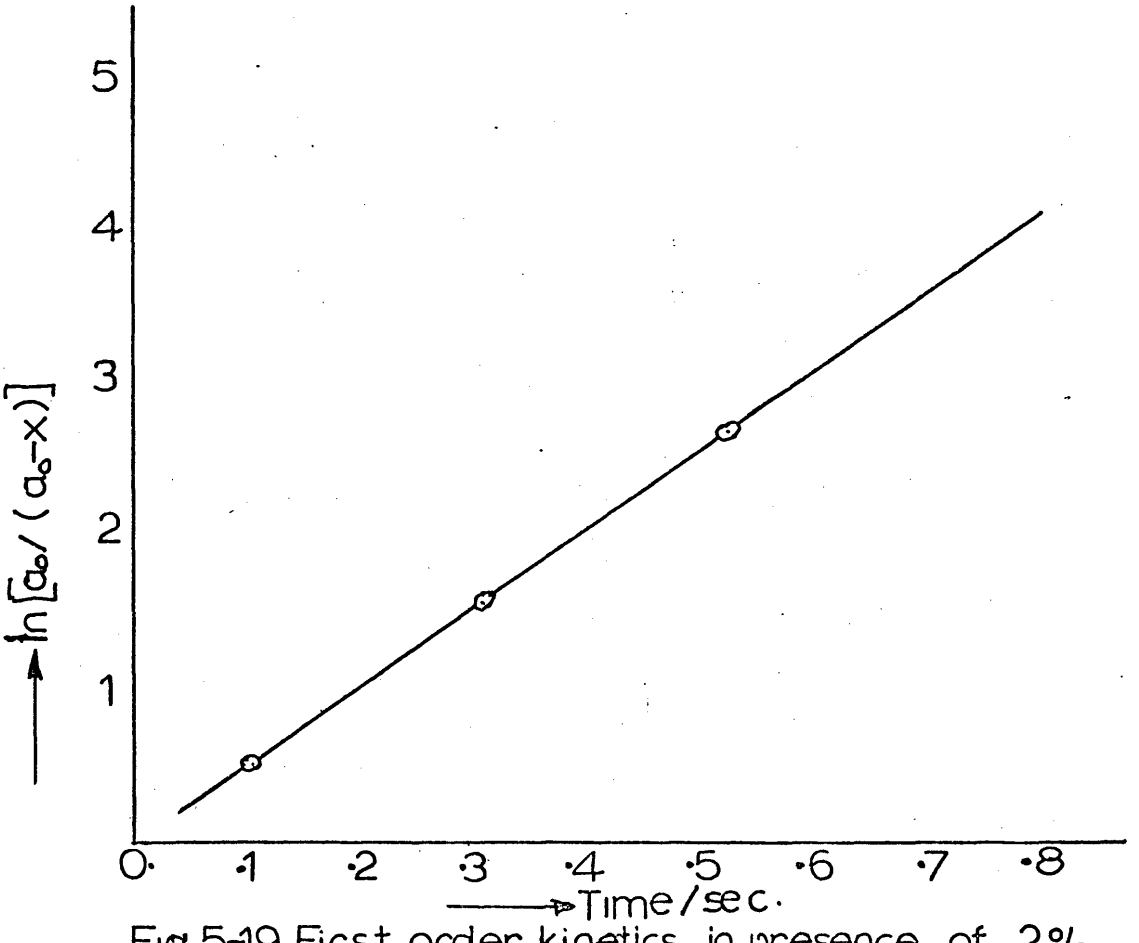

Fig 5-19 First order kinetics in presence of 2% acetaldehyde at 750°C

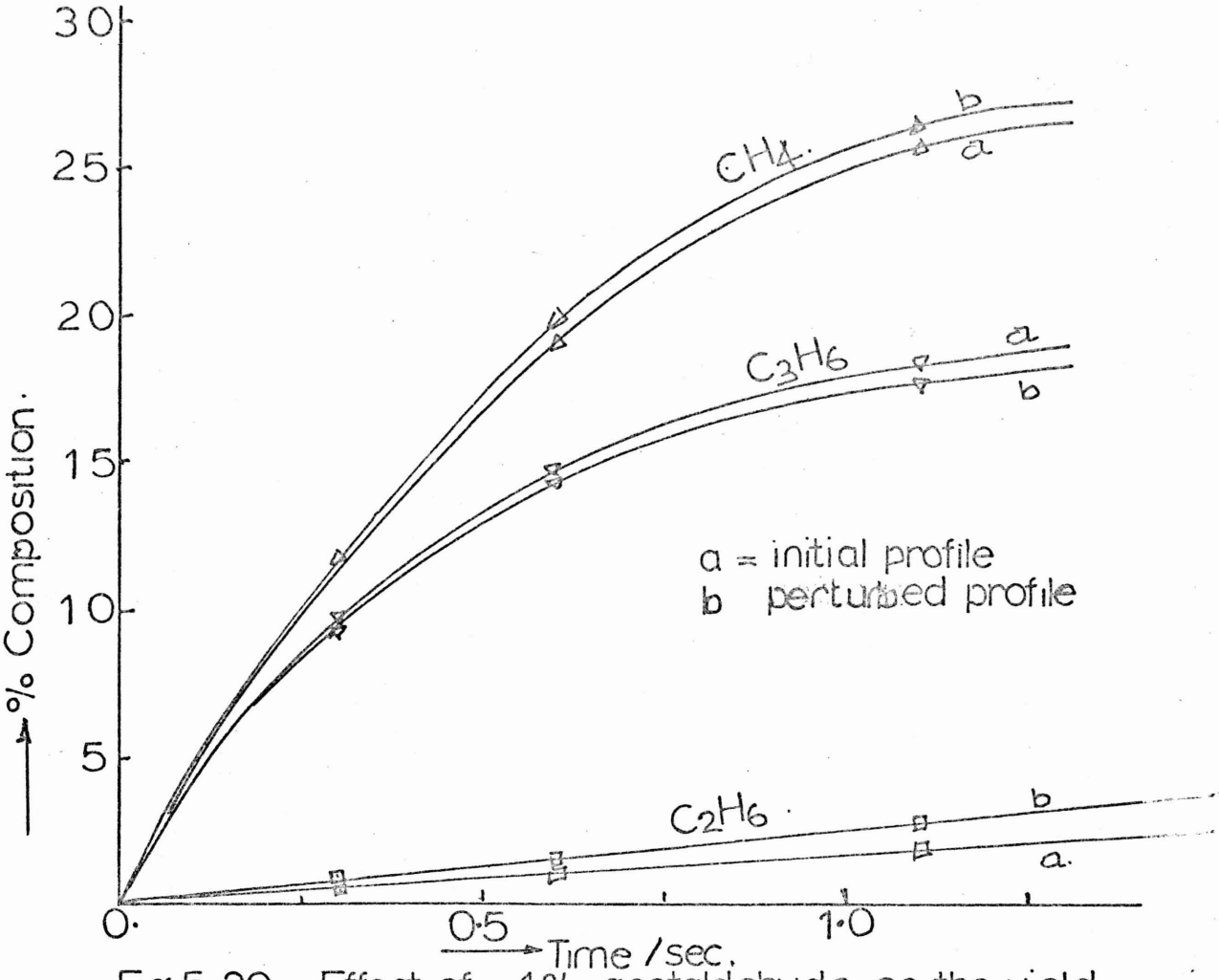

Fig 5-20 Effect of 4% acetaldehyde on the yield of methane propylene and ethane at 700°C

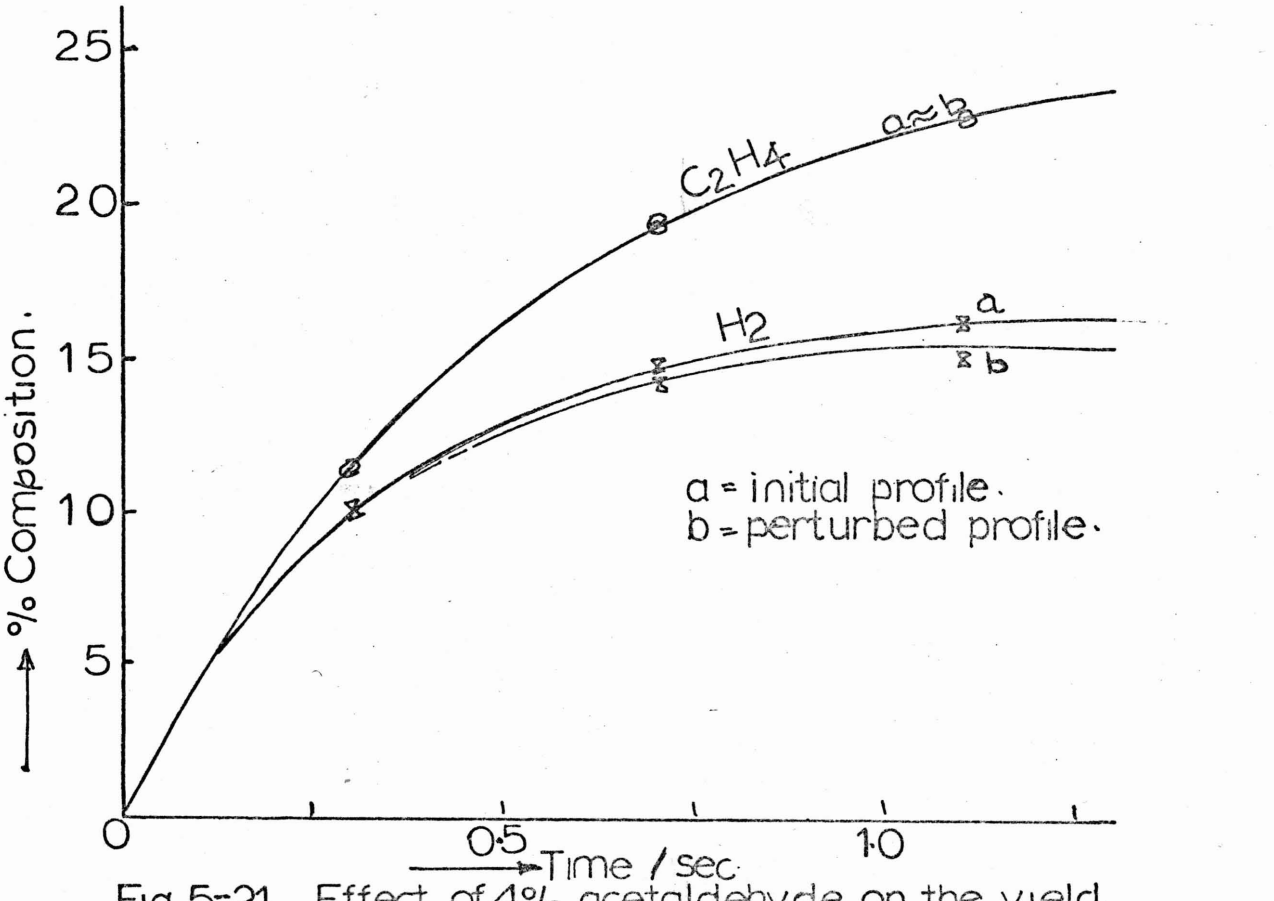

Fig 5-21 Effect of 4% acetaldehyde on the yield of ethylene and hydrogen.

addition of 3% aceone causes its conversion to rise to about 13.5% while 3% acetaldehyde in the fuel effects a 12% conversion. This is the general trend except that the percentage increase in decomposition due to the additives, decreases as temperature increases. That acetaldehyde contributes less than acetone of the same concentration in the propane stream is even more explicit in the kinetic diagram fig. 5.15, where the $\ln[a_o/(a_o - x)]$ versus time plot for the various additions are so close that, for clarity, only a single line is drawn. The same situation prevails at higher temperatures except that, since propane now decomposes very rapidly, the accelerating effect is not easily observed The effect on the product distribution relative to pure propane pyrolysis is shown in fig. 5.20 and fig. 5.21. Acetone contains two methyl groups in its structure such that it generates two methyl radicals.

$$CH_3COCH_3 \longrightarrow CO + 2CH_3$$

(This is schematic, not a concerted decomposition reaction). Acetaldehyde has only one methyl group. Methyl radicals engage mainly in abstraction of hydrogen atoms to form methane and may combine to form ethane. Thus acetone is more effective in producing more methane and ethane than acetaldehyde.

The steady state concentrations of methyl radicals at 700°C are 6.86×10^{-12} mole/cc, 7.3×10^{-12} mole/cc and 9.4×10^{-12} mole/cc for propane, propane perturbed with acetaldehyde and propane perturbed with acetone respectively. It can be seen that the total methyl concentration in either of the perturbed system is higher than in the unperturbed system, and that it is higher in the acetone perturbed system than in the acetaldehyde case. The contribution of extra methyl radicals from aceone is equal to the difference in the concentrations between the acetone-perturbed system and the unperturbed system. This is $(9.4 - 6.8)10^{-12} = 2.6 \times 10^{-12}$ moles/cc. Similarly the contribution

from acetaldehyde would be $(7.3 - 6.86)10^{-12} = 0.44 \times 10^{-12}$ moles/cc. Thus acetone is more effective than acetaldehyde in furnishing methyl radicals. This is because acetone has two methyl groups being released as radicals at a different rate from the single methyl group in acetaldehyde.

Acetone decomposes schematically according to the equation:

$$CH_3COCH_3 \longrightarrow 2CH_3 + CO.$$

At the steady state, the rate of formation of methyl radicals in the acetone system is:

$$\frac{d[CH_3]}{dt} = 0 = 2k_1[CH_3COCH_3] - k[CH_3]^2$$

$$-k[CH_3][C_3H_8]$$

The concentration of C_3H_8 is large and constant

Hence $$\frac{d[CH_3]}{dt} = 2k_1[CH_3COCH_3] - k[CH_3]^2 = 0$$

The second term assumes that the major mode of recombination is second order. $CH_3 + CH_3 \longrightarrow C_2H_6$.

The steady state concentration of methyl radicals is thus

$$[CH_3]_1 = \sqrt{2} \left(\frac{K_1}{K}\right)^{\frac{1}{2}} [CH_3COCH_3]^{\frac{1}{2}}$$

Similarly, in the case of acetaldehyde system, if the methyl fate is mainly recombination.

$$\frac{d[CH_3]}{dt} = k_2[CH_3CHO] - k[CH_3]^2 = 0$$

i.e., $$[CH_3]_2 = \left(\frac{k_2}{k}\right)^{\frac{1}{2}} [CH_3CHO]$$

$$\frac{[CH_3]_1}{[CH_3]_2} = \frac{\sqrt{2}\left(\frac{k_1}{K}\right) [CH_3COCH_3]^{\frac{1}{2}}}{\left(\frac{k_2}{K}\right)^{\frac{1}{2}} [CH_3CHO]}$$

from which $$\left(\frac{k_1}{k_2}\right)^{\frac{1}{2}} = \frac{[CH_3]_1}{[CH_3]_2} \quad \frac{[CH_3CHO]}{2\,[CH_3COCH_3]^{\frac{1}{2}}}$$

$$\frac{K_1}{K_2} = \frac{([CH_3]_1)^2}{[CH_3]_2} \quad \frac{[CH_3CHO]^2}{2[CH_3COCH_3]}$$

The steady state concentrations of CH_3CHO and CH_3COCH_3 are 3.76×10^{-2} moles/cc and 2.2×10^{-2} moles/cc respectively. The ratio of the methyl radicals is $2.6 \times 10^{-12}/0.44 \times 10^{-12} = 5.9$

Hence $$\frac{K_1}{K_2} = (5.9)^2 \quad \frac{1}{2} \quad \times \frac{(3.76)^2 \times 10^{-4}}{2.2 \times 10^{-2}}$$

$$= 1.10$$

In other words, the bond strength in acetone is 1.10 times stronger than that in acetaldehyde. This compares favourably with the ratio of 1.03 reported by Benson et al[122].

CHAPTER VI

CHAPTER VI

OXIDATIVE PYROLYSIS OF PROPANE

6.1 INTRODUCTION

The mechanism and kinetics of the high temperature pyrolysis of propane was discussed in Chapter IV. Chapter V dealt with the effect of acetone (a source of methyl radicals) and acetaldehyde(a degenerate branching intermediate as well as a source of methyl and formyl radicals at high temperatures) on the mechanism of propane pyrolysis. Both acetone and acetaldehyde reduced the induction period and accelerated the decomposition rate, and favoured the higher yield of saturates, methane and ethane while effecting a reduction in the percentage composition of propylene. It is evident therefore that sources of methyl radicals favour the production of saturated hydrocarbons while the opposite effect is observed for olefins. In this chapter, the effects of small amounts of oxygen on the rate of reaction and the changes in products spectrum relative to unperturbed propane, between 600 - 700^{o}C and one atmospheres pressure are analysed.

Knowledge of the branching chain mechanism and behaviour of the relatively stable intermediate products during the slow combustion of many organic fuels, implicates such compounds as playing a degenerate branching role in the oxidation of hydrocarbons. At high temperatures, the mechanism of combustion differs markedly from that responsible for low-temperature oxidation. Combustion can be described as 'fast' with reaction paths being changed or hindered by the decomposition of radicals into stable moecules and other active species. Both acetaldehyde and formaldehyde are not formed in appreciable amounts. The usual route for the formation of acetaldehyde is by the decompositon of alkoxyl radical C_3H_7O

$$C_3H_7O + M \longrightarrow CH_3 + CH_3CHO + M$$

But the alkoxyl radical is formed from alkyl radicals reactions

$$RO_2 + RO_2 \longrightarrow 2RO + O_2$$

At high temperatures, the alkyl peroxyl radicals are preferentially decomposed into olefins and hydroperoxyl radical.

$$RO_2 \longrightarrow R' + HO_2$$ where R' is an olefin.

Similarly the concentration of formaldehyde will be extremely small, suggesting that its removal by radical attack is efficient.

$$\cdot OH + CH_2O \longrightarrow H_2O + CHO$$

$$\cdot OH + CHO \longrightarrow H_2O + CO$$

$$CHO + O_2 \longrightarrow CO + HO_2\cdot$$

It is important to note then that CH_2O need not now lead to branching instead chain branching is believed to occur by the decompostion of hydroperoxides particularly hydrogen peroxide.

$$H_2O_2 \longrightarrow 2OH$$

Thus, at high temperatures, hydroxyl and hydroperoxy radicals are the important propagating species. Knox and Trotman-Dickenson [123, 124, 125] have suggested that the hydroperoxide chain applies in oxidation of paraffins at temperatures as low as 318°C. On the other hand, their work on competitive oxidations[126] showed that the radical which attacks the paraffins displays, like .OH radicals, little discrimination between C-H bonds of varying strength. Hence hydroxyl radicals .OH is the most important radical at high temperatures.

The region of investigation is that corresponding to true ignition where the majority of the enthalpy of reaction is released rapidly in a narrow reaction zone leading to the production of very high temperatures These high temperatures produce steep temperature gradients and the transport of active centres makes the system self-propagating. The

characteristic variation of reaction rate with time observed in hydrocarbon oxidation is as shown in Fig. 6-1.[127]

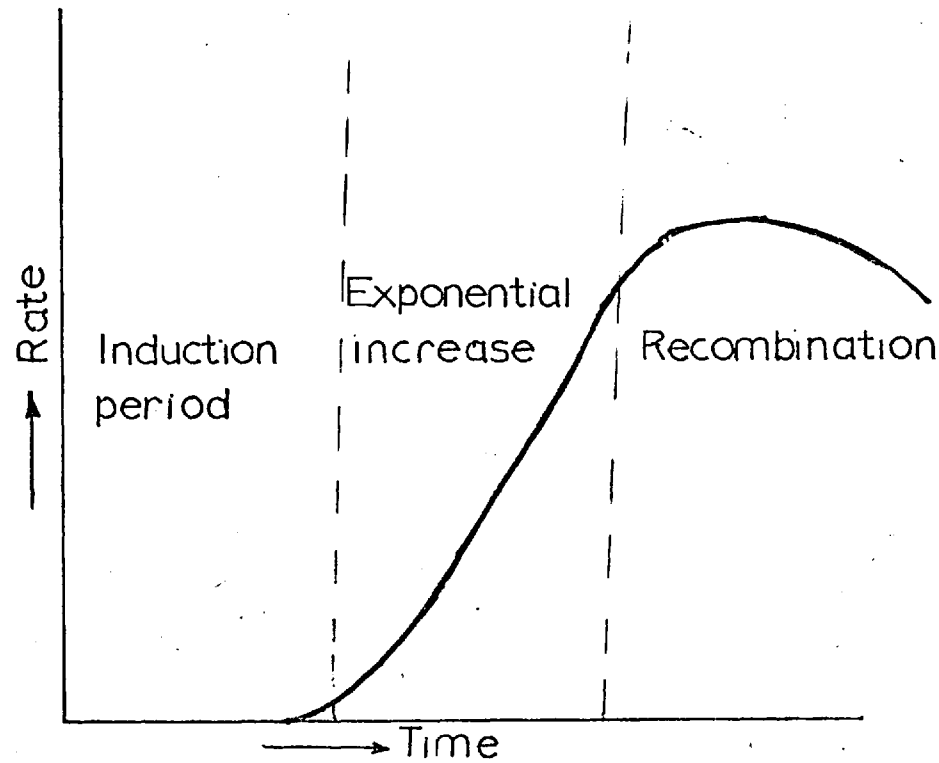

Fig. 6-1 VARIATION OF REACTION RATE IN HYDROCARBON OXIDATION

Three distinct zones - a preheat zone, a true reaction zone, and a recombination zone, may be distinguished. The nature of the reactions in the preheat zone depends on the fuel involved. For a very stable molecule like methane, little or no pyrolysis can occur within the short residence time. With the majority of hydrocarbons however, some degradation occurs and fuel fragments leaving this zone will comprise mainly lower hydrocarbons, olefins and hydrogen. One major effect of this is that the composition in the reaction zone proper is very similar, irrespective of the nature of the fuel, thus explaining why flame temperature and burning velocities vary by only a small amount for a wide range of fuels. In this preheat zone, the oxygen plays only a catalytic role and is itself little consumed. The processes occurring in the reaction zone are mainly propagation and decomposition while in the recombination zone, which is a more extended region, slower recombin-

ation reactions occur. In oxygen-rich fuels, the final composition of the burnt gas is largely determined by the water gas reaction.

$$H_2 + CO_2 \rightleftharpoons H_2O + CO .$$

However, when oxygen is present in small amounts, this reaction does not take place.

6.2 ANALYSIS OF THE RESULTS

The flow system was the same as that employed in Chapter IV. The valve on the preheater was not as widely opened as before. The tap that permits entry into the reactor was similarly not widely opened to prevent any explosion. In addition a nitrogen cylinder was connected to the propane line to quench any ignition that might ensue if propane feed ceased. The Air (from Air Products) was free of water and carbon dioxide. Air was used instead of pure oxygen so that the nitrogen contained could act as a diluent. It was passed into the propane stream at such flow rates that the oxygen to propane ratio was between two and three per cent. With the continuous sampling technique, the mass peak heights were obtained for the products of the reactions of propane containing 2% and 3% of oxygen at 600°, 650° and 700°C respectively. The products spectrum was solved using the deconvolution programme described in Chapter III, and the results compared with computer predictions as shown in Table 6-1. This shows very good agreement. All the peaks normally obtained for pure propane pyrolysis appeared, but in addition, peaks 17 and 18 appeared which indicated the formation of water. No oxygen peak appeared showing that it was almost spontaneously consumed. Similarly there was no indication of the formation of carbon monoxide or of carbon dioxide.

TEMPERATURE = 600°C

SPACE TIME	0.1 SEC.		0.5 SEC.	
	CALCULATED	COMPUTED	CALCULATED	COMPUTED
C_3H_8	80.10	81.33	66.00	66.00
C_3H_6	6.00	6.24	9.31	9.40
C_2H_6	0.01	0.014	0.10	0.08
C_2H_4	3.00	3.07	7.00	7.08
CH_4	3.10	3.08	7.05	7.20
H_2	2.50	2.63	6.00	6.10
H_2O	3.50	3.62	3.10	3.20

TEMPERATURE = 650°C

SPACE TIME	0.1 SEC.		0.5 SEC.	
	CALCULATED	PREDICTED	CALCULATED	PREDICTED
C_3H_8	69.00	69.48	51.20	50.09
C_3H_6	8.90	8.83	12.82	13.00
C_2H_6	0.10	0.073	0.34	0.33
C_2H_4	6.23	6.38	11.70	11.70
CH_4	6.40	6.44	12.35	12.48
H_2	5.30	5.39	9.54	9.60
H_2O	3.26	3.39	3.00	3.00

TABLE 6-1 COMPARISON OF CALCULATED TO COMPUTER PREDICTED VALUES

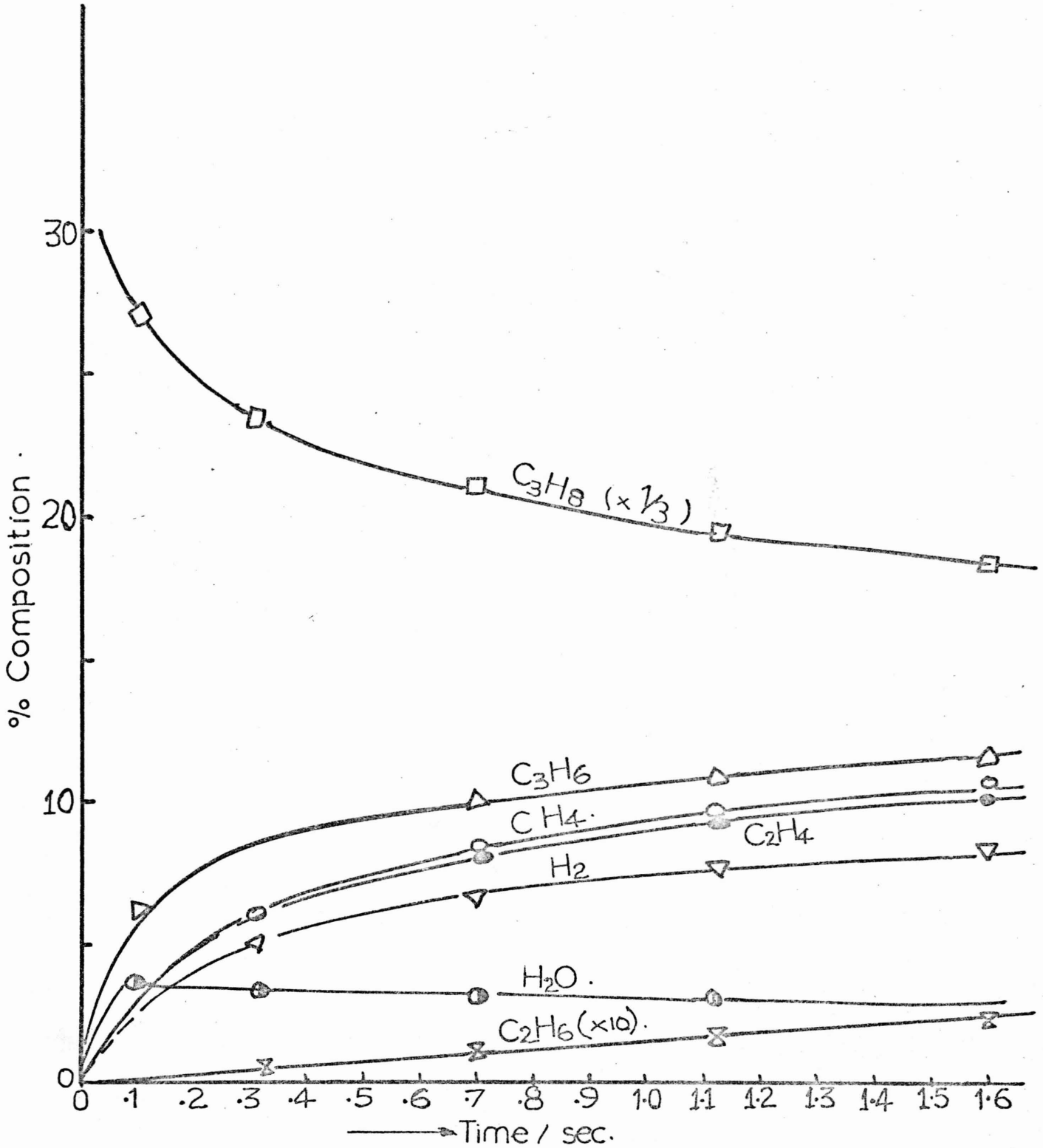

Fig 6-2. Product distribution from propane plus 2% oxygen at 600°C.

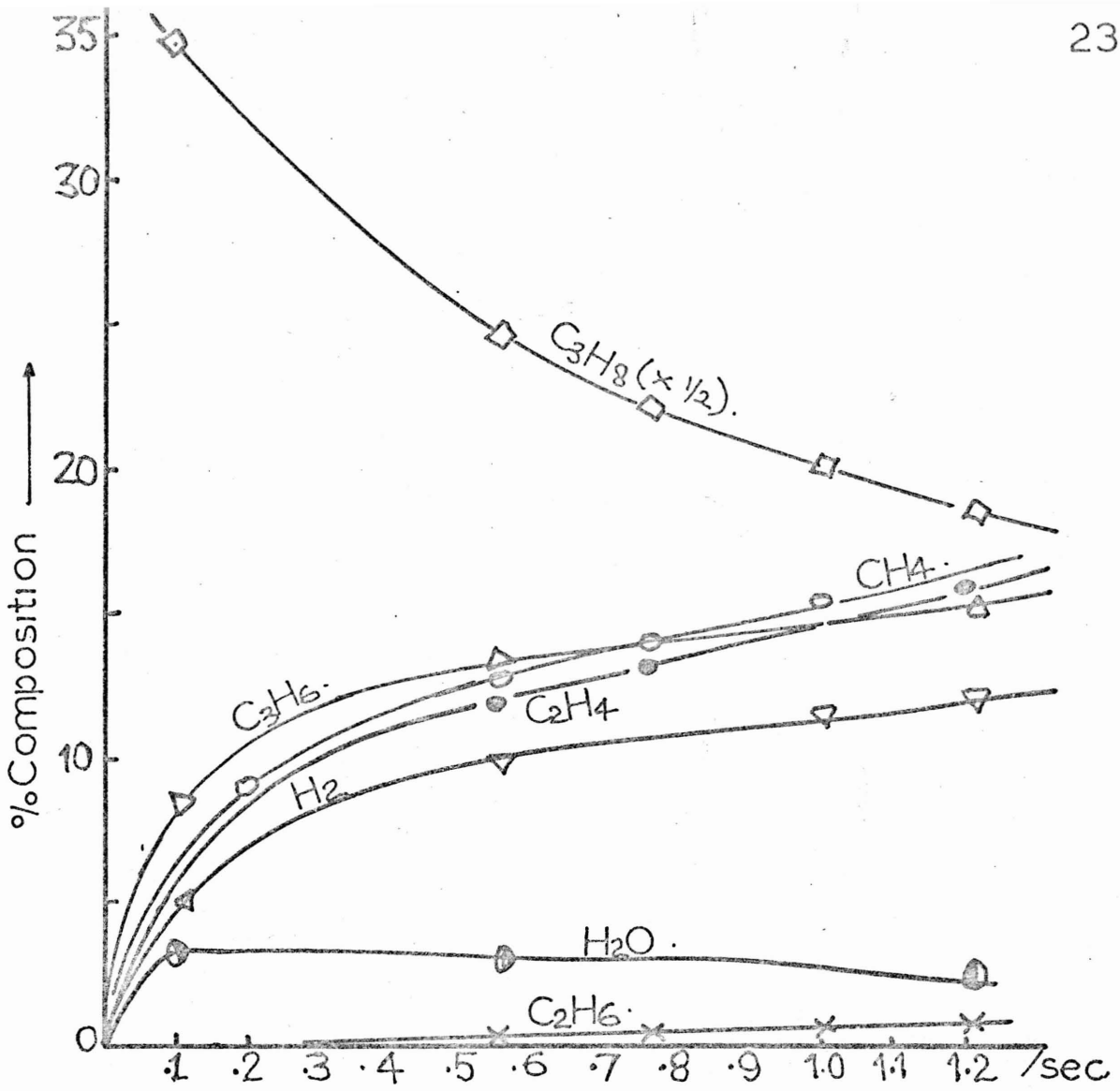

Fig 6-3. Products from propane + 2% O_2 at 650°C.

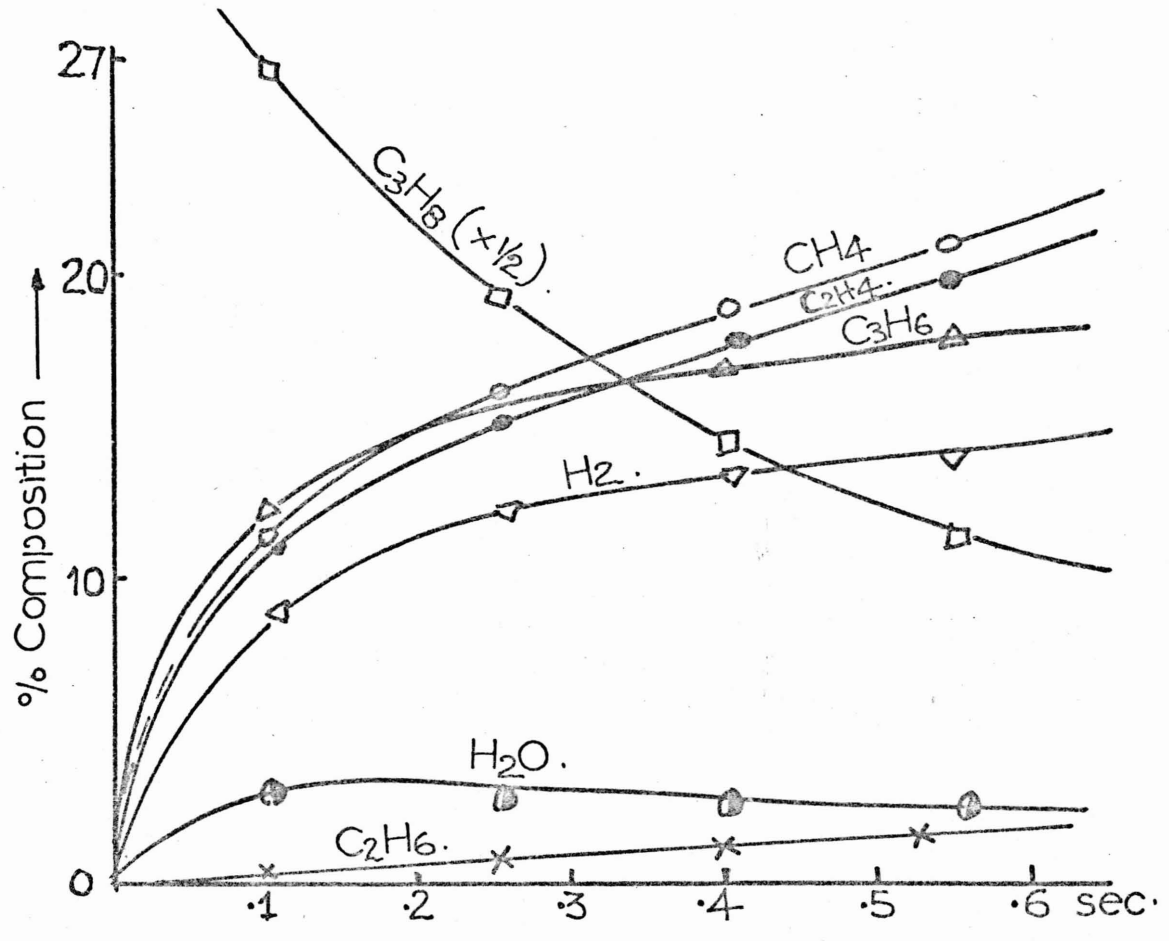

Fig 6-4 Products from propane + 2% O_2 at 700°C

6.2.1 COMPOSITION PROFILES

At 600°C, propylene was the predominant product with a concentration almost twice that of methane at 0.1 secs reaction time. Even water was formed at a faster rate than methane, ethylene or hydrogen at this small reaction time. There was just a trace of ethane. But as the residence time increased, the concentrations of all the other major products; methane, ethylene, hydrogen and ethane were rising much faster than that of propylene. Water quickly attained its maximum concentration and then decreased gradually as space time increased. This is shown in Fig. 6-2. A similar trend was shown at 650°C, but the gap between the propylene yield and that of each of the other products was beginning to close and it can be seen that at a space time of 0.75 seconds methane had almost overtaken propylene while ethylene caught up with propylene at 1.1 seconds reaction time. Fig. 6-3 illustrated this trend. It is worthy of note that the concentration of water at 0.1 second is now lower than the corresponding time at 600°C.

The same course of reaction continued at 700°C as illustrated in Fig. 6-4. It can be seen that methane and ethylene had now overtaken propylene at the shorter reaction times of 0.2 secs. and 0.32 seconds respectively. In addition, the initial yield of water (at 0.1 secs) was lower than at 650°C. Relative to unperturbed propane, all the products increased in concentration at the early stages of the reaction which is an indication of the accelerating effect of oxygen on the rate of pyrolysis of propane. This is well illustrated in Fig. 6-8 and Fig. 6-9.

6.2.2 EFFECT OF OXYGEN CONCENTRATION

The explanation of the observed product spectrum as illustrated by the composition profiles is that the role of oxygen is catalytic at the onset of reaction and that pyrolysis takes over as reaction time increases

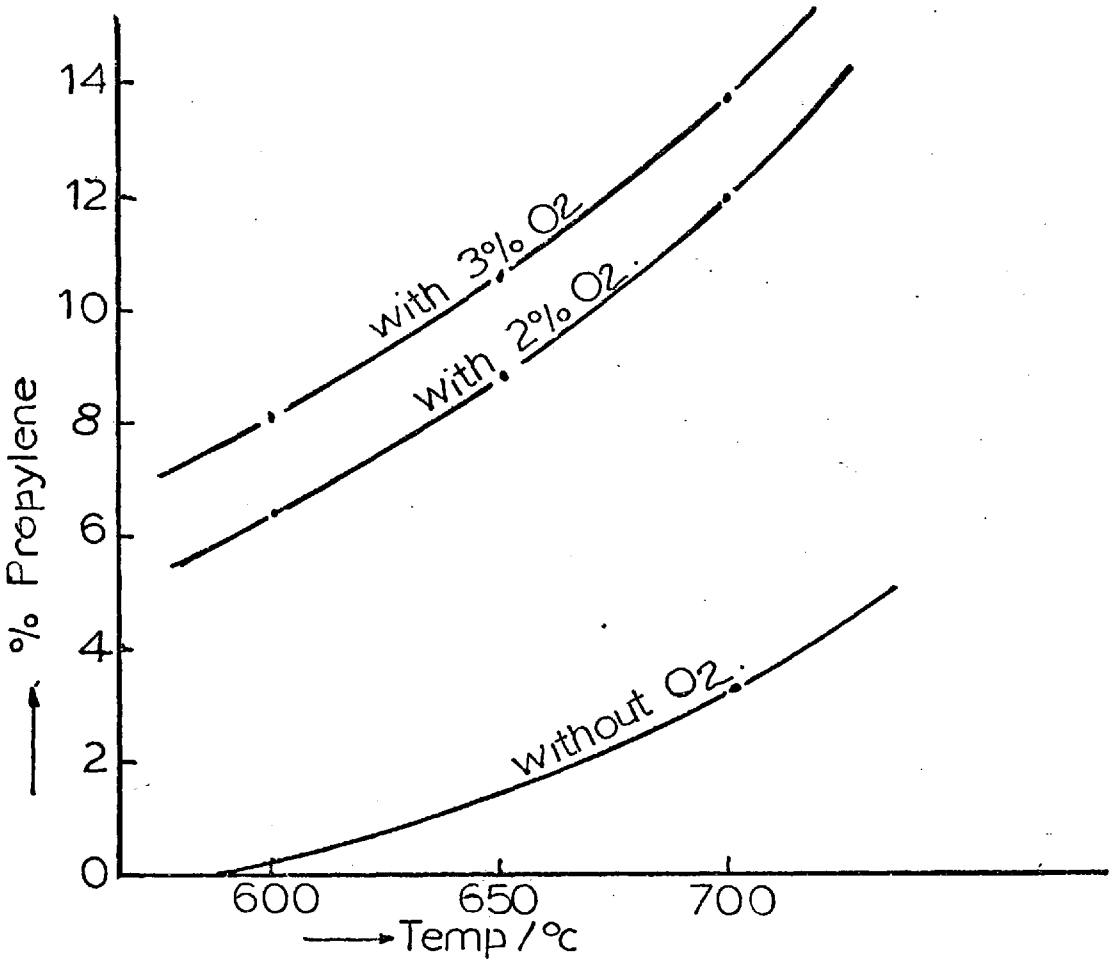

Fig 6-5 Influence of the partial pressure of oxygen on the yield of propylene at 0·1 sec reaction time.

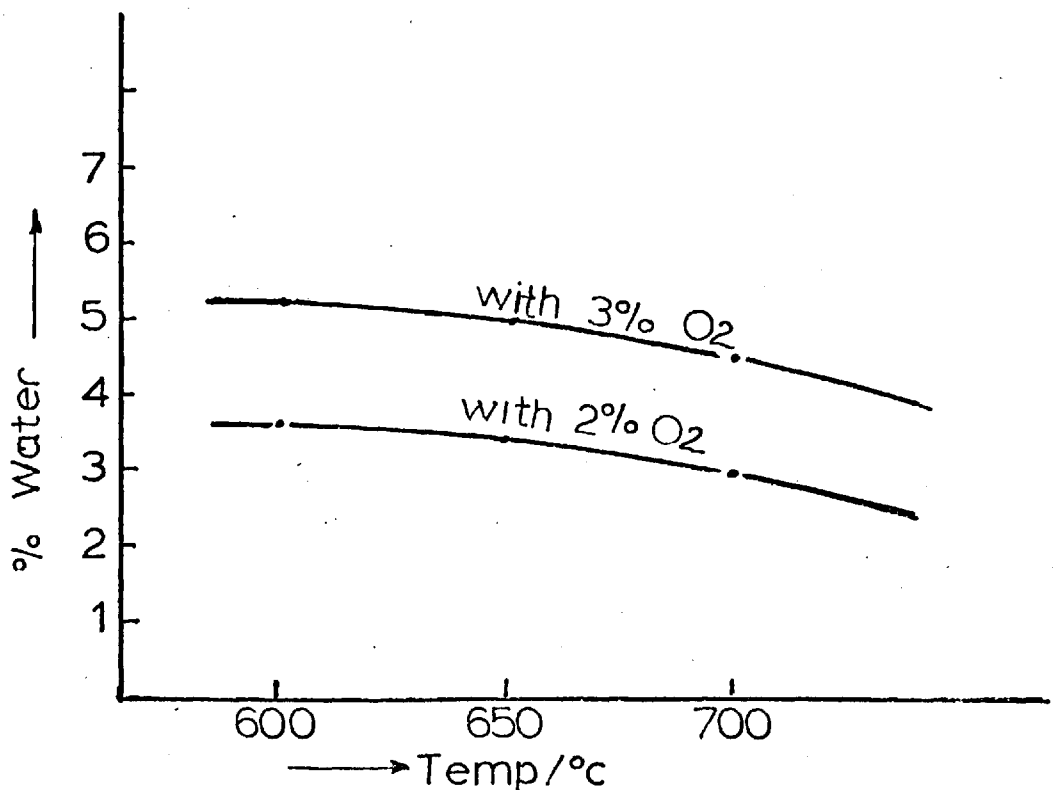

Fig 6-6 Influence of the partial pressure of oxygen on the yield of water at 0·1 sec reaction time.

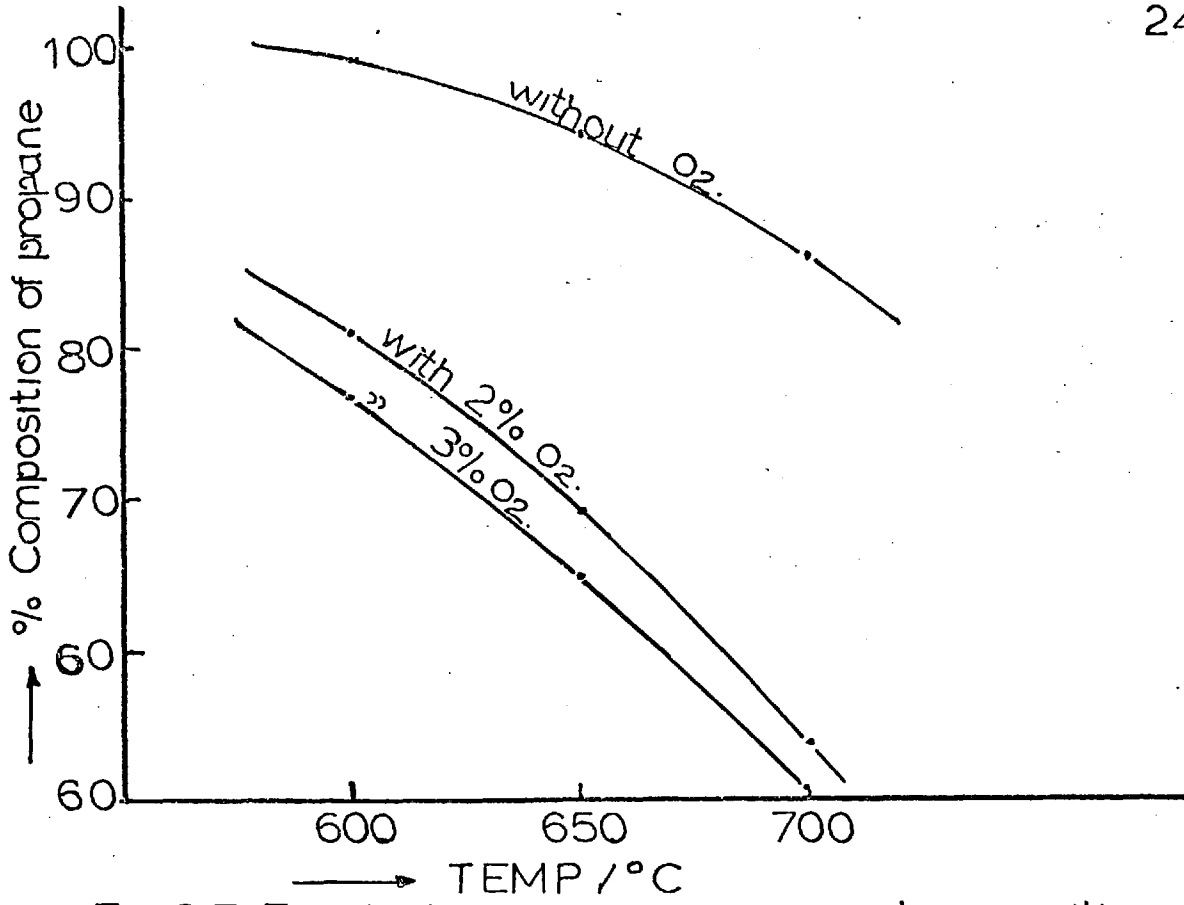

Fig 6-7 Effect of oxygen on propane decomposition at 0·1 sec reaction time.

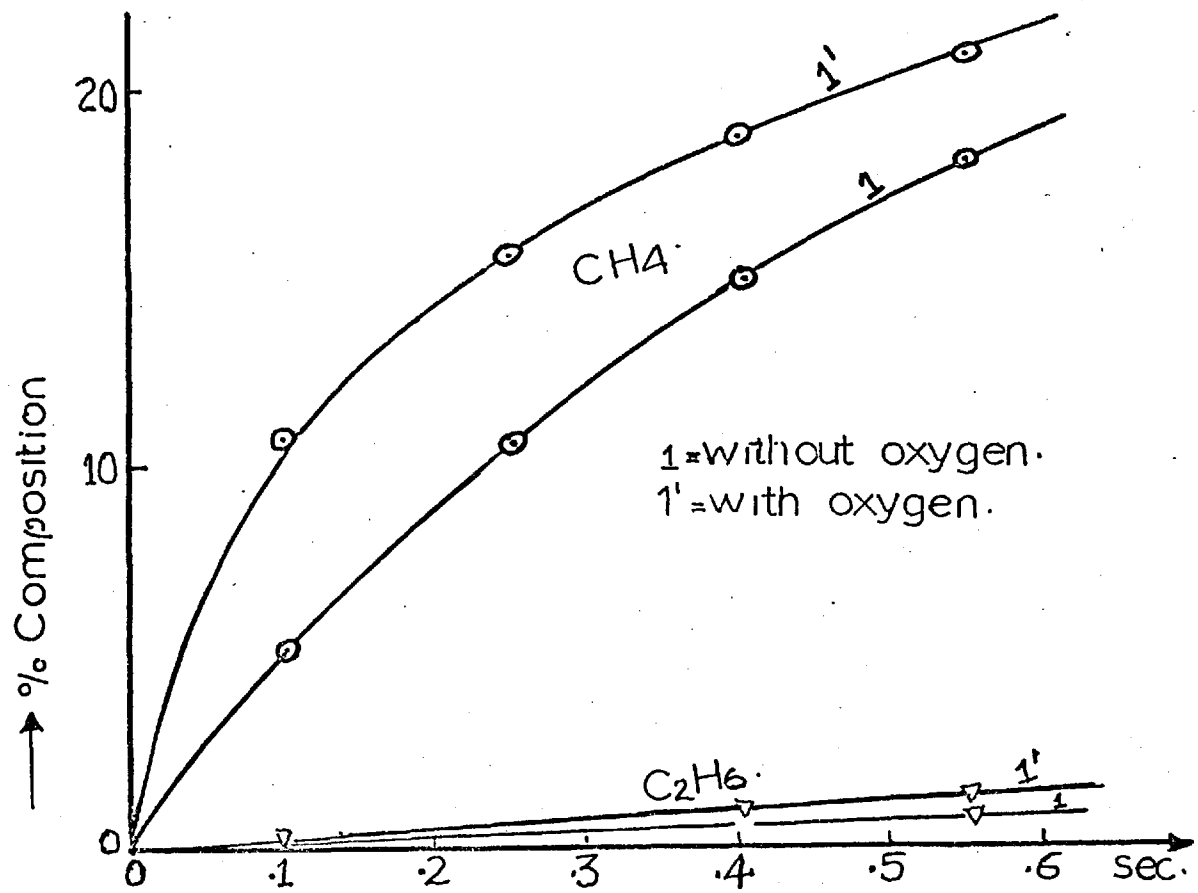

Fig 6-8 Effect of 2% O_2 in propane stream at 700°C on yield of methane and ethane.

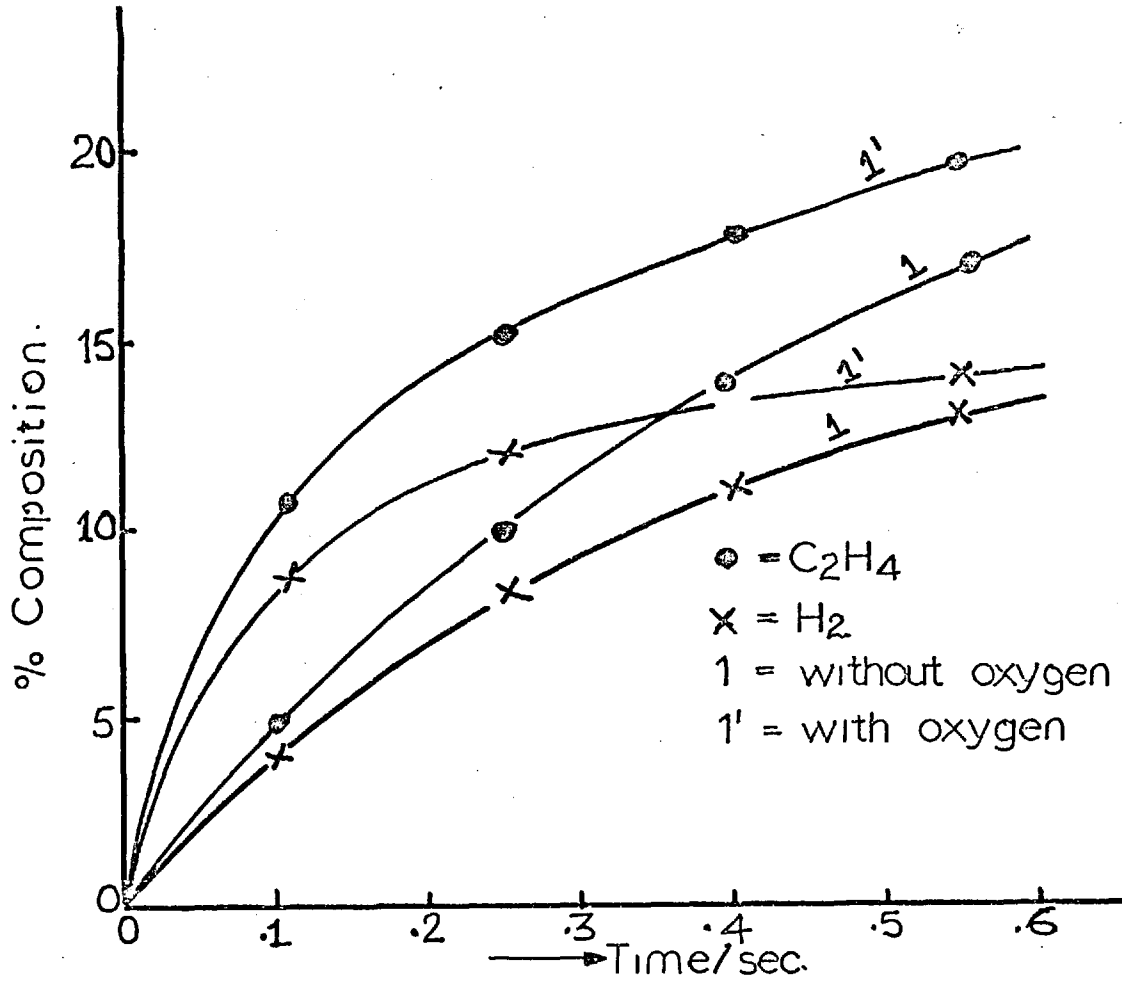

Fig 6-9 Effect of 2% in propane stream at 700°c on yield of ethylene and hydrogen.

and oxygen consumed. By increasing the concentration of oxygen from two to three per cent the rate of formation of propylene increased at a particular temperature for small reaction times. This is illustrated in Fig. 6-5. Two major facts are clearly illustrated: (1) at a particular concentration of oxygen, propylene increases with rising temperature at 0.1 second reaction time. (2) at a particular temperature, increase in oxygen leads to a more rapid formation of propylene.

In contrast to propylene, the formation of water at 0.1 seconds reaction time decreased with rising temperature, but like propylene, at a constant temperature, increase in oxygen concontration leads to an increase in the percentage yield of water. This is summarised in Fig. 6-6.

The overall effect of all this is a rapid decomposition of propane, initially by the catalytic role of oxygen and then by straight pyrolysis of the depleted propane after the exhaustion of oxygen. This accelerating effect of oxygen on propane pyrolysis is illustrated in Fig. 6-7. The following points are well illustrated: (1) The induction period usually observed before the onset of the exponential reaction stage is virtually wiped off. (2) Increase in the oxygen concentration at a particular temperature leads to a faster decay of propane. (3) For small reaction times, the accelerating effect of oxygen (at such small concentrations) decreases as the temperature is increased, i.e., at small extents of reaction. The accelerating effect of oxygen declines as the temperature is raised from 600°C to 700°C.

6.3 MECHANISM OF REACTION

A general mechanistic scheme can be proposed for the oxidation of alkanes as a sequence of reaction steps. The initiation reaction of the oxidation process probably involves the abstraction of a hydrogen atom

from the fuel molecule by a chain carrier x(x = O_2, HO_2., OH., RO_2.);

$$RH + X \longrightarrow R. + XH$$

The next step would be the formation of alkyl peroxy radicals RO_2.[54, 128]

$$R. + O_2 \rightleftharpoons ROO. \qquad (1)$$

This radical is an intermediate product, reactions of which, depending upon the experimental conditions and molecular structure, lead to many intermediate, minor and major products. Its reactions include such steps as:

(a) Isomerization (for C_4 - C_7 hydrocarbons):

$$RO_2. \rightleftharpoons \dot{R}OOH \qquad (2)$$

$$RO_2. \rightleftharpoons A\dot{B}OOH \qquad (2a)$$

The hydrogen atom is transferred from the $-CH^2$ groups in the α, β and position to the peroxidized carbon atom[129,131,132]. For instance in 2-pentylperoxy radicals, α transfer is predominant and in 2-hexylperoxy radicals, γ transfer is predominant.

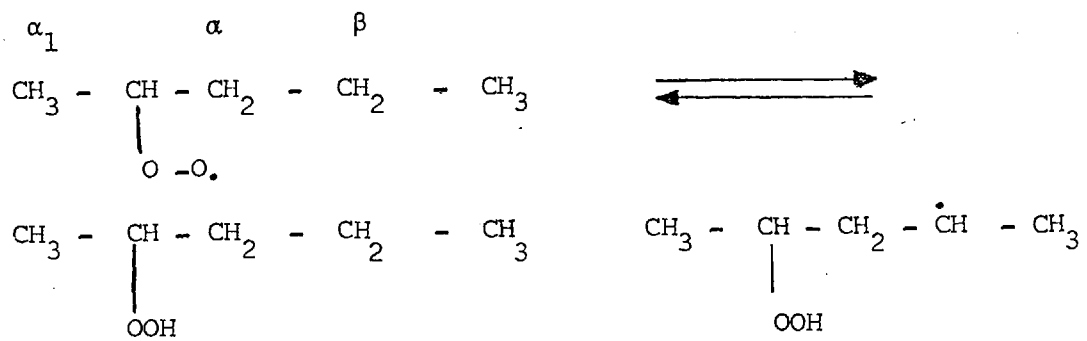

α - transfer

β - transfer

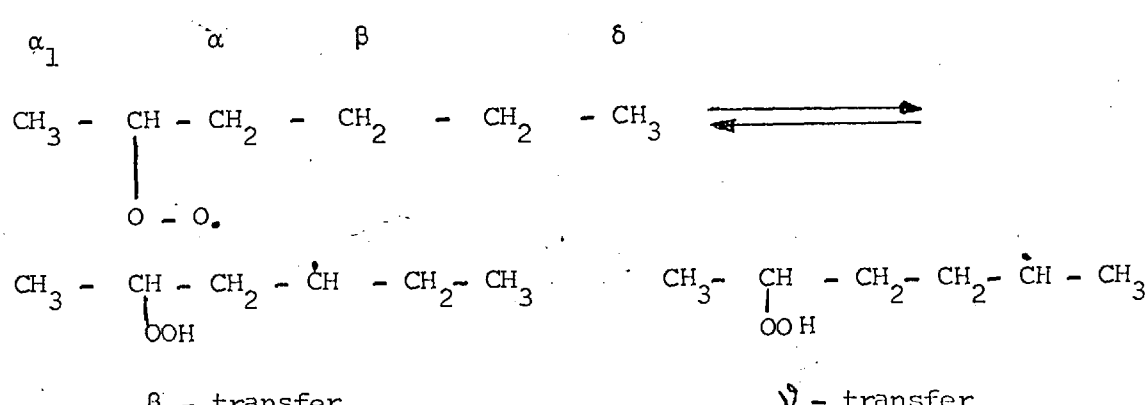

β - transfer

γ - transfer

The $\dot{R}OOH$ radicals produced are isomeric with $\dot{A}BOOH$ radicals which are formed by the reaction of the conjugate olefin AB with $HO_2\cdot$ radicals.

(b) Internal abstraction followed by decomposition

At lower temperatures the internal abstraction products decompose to form aldehyde, Ketone or epoxide.

$$RO_2\cdot \longrightarrow \underline{\text{Intermediate}} \longrightarrow R'CHO + R''O\cdot \qquad (3)$$

But at higher temperatures the alkyl peroxy radicals decompose easily to give conjugate olefins (AB) and an hydroperoxy radical $HO_2\cdot$

$$RO_2\cdot \longrightarrow \text{Intermediate} \longrightarrow AB + HO_2\cdot \qquad (4)$$

(c) External abstraction

At low temperatures they give an alkyl hydroperoxide:

$$RO_2 + HO_2 \longrightarrow ROOH + O_2$$

$$RO_2\cdot + R'O_2\cdot \longrightarrow ROOR' + O_2$$

To understand fully the types of reactions taking place at high temperatures, it is pertinent to summarize what goes on at low temperatures and interprete the difference in the products spectrum of between low and high temperatures in terms of the changes in reactivities of certain intermediates and radicals. Thus at low temperatures, the following scheme would explain the gas-phase oxidation of alkanes.

(1)	$RH + X \longrightarrow R\cdot + XH$	Initiation (abstraction)
(2)	$R + O_2 \rightleftharpoons RO_2\cdot$	addition
(3)	$RO_2\cdot \rightleftharpoons \dot{R}OOH$	1;5 or 1;6 hydrogen atom transfer.
(3a)	$RO_2\cdot \rightleftharpoons \dot{A}BOOH$	1;4 hydrogen atom transfer.
(4)	$R\cdot + O_2 \rightleftharpoons AB + HO_2$	internal abstraction

(5)	$RO_2\cdot + RH \rightleftharpoons ROOH + R\cdot$	abstraction
(6)	$RO_2\cdot + HO_2\cdot \rightleftharpoons ROOH + O_2$	disproportion
(7)	$RO_2\cdot \rightleftharpoons R'CHO + R\overset{\cdot\cdot}{O}$	decomposition
(8)	$AB + HO_2 \rightleftharpoons A\dot{B}OOH$	addition.
(9)	$\dot{R}OOH$, $A\dot{B}OOH \longrightarrow$ products + OH { carbonyl compounds or epoxides	decomposition
(10)	$\dot{R}OOH$, $A\dot{B}OOH + O_2 \longrightarrow \dot{O}OABOOH$	oxidation mainly at lower temp.
(11)	$\dot{O}OABOOH + XH \longrightarrow HOOABOOH + X$	polyperoxidation
(12)	$HOOABOOH \longrightarrow AB + BO + 2OH$ (aldehydes)	heterogeneous decomposition (branching)
(13)	$ROOH \longrightarrow R\dot{O} + \dot{O}H$	homogeneous decomposition (branching)
(14)	$R'CHO + O_2 \longrightarrow RCO\cdot + HO_2\cdot$	aldehyde oxidation
(15)	$2RO_2\cdot \longrightarrow$ products	
(16)	$2R\cdot \longrightarrow$ products	recombustion of radicals (termination)
(17)	$R\cdot + RO_2 \longrightarrow$ products.	

At high temperatures reactions (8), the addition of hydroperoxy radical to an olefin, is not favoured, hence reactions (10), (11) and (12) can only occur, if at all, to a very small extent; and even then the products will decompose very rapidly. The rearrangement reactions of propylperoxy radicals are probably as follows [132].

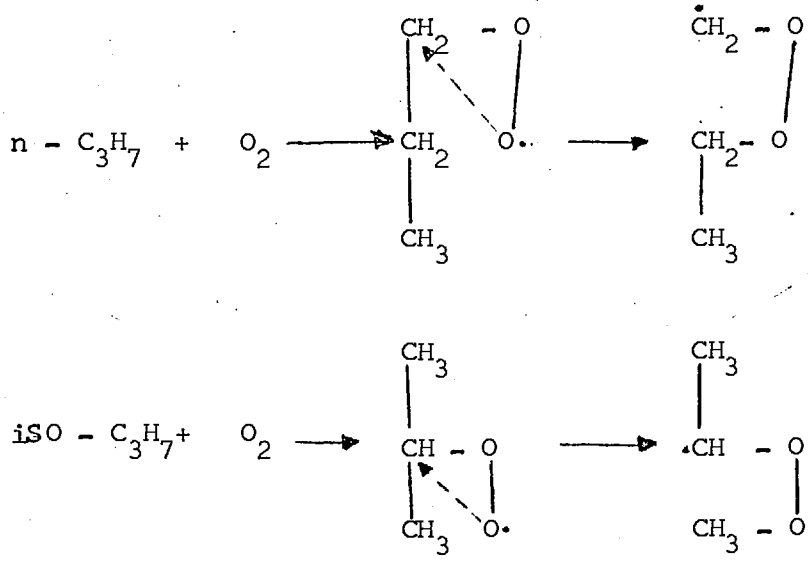

At low temperatures the scission of the O - O link gives formaldehyde, acetaldehyde or epoxide.

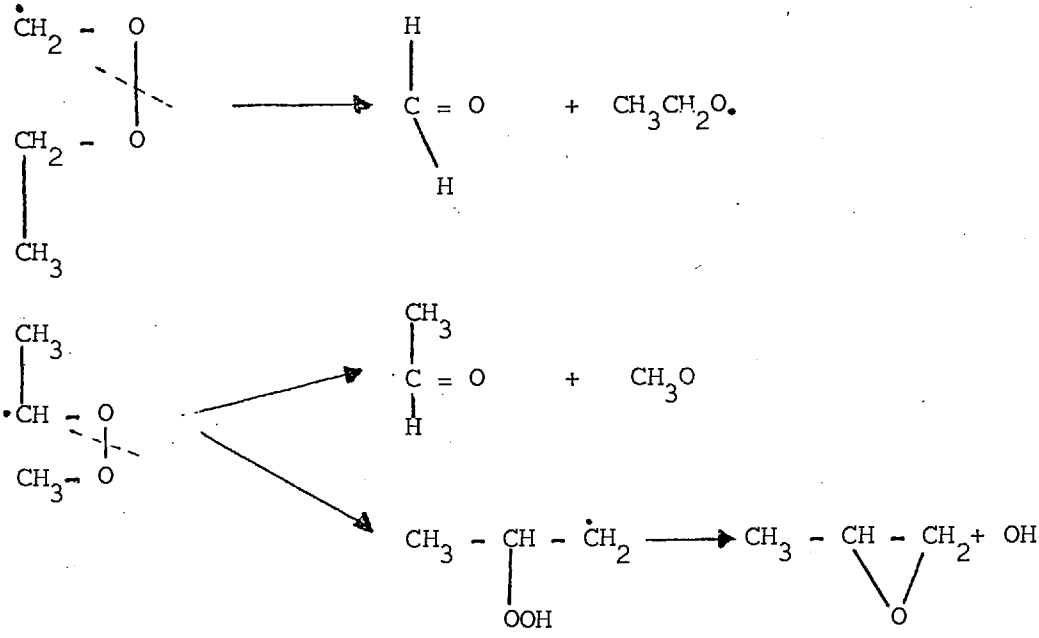

At high temperatures however, isomerization occurs by hydrogen atom transfer.

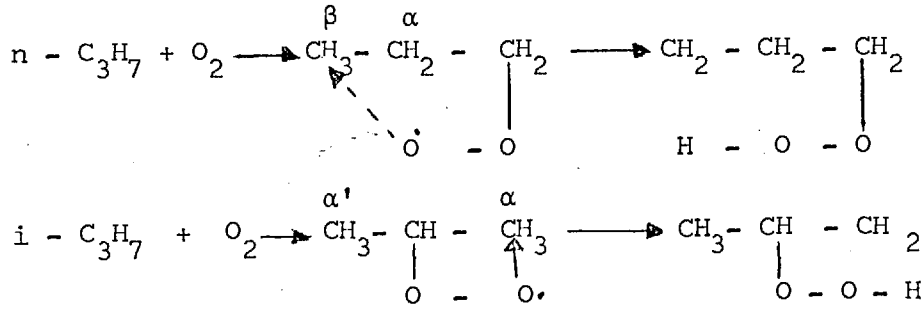

These isomers decompose to give olefins and free radicals;

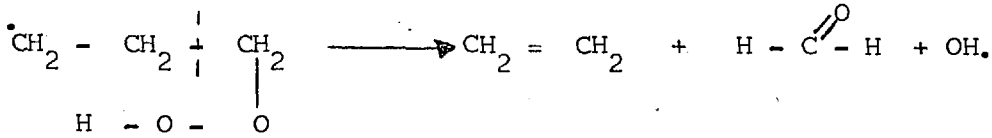

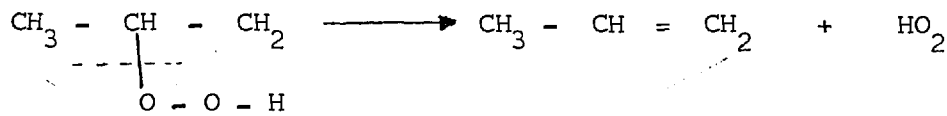

The work of Cullis et al [133] provides additional evidence that peroxy radical rearrangements are essentially high temperature phenomena. They reported the formation of methyl ethyl ketone in cool flames where the carbon atom of the carbonyl group was originally tertiary in the alkane.

6.4 HIGH TEMPERATURE REACTIONS OF ALKYL RADICALS WITH OXYGEN

For alkyl radicals larger than ethyl there is competition between decomposition and reaction with oxygen. As shown above various products can result from the rearrangements and decompositions of the peroxy radicals. There is much evidence that $CH_3\cdot$ reacts with oxygen to produce formaldehyde and hydroxyl radicals above 400°C [134] The initial reaction is;

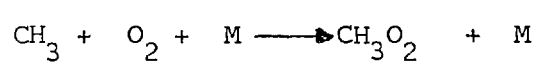

The reverse reaction proceeeds with an activation energy of about 107 KJoules per mole and a pre-exponential factor of about $10^{15.8}$ M^{-1} sec^{-1} [135]

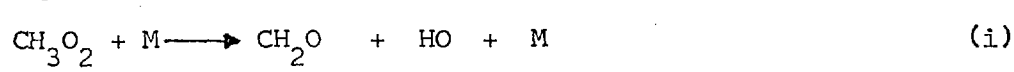

The rate data for this reaction (i) are summarized by McMillan and Calvert [136] The results are greatly scattered, but a number of investigations report a rate constant of 6×10^7 M^{-1} sec^{-1}. This is surely an upper limit, and Benson and Spokes [135] suggest an upper limit

one tenth as large at temperatures from 600° to 1450°K.

Another possible reaction of CH_3O_2 is

$$CH_3O_2 + M \longrightarrow CH_3O + O + M$$

But this reaction is endothermic by 221 KJoules per mole, so it can not be important.

For alkylperoxy radicals larger than CH_3O_2, the decomposition reactions are first-order. Two important reactions are:

$$RO_2 \longrightarrow R\cdot + O_2 \qquad (6)$$

$$RO_2 \longrightarrow \text{olefin} + HO_2\cdot \qquad (7)$$

of which reaction (7) is probably the more important, either to decompose into ethylene and hydrogen atom or react with oxygen to give ethylene and hydroperoxy radical.

$$C_2H_5 \rightleftharpoons C_2H_4 + H\cdot \qquad (8)$$

$$C_2H_5 + O_2 \longrightarrow C_2H_4 + HO_2\cdot \qquad (9)$$

Thus, competition sets in between decomposition of the radical and its reaction with oxygen. As the molecular weight of the radical increases the decomposition reaction becomes more prominent; and in the case of propyl radical C_3H_7, the decomposition rate becomes faster than the lower alkyl radicals.

$$n\text{-}C_3H_7 \longrightarrow C_2H_4 + CH_3\cdot$$

$$i\text{-}C_3H_7 \longrightarrow C_3H_6 + H\cdot$$

$$C_3H_7 + O_2 \longrightarrow C_3H_6 + HO_2\cdot$$

For higher alkyl radicals decomposition will predominate over oxidation, but the radicals generated as a result of their decomposition will react with oxygen to form a stable or intermediate product and hydroperoxy radical.

6.5 DISCUSSION

Since oxygen is added in very small amounts, its role lies mainly in the preheat zone (the induction phase) of fig. 6.1, where propylene is the major product. In agreement with Knox[125] no plausible step leading to its formation other than the following reaction (10) can be envisaged.

$$C_3H_7 + O_2 \rightarrow C_3H_6 + HO_2 \qquad (10)$$

The radical HO_2. is evidently the successor of the alkyl radicals. It is therefore reasonable to suggest that the mechanism which operates in oxidation of paraffins involves attack of HO_2. on the paraffin at least in the early stages before the concentration of primary products has become large enought for attack on them to be appreciable. This situation is described by reaction (11).

$$HO_2 + C_3H_8 \longrightarrow H_2O_2 + C_3H_7 \qquad (11)$$

The amounts of hydrogen peroxide have invariably been considerably lower than those which should be formed if reactions (10) and (11) represent the main chain-carrying steps. This small yield must be attributed to decomposition of hydrogen peroxide (especially on the walls) rather than to its non-formation. The conditions of the present experiment are such that homogeneous decomposition will occur[137] leading to degenerate branching.

$$H_2O_2 + M \longrightarrow M + 2HO. \qquad (12)$$

The hydroxy radicals will then react with the parent molecule to give water.

$$.OH + C_3H_8 \longrightarrow H_2O + C_3H_7 \qquad (13)$$

Another possible fate of HO_2. is dispropornation.

$$HO_2 + HO_2 \longrightarrow H_2O_2 + O_2 \qquad (14)$$

This is a termination step, removing two chain carriers, but it is potentially a source of two further carriers through reaction (12). The observed main products at the induction phase, propylene and water, are

explicable if a high proportion of $HO_2\cdot$ radicals undergo reaction (14) which would be followed by (12).

There is the possibility of surface destruction of the hydroperoxy radical $HO_2\cdot$, which would also lead to the observed products

$$2HO_2\cdot \xrightarrow{\text{wall}} H_2O + 3/2\ O_2 \qquad (15)$$

The alternative fate of $HO_2\cdot$ is its decomposition to hydroperoxy radical and oxygen atom;

$$HO_2\cdot + M \longrightarrow HO\cdot + O + M \qquad (16)$$

But this is endothermic[138] by 262 KJoules per mole, and if it occurred as the major fate of $HO_2\cdot$, would lead to a very rapid branching and isothermal explosion. This effect has not been observed.

The temperature being very high, there will be competition between decomposition of propyl radicals and their reactions with oxygen. Propyl radicals easily decompose to ethylene and methyl radicals.

$$C_3H_7 \longrightarrow C_2H_4 + CH_3$$

The methyl radical can then react with oxygen to give a molecule of formaldehyde and an hydroxy radical:

$$CH_3 + O_2 \longrightarrow CH_2O + HO_2 \qquad (17)$$

The formaldehyde will be rapidly removed by radical attack of, most probably, hydroxy radical

$$OH\cdot + CH_2O \longrightarrow H_2O + CHO$$

$$HCO \longrightarrow H + CO$$

$$CHO + O_2 \longrightarrow CO + HO_2$$

As oxygen becomes exhausted, the formations of $HO_2\cdot$ and hydrogen peroxide will cease and pyrolysis reactions of propane and other molecules in the system will becomes uninhibited.

In the light of the above considerations, the basic features of the

initial reactions are compatible with the following equations:

$$R\cdot + O_2 \longrightarrow \text{olefin} + HO_2\cdot$$

$$R\cdot \longrightarrow \text{olefin} + R\cdot$$

$$HO_2\cdot + RH \longrightarrow R\cdot + H_2O_2$$

$$H_2O_2 + M \longrightarrow \cdot OH + OH + M$$

$$\cdot OH + RH \longrightarrow H_2O + R$$

$$HO_2\cdot + HO_2\cdot \longrightarrow H_2O_2 + O_2$$

where R'. is a methyl radical when R. is a propyl radical.

The following kinetic scheme was integrated and found to describe very well the observed product distribution as a function of time and temperature.

	REACTION	A(SEC^{-1})	E(KJ/mole)	
1.	$C_3H_8 \longrightarrow C_2H_5 + CH_3$	6×10^{14}	326.0	158
2.	$C_3H_7 + O_2 \longrightarrow C_3H_6 + HO_2$	1×10^{6}	0.0	150
3.	$C_3H_8 + CH_3 \longrightarrow CH_4 + C_3H_7$	1.5×10^{12}	20.5	4
4.	$C_3H_7 \longrightarrow C_2H_4 + CH_3$	4×10^{10}	133.7	158
5.	$CH_3 + O_2 \longrightarrow CH_2O + OH.$	6×10^{5}	0.0	150
6.	$HO_2 + HO_2 \longrightarrow H_2O_2 + O_2$	1×10^{11}	0.0	61
7.	$HO_2 + C_3H_8 \longrightarrow H_2O_2 + C_3H_7$	1×10^{7}	50.0	67
8.	$C_2H_5 + O_2 \longrightarrow C_2H_4 + HO_2$	1×10^{6}	0.0	150
9.	$C_2H_5 + C_3H_8 \longrightarrow C_2H_6 + C_3H_7$	2×10^{10}	25.0	158
10.	$C_2H_5 \longrightarrow C_2H_4 + H$	3×10^{11}	146.3	159
11.	$H + C_2H_4 \longrightarrow C_2H_5$	7.5×10^{11}	22.5	158

12.			C_3H_7	$\longrightarrow$	H. +	C_3H_6	3.6×10^{10}	133.7[158]
13.	H.	+	C_3H_6	$\longrightarrow$	C_3H_7		1.8×10^{11}	4.8[158]
14.	CH_3	+	C_2H_5	$\longrightarrow$	C_3H_8		4.2×10^{12}	0.0[158]
15.	C_2H_5	+	C_2H_5	$\longrightarrow$	C_4H_{10}		1×10^{11}	0.0[163]
16.	C_2H_5	+	C_2H_5	$\longrightarrow$	C_2H_6 +	C_2H_4	1×10^{10}	0.0[161]
17.			C_4H_{10}	$\longrightarrow$	C_2H_5 +	C_2H_5	8.7×10^{9}	167.00[162]
18.	H.	+	C_3H_8	$\longrightarrow$	H_2 +	C_3H_7	1.8×10^{12}	19.2[160]
19.	CH_3	+	C_3H_7	$\longrightarrow$	C_3H_6 +	CH_4	1×10^{12}	0.0[158]
20.	CH_3	+	C_3H_7	$\longrightarrow$	C_4H_{10}		1×10^{11}	0.0[158]
21	H_2	+	C_3H_7	$\longrightarrow$	C_3H_8 +	H	5.6×10^{7}	83.6[158]
22.	C_2H_6			$\longrightarrow$	CH_3 +	CH_3	1.2×10^{12}	284.2[4]
23.	CH_3	+	C_2H_6	$\longrightarrow$	CH_4 +	C_2H_5	$8. \times 10^{8}$	50.0[4]
24.	H.	+	C_2H_6	$\longrightarrow$	H_2 +	C_2H_5	1.3×10^{11}	37.6[161]
25.	OH	+	C_3H_8	$\longrightarrow$	H_2O +	C_3H_7	1×10^{6}	40.0[165]
26.	H_2O_2	+	M	$\longrightarrow$	OH +	OH + M	1×10^{6}	46.0
27.	HCOH	+	O_2	$\longrightarrow$	HCO +	HO_2	1×10^{12}	62.7[140]
28.	HCO	+	O_2	$\longrightarrow$	HO_2 +	CO	7×10^{8}	0.0[140]

TABLE 6-2 KINETIC SCHEME FOR THE PYROLYSIS OF PROPANE IN THE PRESENCE OF 2-3% OXYGEN BETWEEN 600 AND 700°C.

The following scheme thus describes the behaviour of the alkyl radicals involved in the autocatalytic reaction of propane,

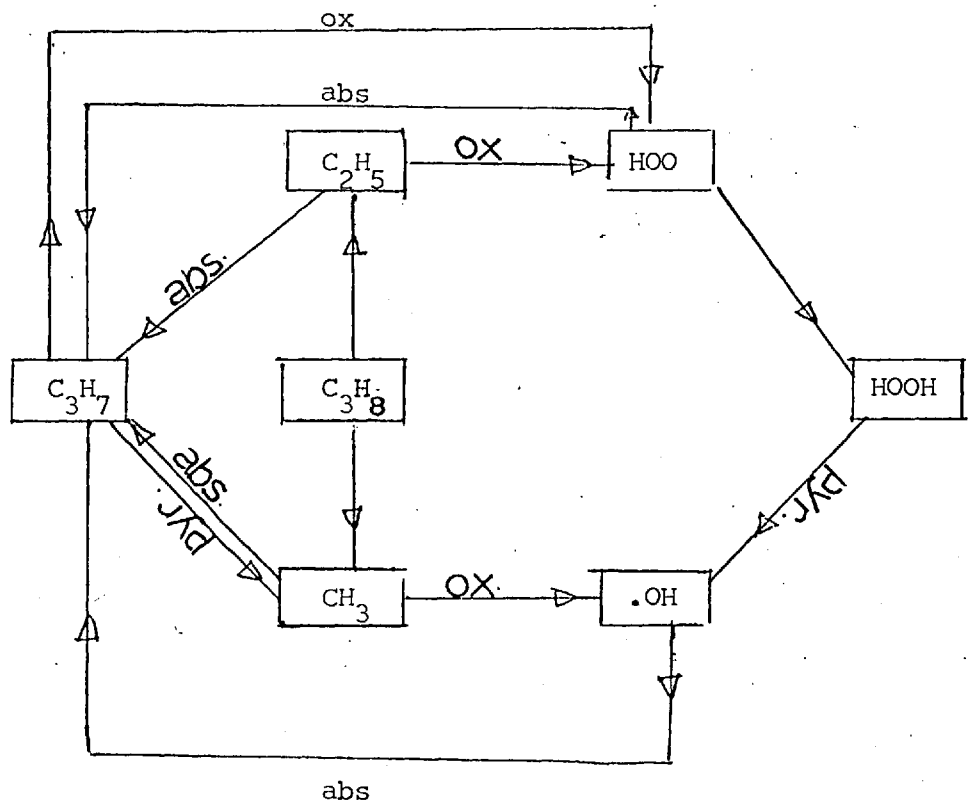

where: abs = abstraction of hydrogen atom from propane

ox = oxidation (reaction with oxygen)

pyr = pyrolysis.

In addition, after the primary initiation, presumably $RH + O_2 \quad R\cdot + HO_2\cdot$, a chain reaction of the types.

$$HO_2\cdot + RH \longrightarrow H_2O_2 + R\cdot, \text{ and}$$

$$R\cdot + O_2 \longrightarrow \text{olefin} + HO_2,$$

would ensue effectively as an induction period. But as reaction proceeds and more radicals become available in the system, the combination reactions of $HO_2\cdot$ competes more and more effectively with its abstraction of hydrogen atoms to form hydrogen peroxide, until ultimately its abstraction reactions take over to constitute the main source of hydrogen peroxide which, in turn, generates the hydroxy radicals. It is also clear that

those fuels which give largely methyl radicals will less frequently lead to the dispropornation of HO_2. radicals as an important feature of their oxidation, because the reaction R. + O_2 ⟶ olefin + HO_2., will be largely replaced by the reaction;

$$CH_3\cdot + O_2 \longrightarrow CH_2O + OH,$$

leading to the reactive .OH radical rather than to hydroperoxy radical.

REFERENCES

1. Rice, F.O.. J. Amer. Chem. Soc. 53, 1959 (1931)
2. Rice, F.O., Herzfeld, K.F., J. Amer. Chem. Soc. 56, 284 (1934)
3. Rice, F.O., Kossiakoff, A., J. Amer. Chem. Soc. 65, 390 (1943)
4. Bradley, J.N., Proc. Roy. Soc. (LONDON) A337, 199 (1974).
5. Leathard, D.A., Purnell, J.H. Proc. Roy. Soc. (LONDON) A305, 517 (1968)
6. Zdonik, S.B., Green, E.J., The oil and Gas Journal June 26, 1967
7. Paul, R.E., Marek, L.F. Ind. Eng. Chem. 26, 454 (1934)
8. Steacie, E.W.R., Puddington, T.E., Can. J. Res. B16, 411 (1938)
9. Laidler, K.J., Sagert, N.H., Wojciechowski, B.W. Proc. Roy. Sco. (LONDON) A270, 242 (1962)
10. Kershenbaum, L.S., Martin, J.J., A.I. Ch. E.J. 13, 148 (1967)
11. Martin, R., Dzierzynski, M., Niclause, M., J. Chim. Phys. 61, 286 (1964)
12. Laidler, K.J., Proc. Roy. Soc. (London) A270, 246 (1962)
13. Crynes, B.L., Albright, L.F. Ind. Eng. Chem. PDD Vol. 8, No. 1. Jan. (1969)
14. Worrell, G.R., Chapman, R.F., Woinsky, S.G., Ind. Eng. Chem. PDD. Vol. 6, 89, 1967.
15. Zdonik, S.B., Green, E.J. Oil and Gas Journal, July 10 1967
16. Knaus, J.A., Yarze, J.C. Paper No. 31, Sec. IV, 6th World Petroleum Congress, Frankfurt. June 1963
17. Frey, F.E., Hepp, H.J. Ind. Eng. Chem. 25, No. 4 (1933)
18. Calingaert, J. Am. Chem. Soc. 45, 130 (1923)
19. Knaus, J.A., Patton, J.L., Chem. Eng. Prog. 57, 57 (1961)
20. Blackmore, D.R., Hinshelwood, C., Proc. Roy. Soc. (LONDON) A268, 21, 36 (1962).
21. Rice, F.O., Rice, K.K., "The Alphatic Free Radicals" John Hopkins Press, Baltimore. P.75 (1935).
22. Hurd, C.D., Ind. Eng. Chem. 26, 50 (1934)
23. Hurd, C.D., Meinert, R.N., J.Am. Chem. Soc. 52, 4978 (1930)

24. Hurd, C.D., Spence, L.U., J.Am. Chem. Soc. 51, 3561 (1929)

25. Hurd, C.D., G ldsby, A.R., J.Am. Chem. Soc. 56, 1812 (1934)

26. Kinney, R.E., Crowley, D.J., Ind. Eng. Chem. 46, 258 (1954)

27. Towell, G.D., Martin, J.J., A. I. Ch. E. J. 7, 693 (1961)

28. Davies, H.G., Williamson, K.D. Paper No. 4, Sec. IV, 5th World Petroleum Congress 1959

29. Rossini, F.D. et al., "Selected Values of Physical and Thermodynamic Properties of Hydrocarbons and Related Compounds. API Research Project 44, Carnegie Press (1953)

30. Zdonik, S.B., Green, E.J. Hallee, J.P. Oil and Gas Journal, August 7, (1967)

31. Berg, L., Summer, G.L. et al, Ind. Eng. Chem. 37, 352 (1945)

32. Weizmann, C. et al. Ind. Eng. Chem. 43, 2312 (1951)

33. Sandler, S., Chung, Y.H., Ind. Eng. Chem. 53, 391 (1961)

34. Frey, F.E., Hepp, H.J. Ind. Eng. Chem. 25, 441 (1933)

35. Rice, F.O., Murphy, M.T. J. Am. Chem. Soc. 64, 896 (1942)

36. Frey, F.E., Hepp, H.J., Ind. Eng. Chem. 41, 827 (1949)

37. Ingold, K.U., Stubbs, F.J., J. Chem. Soc. p1749 (1951)

38. Laidler, K.J. Wojciechowski, B.W., Proc. Roy. Soc. A259, 257 (1960)

39. Amano, A. Uchiyama, M., J. Phys. Chem. 67, 1242 (1963)

40. Kallend, A.S., Purnell, J.H. Proc. Roy. Soc. A300, 120 (1967)

41. Kunugi, T., Kazuhiko, S., Tomoya Sakai, Ind. Eng. Chem. Fund. 9, No. 3, 319 (1970)

42. Hurd, C.D., Eilers, L.K. Ind. Eng. Chem. 26, 776 (1934)

43. Zdonik, S.B., Green, E.J. Oil and Gas Journal July 10, p 196 (1967)

44. Ibid Feb. 19, p93 (1968)

45. Schutt, H.C., Chem. Eng. Prog. 55, 68 (1959)

46. Bone, W.A., Andrew, A.W. J. Chem. Soc. p 1232 (1905)

47. Callender, H.L., Engineering 123, p147, 184 (1927)

48. Bodenstein, M. Z. Phys. Chem. 85, 329 (1913)

49. Christiansen, J.A., J. Phys. Chem. 28, 145 (1924)

50. Semenov, N.N., Z. Physik. Chem. 46 109 (1927)

51. Semenov, N.N., "Chain Reactions" Oxford (1935)

52. Boord, E.C., Third Symposium on Combustion 48, 416 (1949)

53. Knox, J.H. Combustion and Flame 9, 297 (1965)

54. Semenov, N.N. "Some Problems of Chemical Kinetics and Reactivity", Vols I and II. Pregamon Press, London (1958)

55. Minkoff, G.J., Tipper, C.F.H., Chemistry of Combustion Reactions, Butterworths, London 1962

56. Knox, J.H., Oxidation of Organic Compounds. Adv. Chem. Series 76, 3 (1968)

57. Hay, J.M. J. Chem. Soc. B, 1175 (1967)

58. Benson, S.W., J. Am. Chem. Soc. 87, 972 (1965)

59. Hay, J.M., Combustion and Flame 11, 83 (1967)

60. Mayo, F.R. J. Am. Chem. Soc. 89, 2654 (1967)

61. Fish, A., Adv. Chem. Ser. 76, 71 (1968)

62. Knox, J.H., Wells, C.H.J. Trans. Far. Soc. 59, 2786, 2801 (1963)

63. Hay, J.M. Knox, J.H., Turner, J.M.C. Tenth Symposium (International) on Combustion, Combustion Inst., Pittsburgh, Pa, p331 (1965)

64. Zeelenberg, A.P. Bickel, A.F. J. Chem. Soc. (London) 4014 (1961)

65. Cullis, C.F., Fish, A., Trimm, D.L., Proc. Roy. Soc. (London), A273, 427 (1963)

66. Denisov, E.T., Kosarev. V.P., Russ. J. Phys. Chem. 38, 1565 (164)

67. Sampson, R.J., J. Chem. Soc. 5, 5104 (1963)

68. Newitt, D.M., Thomes, L.S., J. Chem. Soc. 1657 (1937)

69. Cullis, C.F., J. City University, London Sep. 16 (1967)

70. Tipper, C.F.H., Quarterly Review II, 313 (1957)

71. Herriot, G.E., Eckert, R.E., Albright, L.F., A.I.Ch. E. J. 18, 84 (1972)

72. Snow, R.H., J. Phys. Chem. 70, 2780 (1966)

73. Edelson, D., J. Comp. Physics., 11, 455 (1973)

74. Gear, C.W. "The Automatic Integration of Ordinary Differential Equations". Comm. ACM 14, 176 (1971)

75. Kershenbaum, L.S., Sena, M.P.: Kinetic Modelling. 65th AICHE, 1972

76. Fort, R., Hinshelwood, C.N., Proc. Roy. Soc. A129, 284 (1930).

77. Spence, R., J. Chem. Soc. p649 (1936)

78. McDowell, C.A., Thomas, J.H., Norrish, R.G.W. Nature 162, 367 (1948)

79. Style, D.W.G., Summers, D. Trans. Far. Soc. 42, 383 (1946)

80. Snowdon, F.F., Style, D.W.G.

81. Askey, P.J., J. Am. Chem. Soc. 52, 974 (1930)

82. Norrish, R.G.W., Thomas, J.H., Nature 210, 728 (1966)

83. Griffiths, J.F., Skirrow, G., Oxidation and Combustion Review, 3, 47 (19 (1968)

84. Markevich, A.M., Fillippdva, L.F. Russ. J. Phys. Chem. 33, 358 (1959)

85. Makellar, J.F., et al, Proc. Roy. Soc. A254, 147 (1960)

86. Vardanyan, I.A., Sachyan, G.A., Nalbandyan, A.B., Doklady Akad. Nauk. SSR. 191, No..1, 130, (1970)

87. Hessam, K. Ph.D. Thesis, University of London (1971)

88. Kerr, J.A. Chem. Rev. 66, 465 (1966)

89. Walsh, R., Benson. S.W., J. Am. Chem. Soc. 88, 4570 (1966)

90. Jenkins, A.D., Style, D.W.G. J. Chem. Soc. p2337 (1953)

91. Steacie, E.W.R., Calvert, J.G. J. Chem. Phys. 19, 176 (1951)

92. Newton, R.H., Dodge, B.F., J. Am. Chem. Soc. 55, 4747 (1937)

93. Nalbandyan, A.B., Markevich. A.M., Russ. J. Phys. Chem. 33, 358 (1959)

94. Galenas, J.R., J. Comp. Phys. 9, 222 (1972)

95. Lange, N.A., Handbook of Chemistry, 10th ed. McGraw-Hill, N.Y. (1961)

96. Thompson, J.J., Phil. Mag. 21, 225 (1911)

97. Aston, F.W., Phil. Mag. 38, 707 (1919)

98. Dempster, A.J. Phys. Rev. 11, 316 (1918)

99. Robertson, A.J.B., Mass Spectrometry, Methuen & Co., New York 1954

100. American Petroleum Inst. Research Project Mass Spectrol Data 1947

101. Parsons, B.N., Danby, C.J., Hinshelwood, C.N. Proc. Roy. Soc. (London) A240, 333(1957)

102. Pease, R.M., J. Am. Chem. Soc. 50, 1779 (1928)

103. March, L.F., McCleur, W.B., Ind. Eng. Chem. 23, 878 (1933)

104. Dintses, A.I., Frost, A.V., J. Gen. Chem. U.S.S.R., 3, 747 (1938)

105. Steacie, E.W.R., Puddington, I.E., Can. J. Res. B16, 176 (1938)

106. Groll, H.P.A., Ind. Eng. Chem. 25, 784 (1933)

107. Schneider, V,, Frolich, P.K., Ind. Eng. Chem. 23, 1405 (1931)

108. Poltorak, V.A., Leitis, L.ya., Voevodskii, V.V., Russ. J. Phys. Chem. 33, 379 (1959)

109. Fusy, J., Scacchi, G. Niclause, M. Compt. Rend. 261, 2223 (1965)

110. Hinshelwood, C.N., Proc. Roy. Soc. (London) A234, 301 (1956)

111. Stevenson, D.P., J. Chem. Phys. 20, 192 (1952)

112. Poltorak, V.A., Voevodsky, Dokl. Akad. Nauk. SSR. 91, 589 (1953) English translation in M.H. Back & K.J. Laidler, "Selected Readings in Kinetics". Pergamon (1967)

113. Niclause, M., J. Chem. Phys. 61, 790 (1964)

114. Martin, R., Dzierzynski, M. Niclause, M. J. Chem. Phys. 61, 286 (1964)

115. De Boodt, H., Ingeniersthesis, Rijksuniversiteit Gent, 1962

116. Goldfinger, P., Letort, M., Niclause, M., Contribution a l'etude de la

117. Lin, M.C., Laidler, K.J., Can. J. Chem. 44, 2927 (1966)

118. Winkler, C.A., Hinshelwood, C.N. Proc. Roy. Soc. A149 640 (1935)

119. Allen, A.O., J. Am. Chem. Soc. 58, 1052 (1936)

120. Laidler, K.J., Liu, M.T.H. Proc. Roy. Soc. A297, 365 (1967)

121. Slater, D.H., Calvert, J.G., Adv. Chem Series 76, 58 (1968)

122. Benson, S.W., Shaw, R. International oxidation Symposium 1, 571 (1967)

123. Knox, J.H. Trans. Farad, Soc. 55, 1362 (1959)

124. Knox, J.H. Smith and Trotman-Dickenson, Trans. Farad Soc. 54 1509 (1958)

125. Knox, J.H. Trans. Farad. Soc. 56, 1225 (1960)

126. Falcomer, W.E., Knox, J.H., Trotman-Dickenson. J. 782, 9288 (1961)

127. Bradley,J.N. Flame and Combustion Phenomena Menthuen 1969 p. 88

128. Ubbelodhde, A.R., Small, N.J.H. J. Appl. Chem (London) 3, 193 (1953)

129. Cullis, C.F., Fish, A., Trimm, D.L. International Combustion Symposium, Vol. 9, Academic Press N.Y. (1963), 167.

130. Cullis, C.F., Fish,

131. Cullis, C.F., Aseed, M., Trimm, D.L. Proc. Roy. Soc. A298, 402 (1966)

132. Shtern, V. Ya, Zh. Fiz. Khim, 28, 613 (1954)

133. Cullis, C.F., Hardy,F.R.F., Turner, D.W. Proc. Roy. Soc. A244, 573 (1958)

134. Hoare, D.E. "Low temperature oxidation" W. Jost. ed; SNew York 1966, Chap. 6.

135. Benson, S.W. J.Am. Chem. Soc. 87, 972 (1965)

136. McMillan, G.R., Calvert, J.G., Oxidation and Combustion review. 1, 83 (1965)

137. Hdare, Protheroe and Walsh. Trans. Far. Soc. 55, 548 (1959)

138. Gray, P., Trans.-Far. Soc. 55, 488 (1959)

139. Hinshelwood, C.N. Proc. Roy. Soc. A167, 447 (1938) 301 (1956)

140. Vardanyan, I.A., Nalbandyan, A.B., Combustion and Flame. 17, 315 (1971)

141. Blundell, Cook, Hoare and Milne, 10th Int. Comb. Symp., Comb. Inst. p.473 (Pitts. 1965)

142. Hay, J.M., Hesssm. K, Combustion and Flame 16, 237 (1971)

143. Benson, S.W. O'Neal, H. Kinetic data on Gas phase-Unimolecular reactions (1970), 385

144. Benson, S.W., "Radicals and Kinetics of Combustion reactions"., Stanford Res. Inst. 1965

145. Hoare, Nature 194, 283 (1962)

146. Baulch, D.L., Drysdale, D.D., Lloyd, A.C. "High temperature reaction rate data". No. 3 1969

147. Calvert,J.G., Steacie, E.W.R., J. Chem Phys 19, 176 (1951)

148. Klein, Scheer and Schoen. J. Am. Chem. Soc. 78, 50 1956

149. Benson, S.W., O'Neal, H. J. Chem. Phys. 36, 2196 (1962)

150 McMcMillan, G.R., Calvert, J.G., Oxidation combustion review, Vol. 1, 83, (1965)

151. McDowell and Sharples. Can. J. Chem 36, 251 (1958)

152. Schmidt, C. Sehon, A.H., Can. J. Chem. 41, 1819 (1963)

153. Avramenko and Lorentso: Dokl. Akad. Nauk. S.S.S.R. 69, 265 (1949)

154. Baldwin, Jackson and Walker. 10th Int. Symp. Comb. Inst. p. 473 (Pitts. 1965)

155. Julian Hercklen; Adv. Chem; Ser. 76, 23 (1968)

156. Baulch et al., "High temp. reaction rate data" May, 1958

157. Harris and Steacie. J. Chem. Phys. 13, 554 (1945)

158. G.E. Herriot, Roger, E. Eckert; Albright, L.F. AICHE J. 18, 94 (1972)

159. Kerr, J.A., Trotman-Dickenson, A.F. J. Chem. Soc. 1611 (1970)

160. Voevodsky and Kondratiev "Progress in Reaction Kinetics" p8 41 Pergamon press 1961

161. Pratt, G.L. , "Gas Kinetics" John Wiley and Sons, p. 159 1969

162. Purnell, J.H., Quinn, C.P, Proc. Roy. Soc. A270, 267 1962.

163. Benson, S.W., H, Edward O'Nela in "Kinetic Data on Gas Phase Unimolecular Reactions (1970) p. 385.

164. Benson, R.W., Shaw, R. International Oxidation Symposium 1, 567 (1967)

165. Baldwin, Jackson, Walker and Webster, 10th. Int. Symp. Comb. Inst. p. 473 (Pitts. 1965)